Study on tropical rain with special reference to rain Drop Size Distribution and integral rain parameters using ground-based and satellite measurements

Thesis Submitted to the
Cochin University of Science and Technology
for the award of the Degree of

DOCTOR OF PHILOSOPHY

in

PHYSICS

Under the Faculty of Science

by

R. HARIKUMAR

Research Supervisor

Dr. S. SAMPATH

Atmospheric Sciences Division
Centre for Earth Science Studies
Thiruvananthapuram-31, India

Department of Physics, Cochin University of Science and Technology
Cochin-22, India

MAY 2009

Dedicated to

THE MOTHER EARTH

MY FAMILY

and

MY MASTERS

Cloud is a promise; ***Rain*** *is the fulfillment*

-An old Arabic Saying

DECLARATION

This is to declare that the research work presented in this thesis entitled **"Study on tropical rain with special reference to rain Drop Size Distribution and integral rain parameters using ground-based and satellite measurements"** is a genuine record of research work carried out by me in the Atmospheric Sciences Division, Centre for Earth Science Studies, Thiruvananthapuram, (registration through the Department of Physics, Cochin University of Science and Technology) for the award of the degree of ***Doctor of Philosophy in Physics*** is entirely original and has not been submitted earlier in part or full in any University or Institution for the award of any degree or diploma.

Thiruvananthapuram-31

R. Harikumar

8th May, 2009

Research Scholar
Atmospheric Sciences Division
Centre for Earth Science Studies
Thiruvananthapuram-31

Counter signed (Research Guide)

(Dr. S. Sampath)

CERTIFICATE

This is to certify that the research work presented in this thesis entitled **"Study on tropical rain with special reference to rain Drop Size Distribution and integral rain parameters using ground-based and satellite measurements"** has been carried out by **Mr. R. Harikumar** in the Atmospheric Sciences Division, Centre for Earth Science Studies (registration through the Department of Physics, Cochin University of Science and Technology) independently under my supervision and guidance for the award of the degree ***Doctor of Philosophy in Physics***. I also certify that this is his original contribution and has not been submitted for the award of any degree or diploma in any other University or Institution. Certified that **Mr. R. Harikumar** has passed the Ph. D. qualifying examination conducted by the Cochin University of Science and Technology in February, 2008.

Thiruvananthapuram-31

Dr. S. Sampath

8th May, 2009

Head ASD (Retired)
Atmospheric Sciences Division
Centre for Earth Science Studies
Thiruvananthapuram-31

ACKNOWLEDGEMENT

The research work that is presented in this thesis is an effort of about four years. During my journey through out these years, I got lots of help from a lot of individuals. I am very happy now because I have now the opportunity to express my gratitude for all of them. There is a strong enticement to individually acknowledge everyone who has helped me to reach this point. But, such a list would be too long and it is inevitable that many people would be unintentionally omitted. Therefore, I would thus like to thank everyone who has very kindly provided their support, encouragement and assistance during the progress of the thesis. However, there are others who have played a major role in the origin of this thesis and who deserve a more personal note of gratitude.

First of all, I am very thankful to Dr. S. Sampath, my supervising guide, without his constant all-round guidance and support, this scientific mission could not have been completed successfully.

Dr. V. Sasi Kumar was my constant master, who is always with me irrespective of day or night from the beginning to the end of this effort. I am grateful to him. The all round development through nice scientific discussions that I had with Dr. G. Mohan Kumar and Dr. S. Murali Das is also thankfully acknowledged. Dr. P.V.S.S.K Vinayak extended a lot of helps during this course. Dr. N. Subhash, Head ASD, deserves my great thanks because of his encouraging comments especially during the chances to get exposures in scientific field. Supports from the scientists Dr. E.J. Zacharia, Mr. K.J. Mathew, Dr. Vijaya Kumar, Dr. V. Muraleedharan are also thankfully acknowledged. The support from T.K. Krishnachandran Nair and Mohamed Ismail were worth acknowledging. All the administrative supports from Mrs. Prabhavathi and Bhaskaran, camp office, Kochi are thankfully acknowledged.

I am very grateful to Dr. M. Baba, Director, Centre for Earth Science Studies (CESS) for his all support. The administrative suppot from Mr. P. Sudeep, Registrar, and Mr. A. Gopinath., SO (Admn) CESS is thankfully acknowledged. Motivation from scientists Dr. Padma Lal, Dr. Kurian and Dr. Raveendra Kumar from CESS is thanked. The supports from all the administrative as well as scientific staffs of CESS are thanked.

Supports from Dr. Satheesh Shenoi, The Director, Indian National Centre for Ocean Information Services (INCOIS), Hyderabad: where I have joined to pursue my research career after this scientific mission. All the support and motivation from Dr. Ravi Chandran, Head, MOG and Dr. Francis is hearty thanked. All the support from Dr. Sudheer Joseph, Dr. Rahman, Dr. Bala Krishnan Nair and all the scientific, technical and administrative staffs at INCOIS are thankfully acknowledged.

Supports from Dr. Hamza Varikoden and Ms. Shiny Sara Thomas are thankfully acknowledged. Support fom my colleagues M/s. Vishnu, Rupanand, Jayanthi, Anjali, Anil, Abish, Jeena, Aneesh, Srikanth, Prasanth, George (all from ASD), M/s Shamji, Arjun, Tiju, Praveen, Reji Sreenivas, Ajith G. Nair, Murali, (team MSD) and my other friends at CESS: Eldos, Siju, Rajesh, Nishanth, Srijith, Salaj, Baiju, Aravind, Aneesh, Manjush are thankfully remembered. I am very thankful to my loveable friends: Vijeesh, Toji, Shahin and Kannan who were there at CESS during my initial stages of Ph. D. Security community at CESS extended a lot of help that would be apt to a researcher.

Friends at INCOIS: Gireesh, Vimlesh Pant, Sumisha, Sandhya, Kumar, Sreedhar, Srinivas, Anil, Soumya, Rajesh, Neetu deserve thanks for their motivation to finalyse this thesis.

Supports from Prof. H.S. Ram Mohan as a doctoral committee member; Dr. Mohan Kumar; Head of the Department of Physics; Mrs. Nima: Ph. D. Scholar and all the administrative staffs at Cochin University of Science And Technology are thankfully acknowledged.

Motivation and support from Dr, Sreedharan, Director, Space Physics Laboratory (SPL), VSSC, Dr. K. Rajeev, Dr. Kunhi Krishnan, Dr. K. Parameswaran , Dr. Kiran Kumar, Dr. Manju and all friends at SPL are thankfully remembered.

The work presented in the thesis was carried out as a part of the project funded by the MOP group of Space Applications Centre. I thankfully acknowledge the support both by funding and by scientific inputs from this group, especially the expert advice from Dr. M. S. Narayanan the then Group Director. Scientific discussions with Dr. R.M. Gairola, Space Applications Centre, ISRO, Dr. T. Narayana Rao, NARL, Gadanki, Dr. Sanjay Sharma, Kohima Science College, Dr. Animesh Maitra, Culcatta University helped me a lot for the refinement of my this effort.

The support received from the authorities at SHAR and Tata Tea Estates, Munnar for installation and running of the instruments in their premises is thankfully acknowledged. The authorities of Ministry of Communications, Government of India for the experimental license to operate the Micro Rain Radar and the help received from Mr. Sayeenathan of ISRO Headquarters for his guidance in this are thanked.

Supports from the International scientific community, especially Prof. Martin, da Aeronautica-ITA, sao Jose dos campos, SP, Brazil, Dr. Remy Rocca, LMD, France are thankfully acknowledged.

Thanks are due to NASA/GSFC for providing the TRMM-3B42 data on their ftp site, Wyoming Radiosonde data through their web site. Acknowledgemnt is also due to Ferret program for one of the graphics in this thesis. Ferret is a product of

NOAA's Pacific and Marine Environmental Laboratory (PMEL). More information is available at http://ferret.pmel.noaa.gov/Ferret/.

I am happy to mention here my deep gratitude to Committee on Space Research (COSPAR), ICSU (International Council for Science Unions), who selected me as a COSPAR ASSOCIATE and invite with all the support (including financial support) to present my 4 papers in the 37th COSPAR Scientific Assembly held at Montreal, Canada during July 13 to 21, 2008. I am also very grateful to Council for Scientific and Industrial Research (CSIR), who selected me and assisted me with good financial support for my travel to Canada under its "Foreign Travel Grant Scheme". This above mentioned assembly was very fruitful motivation for me to explore more in science with the help of great exposure to the international scientific community, through my interaction during my presentations there.

I am grateful to Indian Space Research Organisation (ISRO), for financial support extended through its projects considering me as a beneficiary of the same that eventually leads to the completion of my effort with out any difficulties. During the later stage of my work, the sanction of the project proposal submitted by me along with scientists of CESS to ISRO under its Announcement of Opportunity (AO) for the Megha-Tropiques Utilisation projects, gave me motivation to do more in the current field of interest. During that stage, the great encouragement given by Dr. C.B.S. Dutt in the form of 4 lines in his e-mail reply is very seriously and thankfully acknowledged.

I am very grateful to all the organizers who have conducted the scientific symposia/conferences/seminars that are mentioned in the list of publications by the author.

Last but not least, I would like to express my gratitude towards my father M.S. Rajasekharan Nair and mother N.R. Santhamoney Amma both who gave sustained motivation and mental support with their cool dialogues that helped me to overcome all my frustrations that a research scholar would be having during the course of my research and also through out my life, that cause good health and mind in its correct way to complete this great effort. My loveable brother Sreekumar gave me limitless support to all the facets of life, especially during the course of this research work.

R. HARIKUMAR

PREFACE

Tropical rain comprises more than two thirds of the global rain. The evaporation and condensation processes involved in the form of clouds cause this rain is the primary distributor of heat through the circulation of the atmosphere. Characterizing tropical rain and its variability is very useful for understanding the global climate. Satellite-borne rainfall measurements are fast becoming important to get a complete global coverage. The models and the algorithms developed so far for measurements and the retrieval of rain parameters from satellite need to be fine-tuned using measurements from in-situ and remote sensing techniques. The knowledge of rain Drop Size Distribution (DSD) is very essential for calibrating the instruments/sensors, especially the Z-R (radar reflectivity-rain rate) relations, used for radars onboard satellites. This study will have potential application in rain retrieval by using the parameterization techniques and to study the variability of the DSD parameters with respect to different seasons. The study will be useful for the Megha-Tropiques programme. Results from this study find application for those who are investigating radio propagation in India. The understanding about the drop size from which the contribution to the total rainfall is maximum at each location, would give an idea about the impact of rain on soil erosion at different locations. Therefore, the study of rain DSD and integral rain parameters on the tropics and its spatial, vertical and temporal variations are very important. The study presented in the thesis will help in this.

The number of rain drops per unit volume per mm interval of the diameter is called the rain DSD. The rain parameters viz. Rain Rate (R), Radar Reflectivity Factor (Z dB) and Liquid Water Content (LWC) are rain DSD integrals and thus these could be derived from rain DSD. In general understanding of rain DSD finds applications in fields like satellite meteorology, cloud microphysics, soil erosion, micro wave communication etc.

The main focus of this investigation is to study the different aspects of the tropical rain with special reference to rain DSD, rain rate and radar reflectivity factor. Rain DSD and other rain parameters data from 4 stations viz. Thiruvananthapuram

(Lat: 8.29 N, Long: 76.59 E; 4 m amsl), Kochi (9.58 N, 76.17 E; 5 m amsl), Munnar (10.08 N, 77.07 E; 1500 m amsl) and Sriharikota-SHAR (13.58 N, 80.29 E) during various monsoon periods from the year 2001, was measured using a Joss-Waldvogel impact type Disdrometer and the data from these measurements are used for this study. Rain DSD data at different heights has been collected using a Micro Rain Radar (MRR) that was installed during September 2005 at Thiruvananthapuram. The Tropical Rainfall Measuring Mission (TRMM) and other satellite rain rate data (3B42-V6) for the period 2001 to 2008 has also been used in the present study.

The thesis is arranged in eight chapters. At the end of the thesis, the publications referred in the thesis are listed out. The list of publications [published (4 in number) and under review (3 in number)] including presentations/proceedings in symposia/conferences (21 in number) have been listed in the beginning.

Section 1 of the Chapter I gives an introduction to the present study. A brief review of literature on rain DSD, rain rate and Z-R relation studies are presented in the second section of this chapter to bring out the current status of the subject. The objectives of this study in relation to the current knowledge in this field are detailed in this chapter.

Experimental techniques used for the measurements are covered in Chapter II. The details of the hardware and software of the instruments/sensors Disdrometer and Micro Rain Radar (MRR) used for the present study are explained. A brief outline of TRMM satellite sensors is given. The data availability, data analysis and the corrections to be applied for the data retrieval are also discussed in this chapter. The complete details about the stations are given at the end of this chapter.

Chapters III to VII present the analysis and the results from this study.

The rain rate characteristics at all the four stations are explained in detail in the Chapter III. It is seen that the rain rate temporal cumulative distribution could be fitted with a Weibull distribution function. Thiruvananthapuram showed a different behavior compared to other stations. Rain rate below 5mm/h was seen only around 65 % of the time while at other stations it was around 90 % of the time. This indicates about the relative prevalence of cumuliform and stratiform clouds in these stations.

The rain DSD characteristics have been brought out in the first section of Chapter IV. The rain DSD data for all the stations were fitted with Marshall-Palmer distribution, Gamma distribution and log-normal distribution those have been used by different earlier workers to describe the DSD variation. It has been found that the log-normal distribution fits our stations better than the other two distributions. From this log-normal distribution, three physical parameters viz. total number of drops (N_T), Geometric mean diameter (D_g) and Standard geometric deviation (σ) were derived. The behaviour of these physical parameters at these four sites has been compared to evaluate the rain characteristics at these stations. Comparison between coastal sites on the west coast (Kochi and Thiruvananthapuram) and east coast (SHAR) has been done. Behaviour at Munnar (a station on the western ghat at 1500m altitude) has brought the possible effects of orography on the rain DSD.

In the second section of this chapter, an empirical model to represent the DSD variation has been derived to describe the DSD variation with rain rate at all the stations. Using this empirical model, the average DSD variation with rain rate at these stations could be obtained. The empirical model has been verified and the statistical significance of this relation was also evaluated.

As rains occur in spells, the characteristics of spells in terms of DSD variations are studied. These results are discussed in Chapter V.

Chapter VI discusses the measurements done using the Micro Rain Radar. The variations of the DSD with altitude at the station Thiruvananthapuram are explained in this chapter.

The radar reflectivity (Z) and its relation with rain rate (R) play an important role in satellite measurements. Using the DSD data this relation (Z–R) has been derived and its variation with altitude has been studied. This relation is compared with similar results from other parts of the world. These results are also presented and discussed in this Chapter.

TRMM and other satellite derived rain rate data (3B42-V6) is compared with the ground based rain rate measurements using Disdrometer, MRR and rain gauges with reference to the detection of occurrence of rain and the magnitude of rain or rain

rate. The study reveals that the magnitudes show a correlation of about 0.5 while the simultaneous detection is around 0.78. The details of the study are explained in Chapter VII.

Chapter VIII summarises the results and the conclusions derived from the study. The major results pertain to the development and testing of an empirical model to represent the variation of DSD with rain rate in the tropics. The evaluation of the vertical profiles of Z-R relations for our region is another important result of this study. The correlation between satellite measured rainfall and ground based measurements has brought out the need to have a closer look at the satellite retrieval. The behaviour of the intensity of rain fall or rain rate at the four stations and the possible effect of orography on DSD has been also brought out.

LIST OF FIGURES

LIST OF TABLES

CONTENTS

LIST OF PUBLICATIONS OF THE AUTHOR

A. National and International peer reviewed Journals

1. **Harikumar**, **R.,** Sasi Kumar, V., Sampath, S., Vinayak, P.V.S.S.K. Comparison of Drop Size Distribution between stations in Eastern and Western coasts of India. J. Indian Geophys. Union. 11(2), 111-116, 2007.
2. Sasi Kumar, V., Sampath, S., Vinayak, P.V.S.S.K., **Harikumar, R.** Rainfall Intensity Characteristics at Coastal and High Altitude Stations in Kerala. J. Earth System Sci. 116(5), 451-463, 2007.
3. **Harikumar, R.,** Sampath, S., Sasi Kumar, V. An Empirical Model for the Variation of Rain Drop Size Distribution with Rain Rate at a few Locations in Southern India. Adv. Space Res. 43, 837-844, 2008, DOI: 10.1016/j.asr.2008.11.001.
4. *Hamza, V., **Harikumar**, **R.,** Murali Das, S., Sampath, S., Mohan Kumar, G. Properties of cloud base height during southwest monsoon period over a tropical station, Thiruvananthapuram. Current Sci., 96(4), 562-568, 25, 2009.
5. **Harikumar**, **R.,** Sampath**,** S., Sasi Kumar, V. Variation of Rain Drop Size Distribution with Rain Rate at a few Coastal and High altitude Stations in Southern Peninsular India. Atm. Res. 2008 (Under review)
6. **Harikumar**, **R.,** Sampath**,** S., Sasi Kumar, V. Altitudinal and temporal Evolution of Rain Drop Size Distribution observed over a tropical station using a Micro Rain Radar. Adv. Space Res. 2008 (Under Review)
7. *Hamza, V., **Harikumar**, **R.,** Sasi Kumar, V., Sampath, S., Mohan Kumar, G., Murali Das, S. Features of 2007 monsoon onset: studies using satellite and ground based measurements Adv. Space Res. 2008 (Under Review)

B. National and International conference proceedings/presentations

1. **Harikumar**, **R.,** Sampath, S., Mohan Kumar, G., Sasi Kumar, V. Simultaneous Evidence for the origin of rain from Stratiform or Convective Clouds from the Micro Rain Radar Bright Band Signature and the Vertical profiles of Z-R Empirical relation. Proc. International Conference on Megha-Tropiques Science and Applications, Bangalore, India, March-2009.

2. **Harikumar**, **R.,** Sampath, S., Mohan Kumar, G. Spatial Variability of Rain Drop Size Distribution-Study at High Altitude and Coastal Tropical Stations in Peninsular India. Proc. International Conference on Megha-Tropiques Science and Applications, Bangalore, India, March-2009
3. **Harikumar**, **R.,** Sampath, S., Mohan Kumar, G., Sasi Kumar, V., Gairola, R.M. Preliminary Comparison of TRMM precipitation data with Micro Rain Radar, Disdrometer and Manual Rain Gauge data during different monsoon seasons at Coastal and High altitude Stations in Peninsular India. Proc. International Conference on Megha-Tropiques Science and Applications, Bangalore, India, March-2009,
4. **Harikumar**, **R.,** Sampath, S., Mohan Kumar, G. Simultaneous Evidence from the Micro Rain Radar Bright Band Signature and the Vertical profiles of Z-R Empirical relation of the origin of rain from Stratiform or Convective Clouds. Proc. 45th Annual Convention of the Indian Geophysical Union-2008, Varanasi, November-2008.
5. **Harikumar**, **R.,** Sampath, S., Mohan Kumar, G. Evidence of the Orographic Effect on Rain from Rain Drop Size Distribution at Coastal and High Altitude Stations. Proc. 18th Swadeshi Science Congress, Thiruvananthapuram, November-2008 (Selected for 'Young Scientist-Best paper Award').
6. **Harikumar**, **R.,** Hamza. V., Sampath, S., Mohan Kumar, G., Gairola, R.M. Comparison of TRMM precipitation data with Micro Rain Radar and Disdrometer data during different Monsoon seasons. Proc. 37th COSPAR Scientific Assembly, Montreal, Canada, July-2008.
7. **Harikumar R.,** Sampath, S. Altitudinal and temporal Evolution of Rain Drop Size Distribution observed over a tropical station using a Micro Rain Radar. Proc. 37th COSPAR Scientific Assembly, Montreal, Canada, July-2008.
8. **Harikumar R.,** Sampath, S. An Empirical Model for the variation of Rain Drop Size Distribution with Rain Rate at a few locations in Southern India. Proc. 37th COSPAR Scientific Assembly, Montreal, Canada, July-2008.

9. *Hamza V.**, Harikumar**, **R.,** Murali das, S., Sampath, S., Mohan Kumar, G. Study of Asian Summer Monsoon Onset phase using Satellite and Ground based measurements. Proc. 37th COSPAR Scientific Assembly, Montreal, Canada, July-2008.
10. **Harikumar, R.,** Sampath, S., Sasi Kumar, V. An Empirical relation for the variation of rain Drop Size Distribution with rain rate at a few locations in southern India. Proc. National Space Science Symposium (NSSS-2008), Ooty, February-2008.
11. **Harikumar, R.,** Sampath, S., Sasi Kumar, V. Investigation on the variation of rain Drop Size Distribution with rainfall intensity at tropical stations in peninsular India. Proc. TROPMET 2007, Bhopal, December-2007.
12. *Hamza V, **Harikumar**, **R.,** Sasi Kumar, V., Sampath, S., Mohan Kumar, G., Murali Das, S. Features of 2007 monsoon onset: studies using satellite and ground based measurements. Proc. 44th Annual Convention of the Indian Geophysical Union-2007, Haryana, November-2007.
13. **Harikumar**, **R.,** Hamza, V., Sampath, S., Sasi Kumar, V., Gairola, R.M. Comparison of TRMM precipitation data with Micro Rain Radar and Disdrometer data over a tropical station- Thiruvananthapuram. Proc. 44th Annual Convention of the Indian Geophysical Union-2007, Haryana, November-2007,
14. Sampath, S., Sasikumar, V., **Harikumar, R.** An Empirical Model for raindrop size distribution in the tropical Indian region. Proc. IUGG XXIV General Assembly-2007, Perugia, Italy, July-2007.
15. **Harikumar, R.,** Sasi Kumar, V., Sampath S. Spatial and temporal evolution of rain drop size distribution. Proc. METOC-2007, Kochi, May-2007.
16. **Harikumar**, **R.,** Sampath, S., Sasi Kumar, V. An extensive study on Rain DSD over tropical stations in Peninsular India using a J-W Disdrometer. Proc. Geophysical Research Abstracts, Vol. 9, 00790, 2007, SRef-ID: 1607-7962/gra/EGU2007-A-00790, European Geosciences Union Assembly-2007, Vienna, Austria, April-2007.

17. **Harikumar**, **R.,** Sasi Kumar, V., Sampath, S. Rainfall Intensity and DSD at sea level and at 1500 m altitude in southern India- studies using TRMM and Disrometer data. Proc. 36th Committee on Space Research (COSPAR), Beijing, China. (Reference: 'TC2-0020 COSPAR2006-A-01027; A1. 1-0125-06'), July-2006.
18. **Harikumar**, **R.,** Sasi Kumar, V., Vinayak, P.V.S.S.K., Sampath, S. Rain Drop Size Distribution studies using a Disdrometer and a Micro rain radar. Proc. National Space Science Symposium (NSSS-2006), Visakhapatnam, February-2006.
19. **Harikumar**, **R.,** Sasi Kumar, V., Sampath, S., Vinayak, P.V.S.S.K. Rain Drop Size at different heights. Proc. 18th Kerala Science Congress-2006, Thiruvananthapuram, January-2006.
20. **Harikumar**, **R.,** Sasi Kumar, V., Sampath, S., Vinayak, P.V.S.S.K. Comparison of Drop Size Distribution between stations in Eastern and Western coasts of India. Proc. 42nd Annual Convention of the Indian Geophysical Union-2005, Bhopal, December-2005.
21. **Harikumar**, **R.,** Sasi Kumar, V., Sampath, S., Vinayak, P.V.S.S.K. A Study on Rain Drop Size Distribution. Proc. 14th Swadeshi Science Congress-2004, Thekkady, November-2004.

C. Scientific Report

1. *Mohan kumar, G., Jeena, V.S., **Harikumar, R.,** Sampath, S. Ambient carbon monoxide measurements in the ISRO-GBP land campaign at Jaduguda by Centre for Earth Science Studies, Scientific Report submitted to ISRO, January 2005.

* Work not directly connected with the thesis.

CHAPTER I

INTRODUCTION

CHAPTER-I

INTRODUCTION

1.1. GENERAL INTRODUCTION

Two third of the globe is covered with water. Water is very essential for the existence of life. In the tropics, rainfall is the major source of fresh water. Excess of rainfall causes flood (figure 1.1) and deficiency causes drought (figure 1.2). Both cause a lot of suffering and strain the resources. Therefore, rainfall measurement has been considered as one of the important parts of meteorological studies.

Rainfall measurements are being carried out almost from 1900 in a regular way at many parts of our country by the India Meteorological Department (IMD). Manual Rain Gauges were used to start with and later Self Recording Rain Gauges, Rapid Response Rain Gauges and Digital Recording Rain Gauges have become part of such measurements. Measurements are also carried out by other atmospheric science/meteorological groups for their respective studies. In order to understand the global precipitation, it becomes necessary to have satellite measurements (figure 1.3). To validate the satellite data, other type of measurements apart from rainfall are needed. Therefore, Disdrometers and Ground-based Rain Radars are being used to validate the satellite data.

By using Disdrometers and Rain Radars, the characteristics of rain can be studied, apart from being those used as ground truths. In this thesis, analysis of rainfall from the point of Drop Size Distribution (DSD) has been done. A Disdrometer and a Micro Rain Radar (MRR) have been used for the study. Therefore in this chapter earlier studies pertaining to DSD are discussed to form the back ground. Based on this the need for the present study is brought out in the following sections.

The Earth system comprises of three closely coupled components, viz. the atmosphere, oceans and biosphere. Water is the unifying element of this system. It is the active component of the atmosphere, covers three-quarters of the Earth's surface, and is the basis for all life on our planet. Water is essential to our continued

Figure 1.1. Sever after effects of continuous heavy rainfall: Flooding. Courtesy: Kidd and Muller, School of Geography, University of Birmingham.

Figure 1.2. Severe after effect of lack of rainfall: Drought. Drought in Andhrapradesh, India (top left panel); in Georgea in 2007 (top right panel); at Barcelona in 2008 (bottom left panel) and in Australia in 2003 (bottom right panel). Courtesy: Internet.

existence. Because of the unifying role of the global water cycle, studies of rainfall are essential for a deeper understanding of the Earth as a system. Variability in the global distribution of precipitation is recognized as a key element in assessing the impact of climate change for life on earth. The response of precipitation to climate forcing is, however, poorly understood because of discrepancies in the magnitude and sign of climatic trends in satellite-based rainfall estimates. Quantifying and ultimately removing these biases is critical for studying the response of the hydrologic cycle to climate change (Ecuyer et al., 2004).

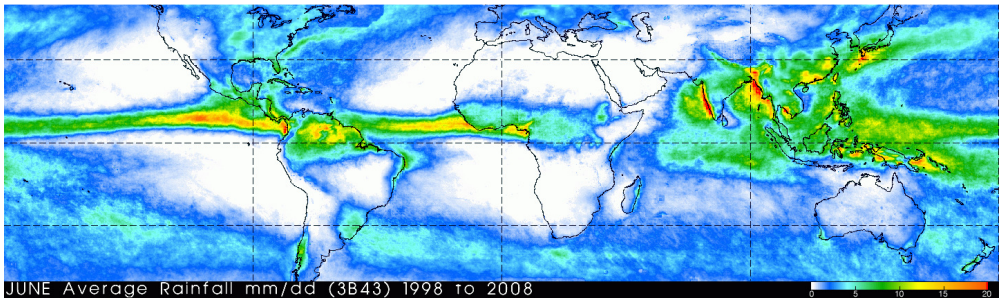

Figure 1.3. Rainfall Climatology (averaged data for 1998 to 2008) for June from 3B43 merged Tropical Rainfall Measuring mission (TRMM), a collaborative satellite mission of NASA (National Aeronautics and Space Administration), USA and JAXA (Japanese Aerospace Exploration Agency), Japan and other sources estimates data (Courtesy: www.trmm.gsfc.nasa.gov)

Rainfall is also the major source of energy that drives the circulation of the atmosphere. As water changes from liquid to vapour and back to liquid, heat is stored and then released. This latent heat can intensify some weather systems, making tropical rainfall an important determinant of atmospheric circulation and short-term climate changes. Along with temperature, rainfall is perhaps the most important factor in defining climate. All these factors emphasise the need to understand more about the global water cycle (Figure 1.4) with special reference to characteristics of the tropical form of precipitation -"rain" in detail.

Evaporation and transpiration processes return a part of the rainfall to the atmosphere. The environment recycles a large portion of this returned water. During a rainstorm, clouds transport atmospheric trace constituents into the free atmosphere while cleaner air flows down to the surface. This exchange reveals a

direct link between tropical rainfall and the global cycles of carbon, nitrogen and sulphur, which are important in biological processes.

Tropical rainfall comprises more than two thirds of global rainfall. It is the primary distributor of heat through the circulation of the atmosphere. Understanding rainfall and its variability is crucial to understanding and predicting global climate change. In-situ measurements of the rainfall parameters are few and have so many limitations, especially in the tropics. The main reason for this is that about $3/4^{th}$ of the tropical region is covered by not merely forests, but rain forests. Because of that, the deployment of instruments and data collection is virtually impossible at these sites. Satellite-borne rainfall measurements are fast becoming important to get a complete global coverage. The models and the algorithms developed so far for measurements and the retrieval of rain parameters from satellite need to be fine-tuned using measurements from in-situ and remote sensing techniques. Therefore, study of rainfall and its variability is important.

Measurement of rainfall is being made for a long time using the conventional manual rain gauges. These rain gauges give the daily rainfall at the site of installation. To get the rainfall distribution during the course of a day, self-recording rain gauges (SRRG) were installed and rainfall during every hour could be obtained at select sites. As rainfall has impact on radio communication, rainfall measurements were automated with closer interval data being made available. To get the rainfall over larger areas, rain radars or precipitation radars (PR) were installed. These give rainfall over a large area compared to the rain gauges with good temporal resolution. Intensity rain gauges also called fast response rain gauges were developed to make measurements with a higher time resolution.

With rainfall measurements making their importance felt, rain drop size distribution (DSD) has become another important parameter. For calibrating the radar and also for understanding the attenuation and other effects of rainfall on communication (a need for GSAT–4), knowledge of DSD has become essential. With satellite measurements of rainfall becoming a reality, measurements of rain rate and DSD at the surface to serve as ground truth for satellite data have gained importance (Doviak and Zrnic, 1993; Vivekanandan et al., 1999). The Tropical

Rainfall Measuring Mission (TRMM) has shown the importance of such measurements. With the proposed *Megha-Tropiques* satellite and the Global Precipitation Mission (GPM) on the cards, it is essential that tropical rainfall characterisation in terms of rain rate and DSD is taken up. This thesis is directed also towards this objective.

Rain rate estimation from radar measurements is based on empirical models such as the Z-R relation, $R(Z,Z_{DR})$ and $R(K_{DP})$ – where Z_{DR} is the differential reflectivity and K_{DP} is the specific differential phase shift measured by a polarimetric radar (Bringi and Chandrasekar, 2001; Ulbrich, 1983). Accurate rain rate estimation requires detailed knowledge of rain DSD (Doviak and Zrnic, 1993; Tokay and Short, 1996). In the past, rain DSD was commonly assumed to be exponential. Some observations, however, indicate that natural rain DSD contains fewer of both very large and very small drops than exponential distribution (Tokay and Short, 1996; Ulbrich, 1983). Thus there exists a need to estimate the rain DSD (particularly for monsoonal and non-monsoonal rainfall) to deduce the rain rate from satellite data.

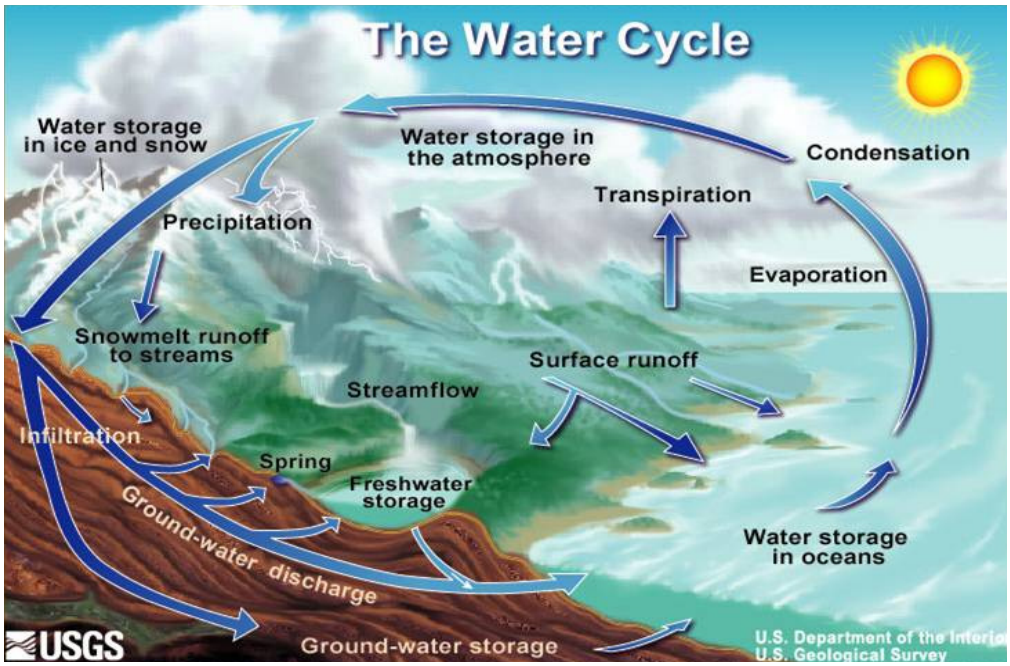

Figure 1.4. The Hydrological Cycle.

The Intergovernmental Panel for Climate Change (IPCC), in its third report (Houghton et al., 2001), made it clear that the study of clouds, especially the kind

and number of condensation nuclei, liquid water content and drop size distribution, is a very important aspect of climate and climate change studies today. Clouds do largely influence weather and climate but the knowledge with respect to 'how and why' is still lacking. Since rain is the end product of the hydrological cycle and it originates from clouds, deep understanding about the rain microphysics is mandatory to understand the physics and dynamics of the clouds. In tropics, this problem is crucial because the tropics is the region which receives the maximum energy from the sun, and thus plays a vital role in the energetics of the atmosphere and also studies have traditionally been relatively less in this region. Clouds also strongly influence heat transfer in the atmosphere through the transport of moisture and hence the latent heat and through influencing the albedo. This heat then influences the atmospheric circulation. Clouds thus play a vital role in determining the consequences of global warming. Thus the study of clouds and precipitation is important from the point of view of climate and climate change.

India depends on the monsoon for much of its water needs. Water scarcity and droughts are becoming threatening problems. Under such conditions, people are increasingly looking towards technologies like artificial rain making to mitigate their problems. Some of the states in our country have tried this a few times and efforts to make it perfectly fruitful are being carried-out by many organisations like the Indian Institute of Tropical Meteoroloty (IITM) in India. However, it may not be long before such trials increase for whatever they are worth. Understanding the structure and properties of the clouds and rain as well is becoming a necessity from this point of view.

Indian peninsula is a unique land mass with varying orography that experiences seasonal reversing monsoon resulting in intense air-sea interactions on several spatio-temporal scales. So, the rain study over those stations in this peninsula has good impact with special reference to climate change.

1.1.1. Precipitation

When cloud particles become too heavy to remain suspended in the air, they fall to the earth as precipitation. Precipitation occurs in a variety of forms – hail, rain, freezing rain, sleet or snow.

When clouds develop, something is making the air rise. When air rises it expands and gets colder and since colder air cannot hold as much moisture as warm air, the water condenses to form clouds and sometimes rain or ice or snow.

Forms of Precipitation

There are different forms of precipitation. In this section we discuss only those which are commonly observed. The kind of precipitation received depends on the variation of temperature above the surface. Rain is precipitation in liquid form. Snow is precipitation in solid form as (typically) a hexagonal crystal shape. Size and shape of the crystal are dependent on moisture content and temperature of the air. In the middle and high latitudes rain begins as snow. If the air temperature near the surface is above zero, the snow will melt into rain and fall in liquid form. If the air temperatures are below freezing on its journey toward the surface, precipitation will be in the form of snow. Sleet is caused by rain falling into a cold layer of air aloft which has to be below freezing. As the raindrops fall through the cold layer of air, they freeze and become small ice pellets. Freezing rain is basically rain that falls onto the ground and then freezes after it hits the ground. It causes a glaze of ice on any surface that is below freezing. A temperature inversion causes the conditions that result in freezing rain. This means that it is warmer aloft than it is at the surface.

1.1.2. Rain

The term rain refers to precipitation in liquid state. It consists of drops of water falling from clouds; if the drops are very small, they are collectively termed as drizzle. Rain plays a key role in the hydrologic or watercycle in which moisture from the oceans evaporates, condenses into clouds, precipitates back to earth, and eventually returns to the ocean via runoff into streams and rivers to begin the cycle again.

Clouds contain huge numbers of tiny droplets of moisture. Raindrops are formed when these tiny droplets grow, first by moisture from the surrounding air condensing on them and then by coalescing with other droplets during their descent. The size of raindrops can vary considerably from diameters of .1 mm to 5 mm. They vary in size from about 0.5 mm to as much as 8 mm in thunderstorms.

There is a natural limit for the size of raindrops; large drops falling through air break up into smaller drops when they attain a velocity of about 30 km/hr. Raindrops are often large enough to have a size dependent shape that cannot be characterized by a single length, so there is some difficulty to describe the size spectra of rain drops. The conventional solution is to describe rain spectra in terms of the equivalent diameter D_0 defined as the diameter of a sphere of the same volume as the deformed drop. When falling at terminal velocity, drops are nearly perfect spheres if $D_0 < 280$ μm. Larger drops are slightly deformed and resemble oblate spheroids if $280 < D_0 < 1000$ μm. For $D_0 > 1000$ μm, the deformation becomes larger and drops resemble oblate spheroids with flat bases. Drops larger than about 10 mm in diameter are hydrodynamically unstable and break up during fall.

In addition to equivalent diameter D_0, there are three other quantities commonly used to characterize rain. (1) the size distribution $n(D_0)$ expressed here in terms of the number of drops per unit size interval per cubic metre of air, (2) liquid water content (w_L) and (3) the Rain rate (R)

Raindrop spectra may extend to drop diameters as large as 6 mm. Such drops are rather rare since they are found in very heavy rain with $R > 100$ mm/hr. At smaller rainfall intensities raindrop spectra usually extend only to drop diameters of 2 to 3mm. Larger drops tend to break up as a result of collision with other drops.

Several factors affect the spectral shape of rain at the small size end. Since rain must fall through the cloud draft, the strength of the latter tends by itself to truncate the spectrum at minimum size. This effect is largely masked by further modification of rain after it leaves the cloud. In particular, small drops continue to be produced by break up and evaporation. Also, at the beginning of a shower, the drop spectrum at the ground may be expected to be biased towards larger size owing to the greater fall speed of larger drops, and possibly small size owing to an initially high evaporation rate. Observations show that most precipitating drops which reach the ground have $D_0 > 200$ μm.

Formation of rain

Cloud droplets are tiny, averaging less than 20 micrometers in diameter. Because of their small size, the rate at which cloud droplets fall is extremely slow. Even falling through humid air, a cloud droplet would evaporate before it fell a few meters below the cloud base. Clouds consist of many millions of these droplets, all competing for the available water; thus, their continued growth via condensation is slow. In order to form precipitation, these cloud droplets must somehow coalesce to form large drops to sustain themselves during descend. It is not easy for a cloud droplet to continue to grow into a raindrop. Several conditions must exist within the cloud in order for the droplet to grow large enough to fall to the ground as precipitation. There are two major mechanisms that explain how cloud droplets become large enough to fall to the ground without evaporating. They are

1) The Bergeron or "Ice Crystal" Process and
2) Collision and Coalescence

Bergeron Process

The Bergeron Process, named after its discoverer, Tor Bergeron, involves supercooled water droplets. For Bergeron process to occur, the cloud should comprise of both supercooled water and ice crystals. This process explains how ice crystals grow at the expense of liquid cloud droplets within a mixed cloud. There are more water molecules surrounding the water droplets than the surrounding ice crystals. This occurs because the saturation vapour pressure over a water surface is greater than that over an ice surface at the same (subfreezing) temperature. The supercooled liquid droplets are more readily able to evaporate and contribute to the vapor pressure in the surrounding air than the ice crystals are able to sublimate and contribute to the vapor pressure. Therefore, when ice and liquid coexist within a cloud, water vapor must evaporate from the drop and flow toward the ice crystal in order to maintain equilibrium. As this water vapor diffuses toward the ice crystal, the droplet must evaporate more in order to keep the vapor pressure in equilibrium with its surroundings. Therefore, what happens is a vicious cycle of water vapor evaporating from the drop, collecting on the ice crystal, and freezing so that the crystal continuously grows at the water droplet's expense.

The Collision - Coalescence Theory

The process of formation of bigger liquid drops through collision of small liquid drops is known as coalescence. All collisions can't lead to coalescence but lead to break up also. The collision–coalescence process is the major source for the formations of raindrops in the warm rain. The coalescence efficiency increases when the drops are electrically charged or an electric field is present in the surroundings.

1.1.3. Coalescence and Break up

Coalescence is the process by which two or more droplets or particles merge during contact to form a single daughter droplet (or bubble). It can take place in many processes, ranging from meteorology to astrophysics. For example, it is both involved in the formation of raindrops as well as planetary and star formation.

The dynamics of bubble coalescence plays an important role in many engineering processes. For example, in mixing, bubbles or drops can generate large changes in interfacial areas through the action of vorticity via stretching, tearing and folding which facilitates the mixing processes. A good understanding of the fundamental mechanism of multiple bubble coalescence can be crucial in maintaining the dispersion process.

Discontinuous fluid properties in a flow system can produce a complex flow structure with rich physical length scales, which presents both computational and experimental challenges. Numerically, a robust algorithm for solving multi-phase flows with an accurate representation of interfaces is required to accommodate the complex topological changes in bubble coalescence.

It is found that the interaction between the leading and following bubbles depends mainly on the liquid viscosity. The higher the liquid viscosity, the easier the bubbles interact. Therefore, bubble coalescence is more likely for high viscosity. On the other hand, for low viscosity, the liquid jet behind the leading bubble becomes stronger which prevents the bubble interaction. A postponed or non-coalescence is obtained. It confirms that the leading bubble travels with a constant velocity until it merges with the following bubble but the following bubble slightly accelerates due to the wake of the leading bubble. Regarding the surface

tension effect, high surface tension results in a weak liquid jet, and high surface tension force prevents the surface from stretching. Therefore a late coalescence occurs.

Experiments supported that in quiet air,drops may be as large as 4.5mm in equilent radius before breaking up. The mechanism of breakup of such drops is closely tied to the development of the previously mentioned concave depression almost explosively deepens and develops rapidly into an expanding bag supported by an annular ring which contains the bulk of the water. As this bag like drop bursts the bag portion bursts into a large no of drops,while the annular ring breaks into a smaller no of larger drops.

Small raindrops (radius < 1 mm) are spherical; larger ones assume a shape more like that of a hamburger bun. When they get larger than a radius of about 4.5 mm they rapidly become distorted into a shape rather like a parachute with a tube of water around the base – and then they break up into smaller drops.

This remarkable evolution results from a tug-of-war between two forces: the surface tension of the water and the pressure of the air pushing up against the bottom of the drop as it falls. When the drop is small, surface tension wins and pulls the drop into a spherical shape. With increasing size, the fall velocity increases and the pressure on the bottom increases causing the raindrop to flatten and even develop a depression. Finally, when the radius exceeds about 4 mm or so, the depression grows almost explosively to form a bag with an annular ring of water and then it breaks up into smaller drops.

Raindrop sizes

In order to have rain we must have a cloud – a cloud is made up of water in the air (water vapor.) Along with this water are tiny particles called condensation nuclei – for instance, the little pieces of salt leftover after sea water evaporates, or a particle of dust or smoke. Condensation occurs when the water vapor wraps itself around the tiny particles. Each particle (surrounded by water) becomes a tiny droplet between 0.0001 and 0.005 centimetre in diameter. (The particles range in size, therefore, the droplets range in size.) However, we can call the growing droplet a raindrop as soon as it reaches the size of 0.5 mm in diameter or bigger. If

it gets any larger than 4 millimeters, however, it will usually split into two separate drops.

In meteorology, its role is crucial in the formation of rain. As droplets are carried by the updrafts and downdrafts in a cloud, they collide and coalesce to form larger droplets. When the droplets become too large to be sustained on the air currents, they begin to fall as rain. Adding to this process, the cloud may be seeded with ice from higher altitudes either by the cloud tops reaching 40 degrees Celsius or the cloud being seeded by ice from cirrus clouds. The smaller drops are the ones that didn't run into as many droplets. Raindrops are different sizes for two primary reasons, (1) initial differences in particle (condensation nuclei) size and (2) different rates of coalescence.

1.1.4. Monsoon

A monsoon is a periodic wind, especially in the Indian Ocean and southern Asia. The word is also used to label the season in which this wind blows southwest in India and adjacent areas that is characterized by very heavy rainfall, and specifically the rainfall that is associated with this wind. The southwest monsoon onset on the Kerala coast of India usually begins within two weeks of June 1st. The north-east monsoon in Tamilnadu begins typically in October. All the stations in the present study is in tropical peninsular India which experiences an intense precipitation during the Indian summer monsoon (Xie et al., 2006)

Monsoons are caused by the fact that land heats up and cools down quicker than water. Thus, in summer, land reaches a higher temperature than the ocean. Air thus rises over the land. This causes an area of low pressure. Since wind blows from areas of high pressure to areas of low pressure, an extremely constant wind blows from the ocean. The rainfall is caused by the moist air rising up mountains and cooling.

In winter, since the land cooles down quickly, the ocean is warmer. Air then rises, causing a low over the ocean. The wind then blows back out over the ocean. Since the temperature difference between the ocean and land is less than in summer, this wind is not a constant. Monsoons are therefore similar to sea breezes,

but they are much larger in scale, stronger, affect a wider area, and are more constant.

The word monsoon owes its origin to the Arabic word "mawsim" meaning "season" to describe a system of alternating winds over the Arabian sea. These winds appear to blow from the northeast for about six months and from the southwest for another six months. The monsoon is a seasonal wind, which blows with consistency and regularity during a part of a year, and which is absent or blows from another direction for the rest of the year. Such seasonal changes of the wind are primarily the result of differences in the quantity of heat received from the sun by different parts of earth. There is a striking difference in the response of the continents and the ocean to seasonal changes in solar energy. Most of the solar energy received by the land is used up in heating the air rather than the earth's surface. On the other hand solar energy is able to penetrate to much greater depths in the oceans because of the stirring which goes on under the action of the wind and also because light can penetrate below the surface. The overall result is that the rise in temperature in summer is much less over the ocean than over the continents. In winter the situation is reversed.

Generally, monsoon is a system of winds which possesses the following characteristic features: (1) Marked seasonal wind shifts, caused by the differential heating of land and sea, that is, by the different response of land and ocean to incoming radiation from the sun and (2) Highly confined to the tropics, by which we mean the region between 20^0 N and 20^0 S on both sides of the equator.

Summer monsoons over the northern hemisphere may be thought of as the south east trades or the trade winds of the southern hemisphere which, on crossing the equator, are deflected to the right by the earth's rotation and, as a consequence, approach land areas from the south westerly direction.

Southwest (Summer) Monsoon

The South-western summer monsoons occur from June to September, after the winds shift during the months of March to May. An area of intense low pressure develops over central Asia, and the jet stream blows over this area.

The south-eastern winds blow towards the area of low pressure over Asia, passing over south-east Asia, which experiences large amounts of rainfall in this period. Meanwhile, the south-west monsoon is drawn towards the Himalayas, creating winds blowing rain clouds towards India, which receive up to 10,000 mm of rain in some areas.

Northeast (Winter) Monsoon

The north-eastern winter monsoons take place from October to December. The temperature over central Asia is lower, creating a zone of high pressure there. Meanwhile, a low pressure system develops over northern Australia and winds are directed towards Australia. During the NE winter monsoon, Australia and south-east Asia receive large amounts of rainfall.

1.2. BACK GROUND

1.2.1. Rain Drop Size Distribution (DSD)

Variability in the global distribution of precipitation is recognized as a key element in assessing the impact of climate change for life on earth. The response of precipitation to climate forcing is, however, poorly understood because of discrepancies in the magnitude and sign of climatic trends in satellite-based rainfall estimates. Quantifying and ultimately removing these biases is critical for studying the response of the hydrologic cycle to climate change (Ecuyer et al., 2004).

The Tropical Rainfall Measuring experience has confirmed that one of the main difficulties surrounding the retrieval of rain profiles from space-borne radar reflectivity measurements is the unknown Drop Size Distribution. (Haddad and Li, 2003). Their natural conclusion is that in spite of the dual-frequency radar that GPM will carry, the careful a-priori modeling of the DSD, at scales commensurate with the GPM radars' resolution, will be crucial to the success of the GPM core retrieval algorithm. And they offered a new, robust method to quantify the characteristics of the DSD at these scales using dual-frequency wind profiler data.

All the rain parameters are integral parameters of rain DSD. So the understanding about DSD is very crucial. The transformation of remote sensing measurements of clouds and precipitation into quantities of interest requires the knowledge of DSD (Lee et al., 2006). Study of rain drop size distribution (DSD) is

very useful in different areas like microwave communication, satellite meteorology, soil erosion and cloud physics. There is big interest in these areas for several reasons, including climatic change and increasing soil erosion due to expanding human activities. Accurate measurements of drop size distributions are important for many meteorological applications, including estimation of rainfall, cloud radiative transfer studies, and cloud model initialization and verification. For example, McGaughey et al. (1996), Viltard et al. (1998) and McKague et al. (1998) all demonstrated the large sensitivity of passive microwave algorithms to the prescribed drop size distribution of the precipitation originated from both convective and stratiform clouds. By tracking the rain DSD along their falling path is a direct way of even measuring rain evaporation (Li and Srivastava, 2001)

To overcome the time height ambiguity in radar measured reflectivity and surface rain rate, knowledge of hydrometeor size distribution within the precipitation layer is essential. The rain DSD is a critical factor in estimating rain rate using advanced dual-polarized weather radars (Vulpiani et al., 2006). A new neural-network algorithm to estimate the DSD from S-band dual-polarised radar measurement is presented in their paper. The corresponding rain rates are then computed assuming a commonly used raindrop diameter-speed relationship. Satellite measured rain parameters would be reliable and dependable if and only if the retrieval from the satellite primary data using the algorithm is accurate. Unfortunately, errors due to the seasonal dependence, back ground dependence etc. is very clear from the retrievals carried out so far. Retrieval of the precipitation parameters from the active satellite measurements is found to be less accurate. The errors associated with the retrieval of rain rate from radar reflectivity factor can be eliminated, by knowing the target, which is the rain drop size distribution, from which the scattering of the electro magnetic radiation takes place. The same reflectivity may be obtained from different targets having different drop size distributions. Hence, there is a need to know the rain DSD in detail. The spatial, altitudinal and temporal variability of the Z-R relation is evident from the past measurements. Since the radar reflectivity factor is the 6^{th} moment of rain DSD, the radar back scattered power is not only merely dependant on the rain rate, but also it

depends purely on the number and size distribution of the rain drops. So the radar reflectivity factor should necessarily be derived from the rain DSD, for the derivation of an empirical relation for the altitudinal and spatial variation of Z-R equation and here lies the importance of the need of more rain DSD data and analyses. Since there is no one to one relation between this Z and R, a wide range of Z-R relations are mentioned in the literature (Battan, 1973). A common technique for radar estimation of rainfall is to develop relationships between the backscattered energy return to the radar (i.e., reflectivity, *Z*) and rainfall rate (*R*). Both *Z* and *R* are dependent on the drop size distribution. The *Z–R* technique has the advantage of producing rainfall estimates over large areas (50 000 km^2) in relatively short time (several minutes). Unfortunately, the existence of various range-dependent errors can produce significant biases in the scanning radar estimate of rainfall (e.g., Wilson and Brandes 1979; Zawadzki 1984; Austin 1987). Moreover, many previous observational studies have shown that natural variations of the drop size distribution in time and space can lead to different *Z–R* parameterizations, ultimately producing different estimates of rain rates (e.g., Battan 1973; Ulbrich 1983; Austin 1987; Huggel et al. 1996). Different Z-R relations should be used for each rain rate range, for better rain DSD derivation (Mali et al., 2003).

In the context of microwave communication, the performance of the microwave links at frequencies above 10 GHz is constrained by the excess attenuation due to precipitation, especially, rainfall. The lower atmosphere is absorptive, dispersive and inhomogeneous and therefore plays an important role in radio communication in the frequency range UHF to mm waves. The important parameters affecting the propagating wave are the shape of each rain drop and rain DSD. Rain attenuation increases with rain drop size and attains a maximum value at a particular drop size. Beyond this value of drop size, rain attenuation either remains constant or decreases (Verma and Jha, 1996b). Since the wavelengths of mm waves are of the same order as the rain drop sizes, the rate of attenuation is highly dependant on rain DSD (Verma and Jha, 1996a). In tropical climates, rain attenuation is severe due to higher rain rates (Jassel et al., 1994). “Sufficient data on

propagation attenuation, rain rate and DSD are not available for tropical region and, in particular, for India where rainy season is characterised by the heavy monsoon rains. Due to the lack of rain DSD data in the tropics, the usage of available DSD data that are collected from the low rain rate regime like temperate regions, causes the attenuation prediction models are found to be very inadequate for tropics" they continued. These authors have developed a rain attenuation model based on the DSD data and compared with CCIR (International Radio Consultative Committee) and other models. The usage of regional DSD data with its lognormal fit is very clear from their studies (and also Verma and Jha, 1996b) and the specific attenuation calculated using DSD with lognormal representation was more realistic compared to DSD with MP and gamma representations. So, these DSD measurements, its lognormal modelling and deep quantitative understanding have much relevance in the special scenario of attenuation of electromagnetic radiation with rain, especially with tropical heavy rainfall. Rain attenuation can be obtained directly through experiments or predicted from a knowledge of rain rate and DSD (Medhurst, 1965; Maciel and Assis, 1990; Ajai and Olsen, 1985); i.e., a model for the variation of DSD with rain rate is very essential. The difference in the experimental and theoretical attenuation results are due to the non-uniformity of DSD, which varies with the geographical locations (Medhurst, R.G., 1965). So, it will be helpful to understand more about the rain DSD for tropical climates, for improving the efficiency of communication. Selection of frequency bands can be made on the basis of the DSD model derived for each location.

A number of recent studies have examined the applicability of separate *Z–R* relations for rain originated from convective and stratiform clouds. Short et al. (1990) and Tokay and Short (1996) have shown, using disdrometer data from Darwin, Australia, and the tropical western Pacific, that the DSD undergoes abrupt shifts between convective and stratiform precipitation and that rainfall rates derived are improved when two *Z–R* relations are used instead of one. However, Steiner and Houze (1997) showed that the use of two *Z–R* relations instead of one did not significantly improve monthly rain totals using radar data at Darwin, Australia. Also, Yuter and Houze (1997) have argued that convective and stratiform DSDs in

the tropical western Pacific are not statistically distinct. Clearly, more research on the variability of the DSD in different precipitation regimes is required. The profiler retrievals for the MCS were partitioned into a three-tier classification scheme (i.e., convective, mixed convective–stratiform and stratiform) following a modified version of Williams et al. (1995) in order to isolate the microphysical characteristics in different precipitation types.

Kenji et al. (1999) has made measurements of rain DSD and kinetic energy of the rainfall at T-sukuba for 2 years and Ishigaki for 1 year, and compared the energy-rain rate equations. Their main finding on regional characteristics of Ishigaki was that, there were large sized raindrops below 30 mm/h rain rate and the distribution of raindrop size was from 1 mm to 5 mm in diameter. But in Tsukuba the distribution of raindrop size concentrated between 1 mm to 2 mm. The impact of rain on soil that causes soil erosion at these different locations will be different because of the difference in DSD. So, the understanding about rain DSD will help us to take precautions in determining the agriculture field structure.

The gamma parameters have been derived on the ground with the disdrometer and aloft with VHF and UHF radar measurements made at Gadanki in the southwest monsoon season by Narayana Rao et al. (2006). This is to study the μ-λ (shape parameter-slope parameter) relation (parameter derived from the gamma fit to the rain DSD) with respect to this climatic regime and also as a function of height. This relation is different at Gadanki compared to other places like Florida and Oklahoma and also this relation is found to be varying with height. An experimental study of small scale variability of DSD has been carried out at Wallops Island, Virginia by Tokey and P.G. Bashor (2007). They also recognised the sampling issues of the disdrometer and thus itself presented the findings for 1-, 3-, 6-, 10- and 15-minute averaged disdrometric measurements. Using the disdrometer measurements at different climatic regions, constraints on the gamma distribution has been developed to retrieve DSD from the dual-frequency radars by Munchak and Tokey (2008). DSD data obtained from Disdrometer could be used for the simulation of algorithms to derive back the DSD (Tokey and Dickens, 2000).

The natural conclusion by Haddad et al. (2003) is that, in spite of the dual-frequency radar that GPM will carry, the careful a-priori modeling of the DSD, at scales commensurate with the GPM radars' resolution, will be crucial to the success of the GPM core retrieval algorithm. This enforces the fact that DSD should be modeled for its variation with rain rate very region specific.

According to Weischet (1969), the tropical area characteristically has a rainfall maximum between 1000 metres and 1500 metres. Still, there is possibility of many local or regional complications to occur (Barry, 1981). The rainfall characteristics over mountains are determined by several factors such as latitude, altitude and orography. A convective pattern of vertical precipitation distribution is widely found in the tropics. According to Rao (1958), the monsoon currents become convectively unstable when it is lifted by the mountains during travel along a short distance. The amounts of orographic precipitation depends on the air mass characteristics and synoptic-scale pressure pattern, local vertical motion due to the terrain, microphysical processes in the cloud and the evaporation of the falling rain drops (Sawyer, 1956).

Orographic effect of the Western Ghats on the monsoon rainfall has been studied for the southwest and northeast monsoon using normal rainfall data of 50 years (1901 to 1950). The precipitation is dependant on altitude over the western slope which is on the windward side with respect to the southwest monsoon, whereas it is independent of altitude over the eastern slope which is on the leeward side. The situation exactly reverses during the northeast monsoon rainfall. The study of Muralidharan et al. (1985) reveals that the amount of precipitation on the western slope of the Western Ghats above an altitude of about 600 metres increases with the altitude to a maximum at a height of about 1300 meters; and further up it decreases. Almost in a similar manner on the eastern slope of the Ghats above an altitude of about 370 metres the rainfall increases to a maximum about 1800 metres above mean sea level, and thereafter decreases continuously. Their rainfall profiles more or less agree with the results obtained from the global survey carried out by Lauer (1975) and also by Lauscher (1976) for other tropical mountains.

With the development of instruments that can give drop size data continuously and at relatively low costs, DSD measurements are becoming more common. However, there haven't been many measurements in India. Some of them are Jassal et al. (1994), Verma and Jha (1996a and 1996b), Reddy and Kozu (2003), Sasi Kumar et al. (2003), Mali et al. (2003), Krishna Reddy et al. (2005), Soma Sen Roy et al. (2005), Rao et al. (2006) and Harikumar et al. (2007; 2009). We present here the characterization of rain DSD and derivation of a rain DSD model for 4 different locations in southern India, viz. Thiruvananthapuram and Kochi, which are west coast stations; Munnar, a high altitude station in the Western Ghats and Sriharikota (SHAR), a station on the east coast, (Details of these stations are explained in the Chapter II) using a Joss-Waldvogel Disdrometer (JWD; Joss and Waldvogel, 1967). Some preliminary results from Thiruvananthapuram were presented in an earlier paper by Sasi Kumar et al. (2003) and the comparison of rain DSD between the stations in the eastern (SHAR) and western (Thiruvananthapuram and Kochi) coasts of India has also been presented by Harikumar et al. (2007).

Three different distribution functions are commonly used by different authors to describe rain drop size spectra, namely, the Marshall and Palmer (1948) type of exponential distribution, the gamma distribution (Ulbrich,1983) and the lognormal distribution (Feingold and Levin, 1986). It is generally agreed that the exponential distribution is valid only for data averaged over long periods of time (Joss and Gori, 1978), or over large volumes of space. However, the negative exponential is not appropriate for use in tropical regions and gamma model distribution must be too modified (Awang and Din, 2004). Thus, lognormal raindrop size distribution models are suitable and thus used it to estimate rain attenuation and compared to rain attenuation measurements from microwave links installed at Wireless Communication Centre (WCC), Universiti Teknologi Malaysia, UTM Skudai, Johor by these authors. Raindrop spectra often tend to have a monomodal distribution, which can be modelled by the gamma distribution function. This has the advantage that it tends to the exponential function as one of the parameters tends to zero. In the cases of the exponential and gamma distributions, however, the parameters have no physical significance.

The Lognormal distribution was explored by Feingold and Levin (1986) and was found to be as good as, if not better than, the gamma distribution in terms of fitting with observations. While the former showed better fit with the observed raindrop size distribution, the computed rain rate was marginally better when the gamma function was used. However, the Lognormal distribution has the advantage that the parameters have physical significance (Feingold and Levin, 1986). The variations in these parameters with rain rate or with time would, therefore, have implications on the physical processes that lead to the formation of rain drops and the processes that take place as the drops fall from the cloud to the ground.

Testud et al., (2000) developed a concept of normalization of DSD as normalizing raindrop spectra is an appropriate way to identify the shape of the distribution. The concept of normalization of DSD is based upon two reference variables, the liquid water content LWC and the mean volume diameter *Dm*. This normalization procedure helps in clearly defining the stratiform and convective rain types and hence a better insight into the cloud microphysics. The major point of this approach is that this normalisation is totally free of any assumption about the shape of the DSD. This new normalization has been successfully applied to the airborne microphysical data of the Tropical Ocean and Global Atmosphere Coupled Ocean–Atmosphere Response Experiment (TOGA COARE) collected by the National Center for Atmospheric Research Electra aircraft. The classification of the TOGA COARE raindrop spectra into stratiform and convective have been done to impress on the usefulness of this approach.

Since rain produces a loud and unique sound underwater that can be used to detect and quantify rainfall. Using the acoustical rainfall analysis (ARA) algorithm, the rain parameters are derived from this naturally generated underwater ambient sound field (Nystuen, 1996). Ulbrich and Atlas (2007) focus on continental tropical convective storms and their comparison with their maritime counterparts. They found out that in both maritime and continental storms the DSD in the convective portion of the storm approaches equilibrium. The coefficient *A* in the $Z=AR^b$ relation increases with median volume diameter while the exponent *b* approaches unity.

Since the DSD characteristics at 1 to 3 mm/h and 10 to 30 mm/h ranges roughly represent characteristics of stratiform and convective DSDs, rainfall type classification was not seriously examined by Koshu et al. (2006). But Roy et al. (2005) separated the rainfall events into convective and stratiform type, based on variation DSD parameters. At lower rain rates, the convective phase was marked by DSD spectra that have greater population of small droplets as compared to stratiform DSDs at the same rain rates. But at higher rain rates, the convective regime is characterised by narrow spectra centred at higher diameters. Using the gamma distribution to represents the DSD, then from the gamma parameters, from the No jump in the No-R relation, they classified the rain with respect to origin.

Based on the information on the time variability of DSDs, a method to generate the space time variability of the distributions of the size of the raindrops is developed by Lee et al. (2006). The model developed can be used to calculate DSDs and integral rain parameters, based on the fact that two moments of the DSDs are sufficient to capture most of the DSD varibility. The model is validated using concurrent radar and disdrometer data. Observation with disdrometer and optical rain gauge were made at Gadanki and their application in rainfall estimation are evaluated (Reddy et al., 2003). Ecuyer et al. (2004) explores the potential for refining assumed drop size distributions (DSDs) in global radar rainfall algorithms by establishing a link between satellite observables and information gleaned from regional validation experiments where polarimetric radar (Doviak and Zrnic, 1993), Doppler radar, and disdrometer measurements can be used to infer raindrop size distributions. The measured shape of the rain DSD depends significantly on the sample size, and that adding many “instant” distributions from different conditions leads to an exponential distribution such as proposed by Marshal and Palmer. “instant” distributions, i.e., distributions accumulated during 1 min or less, deviate strongly from exponential distributions in the direction towards monodispersity (Joss and Gorri, 1978). Toress et al. (1994) proposed a general phenomenological formulation for DSD, written down as a scaling law, accounts for all previous fitted DSDs.

Rain DSD data has been used to derive the rain rate and radar reflectivity factor and then the standard deviation of the rain intensity R and the radar reflectivity factor Z are derived theoretically for R and Z values by Joss and Waldvogel (1968)

One method for obtaining drop size distribution (DSD) functions requires previous normalization of both measured drop diameters and concentrations. This normalization, proposed by Sekhon and Srivastava (1971, 1978), and later by Willis (1984), was meant to comprise the entire dataset, thus achieving a universal distribution function independent of observation site or rain type. An alternative method is based on previous grouping of rain registers in different rain-rate classes to obtain mean size distributions. These distributions can then be fitted to theoretical models whose parameters will depend on the rain rate, usually through a power law. (Cerro et al., 1999).

In developing the upcoming Global Precipitation Measurement (GPM) mission, a dual-frequency Ku–Ka-band radar system will be used to measure rainfall in such a fashion that the reflectivity ratio intrinsic to the measurement will be sensitive to underlying variations in the drop size distribution (DSD) of rain. This will enable improved techniques for retrieving rain rates, which are dependent upon several key properties of the DSD (Kuo et al., 2004). The results of their study have bearing on how future dual-frequency precipitation retrieval algorithms could be formulated to optimize the sensitivity to underlying DSD variability, a problem that has greatly upheld past progress in radar rain retrieval.

The drop-size distributions associated with a range of high rainfall rates are examined using data from tropical storms and hurricanes by Willis and Tattelman (1998). Mean drop-size distributions are presented for a range of high rainfall rates, as well as a Gamma distribution fit to the entire set of normalized drop-size distributions. This fit forms the basis for a model drop-size distribution for intense rain. Except at small diameters, the experimental (measured by died filter and by radar echos) could be fitted by the negative exponential expression (Marshal and Palmer, 1948).

The dual-frequency radar which the GPM core satellite will carry should prove a much more effective tool in sorting out at least part of this DSD-induced ambiguity. Indeed, with two radar reflectivity profiles, one would expect to be able to retrieve not just a single rain rate profile, but also at least one additional "first order" DSD profile, such as a profile of the (mass-weighted) mean drop diameter D* (Haddad and Li, 2003). Two proposed algorithms to retrieve the governing parameters of the gamma DSD from polarimetric measurements have been compared by Brandes at al. (2003). The beta method (Gorgucci et al., 2002; Bringi et al. 2002) is found to be comparably erroneous than the constrained-gamma DSD (Zhang et al. 2001; Brandes et al. 2003; Vivekanandan et al. 2004)method.

Awand and Din (2004) reports the comparison of the rain attenuation measurements from 38 GHz microwave links conducted at Wireless Communication Center, Universiti Teknologi Malaysia (UTM) with the DSD model from Malaysia (KL-Lognormal), Singapore, Brazil and Nigeria using lognormal distribution model. The rapid growth of telecommunication services, both in satellite and terrestrial links using higher frequency bands is above 10 GHz has highlighted need for estimating the effect of hydrometeors such as rain, clouds, fog and gaseous. The presence of hydrometeors in radio wave propagation, particularly rain, can produce major impairments to microwave propagation. Raindrops can absorb and scatter radio wave energy results in signal attenuation, which can degrade the reliability and performance of the communication links. However, the negative exponential is not appropriate for use in tropical regions and gamma model distribution must be too modified. Thus, lognormal raindrop size distribution models are suitable, used to estimate rain attenuation and compared to rain attenuation measurements from microwave links installed at Wireless Communication Centre (WCC), Universiti Teknologi Malaysia, UTM Skudai, Johor.

Roy et al. (2005) studied the Drop DSDs associated with tropical rainfall at Cuddalore in the south-eastern part of India, measured by a Joss-Waldvogel disdrometer (RD–80 model) during September to November 2002. They have separated the rainfall events into convective and stratiform. Even using microwave

brightness temperature, a new scheme has been developed to classify convective and stratiform (C/S) precipitation areas over oceans by Hong et al. (1999).

Zhang et al. (2001) studied the error propagation from moment estimators to rain DSD parameter estimators. Consequently, the derived μ-λ (shape parameter-slope parameter) relation is believed to contain useful information in that it describes the mean behavior of the DSD parameters and reflects a characteristic of actual raindrop size distributions. The μ–λ relation improves retrievals of rain parameters from a pair of remote measurements such as reflectivity and differential reflectivity or attenuation, and it reduces the bias and standard error in retrieved rain parameters.

Here an effort has been made to understand the average rain DSD spectrum. The characteristics of the rain DSD, whose variation with rain rate has been explored in detail. An empirical lognormal model for this variation of DSD with rain rate is also derived. The model would be very useful to communication engineers to design their instruments considering this knowledge. This can be used to derive the Z-R relation to apply for calibration of satellite sensors and weather radars (Soto, 1989). Kinetic energy imparted by the rain could be derived using it, that will eventually help agro meteorologists in the field of soil erosion. Cloud microphysics modellers are also would be the beneficiaries of this model.

1.2.2. Rain Rate

The measurement of rain rate and understanding about its temporal and spatial distribution is of importance in many respects. These data are needed, for instance, in the modelling of soil erosion (using models like RUSLE or WEPP). These models usually require a time series of rain rate with moderate to high time resolution. A knowledge of rain rates that can be expected to help design structures like culverts so that they can handle the storm waters during heavy rainfall. Rain rate is also important to understand the rate of recharge of the water table and to estimate runoff. Apart from these, the effects of climate change are now making rain rate measurements even more important. For instance, Gordon et al (1992) report results from a model that point to increase in rain rate due to enhanced greenhouse effect. A study in Australia by Haylock and Nicholls (2000) showed an

increase in the total rainfall and number of rainy days in the northern and southern regions and a decrease in the western and southwestern regions. Their study implied a significant change in the number of heavy events in the southwest and a significant change in only the number of lighter events in the north. Most of the rainfall measurements in India are limited to daily rainfall, with only a relatively few stations recording rain gauges that can give hourly rainfall values. Rainfall data have been used in many studies (for instance, Ananthakrishnan et al., 1979; Muralidharan et al, 1985; James et al., 1987; Sreedharan and James, 1988; Sampath et al., 1989). Ananthakrishnan *et al* (1979), after analysing hourly rainfall data for the monsoon seasons of 1969 and 1970, found that "falls of intensity ≥10 mm/h account for 14% of the rainfall at Thiruvananthapuram in less than 2% of the rain hours". They continue to state that "Such falls account for about a third of the rainfall at stations from Cochin to Goa and 40 to 50% at Vengurla and Bombay." Ananthakrishnan *et al* used the hourly rainfall value in place of rain rate, in the absence of rain rate measurements. A rainfall of 1 mm depth that lasted for one minute would be counted as a 1mm/h rain event, while, in fact, the intensity should be taken as 60mm/h. Thus, the intensity values used by Ananthakrishnan *et al* could be highly underestimated.

While daily rainfall data are quite useful for such studies, the distribution in shorter intervals of time is important in many fields. The data from recording rain gauges show that rainfall is often confined to a few hours a day, and sometimes even for periods shorter than an hour. The period during which a given amount of rain occurs is important because heavier rainfall leads to greater runoff, greater soil erosion and less infiltration into the water table. A knowledge of rain rate therefore becomes important from the point of view of better management of our dwindling fresh water resources and improved control of soil erosion.

In the present study some of the first results from the measurement of rain rate with high temporal resolution of 1 minute at a few stations in Kerala State are presented. Distribution of rainfall, temporal distribution of rain rate, cumulative distribution of rain rate and contribution of each rain rate range to total rainfall are analysed and discussed in detail. In tropical climates, rain attenuation is severe due

to higher rain rates (Jassel et al., 1994). "Sufficient data on propagation attenuation, rain rate and DSD are not available for tropical region and, in particular, for India where rainy season is characterised by the heavy monsoon rains. So, the micro wave communication design engineers could consider the rain rate distribution and its spatial variability spectrum while design mm wave communication devices.

1.2.3. Vertical profiles of rain DSD

Knowledge of the vertical profiles rain DSD are very useful for the fields like microwave communication, radar/satellite meteorology and cloud micro-physics. But such measurements that will help in measuring precisely the atmospheric parameters using remote sensing techniques need to be carried out more especially in the tropics. Since the global circulations are driven mainly by tropical weather, understanding on its variability using observational techniques especially satellite-based is very crucial. Satellites like TRMM (Tropical Rainfall Measuring Mission), upcoming Indo-French satellite Megha-Tropiques, GPM (Global Precipitation Measurement) constellation etc. are exclusively measures the tropical atmospheric parameters. So, for the retrieval of atmospheric parameters from the satellite-borne measurements and for calibration of the satellite sensors, vertical profiles of DSD and Z-R relations in the tropical sites are very essential. In this chapter, study of the variation of DSD with altitude has been carried out. The vertical variation of the Z-R relation is also derived and studied during radar bright band (BB)/stratiform and non-bright band (NBB)/convective conditions/rains of the southwest monsoon and premonsoon seasons.

In the Indian region, monsoon is a major phenomenon affecting agriculture, drinking water, potential of hydro electric energy and the overall economy. The lives of a large number of people within and nearby countries get affected. Hence we need to study and understand the vertical distribution of DSD parameters, which gives information concerning the generating processes of the monsoon precipitating systems (Reddy et al., 2005).

Understanding of the characteristics of melting layer is very useful to weather forecasters in predicting and monitoring the snow level, defined as the lowest level in a melting layer where snow or ice completely changes to rain. This

information can also be useful to road maintenance workers, hydrologists, emergency managers, aviators and the ski industry (White et al., 2002). More importantly, the information of the freezing height and the melting layer are critically important in making decision to do seeding experiment or not and in establishing an optimal seeding strategy that may lead to most profitable output (Cha et al., 2007). They have explained in detail the method to estimate the freezing height and the melting layer depth, the altitude interval throughout which ice-phase precipitation melts as it descends, from the Micro Rain Radar (MRR) output product.

Numerical modeling studies have demonstrated large sensitivity in terms of surface rainfall production, evaporation, and downdraft intensity to the parameterized hydrometeor size distribution below the melting level, especially in tropical mesoscale convective systems (MCS; Ferrier et al. 1995). Drop-size distributions in clouds are difficult to observe directly. These measurements are typically recorded using probes mounted on aircraft. The observations are limited to the regions where the planes fly, thus producing sporadic measurements in time and space (e.g., Rogers et al. 1993). Moreover, the sample volume is typically small so that it may not always be possible to obtain representative drop-size distributions (e.g., Richter and Hagen 1997). Three different algorithms of DSD retrieval by vertically pointing radar have been simulated utilising JWD measurements from Amazon basin of Brazil by Tokey and Dickens (2000). Thus they used the DSD data obtained from Disdrometer for the simulation of algorithms to derive back the DSD.

Li and Srivastava (2001) derived an analytical solution for the evaporation of a single raindrop. The results show that, for the detection of rain evaporation, reflectivity is more sensitive than differential reflectivity, whereas for the estimation of rainfall rate R, an empirical ZDR–Z–R formula is more robust and accurate than a Z–R formula. Lee at al. (2006) concluded that, when using the ground disdrometer to establish proper Z-R relationship, the spatial and temporal extends should be considered very carefully. It is well established that rain evaporation plays an important role in inducing and maintaining downdrafts under

cloud bases, in both convective-scale and mesoscale precipitation. It is also an important sink of atmospheric latent heat. However, quantitative measurement of rain evaporation remains extremely difficult (Li and Srivastava, 2001). A direct way of measuring rain evaporation is to track the drop size distribution (DSD) along their falling paths. Gori and Joss (1980), and Levin et al. (1991) used this approach in their investigations. They measured DSDs simultaneously along steep mountain slopes at different heights.

Weather radar yields improved hydrometeor detection and area coverage, but has other limitations when it comes to ground truth or quantitative precipitation estimation (QPE) due to the very variable relation between radar reflectivity (Z) and rain rate (R; Diederich et al., 2004). In this article, they present the MRR (Micro Rain Radar), which gives an alternative QPE method. This low cost Doppler radar measures vertical profiles of radar reflectivity as well as spectra of fall velocity of hydrometeors, and estimates the drop size distribution (DSD) of rain using a relation between terminal fall velocity and drop diameter for liquid precipitation. Tian et al. (2006) presents an initial investigation using airborne Doppler radar operating at 10 and 94 GHz to measure the light stratiform rain ($\leq$5 mm/h). It has been shown that the combination of 10 and 94 GHz is more sensitive to resolve the rain DSD in light rain than that of 14 and 35 GHz (Frequencies that will be used in the dual-frequency radar of Global Precipitation Measurement mission). The sensitivities of the retrieval to Gamma shape parameter are discussed.

Characteristics of precipitating clouds, such as microwave irradiance, cloud-top infrared irradiance, and radar reflectivity, can be measured remotely over large regions by sensors on satellites, aircraft, ships, and on the ground. The information from these indirect measurements of precipitation must be converted to the rain rate by using an appropriate algorithm. Although the basic physics behind these algorithms may be understood, algorithm parameters typically must be calibrated to the particular rain regime under study in order to produce accurate results. Often the approach to calibration is one of bootstrapping—using a small-scale direct measurement to calibrate a larger-scale indirect measurement, which in turn is used to calibrate a still larger scale measurement successively until the scale

needed is reached. Thus, it is vital that the initial relation upon which this sequence of calibrations is based be as accurate as possible (Yuter and Houze, 1995)

Application of the information on vertical profiles of rain DSD and integral rain parameters is to correct algorithms for weather radar data. But the problem exists as weather radar measurements take place at a certain altitude whereas their calibration is usually done by ground based data-either the radar data is adjusted to surface based sensors or transferred to rain rate by Z-R-relationships established at ground-level. The vertically pointing radar provides measurements at different altitudes and thus closes the gap between ground based measurements and the weather radar as has been reported before (Wagner et al., 2004). Within the framework of APOLAS (Areal Precipitation measurements Over Land And Sea), a project under the German Climate Research Programme DEKLIM in the Baltic area (http://miraculix.dkrz.de/gerhard/apolas.html), they addressed this problem of understanding the vertical structure of precipitation. Diederich et al. (2004) studied the variability in the drop size distribution inside an area of 200 by 600 meters with a temporal resolution of 30 seconds using 3 Micro Rain Radars/disdrometers and a 2d-video disdrometer.

Whenever the weather radar has been used for areal precipitation measurement, the quantitative estimation and investigation of rain rate from radar reflectivity has been hampered by (1) The highly variable and ambiguous relation between rain rate and radar reflectivity, which depends strongly on the drop size distribution (DSD), (2) The occurrence of ice in the illuminated volume, (3) The evolution of rainfall from the height of the radar beam to the ground and (4) The dissimilar volumetric and temporal scales involved when measuring different rain characteristics. These effects have been investigated in numerous publications, but the progress in applied areal rainfall measurement with radar has been modest. Often additional information is needed to correctly identify, predict and correct the named effects. Fabry et al. (1992) suggested the use of a network of low cost vertically pointing radars to enhance weather Radar scans by measuring the vertical reflectivity profile and detecting the melting layer, which yields potential to counter the errors caused by issue 2 and 3. For issue 1, the measurement of the drop size

distribution (DSD) allowed the investigation of methods to associate rainfall structure with DSD characteristics at ground level (Uijlenhoet et al, 2003). This represents a significant progress compared to separately measuring reflectivity with radar and rain rate with gauges, as this is too strongly affected by issue 4 (Diederich et al., 2004).

Z-R relation shows a clear distinction between southwest and northeast monsoon seasons (Reddy et al., 2003). During southwest monsoon precipitation generally has bigger drops than during northeast monsoon. Wilson et al. (2001) made study using the disdrometer and found out that no significant differences in DSDs in southwest and northeast monsoons. In the model study in this thesis, it is getting more or similar lognormal parameters during different monsoon seasons at a particular station.

Measurements of rain were obtained with a vertically pointing micro radar (MRR) with 1 min time resolution and 50 (100) m height resolution at the German Baltic coast on the Zingst peninsula (54.43°N, 12.67°E) by Peters et al. (2002). Simultaneous estimates of rain rate and reflectivity factor with data of a C-band (frequency=6 GHz) weather radar suggest that the MRR may be used to support quantitative rain rate estimates with weather radars.

Conventional weather radar retrieval of areal quantitative precipitation suffers from mainly two problems (Peters et al., 2002). They are (1) The relation between the radar reflectivity and rain rate depends on the structure of the drop size distribution. Parameterized distributions can deviate considerably from actual distributions. Richter and Hagen (1997) demonstrated that this problem can be mitigated by advanced radar techniques including for example polarimetry and (2) The height of the measuring volume increases with increasing distance from the radar due to the earth curvature. In moderate zones the majority of weather radar data are obtained above the freezing level. Stratiform shallow rainclouds may be totally below the sampling height of the radar. In general the extrapolation from the radar measuring volume to the surface includes significant uncertainties. The influence of vertical wind and turbulence was neglected in these MRR

measurements, which represents probably the most important source of error of this method (e.g. Joss and Dyer, 1972, Richter, 1994).

Zhang et al. (2002) studied the sampling effect on radar measurements of inhomogeneous media and the resultant rain estimation. The dependence of statistical moments on the variation of DSD parameters are calculated and applied to radar-based rain estimation. Quantitative estimation of fallen precipitation at ground level using weather radar is hampered by numerous well documented problems: the variable relation between radar reflectivity and rain rate, a vertical evolution of rain intensity from ground to beam-height, attenuation, changes in water-phase, attenuation, and eventually insufficient temporal sampling (Diederich et al., 2004). Bendix at al. (2004) used MRR to study the rain in a tropical montane cloud forest of southern Ecuador and its chemical composition.

A bright band is the enhanced radar echo area that is associated with the melting of hydrometeors in stratiform precipitation (Cha et al., 2009). The top of the bright band can be considered as the melting level (or freezing height), commonly accepted as the altitude of the 0◦ C isotherm (Glickman, 2000).

Data from a long term measurement of MRR at a mountain site (Daegwallyeong, DG, one year period of 2005) and a coastal site (Haenam, HN, three years 2004–2006) in South Korea were analyzed by Cha et al. (2009) to compare the MRR measured bright band characteristics of stratiform precipitation at the two sites. On average, the bright band was somewhat thicker and the sharpness (average gradient of reflectivity above and below the reflectivity peak) was slightly weaker at DG, compared to those values at HN.

The characteristics of the bright band may reveal important cloud microphysical processes. Fabry and Zawadzki (1995) reported that the mixture of ice, air, and water leads to a greater increase in the radar reflectivity than that expected from the change from ice to water. They suggest several other factors that contribute to this bright band phenomenon. One such factor is the distribution of water within the particle, so called the density effect. That is, the distribution of melted water within the snow particle will appreciably affect the reflectivity value. Zawadzki et al. (2005) focused more on the density effect and proposed a bright

band model, showing that the difference between the peak reflectivity and the snow reflectivity increases with a decreasing density of snow particles.

Melting precipitation in stratiform rain produces a distinct signal in radar data, ie., the "bright band" (BB; Gettys et al., 2000). The case of the convective rain is different. The strong convective currents in active showers and thunderstorms tend to destroy the horizontal stratification essential for creating and sustaining the BB. As a result, the BB is broken (Farby and Zawadkzki, 1995; Neiman et al., 2005). The stratiform condition gives rise to radar bright band (BB) and during convective regime of rain there will not be any radar bright band (NBB). High-frequency radars do not measure an enhanced 'bright band' at the melting layer, rather a sudden increase of reflectivity as the ice particles become coated in water. This sudden step can be used to locate accurately the height of the WBZ (Wet-Bulb zero degree isotherm). The studies of Mittermaier and Illingworth (2003) suggests that, at least in the UK, operational model predictions of the freezing-level height are within the specified 200 m error, but that the use of volumetric scans, even under idealized conditions, cannot achieve this accuracy.

Recently, however, Loffler-Mang and Kunz (1999) and Harikumar et al. (2006) demonstrated that a MRR, a vertically pointing Doppler radar, could be a very useful instrument to measure the vertical profiles of precipitation and the bright bands, with the advantage of a higher time resolution, a significantly lower cost than X-band radars, and the easiness of operation. The electronic noise correction rendered the radar particle size retrievals below 0.7 mm drop diameters invalid; exponential extrapolation of the spectrum below drop diameters of 0.7 mm decreased the rain intensity up to 20% (Loffler-Mang and Kunz, 1999).

For the first time in Korea, monthly mean melting layer height data measured by a MRR. Measurements were made at the Cloud Physic Observation System (CPOS) site at Daegwallyeong Weather Station (37º41 N, 128º46 E, 842 m ASL), located in Gangwon Province. An easy method is introduced to estimate the melting layer height from the MRR rain rate data in association with the bright band regions (Cha et al., 2009). In the Tropics, freezing levels are highest (~5000 m) and both intramonth and interannual variability is lowest. Freezing levels are lower

and variability is higher in the subtropics and midlatitudes (harris et al., 2000). Sudden changes in the temporal behaviour of the DSD spectra are accompanied by rapid modifications in corresponding integral relationships of Z-R are seen (Clemens et al., 2006). So, the DSD evolution of the rain DSD has been studied in detail by these authors. The initial spectra below the melting layer seem to play an important role in the change of these modifications of the integral parameter's relation. In addition, the height of the melting layer or even the fall-distances allows for modifications of drop size distributions in terms of coalescence and drop-break up. Most of these described processes result in a vertical variability of the estimated reflectivity in contemporaneous constant rain intensity. This leads to height-dependent Z-R relationships in spite of temporal homogeneity which is of importance especially for quantitative radar rainfall estimation (Clemens et al., 2006)

1.2.4. Altitudinal variation of rain DSD

Deep awareness of altitudinal and temporal evolution of rain DSD are very also useful for the fields like microwave communication, radar meteorology and cloud micro-physics. But such measurements have been very few in the tropics. The altitudinal and temporal evolution of rain DSD is of much interest. According to Low and List, significant collisional growth, i.e., coalescence, occurred only when drops < 0.6 mm in diameter struck by larger ones (Low and List, 1982). The coalescence efficiencies of raindrop pairs has been established by Low and List and using it, the collision breakup equations were expanded into general overall equations for all drop pairs as expected in natural rain. Special procedures have been developed by Philips and Brown (1986) to deal effectively with several computational problems that arise in calculating both the fragment distribution function and the Bleck expansion coefficients that appear in the discrete coalescence/breakup equation of Low and List. Theoretical and observational studies on the evolution of rain DSD by coalescence, breakup and evaporation have been done by Hu and Srivastava (1993 and 1995). They considered two models of evolution of the rain DSD. Model 1 was spatially homogeneous and model 2 was one dimensional (vertical), conditions being uniform in horizontal. In both models,

the size distribution evolved with time by the process of coalescence, collisional breakup and evaporation. In model 2, they also considered vertical air motion. The model 1 may be considered to be a crude approximation to showery precipitation while model 2 approximates continuous stratiform rain. According to these authors, either the Low and List parameterization is greatly over estimating drop breakup and/or the number of drops formed by breakup or evaporation played a dominant role in shaping the DSD.

There are two currently accepted mechanisms for raindrop formation: Wegener (1911) first suggested that rain originates from the melting of ice particles, an idea which was later elaborated by Bergeron (1935) and Findeisen (1938). According to a second theory, which is applicable to cloud regions not containing ice, raindrops could form directly by collision and coalescence of cloud droplets (Twomey, 1964). Reynolds (1876) proposed the collision process as a possible growth mechanism but a quantitative presentation of the concept was not formulated until Langmuir (1948) suggested a chain-reaction scheme of rain production from warm clouds. The fragmentation of large drops via aerodynamic breakup was thought to provide the feeder droplets for further collisional growth. Aerodynamic breakup involved the assumption that drops become unstable once they reach diameters of 0.6 cm. This limiting size proved to be incorrect according to experimental and theoretical (Prupacher and Pitter, 1971) studies which moved this limit to drop sizes of 1.0 cm in terms of equivalent spherical diameters. Hence, aerodynamic breakup is now considered unimportant. It is breakup after drop collisions which seem to govern the drop evolution in the larger size ranges (Magarvey and Geldart, 1962; McTaggart-Cowan and List, 1975b; Ryan, 1976; List and Gillespie, 1976), regardless of the origin.

The importance of collection process in warm rain is well established (Riehl, 1954). Although cloud droplets can grow to radii of approximately 10 μm by diffusion and condensation of water vapor, the time required for growth to raindrop sizes by the same process is prohibitive. Growth to drops of precipitation size is accomplished by two other processes. Clouds with tops above the freezing level, solid precipitation particles grow at the expense of super-cooled droplets, fall,

accrete cloud droplets and finally melt at temperatures above 0°C to form rain. In warm clouds, however, raindrops grow by gravitational collection: larger drops, which fall faster, collide and coalesce with smaller drops in their path. Even under conditions in which the ice phase is responsible for the initiation of precipitation, collection is the dominant growth mechanism in the non-freezing regions of the cloud (Houghton, 1968) and is thus important in shaping the rain DSD.

In studies of the growth of cloud droplet populations into precipitation particles, it is found that the collision of droplets does not necessarily result in 100% coalescence and that ice crystals do not always rebound. Information on the percentage coalescence of the colliding drops, usually defined as the coalescence efficiency, and on the percentage bounce of ice crystals, the separation probability, is so scarce and so poor that both coalescence and bounce are often assumed to occur 100% of the time. It has been known for a long time that drops with the order of one millimeter bounce almost 100% of the time if uncharged and not in an electrical field (Rayleigh, 1879). The addition of charges and electric fields increases the probability of coalescence following collision to the point where small charges and small fields cause almost 100% coalescence. In the presence of electric fields, or when the drops are charged, observations of Gunn (1965a, 1965b) and Sartor (1967) show that by controlling their relative velocity they can be made to coalesce with subsequent disruption and the production of rain drops. Further it has been showed by Sartor (1967) that even a small percentage of cloud and precipitation drops bouncing or disrupting in an electric field can be significant in the problems of cloud electrification.

The spatial variation in the rain DSD has been brought out by conducting study at a few stations in the southern peninsular India by Harikumar et al. (2007). An empirical model for the variation of rain DSD with rain rate at these locations in peninsular India has also been developed by Harikumar et al. (2009). The first experimental measurements of rain DSD at Thiruvananthapuram using the MRR were also presented by Harikumar et al. (2006). In that work, the averaged DSD over one hour of a continuous rain episode were presented and compared with the average over a five-minute interval of the same rainfall event.

1.2.5. Z-R Relation and its Vertical profiles

Usually the Z-R-relationship ($Z=aR^b$) is established by using drop size spectra from disdrometers at ground level and transferring it to radar data aloft. But the changes of spectra with height indicate that also Z-R relationships will be affected. Therefore, these relationships have been calculated from the mean spectra described before by regression with the independent variable R (rainfall) and the dependent variable Z (reflectivity). Variable *b* is equal to the regression coefficient (Wagner et al., 2004).

Within stratiform precipitation, the same rain rate could be produced by a drop spectrum dominated by numerous small drops (lower reflectivity) or by a few large drops (higher reflectivity) (Yuter and Houze, 1995). The usual specific Z-R relations are usually established on the basis of climatologies of rain gauge data versus simultaneous radar reflectivities (e.g. Michelson and. Koistinen, 2000). Lee and Zawadzki (2006) demonstrated that distrometer-based radar calibration providing the actual Z-R relation via the drop size distribution has the potential to eliminate important calibration uncertainties.

Reflectivity–rainfall (*Z–R*) relations of the form $Z = AR^B$ were developed for each precipitation category as a function of height using linear regressions to the radar retrievals of *R* and *Z* in log space by Cifelli et al. (2000). The results of this study show that, despite large overlap in the distribution of the drop-size parameters, significant differences occur in the mean *Z–R* parameterization for each category as a function of height. Similar to findings from previous studies, the rainfall decreased *for a given reflectivity* as the precipitation type changed from convective to stratiform. The coefficient *A generally* increased downward with height in each category; the exponent *B* showed a small decrease (stratiform), almost no change (convective), or a slight increase (mixed convective–stratiform). In the stratiform region, the coefficient *A* increases by ~37% with decreasing height. Exponent *B* also decreases slightly in the stratiform category. There are large differences in the convective and stratiform rain rates (15%–85%) for a given reflectivity and emphasizes the fact that the *Z–R* relation varies, not only by precipitation category, but also as a function of height. The combined signature of *A* increasing and *B*

decreasing in the stratiform category is consistent with the expected change in *Z–R* due to one or more of the following: coalescence, evaporation, or size sorting (Gunn and Marshall 1955; Atlas and Chmela 1957; Wilson and Brandes 1979; Ulbrich and Atlas 1998). The coefficient *A* in the $Z=AR^b$ relation increases with median volume diameter while the exponent *b* approaches unity (Ulbrich and Atlas, 2007). Apart from using the lognormal distribution to represents the rain DSD, radar reflectivity factor also has been derived by these authors (Feingold and Levin, 1986). It is found out that the use of MP Z-R relation ($Z=200R^{1.6}$) gives bias errors of about 1.5 dB or less in their measurements (Kozhu et al., 2006). Z-R relation will have significant variation in the area where the origin of rainfall and surrounding environment depend heavily on the season.

Using MST, LAWP and Disdrometer, Z-R relation has been studied for different tyepes of rain, stratiform, transition and convective type and also for different seasons by Rao et al., (2001). The exponent b (coefficient A) has been found to be smaller (larger) in the case of stratiform (convective) precipitation than in convective (stratiform) precipitation, in contrast to the earlier studies. The observed discrepancies are partially due to different methods of precipitation classification and partially due to different data set at different locations. As per the shape of the Z-R relation, if we use a single Z-R relation for all the regions and also to different precipitation systems, there will be underestimation in the convective rain and overestimation in the stratiform rain (Rao et al., 2001).

According to Wagner et al. (2004), from 200 m 2000 m height, the b has been reduced from 1.3 to 0.9. a is also decreasing with height (same result as ours). Factor a is ranging between 60 and 210 for light, moderate and total rainfall, but for heavy rain it exceeds 500 at lower altitudes corresponding to Z-Rrelationships for severe convection (Wagner, 2004). Some kind of linearity between Z and R seems to exist (Jameson and Kostinski, 2002). Within stratiform precipitation, the same rain rate could be produced by a drop spectrum dominated by numerous small drops (lower reflectivity) or by a few large drops (higher reflectivity) (Yuter and Houze, 1995). A probability-matched Z–R relation for all the raindrop image data from the Electra collected between altitudes of 2.7 and 3.3 km in TOGA COARE is

similar to the Z–R relation obtained at the sea surface in the Global Atmospheric Research Program Atlantic Tropical Experiment. I.e., A single Z-R relation using all the data hs been derived rather than classifying as stratiform and convective type.

Study by Cerro et al. (1999) shows the results of the modeling of drop size distributions (DSD) observed during a 2 year study in Barcelona. They collected the rain DSD and velocities and then grouped in to classes according to the rain rate. Good results of Z-R relations are obtained when the DSD is modelled with an exponential distribution. According to Jamson and Kostinski (2002), the non-linear power relations between them are purely depends on the number of samples. I.e., as per these authors, the shape of the power relations depend on the numebr of drops are considered in the analysis.

O. Fiser (2004) describes the accuracy of the Z-R relationships through the RMSE and correlation and to improve the accuracy using distinguished rain (DSD) types using the Czech DSD data that has been collected for one year. Marshal and Palmer published the Z-R approximation firstly. Later Sokol et al. (2002) discussed the of Z-R relations through the RMSE and correlation and tried to improve the accuracy using distinguished rain (DSD) types. Using this data, the power Z-R law is $Z=229R^{1.278}$. This paper ensures thoroughly that power-law relation fits very well for the relation between these two integral rain parameters. The accuracy is perfect when DSDs are distinguished in two classes according to Waldvogel criterion (Waldvogel A., 1974).

The Z-R relation derived by Baltas and Mimikou (2002) for a specific event was $Z=407R^{1.26}$, whereas for all events is $Z=431R^{1.25}$. The rain rate could be derived from the radar reflectivity factor using the power Z-R law (Brandes, 1974). Lee and Kyung (2006) got Z-R relation as $Z=333R^{1.08}$. They concluded that, when using the ground disdrometer to establish proper Z-R relationship, the spatial and temporal extends should be considered carefully. Early classification for Z-R relation by rain type by Fujiwara (1965), gives values of A and B as for thunderstorm (A=450; B=1.46), rain showers (A=300; B=1.37) and continuose rain (A=205; B=1.48). Atlas (1964) noted a tendency toward convergence of a number

of *Z–R* relations on the rain parameter diagram of Atlas and Chmela (1957) at a median volume diameter D_o ~ 2 mm near R ~ 50 mm h^{-1} and Z = 46 dB*Z*.

Uijlenhoet et al. (2003) presented a case study of the variability of raindrop size distributions for a squall line passing over a small watershed in northern Mississippi. The intrastorm variability of raindrop size distributions as a source of uncertainty in single-parameter and dual-parameter radar rainfall estimates is studied using time series analyses of disdrometer observations. Two rain-rate (*R*) estimators are considered: the traditional single-parameter estimator using only the radar reflectivity factor (*Z*) and a dual-polarization estimator using a combination of radar reflectivity at horizontal polarization (*ZH*) and differential reflectivity (*Z*DR). A scaling-law analysis reveals that the shapes of the scaled spectra are bent downward for small raindrop sizes in the leading convective line, slightly bent upward in the transition zone, and strongly bent upward in the trailing stratiform rain. The exponents of the resulting *Z–R* relationships are roughly the same for the leading convective line and the trailing stratiform rain (~1.4) and slightly larger for the transition region (~1.5), with prefactors increasing in this order: transition (~200), convective (~300), stratiform (~450). In terms of rainfall estimation bias, the best-fit mean *R*(*ZH*, *Z*DR) relationship outperforms the best-fit mean *R*(*Z*) relationship, both for each storm phase separately and for the event as a whole.

A fundamental step in the hydrometeorological application of single-parameter weather radar is the conversion of radar-measured reflectivities aloft to estimates of the spatial and temporal distribution of rainfall at the ground. Although many different sources of error and uncertainty affect this conversion (e.g., Wilson and Brandes 1979; Zawadzki 1984; Joss and Waldvogel 1990; Steiner et al. 1999; Sa´nchez-Diezma et al. 2001), a key issue is the limited spatial and temporal representative ness of radar reflectivity–rain rate (*Z–R*) relationships. Fixed *Z–R* relationships will inevitably lead to errors in radar rainfall estimates, because raindropSize distributions exhibit an appreciable amount of spatial and temporal variability e.g., Dingle and Hardy 1962; Waldvogel 1974; Carbone and Nelson 1978; Smith 1993; Smith and De Veaux 1994). Although the storm-to-storm (i.e.,

*inter*storm) variability of *Z–R* relationships is relatively well established (e.g., Fujiwara 1965; Battan 1973; Smith and Krajewski 1993; Steiner and Smith 2000), the variability within storms (i.e., *intra*storm variability) has received less attention until recently (e.g., Waldvogel 1974; Carbone and Nelson 1978). Yet, there exist appreciable spatial variations in microphysical environments within a storm at any given time and corresponding temporal variations through the course of a storm at any given place within that storm (e.g., Steiner et al. 1995; Houze 1997; Petersen et al. 1999). Since the coefficients of *Z–R* relationships are closely related to the microphysical structure of rainfall (e.g., Marshall and Palmer 1948; Battan 1973; Waldvogel 1974; Jameson and Kostinski 2001a), the intrastorm variability of *Z–R* relationships is inevitably a source of uncertainty in radar rainfall estimates.

Drop size distributions (DSD) associated with tropical rainfall at Cuddalore in the south-eastern part of India has been measured by a Joss-Waldvogel disdrometer (RD–80 model) during September to November 2002 by Roy et al. (2005). Rainfall events were separated into convective and stratiform. During the rain event, at low rainrates, the convective phase of the rainfall event was marked by DSD spectra that have greater population of small droplets as compared to stratiform DSDs at the same rainrates. In our case the stratiform (BB)-Z is large for a particular rain rate compared to convective (NBB). This also shows that stratiform rain consists of more large drops. At higher rain rates, the convective regime is characterised by narrow spectra centred at higher diameters.

An empirical stratiform-convective classification method based on N_0 (Intercept parameter of the gamma distribution fit to the DSD) and R is presented by Tokey and Short (1995). Regarding the Z-R relation, the exponent is lower and the intercept is higher in the tropical stratiform classification than in the tropical convective classification. Precipitation is generally considered to be of two clearly distinguishable types-stratiform and convective. Stratiform precipitation falls from nimbostratus clouds, while convective precipitation falls from cumulus and cumulonimbus clouds (Houze, 1993). Atlas et al. (1984) stated that “when rain is composed of many small drops of low fall speed, the liquid water content is bound to be higher and the reflectivity lower than with an equal rain rate of larger fast

falling drops. The Z-R relation obtained by Tokey and Short (1995) are $Z=315R^{1.20}$ when all data is used, $Z=139R^{1.43}$ for convective and $Z=367R^{1.30}$ for stratiform. A value for stratiform is larger than convective.

1.2.6. Comparison of TRMM precipitation data with other measurements

Tropical Rainfall Measuring Mission (TRMM) is the first satellite mission of National Aeronautics and Space Administration's (NASA), United States of America, launched in November 1997, dedicated for observing and understanding tropical precipitation and its relation with global climate. TRMM Merged High Quality/Infrared Precipitation estimates obtained from the TRMM '3B42' algorithm provide high resolution satellite-based rainfall estimates. To understand these measurements and to use the derived data products, it would be needed to compare/validate with ground-based measurements and also be aware of the seasonal and coastal dependence of the satellite measurements.

TRMM provides a unique platform for measuring rainfall from space using a passive sensor TRMM Microwave Imager (TMI; Kummerow et al., 1998), an active Precipitation Radar (PR) operating at 13.6 GHz, and a visible and infrared scanner (VIRS) radiometer. Precipitation Radar is the first satellite-based radar (active sensor) to measure rain parameters. TMI is a multi-channel/dual polarized (except in 22 GHz) microwave radiometer (10, 18, 22, 37 and 85 GHz), which provides rain rates over the tropical oceans besides sea surface temperature (SST), sea surface wind speed (SSW), total water vapor (TWV) and cloud liquid water content (CLW).

But by comparison, the more direct measurement of hydrometeors by the TRMM PR would seem to have less uncertainty; however, the PR operates at a single frequency (13.8 GHz) so that microphysical assumptions regarding drop size distributions come into play in the process of correcting the measured reflectivity for attenuation and relating reflectivity structure to rainfall rate (Franklin et al., 2003). Since the PR is a single-frequency, single-polarization, and non-Doppler one, the retrieval of rain intensity from the echo intensity data requires careful interpretation based on sophisticated algorithms which incorporate with peripheral ground validation data (Koru et al., 1996). Since 13.6-GHz radar will only be

sensitive to reflectivities higher than about 17 dB, there is disagreement between PR and TMI (Berg et al., 2006). Anyway, the upcoming Global Precipitation Measurement (GPM) mission will improve upon TRMM by employing a dual-frequency precipitation radar. The 13.6-GHz radar will only be sensitive to reflectivities higher than about 17 dB, whereas at 35 GHz, the minimum sensitivity will be 12 dB, according to recent design specification (Iguchi et al., 2003).

TRMM algorithm 3B42 provides adjusted 3-hour cumulative estimates of rain using merged microwave and infrared (IR) precipitation information (Adler et al., 2000). The TRMM adjusted Geostationary Observational Environmental Satellite (GOES) precipitation index (GPI) (AGPI) is produced by single cases of (nearly) coincident TRMM combined instrument (TCI) using the combined TMI and PR algorithm (Haddad et al., 1997) and VIRS IR data to compute a time and space varying IR-rain rate relationship that matches the TCI IR rain rate. This relation is used to calibrate IR estimates from geosynchronous satellite IR data to form the 3B42 product. Global estimates are made by adjusting the geosynchronous satellite Precipitation Index (GPI) to the TRMM estimates. The monthly TRMM and merged estimate is produced by merging the AGPI with information from rain gauges. The gauge analysis used in this procedure is from the GPCP (Rudolf, 1993). The merger is computed following Human et al. (1997). The 3B42 algorithm provides daily precipitation and root mean square (RMS) error estimates at 1º x 1º latitude/longitude grids in the TRMM domain 40º N to 40º S (Hu_man et al., 2001) for 3B42-V5 and in 3-hourly at 0.25º x 0.25º latitude/longitude grids over 50º N to 50º S for 3B42-V6.

Even though we have been using the data from TRMM satellite for more than 10 years, the effect of coastal dependence and seasonal dependence on data products at each location is still a dilemma. Validation of TRMM 3B42-V5 data has been done using IMD rain gauge data by Narayanan et al. (2005) over Indian land. They found out that 3B42-V5 does not pick up small (< 1mm) and very high (> 80 mm per day) daily average rainfall. Thus, the daily variance (day-to-day variations within the season) estimated by 3B42-V5 is poor compared to the gauge data. The reasons may be related to deficiencies in the IR estimates. However at

pentad (five-day) time scale the correspondence between the two datasets improves and intraseasonal and interannual variations are reasonable. The correlation coefficient over all of India on the monthly scale is high (r^2=0.92) in comparison to 5-day (r^2=0.89) and daily (r^2=0.79) time scale. Chokngamwong and Chiu (2005) have validated 3B42 data using rain gauge data from more than one hundred gauges over Thailand. Their results show that 5-year (1998-2002) daily average rainfall for gauge, 3B42-V5 and 3B42-V6 are 4.73, 5.62 and 4.58 mm/day respectively. The bias and root mean square deviation (RMSD) for V5 are 0.88 mm and 9.71 mm whereas for V6 it is 0.15 mm and 9.60 mm respectively. Scatter plots of daily gauge data versus 3B42 data show that 3B42-V6 correlates better with gauge (r^2=0.44) than V5 (r^2=0.37). The distribution of daily 3B42-V6 rain rate is quite similar to gauge while 3B42-V5 has more rain in the range 5-20 mm/day. The 3B42-V6 TRMM algorithm shows improvement over 3B42-V5 in terms of the bias, RMS difference, and mean absolute difference. Long-term mean rainfall rates from the Tropical Rainfall Measuring Mission (TRMM) Microwave Imager (TMI) and Precipitation Radar (PR) are compared with in-situ measurements by rain gauges on the NOAA TAO/TRITON buoy array in the tropical Pacific by Kenneth et al (2003) [12]. The buoy rain gauges have an advantage over most of the available ground truth data in that the local meteorological effects do not influence them.

The TRMM 3B42-V5 and 3B42-V6 daily rainfall data has been compared both with GPCP as well as IMD Indian gauge data for the duration 1998 to 2003 by Rahman and Gupta (2007). They have compared the all India seasonal (JJAS) total rainfall derived from IMD data with GPCP and 3B42-V6. In all the years the former is having more difference from the later two. Among known sources of errors in the rain retrieval, Toru et al. (1996) studied the vertical variability of the DSD and examined the partial beam-filling effect in terms of their significance with numerical simulations based on the MU radar data. Here, they examined the effect of the height variations of DSD using the MU radar data as realistic examples of the given 'truth' in the simulation. An accurate mean of the ground truth for the TRMM precipitation radar has been developed with the MU radar. Adeyewa and Nakamura (2003) have shown that TRMM PR data overestimates rain in the

tropical rain forest region of Africa when compared with Global Precipitation Climatology Centre (GPCC) rain gauge data (Rudolf, 1993). The 3B43 product, which is the TRMM merged analysis on monthly scale, has the closest agreement with rain gauge data. Nicholson et al. (2003a), using rain gauge data from 515 stations over North Africa shows 3-4% bias for GPCC or GPCP with reference to seasonal rainfall fields (1988-1994). Nicholson et al. (2003b) and excellent agreement of TRMM-adjusted GOES precipitation Index (AGPI) and TRMM merged rainfall analysis with high density (920 stations) gauge data over West Africa on monthly to seasonal time scale. The RMSD of both satellite-derived products is 0.6 mm/day at seasonal scale and 1 mm/day at monthly resolution. The bias of AGPI is only 0.2 mm/day whereas the TRMM-merged product shows no bias over West Africa. The 1ºx1º latitude/longitude product also shows excellent agreement at the seasonal scale and good agreement at monthly scale.

1.3. PRESENT STUDY

The studies of rain rate; rain DSD, its vertical variation and its temporal and altitudinal evolution; Z-R relation and its vertical variation and comparison of the TRMM satellite data have been carried out. Studies of the rain rate characteristics pertain to the stations in Kerala. The rain DSD characteristics in terms of lognormal parameterisation have been brought out and an empirical lognormal model for the variation of rain DSD with rain rate has been derived and validated with data that has not been used in the model derivation. To understand the possible effects of orography on the rain DSD, study and comparison of the behaviour of the DSD at Munnar (a station on the Western Ghat at 1500m altitude) and Kochi (western coastal station) that are situated in the same latitude has been carried out. The vertical profiles of rain DSD has been studied for events with short term and long term averaged data and this eventually leads to the understanding of the effect of averaging in DSD spectrum modification. Altitudinal and temporal evolution of rain DSD for rain spells have been studied experimentally and those results are found to be a proof for the theoretical formulations done in the past. Empirical relations for the Quantitative Precipitation Estimator (Z-R relation) have been derived for different types of rain viz. stratiform and convective during

southwest and premonsoon seasons. This derived relation has been compared with similar results from other parts of the world. The empirical relation for the vertical variation of this Z-R relation has also been derived. TRMM and other satellite derived rain rate data (3B42-V6) is compared with the ground based rain rate measurements with reference to the detection of occurrence of rain and the magnitude of rain or rain rate.

CHAPTER II

EXPERIMENTAL TECHNIQUES, OBSERVATION STATIONS AND DATA AVAILABILITY

CHAPTER II

EXPERIMENTAL TECHNIQUES, OBSERVATION STATIONS AND DATA AVAILABILITY

2.1. INTRODUCTION

Details about the instruments are dealt in this chapter. The principle of operation/measurement, hardware parts of the instruments, installation details, software that handles the instruments, errors in the measurements, data collection and sample data pertains to all the instruments used are being discussed in detail. A Joss waldvogel impact type Disdrometer, a Micro Rain Radar, manual Rain Gauge and a Rapid Response Rain Gauge (RRG) have been used for the current study. The possible errors in the measurements are also discussed. The care to be taken in the deployment of these instruments to reduce these errors is explained. The TRMM satellite-based remote sensing measurements have been also used. The details of this satellite and its precipitation measuring sensors are presented. A brief note on the 3B42 algorithm that will give 3-hourly, .25X0.25 degree spatial resolution data is also given. The data availability and the details about the stations are explained in detail. The proper validation of all these instruments by mutual comparison of the data from all these instruments is explained at the end of this chapter.

2.2. TECHNIQUES OF MEASUREMENTS

The rain DSD and integral rain parameters data are collected using a Disdrometer and a Micro Rain Radar (MRR). Joss Waldvogel Disdrometer is an electromechanical impact type disdrometer made by M/s Distromet Ltd., Switzerland. The momentum imparted by the raindrops that hit the sensor is converted into corresponding an electrical signal. From the amplitude of the signal, the drop size is determined using the terminal velocity-dropsize relation. Then the number density is being measured for each diameter class. This DSD and all the integral rain parameters are given as the output. The temporal resolution could be set from 30 seconds to one

hour. MRR is a continuous wave, frequency modulated, vertically looking Doppler radar operating at a frequency of 24.2 GHz made by M/s METEK GmbH, Germany. The radar used for the present study is Micro Rain Radar-2. The Doppler shift, which is a function of the relative velocity of the raindrops, is measured from the back-scattered power and this determines the size of the drops. The number density in each diameter class is measured and gives the DSD output and also all the integral rain parameters. The temporal resolution could be set from ten seconds to one hour. The conventional Manual Rain Gauge is also used for the present study to measure the accumulated rainfall. A Rapid Response Rain Gauge (RRG) is a fast responding pluvial instrument that gives the rain rate with a finer resolution of one minute. Tropical Rainfall Measuring Mission (TRMM) is the first satellite mission of National Aeronautics and Space Administration's (NASA), United States of America, launched in November 1997, dedicated for observing and understanding tropical precipitation and its relation with global climate. The TRMM and other satellite combined, IR calibrated rain product 3B42 data is also used. The first satellite-based radar Precipitation Radar (PR) and TRMM Microwave Imager (TMI) are the rain measuring instruments onboard TRMM. The details about all the aspects of these instruments/sensors are explained in the following sections.

2.3. DISDROMETER

Disdrometer is an instrument for measuring raindrop size distribution and integral rain parameters continuously and automatically. It can give statistically meaningful samples of raindrops, which could not be obtained previously without a prohibitive amount of work. The instrument transforms the vertical momentum of an impacting drop into an electric pulse whose amplitude is a function of the drop diameter. M/s Distromet Ltd., Switzerland, offers all the necessary equipment for completely automatic drop size data acquisition. An example of a system is shown in Figure 2.1. It consists of a Disdrometer RD-80 and a personal computer or a notebook.

2.3.1. Principle of operation

According to it's principle of operation, the Distrometer RD-80 measures the size distribution of raindrops falling on the sensitive surface of the sensor. From this it is easy to calculate the actual drop size distribution in a volume of air. The range of drop diameters that can be measured spans from 0.3 mm to 5 mm. Drops smaller than 0.3 mm cannot be measured due to practical limits of the measuring principle and are usually of minor importance in applications for which the instrument is intended. Drops larger than 5 mm are very rare because of drop break-up due to the instability of large drops.

The sensor is exposed to the raindrops to be measured. It produces an electric pulse for every drop hitting it. In the processor RD-80, these pulses are divided into 127 classes of drop diameter, and for every drop hitting the sensor a seven bit ASCII code is transmitted to the serial interface of the PC. A computer program, which is delivered with the Distrometer system, can be used to put the data in a suitable format for recording in a file. To reduce the amount of data and to get statistically meaningful samples, the 127 drop size channels are combined into 20 drop size classes distributed more or less exponentially over the available range of drop diameters.

Derivation of the rain parameters

To calculate the drop size distribution, the quantity $N(D_i)$ the number density of drops of the diameter corresponding to size class i per unit volume must first be calculated from the data for every drop size according to the formula

$$N(D_i) = \frac{n_i}{F \times t \times v(D_i) \times \Delta D_i} \qquad (2.1)$$

where n_i = number of drops measured in drop size

D_i = average diameter of the drops in class i

F = size of sensitive surface of the distrometer

$v(D_i)$ = fall velocity of the drop with the diameter *Di*

ΔD_i = diameter interval of drop size class *i*.

The value of n_i is obtained from the measurement. The size of the sensitive area of the distrometer sensor is given by the manufacturer as 50 cm^2. D_i is the average diameter of the drop size class.

Equations by which the rainfall parameters are derived from the rain drop size distribution data are given below. The integral rain parameters are rain rate, accumulated rainfall, liquid water content, radar reflectivity factor and kinetic energy.

Rain rate, $$R = \frac{\pi}{6} \times \frac{3.6}{10^3} \times \frac{1}{F \times t} \times \sum_{i=1}^{20} (n_i \times D_i^3) \quad (2.2)$$

Rainfall, $$RA = \frac{(R \times t)}{3600} \quad (2.3)$$

Accumulated rainfall $$RT = \sum RA \quad (2.4)$$

Liquid water Content, $$W = \frac{\pi}{6} \times \frac{1}{F \times t} \times \sum_{i=1}^{20} \left(\frac{n_i}{v(D_i)} \times D_i^3 \right) \quad (2.5)$$

LWC in g/m^3, $$W_g = \frac{W}{1000} \quad (2.6)$$

Radar Reflectivity Factor, $$Z = \frac{1}{F \times t} \times \sum_{i=1}^{20} \left(\frac{n_i}{v(D_i)} \times D_i^6 \right) \quad (2.7)$$

RRF in Db, $ZdB = 10 \times LogZ$ (2.8)

Kinetic Energy, $EK = \frac{\pi}{12} \times \frac{1}{F} \times \frac{1}{10^6} \sum_{i=1}^{20} (n_i \times D_i^3 \times v(D_i)^2$ (2.9)

Marshal Palmer Intercept parameter,

$$N_0 = \frac{1}{\pi} \times \left(\frac{6!}{\pi}\right)^{4/3} \times \left(\frac{W}{Z}\right)^{4/3} \times W \quad (2.10)$$

Marshal Palmer Slope parameter,

$$\lambda = \left(\frac{6!}{\pi} \times \frac{W}{Z}\right)^{1/3} \quad (2.11)$$

2.3.2. Block diagram/components of the Disdrometer

The RD-80 Disdrometer consists of 2 units (see Figure 2.1). The processor and the sensor which is exposed to rain. A cable, 20 metre long, is used to connect the sensor and the processor.

The sensor transforms the momentum of an impacting drop into an electric pulse, whose amplitude is roughly proportional to the momentum. The sensor consists of a cylindrical metal housing, containing an electromechanical transducer and an amplifier module. The processor contains circuitry to eliminate unwanted signals, mainly due to acoustic noise to reduce the 90 dB dynamic range of the sensor signal and to digitize it into a 7-bit code at the output for every drop, hitting the sensitive surface of the sensor.

The sensor consists of an electromechanical unit and an amplifier module in a common housing. A conical Styrofoam body is used to transmit the mechanical impulse of an impacting drop to a set of moving coils in a magnetic field. The Styrofoam body and the two coils are fixed together rigidly.

Figure 2.1. The Disdrometer processor and sensor.

At the impact of a drop the Styrofoam body together with the two coils move downwards and a voltage is induced in the sensing coil. This voltage is amplified and applied to the driving coil such that a force counteracting the movement is produced. As a consequence the excursion is very small and it takes very little time for the system to return to its original resting position and therefore to get ready for the next impact of another drop. The amplitude of the pulse at the output of the amplifier is the measure of the size of the drop that caused it.

2.3.3. Installation of the Disdrometer

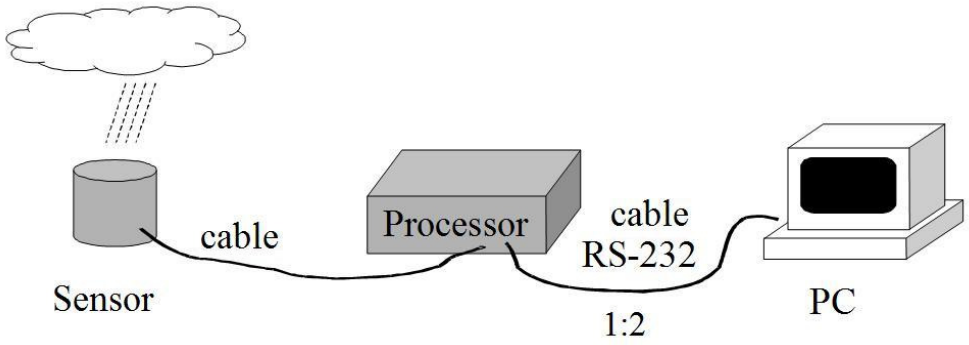

Figure 2.2. Schematic diagram shows the connection of the components of the Disdrometer.

The processor serves three functions, (1) It supplies power to the sensor, (2) It processes the signal from the sensor and (3) It contains circuits for testing the performance of the instrument. The processor contains circuits to eliminate unwanted signals, mainly due to acoustic noise. It is connected to a personal computer, which acquires the data through a program. In the processor RD-80 pulses are divided into 127 classes of drop diameter, and for every drop hitting the sensor a seven-bit ASCII code is transmitted to the serial interface of the personal computer. A computer program, which is delivered with the Disdrometer system, can be used to put the data in a suitable format for recording on a file. In order to get statistically meaningful samples and to reduce the amount of data, the program reduces the number of classes to 20. The schematic diagram that shows the connection of the components is shown in figure. 2.2.

To reduce the error that will be present because of the careless deployment of the Disdrometer, we have taken following steps,

1) Deployed in a quiet surrounding, since high acoustic noise levels will impair the measurement of small drops.

2) Deployed such that the effect caused by strong winds (producing turbulence at the edges of the transducer) is absent.

3) The prevention from flooding and

4) Without resonance and splashing by raindrops.

Error possibilities

The possible errors associated with this instrument are discussed here. First, the Disdrometer has a self-noise control. When the ambient noise is loud, smaller drops are not counted. When the noise level is high during extremely high rainfall rates, a noise suppression circuit is activated. This results in a reduction in the small drop count. This is a design feature built into the Disdrometer to minimise the likelihood of

noise being counted as small drops. Extrapolating to include the ‘‘missing’’ small raindrops reduces, but does not eliminate, this underestimation. (Nystuen, 1998). Another reason for underestimation during extremely high rainfall rates is that a finite time is needed for the instrument to recover from a drop strike and be ready for the next drop. This error is called dead time error and it can be corrected using a correction algorithm that is a multiplication matrix. This dead time correction was first applied by Sheppard and Joe (1994) and the details of applying the correction are explained in that publication. Based on this, the manufacturer now supplies the correction matrix along with the instrument. Here, the dead time correction is applied, using the correction matrix supplied by the manufacturer and following Sheppard and Joe (1994). A third possibility of error is that water accumulation on the sensor head may change its calibration, especially for drops directly striking pools or existing drops of water on the sensor head. The detection of smaller drops during high rain rates is a possible source of error, but there is no way as on today to eliminate it completely. Another possibility is the erroneous measurement of number density especially on large drop end (Tokey et al., 2005). The estimated accuracy of the Disdrometer system is ± 5% (Verma and Jha, 1996). In the present case, the sensor is mounted such that acoustic noise and wind effects are reduced to a minimum.

The accumulated rainfall derived from the rain rate data from the Disdrometer deployed at Thiruvananthapuram has been validated using a manual rain gauge deployed nearby. They have been found to agree reasonably well (Sasi Kumar et al., 2007).

2.3.4. Data collection

The output data from the Disdrometer is being logged automatically into a computer as per the temporal resolution of the data is set for. The data cables from both the Disdrometer and from the MRR have been connected to one computer and the data has been logged every minute to this computer. The data acquisition system used for

this is shown in the figure 2.3. The processor of the Disdrometer and the connection box of the MRR are seen in the figure.

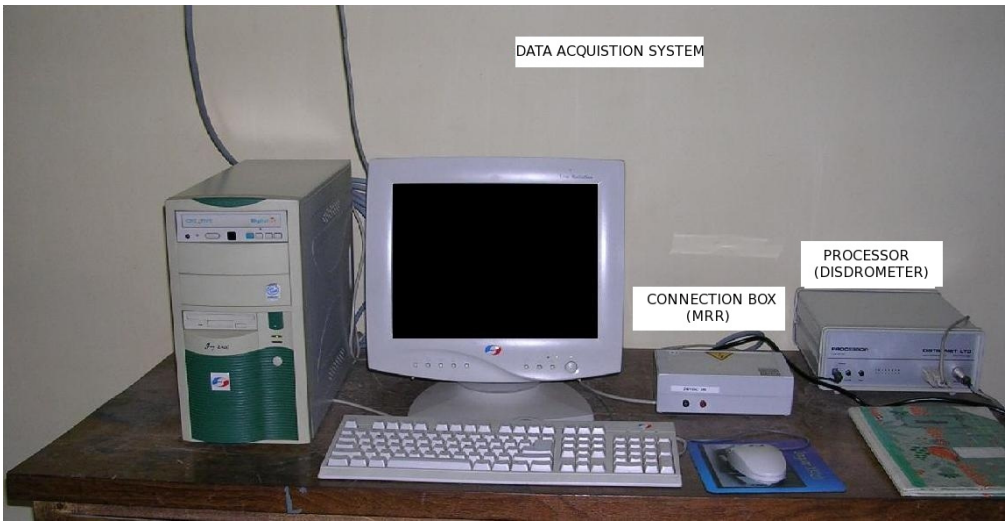

Figure 2.3. The data acquisition system set-up.

Disdrometer program

There is an in-built programme being delivered with the Disdrometer called *Disdrodata.* The purpose of the program *Disdrodata* is to enable users of a RD-80 Disdrometer to record and evaluate drop size measurements with a personal computer or notebook. To calculate the drop size distribution, equation 2.1 could be used. The value of n_i is obtained from the measurement. The size of the sensitive area of the distrometer sensor is given by the manufacturer as 50 cm^2. D_i is the average diameter of the drop size class. The DSD data could found out this way and all the integral parameters could be calculated using the equations given at the beginning of this section.

2.3.5. Sample data

The first two columns of the output file contain date and time. 3rd to 22nd columns give the number of drops in different size classes that hit on the sensor for the duration set as the sampling time. 23rd column gives the size of the large drops present during that time interval. Rain rate is given in the 24th column. A sample data file is shown in the figure 2.4.

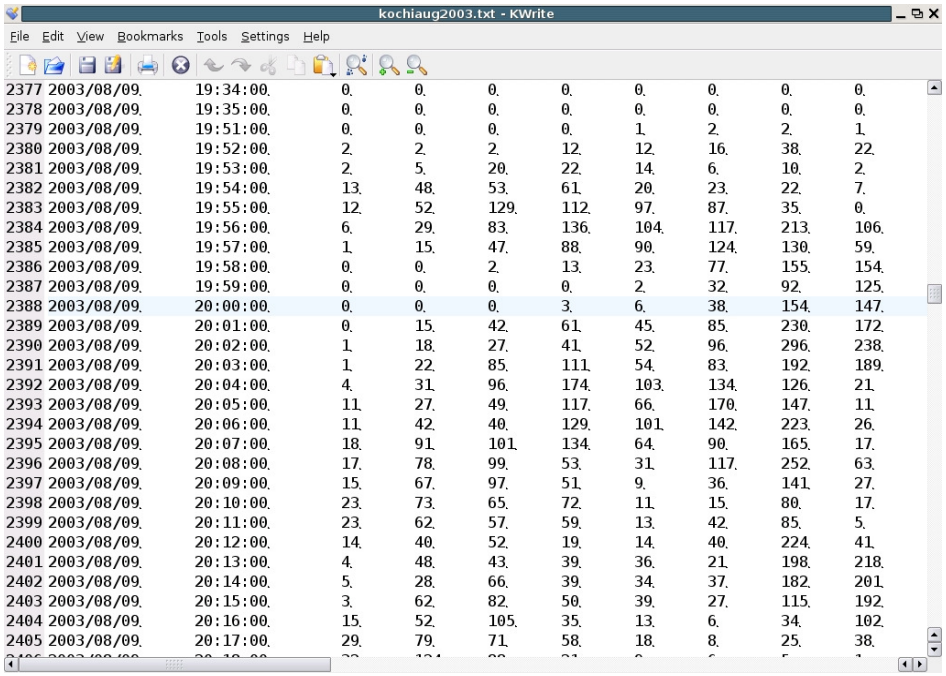

Figure 2.4. A sample Disdrometer raw data file.

The raw data will be corrected for dead time error using the correction matrix that has been provided along with the instrument by the manufacturer (the details about the dead time error is given in the section 2.2.3). Then the number of drops per cubic metre per mm interval (DSD) is derived. All the integral rain parameters can be derived from this DSD using the equations given in the section 2.3.1.

2.4. MICRO RAIN RADAR (MRR)

The MRR used in the current study is MRR-2 manufactured by M/s METEK GmbH, Germany. It is a vertically looking, frequency-modulated, continuous-wave Doppler weather radar capable of giving rain DSD and all the integral rain parameters at different heights operating at a frequency of 24 GHz (K-band) with a beam width of 2º. The radiation is transmitted vertically into the atmosphere where a small portion is scattered back to the antenna from rain drops or other forms of precipitation. Very small amounts of precipitation below the threshold of conventional rain gauges are detectable. Due to the large scattering volume (compared to in situ sensors) statistically stable drop size distributions can be derived within few seconds. The droplet number concentration in each drop-diameter bin is derived from the backscatter intensity in each corresponding frequency bin. In this procedure the relation between terminal falling velocity and drop size is exploited. The backscatter cross section of rain drops increases with the fourth power of the droplet diameter, if the diameter is small compared to the wavelength (Rayleigh scattering). This is why a high frequency is useful in order to increase the sensitivity with respect to small drops. At very high frequencies the quantitatively interpretable height range becomes limited due to attenuation at moderate and higher rain rates. At 24 GHz, which is used here, attenuation effects may be noticeable but should be weak enough to be correctable with sufficient accuracy. The specifications of MRR are given in the table II.1.

The main features of MRR are (1) vertical profiles of rain rate and liquid water content up to 6 km (3.7 miles), (2) computes detailed drop size and distribution output, (3) user adjustable averaging intervals and height resolution, (4) no maintenance, (5) high system reliability, (6) remote/ long term unattended operation, (7) high quality measurements, (8) no wind, sea spray or evaporation induced errors, (9) adjustable averaging intervals 10 - 1800 s, (10) height range more than 2000 m (1.2 miles) with 30 range gates and (11) battery or mains power.

2.4.1. Principle of operation

Due to the falling velocity of the rain drops relative to the stationary antenna there is a frequency deviation between the transmitted and the received signal (Doppler frequency). This frequency is a measure of the falling velocity of the rain drops. Because drops with a different diameter have a different falling velocity the backscattered signal consists of a distribution of different Doppler frequencies. The spectral analysis of the received signal yields a spectrum which does not consist of one single line but of a wide distribution of lines corresponding to the Doppler frequencies of the signal.

The measurements also allow easy detection of the ice phase and the melting layer, and the measured vertical profiles may eventually be used to correct weather radar measurements. The system can be used for the observation of the melting layer, now-casting of precipitation events (it will detect the start of rain from ground level to high above the radar several minutes before the start of rain at ground level) and calibration of weather radar signals. Due to the principle of measurement it is ideal for the determination of rain parameters at wind exposed sites (eg. ships or off-shore), because the measurements are not influenced by wind errors. It is a highly reliable system suitable for use in remote and extreme environments, requiring minimal maintenance and is suited for long term unattended operation.

Scattering at Raindrops

In the case of rain always a large number of drops exist within the scattering volume. Atypical number density at moderate rain (1 mm/h) is 2000 m^{-3}. The scattering volume (500 m height, 50 m range resolution) has a size of about 10^4 m^3. That is $2x10^7$ drops are in the scattering volume. As the drop position is irregular in space the phases of the scattering signals of each drop are statistically independent. Therefore, the total power of the echo is obtained by adding up the power of all individual scattering signals. In this case the spectrum within one range gate consists of

a distribution of lines corresponding to the velocity distribution of the rain drops. The frequency spectra obtained in this way with the FM-CW radar do not differ within the Nyquist interval from those spectra which would be obtained by a pulsed Doppler radar with the same wave length.

Principle of measurement of the MRR

Basic concept

A Doppler radar is a radar that produces a velocity measurement as one of its outputs. Doppler radars may be Coherent Pulsed, Continuous Wave, or Frequency Modulated. A continuous wave (CW) doppler radar is a special case, which provides only a velocity output. Early doppler radars were CW, and it quickly led to the development of Frequency Modulated (FM-CW) radar, which sweeps the transmitter frequency to encode and determine range. The CW and FM-CW radars can only process one target normally, which limits their use.

Continuous-wave radar system is a radar system where a continuous wave radio energy is transmitted and then received from reflected objects. A known stable frequency is transmitted and return signals received from targets are shifted away from this frequency based on the Doppler effect. The main advantage of the CW radars is that they are not pulsed, and thus have no minimum or maximum range (although the broadcast strength imposes a practical limit on the latter) as well as maximizing power on the target. However they also have the disadvantage of only being able to detect moving targets, as motionless ones (along the line of sight) will not cause a Doppler shift and the signal from such a target will be filtered out. CW radar systems thus find themselves being used at either end of the range spectrum, as radio-altimeters at the close-range end (where the range may be a few feet) and long distance early warning radars at the other.

CW radars have the disadvantage that they cannot measure distance, because there is no time reference. In order to correct for this problem, frequency shifting methods can be used. When a reflection is received the frequencies can be examined, and by knowing when in the past that particular frequency was sent out, you can do a range calculation similar to using a pulse. It is generally not easy to make a broadcaster that can send out random frequencies cleanly, so instead the frequency-modulated CW radars (FMCW), use a smoothly varying "ramp" of frequencies up and down. For this reason they are also known as a chirped radars.

The measuring principle of the micro rain radar is based on electromagnetic waves of a frequency of 24 GHz. In contrast to normal rain radar devices, the signals are emitted vertically into the atmosphere. A part of the emitted signal is scattered back to the antenna (paraboloid dish) from rain drops and is registered there. The output signal is transmitted continously (CW mode in contrast to pulsed radars).

The MRR is a Doppler radar. While falling to the ground the raindrops are moving relative to the antenna on the ground, which is both transmitter and receiver. Due to the falling velocity of the rain drops relative to the stationary antenna there is a frequency deviation between transmitted and the received signal. This frequency is the measure for the falling velocity of the rain drops.

Derivation of DSD and integral rain parameters

The droplet number concentration in each drop-diameter bin is derived from the backscattered intensity in each corresponding frequency bin. In this procedure the relation between terminal falling velocity and drop size is exploited. Since the backscatter cross section of rain drops increases with the sixth power of the droplet diameter, if the diameter is small compared to the wavelength (Rayleigh scattering), a high frequency is useful in order to increase the sensitivity with respect to small drops.

MRR uses a frequency modulated Gunn-diode-oscillator with integrated mixing diode while conventional weather radar uses the pulse radar mode. Thus a

MRR can measure hydrometeors particle size distributions. The retrieval of range-resolved Doppler spectra follows the method described by Strauch (1976).

The derivation of the rain drop size distribution and the integral rain parameters is briefly explained below.

The precipitation particle size distribution N(D) is given by

$$N(D) = \frac{\eta(D)}{\sigma(D)}, \tag{2.12}$$

where D is drop diameter, $\sigma(D)$ is the back scattering cross-section and $\eta(D)$ is the spectral reflectivity as a function of D.

The MRR will also give the vertical structure of the radar reflectivity (Z in dBZ), liquid water content (LWC in g/m^3), rain rate (RR in mm/h) and fall velocity (V in m/s).

The differential rain rate is equal to the volume of the differential droplet number density $\frac{\pi}{6} N(D)D^3$ multiplied by the terminal fall velocity V(D). From this product the rain rate is obtained by integration over the drop size distribution.

$$RR = \frac{\pi}{6} \int_0^\infty N(D)D^3 V(D)dD \tag{2.13}$$

The radar reflectivity factor is defined as the sixth moment of the rain drop size distribution and is given by

$$z = \int_0^\infty N(D)D^6 dD \tag{2.14}$$

The liquid water content is obtained by the expression

$$LWC = \rho_W \frac{\pi}{6} \int_0^\infty N(D) D^3 dD \tag{2.15}$$

where ρ_w is the density of water.

A physical reasonable definition for fall velocity would be the velocity of those drops which deliver the maximum contribution to the rain rate. The fall velocity is estimated by the spectra volume density,

$$v = \frac{\lambda}{2} \frac{\int_0^\infty \eta(f) f df}{\int_0^\infty \eta(f) df} \tag{2.16}$$

where λ is the wave length and f is the Doppler frequency shift.

The relation between fall velocity and drop diameter will be obtained by appropriated analytical form by Atlas et al. (1973)

$$v(D) = 9.65 - 10.3 \times Exp(-0.6D) \tag{2.19}$$

where 0.109 mm ≤ D (mm) ≤ 6 mm

To estimate the impact of using Mie theory for computing the backscatter cross-section (Loffler-Mang and Kunz, 1999), The backscattering cross-section σ_{Mie} of a dielectric sphere for a plane electromagnetic wave is given by

$$\sigma_{Mie} = \frac{\lambda^2}{4\pi} \left| \sum_{n=1}^{\infty} (-1)^n (2n+1)(a_n - b_n) \right|^2, \tag{2.20}$$

where a_n and b_n are derived from Bessel and Hankel functions.

2.4.2. Components of the instrument

Radar Frontend

The core component of the radar is a frequency modulated gunn-diode-oscillator with integrated mixing diode. The nominal transmit power is 50 mW. The assembly and function of the radar frontend is explained with reference to of the block diagram in figure 2.5. The linear polarized RF-power is fed through a wave guide and a horn, which represents the feed of an offset paraboloid dish of 60 cm diameter (not shown). The backscattered signal is received with the same antenna assembly (monostatic radar). The received signal is detected by a mixing diode which is mounted in the wave guide between gunn-oscillator and horn. This diode, which is biased with a fraction of the transmit signal, acts as mixer. This simple configuration cannot be operated in pulsed mode, because during shut off of the transmitter, the receiver does not work either. When operated in continuous wave mode, at the diode output a voltage appears, which depends on the phase difference between the transmit and receiving signal (homodyne principle), and which is used for the further signal processing.

The MRR system consists of an antenna dish, radar, receiver unit and RS-232 data transmission interface. PC based software is available for on line control, data visualization, transfer and storage. The MRR can be used to calibrate other radars for better performance

The radar antenna is an offset paraboloid dish, which has a vertical beam orientation without need of a horizontal alignment. Due to this mounting angle the rainwater can drain off without any problem. In order to avoid disturbances from snow, which could precipitate in the antenna dish, the system provides an optional offered heating.

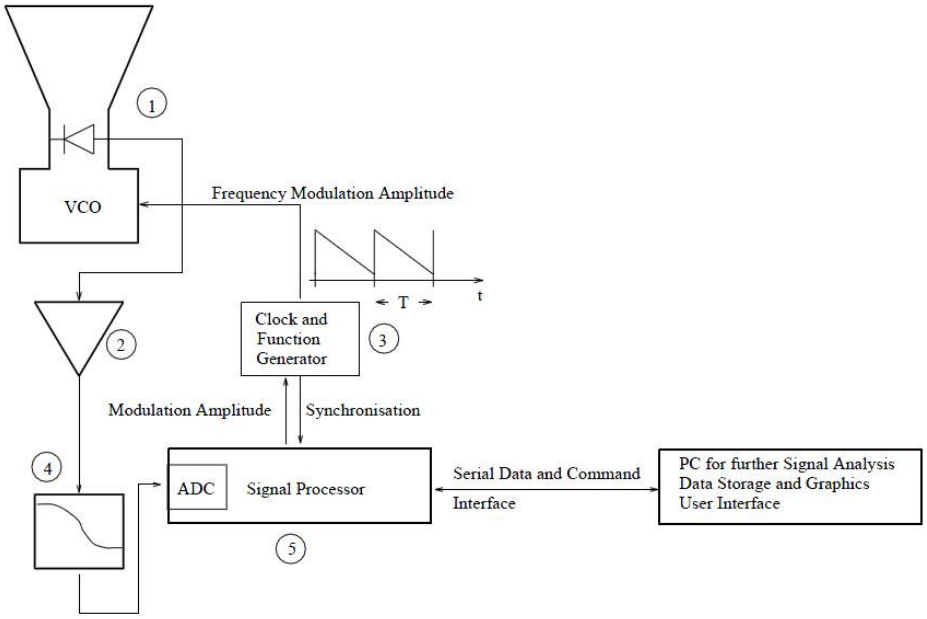

Figure 2.5. Block diagram of MRR. [1: Gunn-Diode-Oscillator with mixing diode, 2: Low noise IF amplifier with equalizer function, 3: Clock- and modulation generator with variable modulation amplitude, 4: Anti aliasing filter, 5: Digitaler signal Processor (23 FFT/s mit 4096^{2} points)].

Figure 2.6. Micro Rain Radar (MRR) deployed in the premises of our institute, Centre for Earth Science Studies (CESS), Thiruvananthapuram.

Sl. No.	Specification	MRR
1	Transmit frequency	24.1 GHz (K-Band)
2	Transmit power	50 mW
3	Receiver-Transmitter Antenna	offset -parabolic, 0.6 m diameter
4	Beam Width	2°
5	Modulation	Frequency modulated continuous wave
6	Height resolution	35 ~ 200 m
7	Averaging time	10 ~ 3600
8	Height range	29 range gates
9	Interface	RS232 9600 ~ 57600 Baud
10	Power supply	24 VDC / 25 W
11	Weight	12 kg
12	Dimensions	0.6 m^3

Table II. I. Specifications of the Micro Rain Radar (MRR) deployed in the premises of CESS, Thiruvananthapuram.

2.4.3. Installation of the MRR

MRR consists of indoor and outdoor units. Indoor unit has a MRR connection and data acquisition system. Out door unit consists of antenna, electronics unit and radar module. There is a data cum power cable that will connect between these components. The platform where the antenna is connected should be very parallel to the earth's surface. Then the default screw that connects the stem and the radar antenna has been set in such a way that the electromagnetic beam will emanate very vertically upward. The MRR deployed on the terrace of our institute is shown in figure 2.6.

Error possibilities in MRR

The possible errors in the measurements of rain DSD and integral rain parameters using the MRR are explained below. For the relation of terminal falling velocity versus drop size (equation 2.19) stagnant air has been assumed.

In real atmosphere the drops are carried with the wind (the inertial length scale of rain drops is on the order of 10 m). Thus the velocity in the equation 6 is relative to the ambient air velocity. But in the present study, most of the analysis has been done for low intensity rain, during which the air velocity will be very less. So, the error due to this assumption does not come into picture. Turbulence, i.e. the random fluctuations of vertical wind within the scattering volume or within the averaging time interval causes a systematic bias because the effects of up and downwind do not compensate each other completely due to the non-linear velocity-diameter relation. Usually turbulence leads to an underestimation of LWC and RR and not affecting much to the DSD measurement. Other chance for error is due to the non-spherical shape of the rain drops. But, since the MRR has been calibrated for natural rain, this error is reduced. Because of the change of phase of water at heights like 0 degree isotherm, the back-scattered power will increase and thus cause an over estimation of measurement. But here our analysis is limited to a height of maximum around 4000 m and thus no possibility of ice phase in these heights. Up to this height the possibility to have pollution in the data due to the effect of bright band is very less. Chances of attenuation of the electro-magnetic radiation during higher rain rates and also at higher altitudes are possible. Since, in the present study we have used rain episodes having low rain rates, the possibility of error due to this fact is absent. The electronic noise correction rendered the radar particle size retrievals below 0.7 mm drop diameters invalid; exponential extrapolation of the spectrum below drop diameters of 0.7 mm decreased the rain intensity up to 20% (Loffler-Mang and Kunz, 1999).

2.4.4. Data collection

Control program

The MRR generates a height range resolved Doppler spectrum. The data processing is performed by a DSP which is placed in housing directly below the antenna support. The measured data are transmitted by a serial RS-232 port. This port is also used for the device control. If the MRR-2 is connected to a PC, the control, the calculation of further values, and the recording of the data can be done with the MRR-2-control program.

The temporal resolution for the data collection could be adjusted from 10 seconds to 1 hour. The height resolution also could be selected from 35 meters to 200 meters. There are 30 range gates for MRR. If we set the resolution as 35 meters, measurements will be done up to 1050 meters and if it is set to a resolution of 200 metre, measurements will be there up to 6000 metres. A software that will be provided with the instrument viz. "Graphic" is useful for data analysis and data visualisation.

2.4.5. Sample data

The sample raw data file is shown in the figure 2.7. The first raw is the header line where the data and time are available. The sampling time is also provided in this line. The second raw gives the height steps horizontally in each column. The back-scattered spectrum which starts from F00 to F64 at the 66^{th} row is given from third raw onwards. From there, the number of drops per cubic meter per mm interval of diameter in each height ranges for 46 diameter classes are given in the next 46 rows. The rain rate, liquid water content, fall velocity and radar reflectivity are given in the last 4 rows. The data pertains to successive one-minute events is gives in the successive rows as sets of rows as explained above.

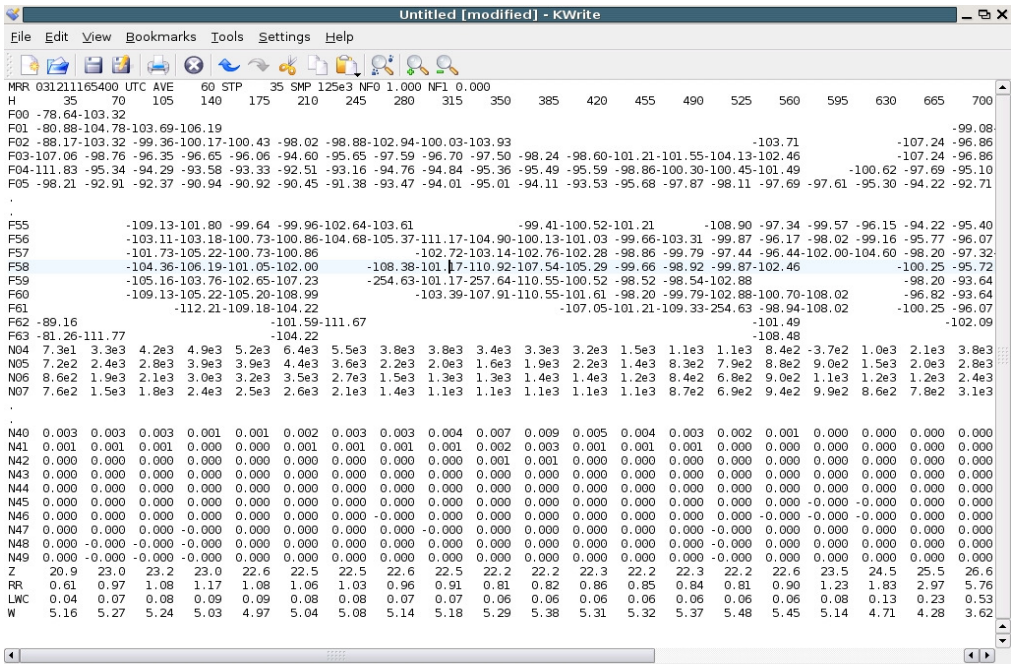

Figure 2.7. Sample raw data file from The MRR.

2.5. MANUAL RAIN GAUGE

Manual Rain Gauge is a simple pluvial instrument by which man started his systematic rainfall measurement. It measures the rainfall accumulation for a particular period for which we make measurement. It consists of a collecting jar with predefined surface area through which the rain water collection is done. The raingauge should be placed in a plane surface such that the plane of the collecting surface should be parallel to the surface of the earth.

The equation to find out the rain rate in mm is, Rainwater measured in mm=Volume of the water collected/surface area through which the water has been collected.

For the measurement of rainfall, a measuring jar is used. Grading in the measuring jar represent the rain in mm. When ever is measurement is needed, the water from the collection jar is poured in to this measuring jar and thus measures the rainfall.

2.6. RAPID RESPONSE RAIN GAUGE (RRG)

Rapid Response Raingauge (RRG) is a microprocessor based system designed for automatic monitoring of Rain rate. The rain gauge consists of a sensor kept outdoors and is connected to a controller kept indoors. The sensor consists of two parts, (1) 100 sq.cm water collector which collects the rain water and (b) Drop forming mechanism that converts the rain to drops with uniform size. Water is guided from the stilling well through a small bore (hole) to the nozzle. Precise bore orifice is used to form the drop. A drain line is provided for the water to get drained. The water collected is channelled to the stilling well which is already filled with water. When extra water from the collector enters the stilling well the excess water comes out through the small bore in the drop forming nozzle where water drops are formed. Platinum electrodes mounted directly on the sensor sense the water drops. A preamplifier with an LED indication is provided to drive long cables where the distance between the sensor and the controller become too large. The drop size is a function of the nozzle diameter and rate at which the drops are formed. From this drop count, the rain rate is measured.

2.7. TROPICAL RAINFALL MEASURING MISSION (TRMM)

Tropical Rainfall Measuring Mission (TRMM) is the first satellite mission of National Aeronautics and Space Administration's (NASA), United States of America, launched in November 1997, dedicated for observing and understanding tropical precipitation and its relation with global climate. There are two sensors that will help in rain retrieval. The details about the sensors are explained in the following sections.

2.7.1. Components of the sensors and Principle of operation

Precipitation sensors [(Precipitation Radar (PR) and TRMM Microwave Imager (TMI)]

TRMM provides a unique platform for measuring rainfall from space using a passive sensor TRMM Microwave Imager (TMI; Kummerow et al., 1998), an active Precipitation Radar (PR) operating at 13.6 GHz, and a visible and infrared scanner (VIRS) radiometer. Precipitation Radar is the first satellite-based radar (active sensor) to measure rain parameters. TMI is a multi-channel/dual polarized (except in 22 GHz) microwave radiometer (10, 18, 22, 37 and 85 GHz), which provides rain rates over the tropical oceans besides sea surface temperature (SST), sea surface wind speed (SSW), total water vapor (TWV) and cloud liquid water content (CLW). Passive estimates from the TMI are a less direct rainfall estimate since the radiometer responds to integrated liquid water, not just to raindrops. But by comparison, the more direct measurement of hydrometeors by the TRMM PR would seem to have less uncertainty; however, the PR operates at a single frequency (13.8 GHz) so that microphysical assumptions regarding drop size distributions come into play in the process of correcting the measured reflectivity for attenuation and relating reflectivity structure to rainfall rate (Franklin et al., 2003). Since the PR is a single-frequency, single-polarization, and non-Doppler one, the retrieval of rain intensity from the echo intensity data requires careful interpretation based on sophisticated algorithms which incorporate with peripheral ground validation data (Koru et al., 1996). Since, 13.6-GHz radar will only be sensitive to reflectivities higher than about 17 dB, there is disagreement between PR and TMI (Berg et al., 2006). Any way, the upcoming Global Precipitation measurement (GPM) mission will improve upon TRMM by employing a dual-frequency precipitation radar. The 13.6-GHz radar will only be sensitive to reflectivities higher than about 17 dB, whereas at 35 GHz, the minimum sensitivity will be 12 dB, according to recent design specification (Iguchi et al., 2003).

The sensors and the scanning geometry of the TRMM are shown in figure 2.8.

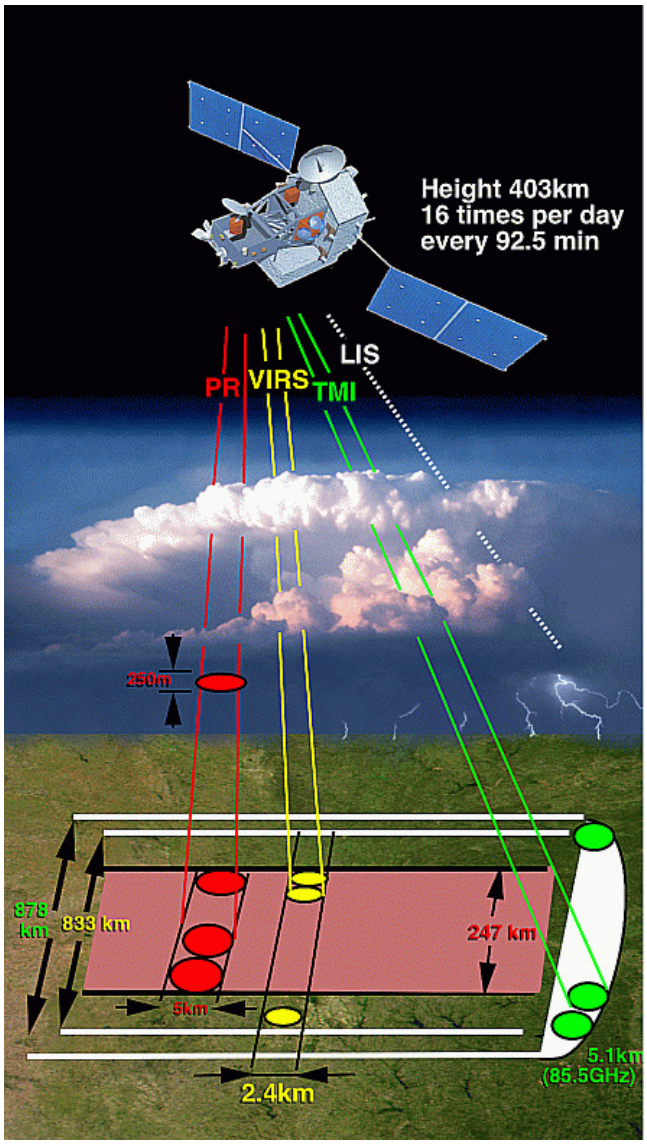

Figure. 2.8. Tropical Rainfall Measuring Mission (TRMM) sensors and scanning geometry.

2.5.2. Data products: TRMM 3B42 algorithm for rain estimates

Algorithm 3B-42 produces Tropical Rainfall Measuring Mission (TRMM) merged high quality (HQ)/infrared (IR) precipitation and root-mean-square (RMS)

precipitation-error estimates. These gridded estimates are on a 3-hour temporal resolution and a 0.25-degree by 0.25-degree spatial resolution in a global belt extending from 50 degrees south to 50 degrees north latitude. The main difference between TRMM 3B42-V5 and 3B42-V6 is that the resolution of 3B42-V5 is on a 1ºx 1º grid and covers the global tropics (40ºS-40ºN latitude), whereas the 3B42-V6 product is in 3-hourly on a 0.25ºx 0.25ºgrid and covers 50ºS-50ºN latitude. The 3B-42 estimates are produced in four stages, (1) the microwave estimates precipitation are calibrated and combined, (2) infrared precipitation estimates are created using the calibrated microwave precipitation, (3) the microwave and IR estimates are combined, and (4) rescaling to monthly data is applied. Each precipitation field is best interpreted as the precipitation rate effective at the nominal observation time.

The data has been downloaded from the web portal of NASA through anonymous FTP. The binary data obtained is converted into ASCII format. The data has a temporal resolution of 3 hours and corresponding to an area averaged over 0.25 X 0.25 degrees latitude longitude grid. The program written in FORTRAN, derives the needed data corresponding to the grid where the each station lies. The 3-hourly accumulated rainfall has then been derived from the 3-hourly rain rate for the comparison with the Disdrometer data. The maximum temporal resolution of the data that has been compared by rahman and Senguptha (2007) is daily. But in the current analysis, we have compared 3-hourly accumulated rainfall that is the maximum temporal resolution of the rainfall data available from TRMM.

2.8. COMPARISON OF THE DATA FROM THE INSTRUMENTS

2.8.1. Comparison between Disdrometer and Manual rain gauge

Daily rainfall was measured using a manual rain gauge at the site where the Disdrometer was installed in Kochi and Thiruvananthapuram. These data were compared with the total rainfall computed from the rain rate values obtained using the Disdrometer, as a means of validating the Disdrometer data. The data from the manual

rain gauge represented the rainfall received between measurements on consecutive days. The Disdrometer data corresponding to this period was taken for comparison. In general, we found that the total rainfall obtained from the manual rain gauge was less than that computed from the Disdrometer data. Direct comparison was difficult because the Disdrometer records data every minute, while manual data were recorded in the mornings of working days only. But the cumulative rainfall from both measurements shows a more or less linear relationship, indicating that the values were more or less consistent, except for the under-estimation in the case of the manual rain gauge. Two examples for June and July 2005 are shown in figure 2.9. The rain gauge data from the National Technical University of Athens station has shown good agreement with rainfall depth data derived from the Disrometer (Baltas and Mimikou, 2002). Despite time-height ambiguity and other physical differences, a good agreement is found between radar and Disdrometer measurements even at high rain rates (Tokey and Dickens, 2000). According to Roy et al. (2005), rainfall data agreed well with self-recording rain gauges.

When comparing the data from the manual rain gauge and the Disdrometer, it is useful to note the following points. The Disdrometer is a very sensitive instrument that detects even a single drop that falls on its sensor. Consequently, rain rates as low as 0.001mm/hr are recorded. But there are certain factors that affect its measurement. The most important factor is that the Disdrometer requires electric power, and hence, loss of power could lead to loss of data. Further, since the Disdrometer is sensitive only to raindrops of diameter greater than 0.3mm, the contribution from smaller drops to total rainfall, though small, is not accounted for. Similarly, since all drops larger than 5.3mm fall into the same size class, there is a possibility that the mean drop size may be underestimated if very large drops are present, as could happen during heavy rain. All these would tend to reduce the total rainfall obtained from the Disdrometer. Another possibility is that of raindrops splashing on the surface, and some of the droplets thus produced falling on the sensor. The company recommends keeping the

sensor at the surface level to reduce the impact of winds that could produce spurious data. The sensor was, accordingly, kept at surface level at Thiruvananthapuram and Munnar. In Kochi, however, it was kept on a low stool, so that the possibility of rainwater splashing on the ground and falling on the sensor was virtually zero. Even in the case of rain water splashing onto the sensor, the drops would have speeds much below the terminal velocity, and hence their contribution cannot be large. On the other hand, there would be some loss of water from the manual rain gauge due to evaporation, as may happen when a generally sunny period is interspersed with light rainfall, and also due to the fact that the water in the container may not always be completely transferred to the measuring jar. In spite of taking into account all these factors, the discrepancy remains unexplained. The only possible reason for the discrepancy seems to be calibration errors. The manual rain gauge is certified by the India Meteorological Department, while the Disdrometer is company calibrated. For the time being, therefore, we leave this discrepancy unresolved.

2.8.2. Comparison between Disdrometer and Rapid Response Rain gauge (RRG)

The RRG data is available in a collocated basis at Thiruvananthapuram and Kochi. The comparison of the rain rate data obtained from these instruments have been done for April 2001, a premonsoon month and for June 2001, a southwest monsoon month (figure 2.10). A good correlation coefficient of 0.77 is there for April and that of 0.88 is obtained for June.

The time series comparison of the rain rate (corresponding to short rain events) data at Kochi is shown in figure 2.11. Sometimes the comparison is found to be excellent as shown for May 31st event. Generally, a visual comparison tells us that both the instruments agree in rain rate measurements.

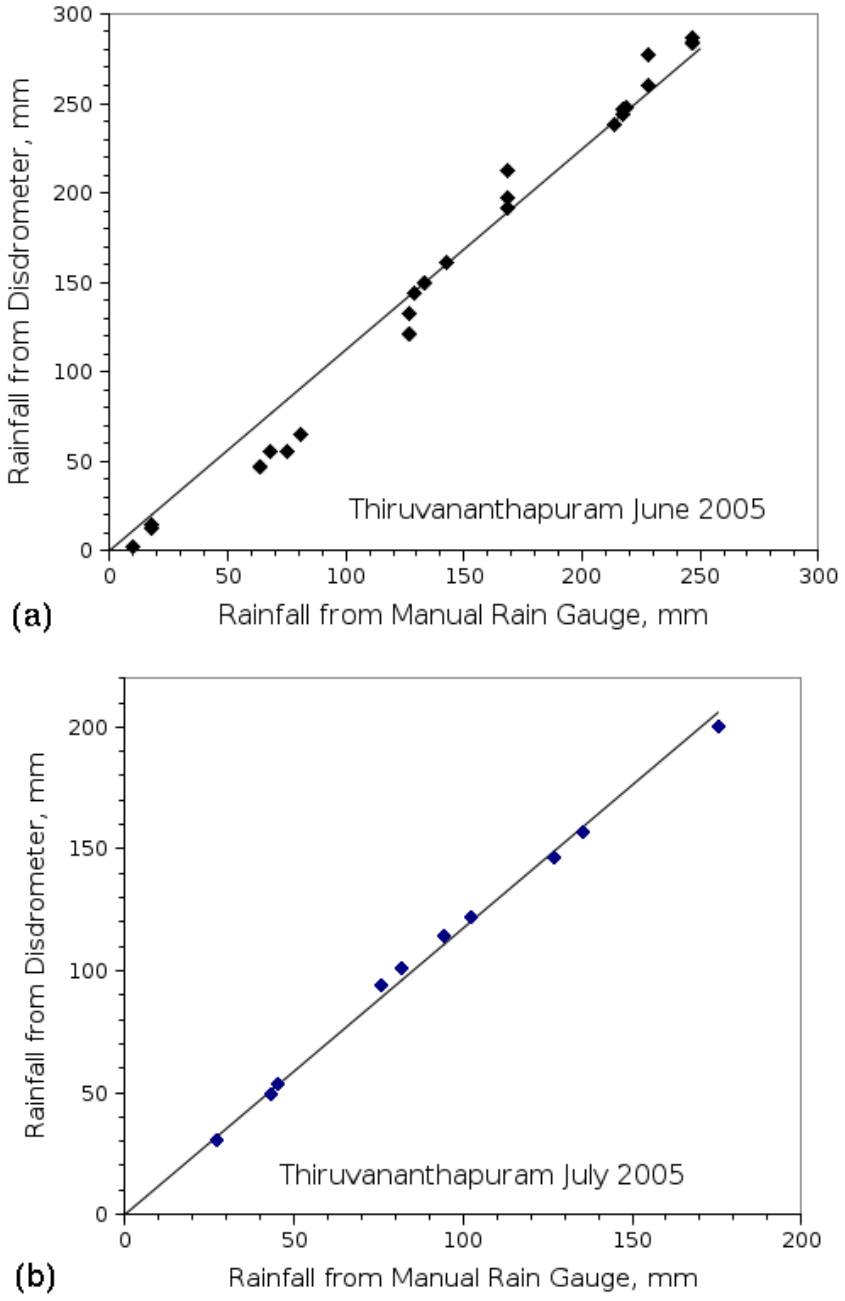

Figure 2.9. Comparison between rainfall data obtained from a Manual rain gauge and a Disdrometer.

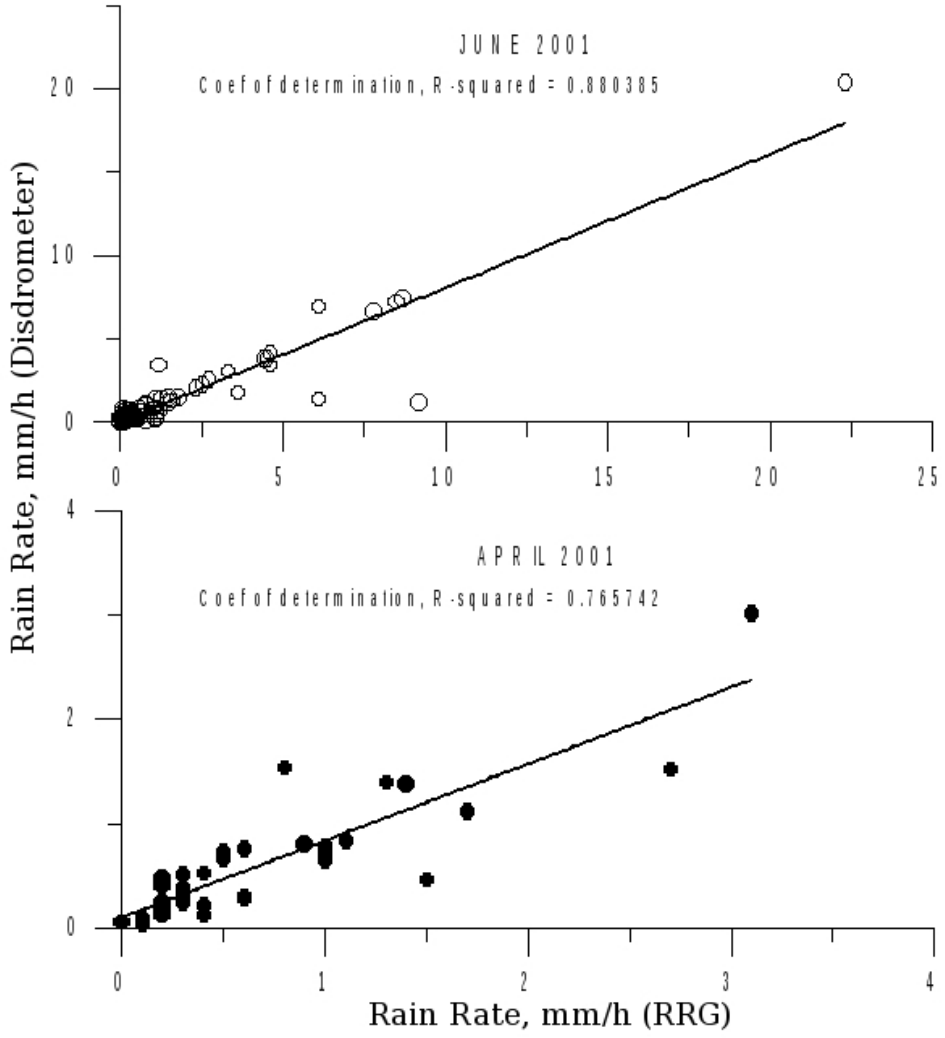

Figure 2.10. Comparison of rainfall measurements from Disdrometer and from Rapid Response Raingauge at Thiruvananthapuram.

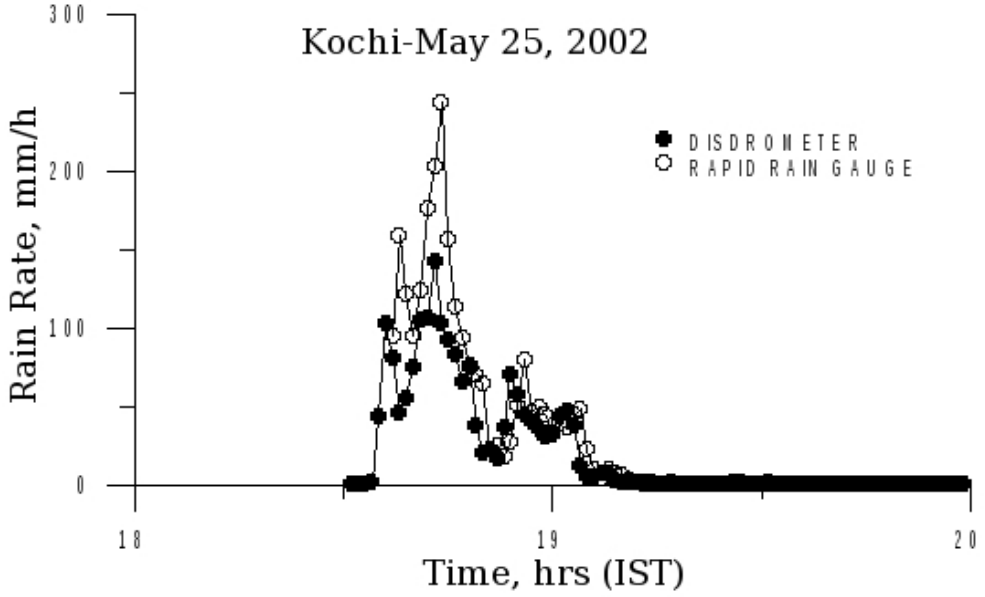
Kochi-May 25, 2002
DISDROMETER
RAPID RAIN GAUGE
Rain Rate, mm/h
300
200
100
0
18
19
20
Time, hrs (IST)

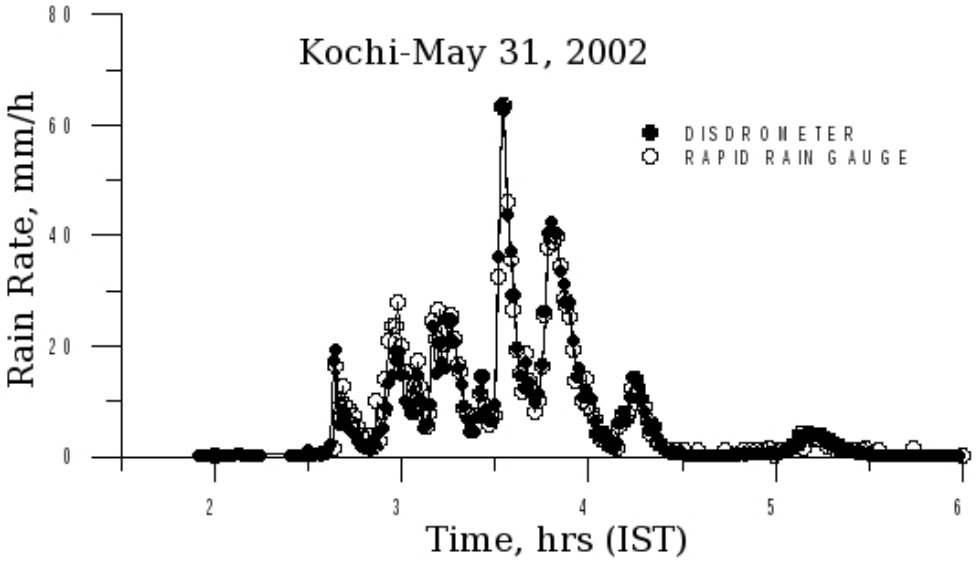
Kochi-May 31, 2002
DISDROMETER
RAPID RAIN GAUGE
Rain Rate, mm/h
80
60
40
20
0
2
3
4
5
6
Time, hrs (IST)

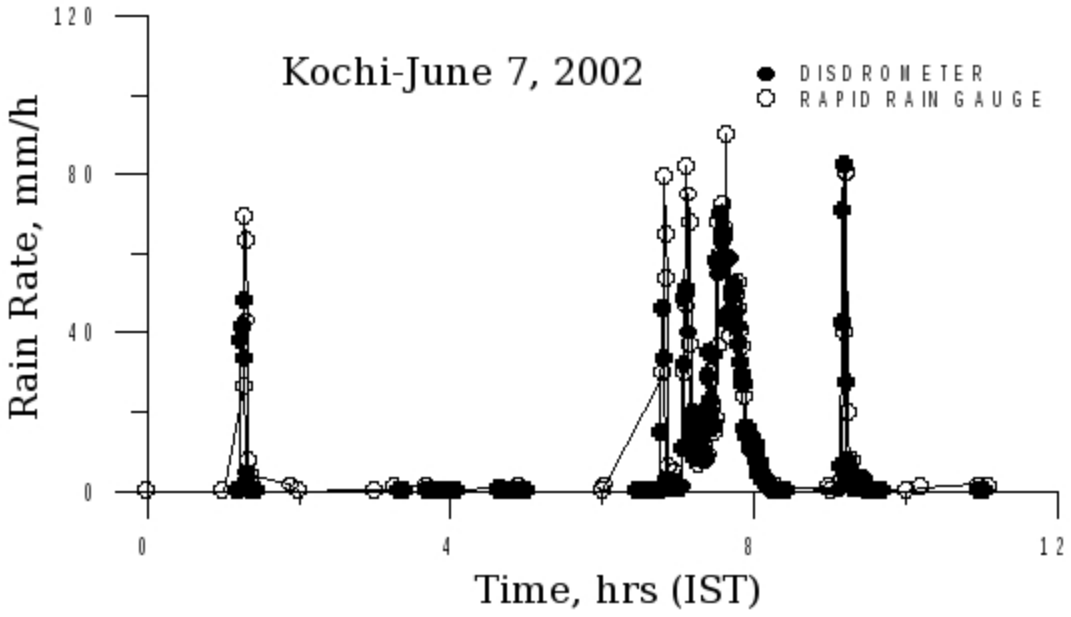

Figure. 2.11. Comparison of the rain rate data from Rapid response rain gauge and Disdrometer for shorter durations at Kochi.

2.8.3. Comparison between Disdrometer, MRR and TRMM 3B42-V6 data

The 3-hourly rain rate derived from Disdrometer and MRR is compared with the TRMM satellite 3B42-V6 data (figure 2.12). It is apparent from the figure that the data from Disdrometer and MRR agree well. Since the TRMM data is an area averaged data, the difference from former 2 instrument's data could be clearly made out. The details of the comparisons are explained in Chapter VII. In order to compare with the Manual raingauge data, the daily accumulations are derived from all other three sensors. This comparison is also shown in the figure 2.10. Agreement between all the four sensors is very clear from such a comparison.

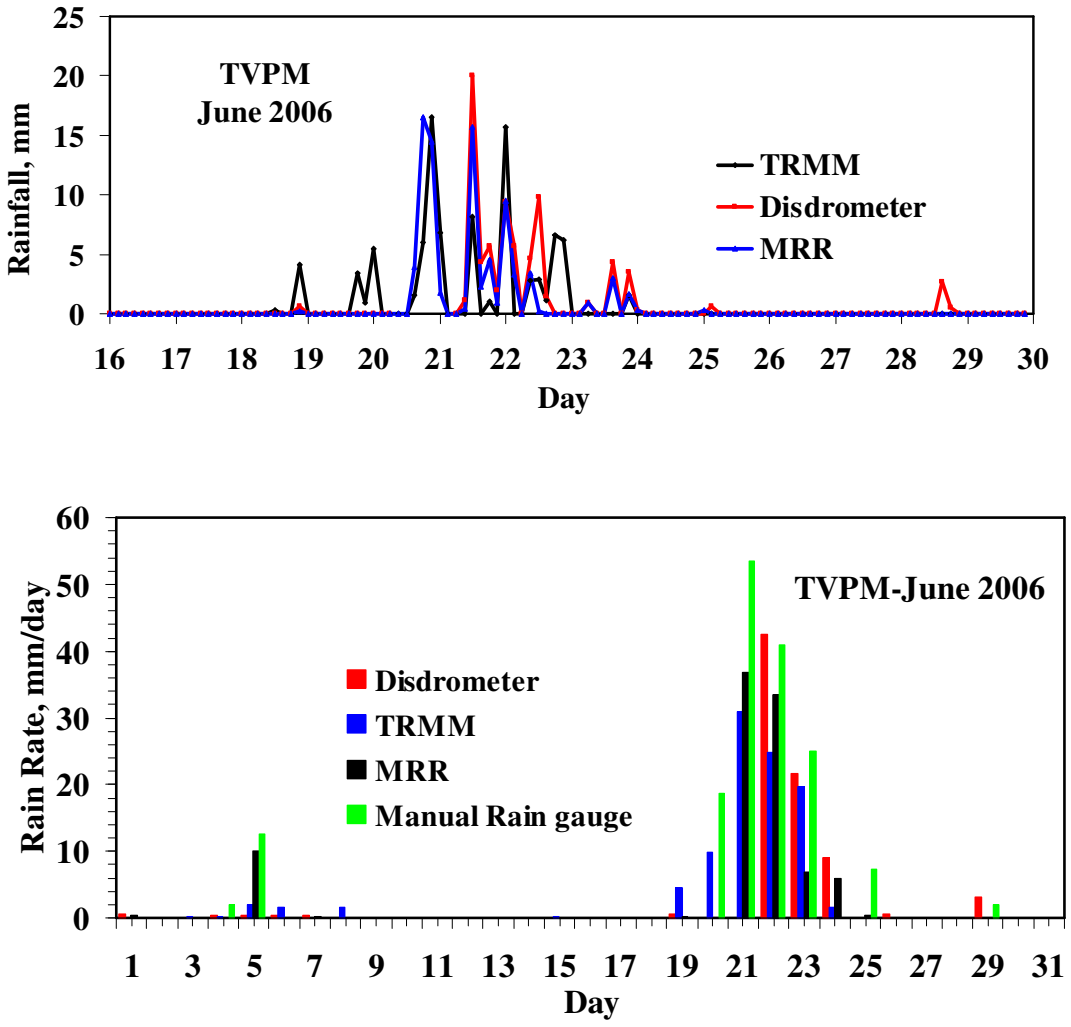

Figure. 2.12. Comparison of July 3-hourly (top panel) and daily (bottom panel) rainfall obtained from TRMM, Disdrometer, MRR and Manual Raingauge at Thiruvananthapuram (Disdrometer data is not available from 20th to 22nd and MRR data is also not available on 20th).

2.8.4. Comparison of the DSD from Disdrometer and MRR

Rain accumulations and rain rate measurements from different instruments has been compared to understand the reliability of the data. Since this thesis mainly depends on the rain DSD data and its integral parameters, it is essential to have a

comparison between the DSD obtained from Disdrometer and MRR. Such a comparison carried for Thiruvananthapuram for a rain event on 12th October 2005, that lasts for hardly five minutes (02:00 to 02:05 hrs) is shown in figure 2.13. The average rain rate of this event was 3.34 mm/h. The decreasing trend as diameter decreases below a diameter of 0.6 mm is shown by both the instruments. The minimum available altitude at which DSD is given by the MRR is 200 m. The DSD data obtained from the Disdrometer and also that given by MRR for a height of 200 m follows a lognormal distribution function. The decreasing trend as diameter decreases below a diameter of 0.6 mm is shown by both the instruments. The tailing end of the DSD spectrum also showed good agreement. The vertical variation of the DSD as explained in the chapter VI, causes the behavior of DSD to be different at 400 m.

Comparison of the DSD data obtained from Disdrometer and UHF wind profiler done by Williams et al. (2000), shows that good agreement was there for the drop size measurements whose diameters > 1.5 mm, but poor agreement was there for small drops (Williams et al., 2000). The magnitude of the difference in small drop estimation was proportional to the reflectivity (and rain rate). MRR has good agreement with optical Disdrometer throughout the drop diameter, as far as the DSD measurements are concerned. But the small drops are being underestimated by JW Disdrometer (Wagner et al., 2004). The comparison with a conventional rain gauge (30 min integration time) for a 5 months summer period show a correlation coefficient of r = 0.87 for the rainrate and agreement within 5% for the total rainfall integrated over the whole period (Peters et al., 2002).

2.9. OBSERVATION STATIONS

The stations selected for this study are tropical stations. Two station are on the west coast of India that experience an intense precipitation during the Indian summer monsoon (Xie et al., 2006), while the third one is on the east coast of India. The fourth station is a high altitude station situated at the western ghat. The geographical locations and altitude above mean sea level are shown in table II.II. A

brief outline of the peculiarities of the stations is given below. The geographical locations in the tropics are shown in the physiographical map (figure 2.14).

Thiruvananthapuram is a western coastal station nearly at the tip of peninsular India with an annual rainfall of 315 cm. Kochi is an important commercial city in Kerala situated close to the western coast and on the shores of state's largest estuary. The average annual rainfall is 310 cm. Munnar is a high altitude station at an altitude of 1500m and about 130 km east of Kochi on the western ghats in south India. Our station is on the wind ward side of the western ghats for southwest monsoon season and experiences enhanced rainfall due to orograpic effect of the western ghats. The average annual rainfall is 380 cm. Sriharikota is an east coast station in India. The site from where we made measurement is situated on an Island. One side of the site faces Bay of Bengal and the others the lake. So this site is very similar to a marine one.

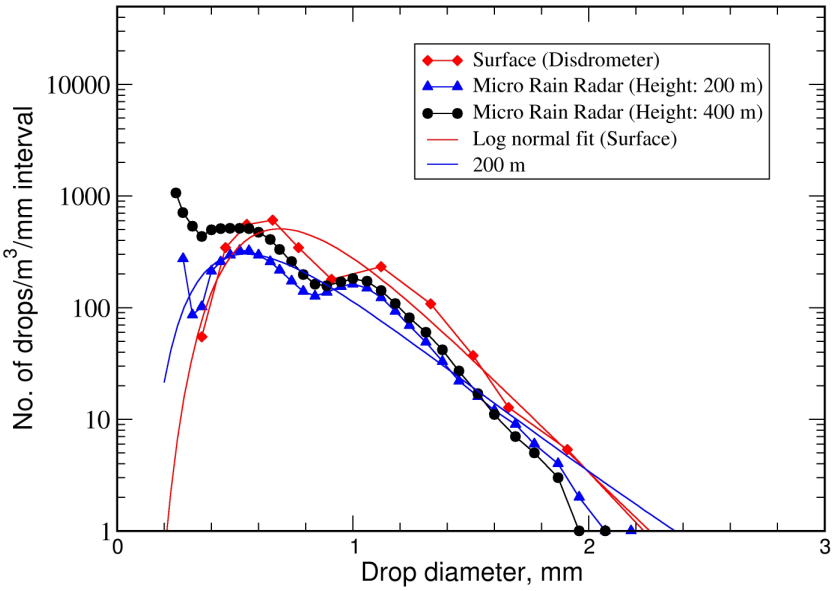

Figure 2.13. Comparison between Disdrometer and MRR DSD (02:00 to 02:05 hrs, 12, October 2005) at Thiruvananthapuram.

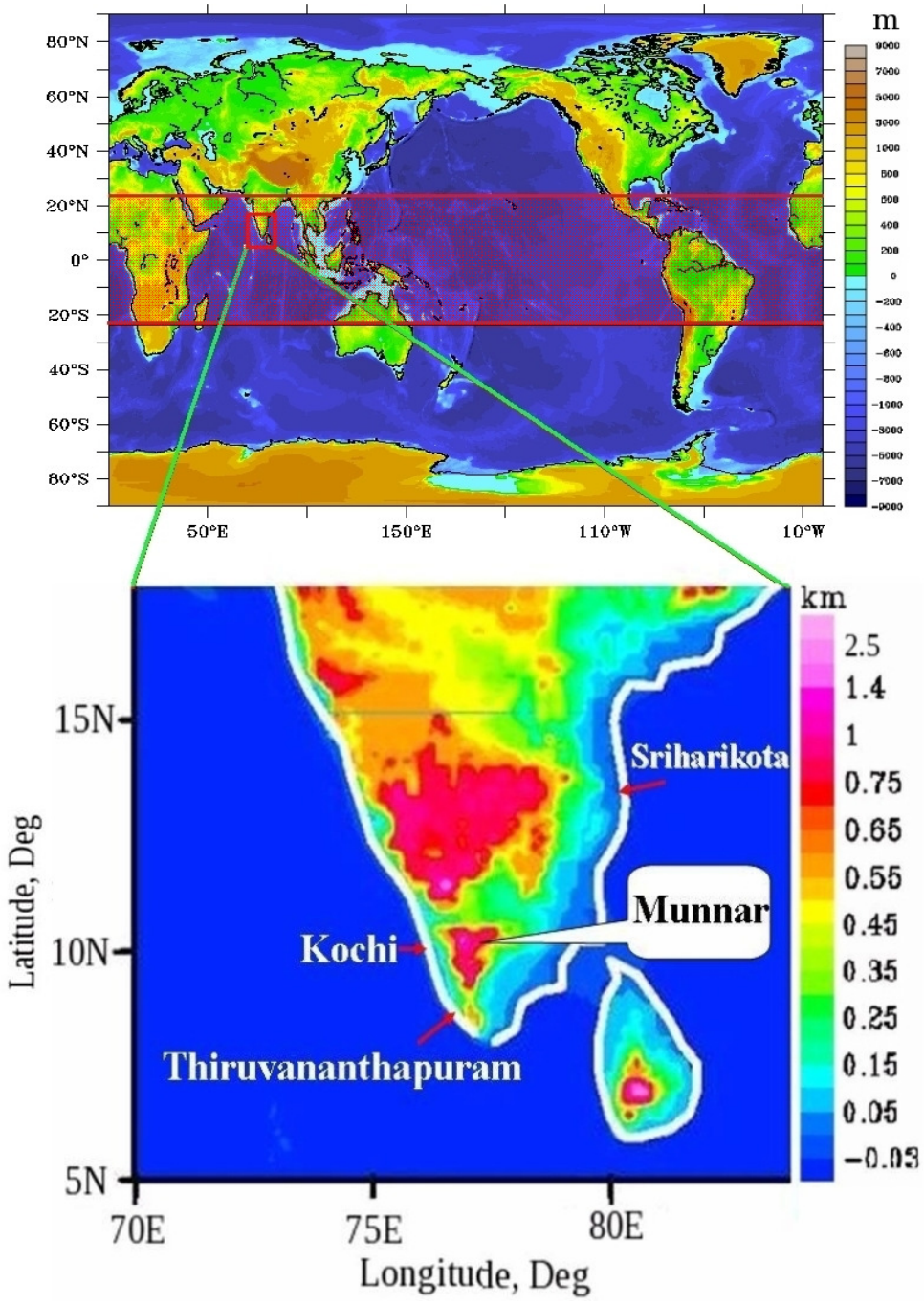

Figure 2.14. The Geographical locations of the 4 stations shown in a physiographical map. The shaded portion in the top figure represents the tropical region (Altitude shown in the legend is in metres in the top figure while that is in kilometres in the bottom figure).

The study region has mainly three seasons, as far as rainfall is concerned. These are the South-West (SW) monsoon (June–September), North-East (NE) monsoon (October–December) and Pre-monsoon (January–May). Rainfall during the SW monsoon is mostly from stratiform clouds, and during the other two seasons is from cumuliform clouds, mostly thunderstorms. Therefore, it is expected that the rainfall during a single season is mostly from similar type of clouds. One important difference is there in the characteristics of rainfall between the stations in the west coast and those in the east coast, which is relevant to this study; i.e, during the SW monsoon period, rain fall over west coast is oceanic while rainfall at east coast is continental because the wind is mostly southwesterly or westerly.

2.10. DATA AVAILABILITY

The Disdrometer is operational at Thiruvananthapuram since April 2001. Then this instrument has been shifted from place to place for further measurements at four different tropical stations. The details of the data availability at each location are given in Table II.II. Micro Rain Radar has been deployed and is operational from September 2005. Data up to the year 2008 has been used for this study. Tropical Rainfall Measuring Mission (TRMM) 3B42 data has been downloaded for the duration year 2001 to 2008 from the website of NASA Data Centre. The TRMM grid box corresponding to each station is given in the table II.III. The stations along with the corresponding TRMM grids are shown in a physiographical map shown in figure 7.1 in the chapter VII. The percentage background covered by ocean or land of each grid is clear from this figure.

2.11. CONCLUSION

The techniques of measurements have been explained in detail in this chapter. The limitations and errors in measurements were also given. The precautions taken in the deployment of the instruments to minimise the errors in measurements are also discussed.

No.	Station	From	To	Lat, Long; Altitude amsl And (corresponding TRMM grid)
1	Thiruvananthapuram	a) April 2001 b) May 2005	August 2001 April 2007	8.52ºN; 76.91ºE; 4 m (8.375º N to 8.625º N; 76.875º E to 77.125º E)
2	Kochi	a) May 2002 b) July 2003 c) May 2004	July 2002 August2003 July 2004*	9.58ºN; 76.17ºE; 5 m (9.375ºN to 9.625ºN 76.125ºE to 76.375ºE)
3	Munnar	July 2004*	October 2004	10.08ºN; 77.07ºE; 1500 m (9.875ºN to 10.125ºN; 76.875ºE to 77.125ºE)
4	Sriharikota (SHAR)	August 2003	October 2003	13.58ºN; 80.29ºE; 3 m (13.375ºN to 13.625 ºN; 80.125 ºE to 80.375ºE)

*Table II.II. Disdrometer data availability. The latitude and longitude of each location is given. The TRMM grid is also shown in the last column. *The Disdrometer was in Kochi up to July 8, and in Munnar from July 9.*

The data collected from these instruments have been mutually compared and their acceptability for the studies has been brought out. The rain rate, rainfall and DSD data obtained from these instruments are found to be agree very well with in the limits of experimental error. Now, with this confidence, analysis of this data for the study being presented in the further chapters can be explained.

CHAPTER III

RAIN RATE CHARACTERISTICS

CHAPTER III

RAIN RATE CHARACTERISTICS

3.1. INTRODUCTION

The measurement of rain rate is of importance in many respects. These data are needed, for instance, in the modelling of soil erosion (using models like RUSLE or WEPP). These models usually require a time series of rain rate with moderate to high time resolution. A knowledge of rain rates that can be expected to help design structures like culverts so that they can handle the storm waters during heavy rainfall. Rain rate is also important to understand the rate of recharge of the water table and to estimate runoff. Apart from these, the effects of climate change are now making rain rate measurements even more important. For instance, Gordon et al. (1992) report results from a model that point to increase in rain rate due to enhanced greenhouse effect. A study in Australia by Haylock and Nicholls (2000) showed an increase in the total rainfall and number of rainy days in the northern and southern regions and a decrease in the western and southwestern regions. Their study implied a significant change in the number of heavy events in the southwest and a significant change in only the number of lighter events in the north. Most of the rainfall measurements in India are limited to daily rainfall, with only a relatively few stations recording rain gauges that can give hourly rainfall values. Rainfall data have been used in many studies (for instance, Ananthakrishnan et al., 1979; Muralidharan et al., 1985; James et al., 1987; Sreedharan and James 1988; Sampath et al., 1989). While daily rainfall data are quite useful for such studies, the distribution in shorter intervals of time is important in many fields. The data from recording rain gauges show that rainfall is often confined to a few hours a day, and sometimes even for periods shorter than an hour. The period during which a given amount of rain occurs is important because heavier rainfall leads to greater runoff, greater soil erosion and less infiltration into the water table. A knowledge of rain rate therefore becomes important from the point of view of better

management of our dwindling fresh water resources and improved control of soil erosion.

This chapter presents some of the first results from the measurement of rain rate with high temporal resolution of 1 minute at a few stations in Kerala State. Distribution of rainfall, temporal distribution of rain rate, cumulative distribution of rain rate and contribution of each rain rate range to total rainfall are analysed and discussed in detail. The rain rate is derived from the Drop Size Distribution data from the Joss–Waldvogel (1967) type Disdrometer. The Geographical features of all the three stations and the comparison/validation of the rainfall derived from the rain rate measurements with that from the manual rain gauge are explained in detail in section 2.6.1 of chapter II.

3.2. DATA AND DATA ANALYSIS

Data used for this study are for the periods as shown in table III.I. The table also shows the number of minutes during which rainfall was measured in each month.

No.	Station	Month	No. of minutes	Highest rain rate
1	Thiruvananthapuram	April 2001	193	140
2		May 2001	140	46
3		June 2001	1074	129
4		July 2001	1358	108
5		May 2005	1142	82
6		June 2005	1886	144
7		July 2005	5250	116
8		August 2005	1695	94
9	Kochi	May 2002	912	171
10		June 2002	5661	223
11		July 2002	2612	107
12		May 2004	1413	108
13		June 2004	6632	102
14		July 2004 (1-8)	652	97
15	Munnar	July 2004 (9-31)	10404	44
16		August 2004	11880	61
17		September 2004	11247	133
18		October 2004	4171	46

Table III.I. Durations for which data from the three stations are presented in this chapter and the highest rain rate observed each month (mm/h).

3.3. RESULTS

3.3.1. Distribution of rainfall

Table III.I shows that the duration for which rainfall was observed in the pre-monsoon months in 2001 at Thiruvananthapuram is very low, though in 2005 the duration of rainfall is longer. Rainfall during the pre-monsoon periods is scattered rather than widespread, and is mainly from cumulonimbus clouds. These clouds generally form in a region towards the east of the city and move in a generally westward direction. Our campus, where the instrument was situated, is at a location which is often missed by these clouds. In April 2001, for instance, there was only one rainfall event that gave heavy rainfall, when a cumulonimbus cloud passed almost overhead, and in May 2001, we received rainfall only on one day.

In Thiruvananthapuram, the month that has maximum duration of rainfall is July in both years (2001 and 2005). But in Kochi, the maximum duration of rainfall is seen to be in June in both years (2002 and 2004). The data are not sufficient to identify whether this is a normal feature. It is interesting to note that Munnar received rainfall almost 25% of the time in the months of August and September, which is much higher than that at the other stations. In July, the instrument was in Munnar only for twenty three days, but recorded rainfall for more than ten thousand minutes, which is about 31% of the time! This suggests that the maximum duration of rainfall may be in July in Munnar also. As we shall see, the rainfall was of very low intensity most of the time at Munnar. This is evident from the fact that the highest rain rates observed in three of the four months the instrument was operated, there are comparatively low, being less than 50mm/hr in two months.

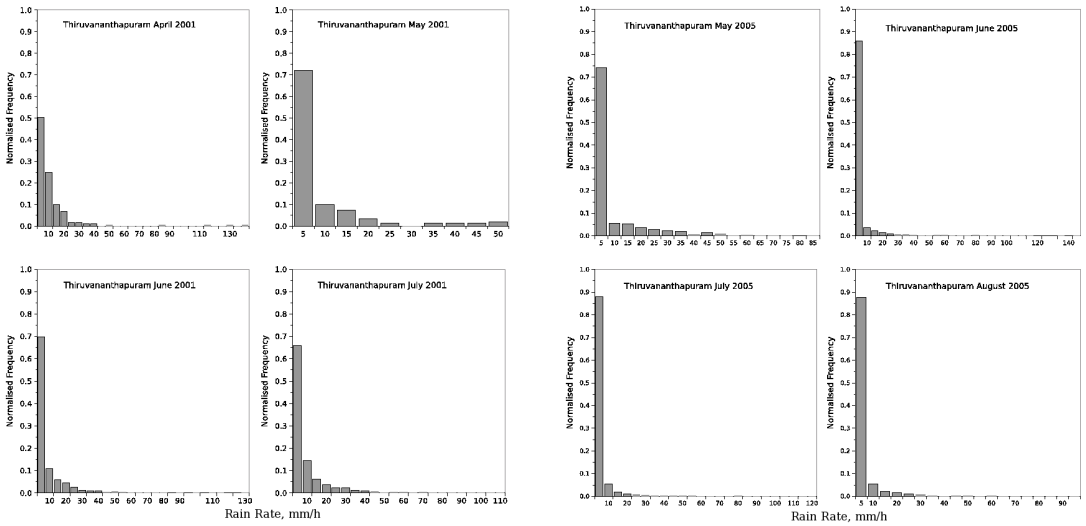

Figure 3.1. Rain rate distribution at Thiruvananthapuram in 2001 (left 2 panels) and 2005 (right 2 panels). Note that the x scale is different in each graph because the maximum rain rate observed is different.

3.3.2. Temporal distribution of rain rate

We shall now examine the distribution of rain rate with respect to time at the three stations. The results show differences in the distribution of rain rate between stations, and between months at the same station. The rain rate distribution at Thiruvananthapuram for four months in 2001 (from April to July) and in 2005 (May to August) is shown in figure 3.1. We see that the lowest rain rate range (0–5 mm/h) dominates in all the months. This range has a probability of occurrence of 50% in April 2001, which is the lowest, and close to 75% in May 2001. This also indicates that the percentage of time rainfall is below 5mm/h, which is relevant in a state like Kerala which has a highly undulating terrain. However, since the data for these months is limited, the distribution seen here could very well be biased and not truly representative. In 2005, however, we find that the probability is more than 75% for rainfall below 5 mm/h in all the months, and in July it is almost 90%, which is the highest for this station. Although the rain rate range 0 to 5 mm/h dominates in all the months, the higher ranges are also seen prominently, especially up to about 50 mm/hr, in most of the months. Interestingly, the distribution does not show any striking difference between southwest monsoon and pre-monsoon periods. We would normally

have expected a greater share for higher intensity rainfall in May. The frequency distribution of rain rate for different months at Kochi is shown in figure 3.2. In all the months except July 2002, the probability of rain rate being below 5 mm/h is 75–85%. In July 2002, this is almost 95%. In the other months, the rain rate distribution is similar to that at Thiruvananthapuram in 2005. In July 2004, the instrument was in Kochi for only 8 days, after which it was shifted to Munnar. The data thus is not for the entire month. The distribution is very similar in both years. Moreover, the highest rain rate observed is in June (223 mm/hr) though the next highest is in May 2002 (171 mm/hr). These two are the highest rain rates observed even when we consider all the stations and all the months. The year 2002 was a rainfall deficient year and the rainfall deficit was mainly in July. Our results appear to indicate a reduction in high intensity rainfall, which means a reduction in cumuliform clouds. It remains to be seen whether this could be the reason for lower rainfall in July 2002.

The distribution for Munnar (figure 3.3) shows that the probability of rain rate being less than 5 mm/h is around 97.5% in July and October, and around 92% in August and September. When we consider the fact that the highest rain rates in July and October are around 50 mm/h, and the highest rain rate range that had at least 5 minutes of rainfall was only 30 mm/h, we see that rain rates are very low during these months at Munnar. We have seen a somewhat similar distribution only in July 2002 at Kochi. There, the highest rain rate recorded was 110 mm/h, but that was only for one minute. The highest rain rate recorded for more than five minutes at Kochi in July 2002 was only 40 mm/h. The corresponding value for June 2004 was 57 mm/h and for June 2002 was 78 mm/h. The limited data available for Munnar appears to show a different rain rate distribution compared to the other two stations. The rain rate distribution indicates that the rainfall in this region is predominantly from stratiform clouds, with cumuliform clouds being relatively rare. On the other hand, the rain rate distributions at Thiruvananthapuram and Kochi show that cumuliform rainfall could be present during 10–20% of the time even during the southwest monsoon period.

3.3.3. Cumulative distribution of rain rate

The cumulative distribution, perhaps, shows the differences more clearly. The cumulative distribution for Munnar, Kochi and Thiruvananthapuram is shown in figures. 3.4, 3.5 and 3.6. The cumulative percentage was computed for values below 5mm/h also because for 5mm/h the percentage contribution is often around 80% and sometimes even 90% and higher. If only the points from 5mm/h are plotted, most of the graphs would not show the rising part of the curve. Beyond about 40mm/h, the graph is almost parallel to the x axis. In the case of Munnar, especially for July and October, the graphs rise almost vertically up to about 80–90% and then become almost horizontal. In the case of Kochi, except for July 2002, the higher rain rates are clearly seen to contribute to a positive slope for the horizontal part of the graph.

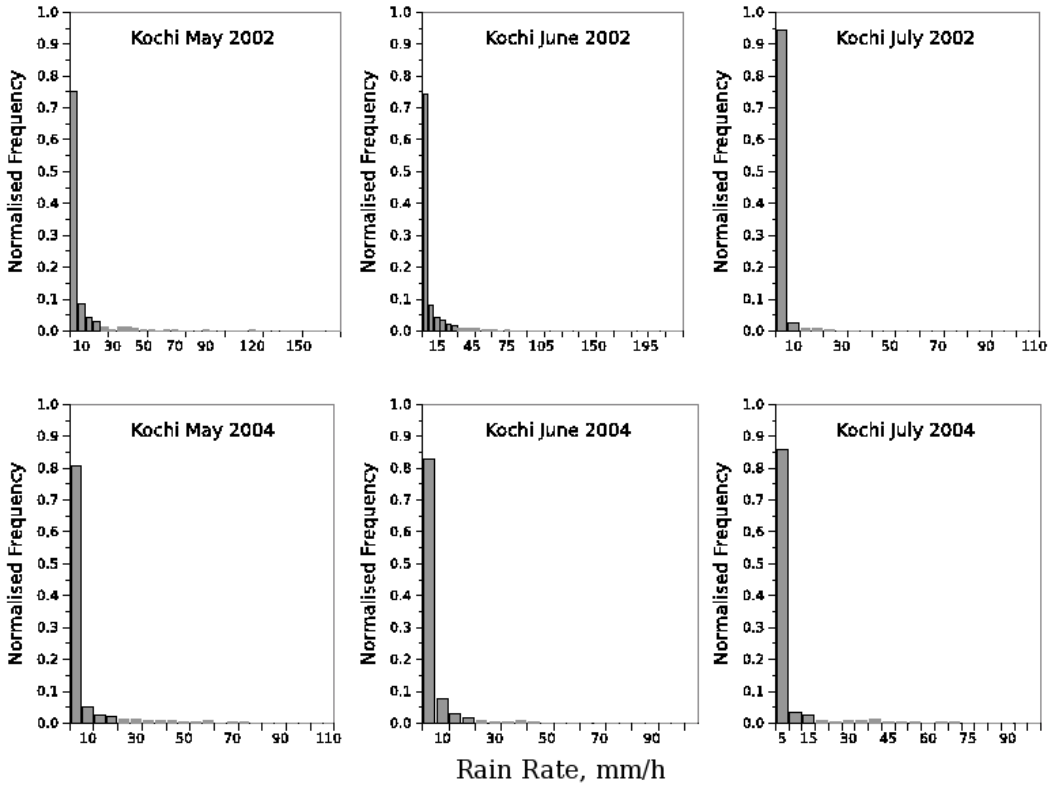

Figure 3.2. Frequency distribution of rain rate at Kochi in three months each in 2002 and 2004.

The cumulative distribution graphs for Thiruvananthapuram (figure 3.6), on the other hand, are very different from these. In order to quantify the differences, the cumulative frequency graphs were fitted with the Weibull function

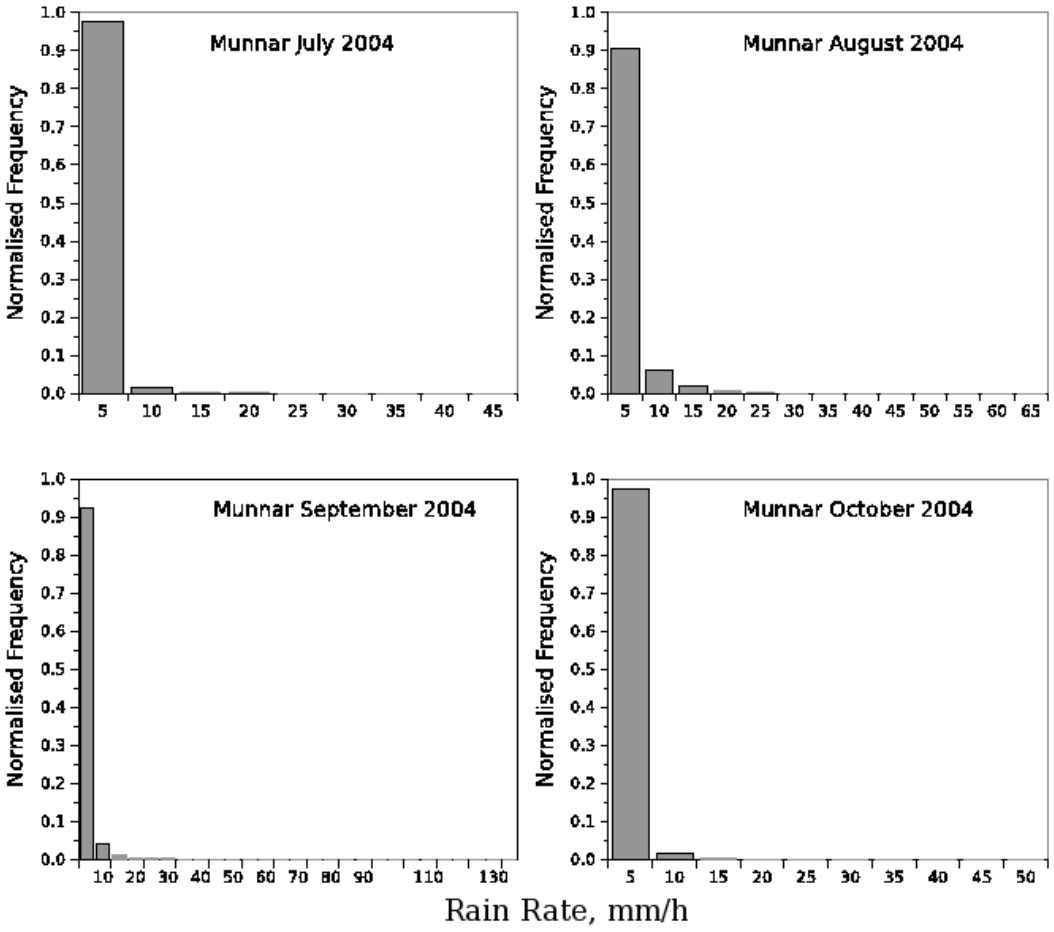

Figure 3.3. Frequency distribution of rain rate at Munnar.

$$y = 1 - \exp\left(1 - \left(\frac{x}{\lambda}\right)^{k}\right) \tag{1}$$

where k is known as the *shape parameter* and λ is known as the *scale parameter* of the distribution. Gnuplot, a free software for plotting graphs, was used for curve fitting. Gnuplot uses the Marquardt–Levenberg algorithm for non-linear curve fitting, which is known to give very good results for a wide variety of datasets. The fitted curves are

shown in the figures, along with the observed values. The fit is very good in most cases, the exceptions being the data for the month of May in both 2001 and 2005.

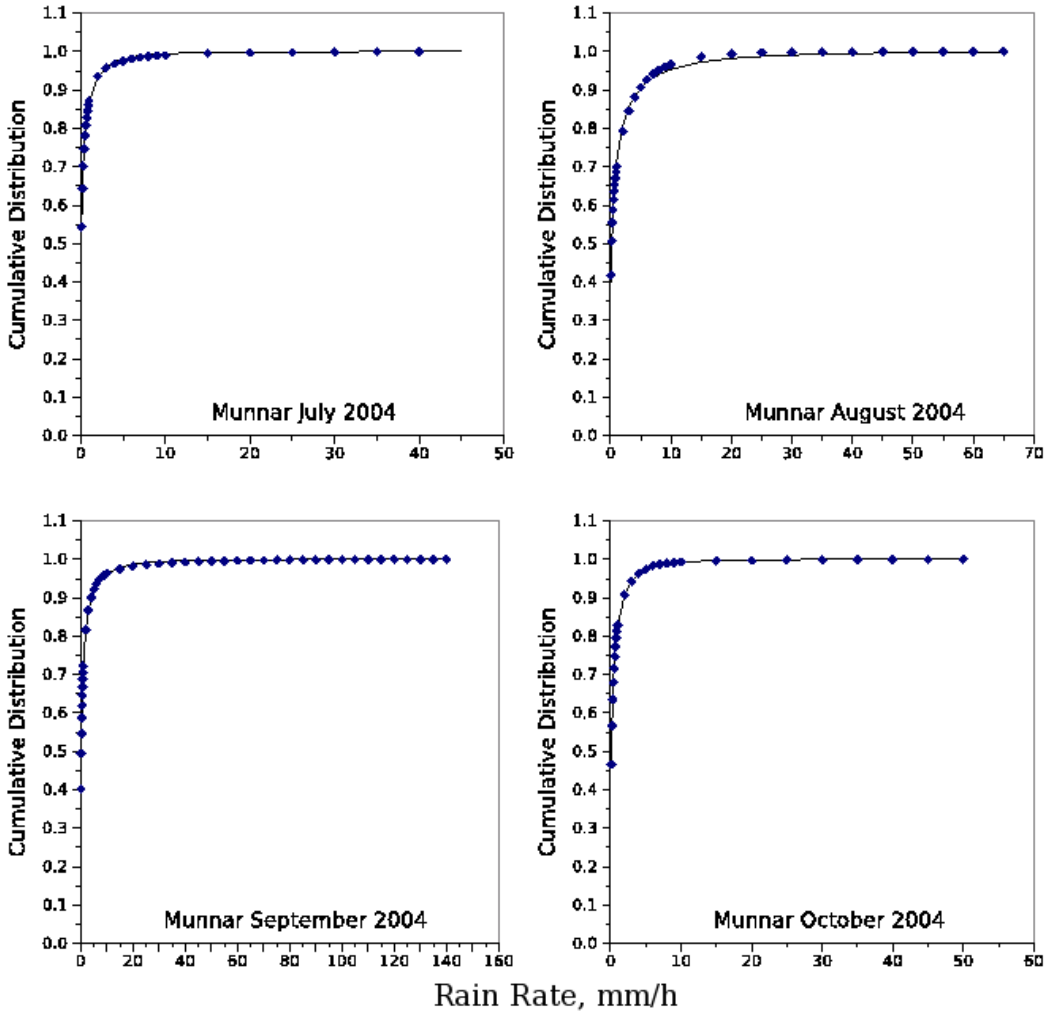

Figure 3.4. Cumulative frequency distribution of rain rate at Munnar. The points represent measured values and the line represents the fitted Weibull distribution.

The fit parameters k and λ for all the months are given in table III.II. What strikes one when observing the table is the high values for both k and λ for Thiruvananthapuram in the year 2001. In both cases, they are the highest, and quite different from the values for the same station for the year 2005. (A higher value of k indicates a more gradual increase, a more rounded curve, and a lower value indicates a sharper curve. A higher value of λ generally means a higher y value for a given x

value.) The reasons for this difference are not clear, and more measurements may be needed to understand these variations. A similar, but much smaller, difference can be seen between the data for the two years at Kochi. The values of k and λ in May and June 2002 are similar and higher than those in 2004, except for the value of k in June 2004. But July 2002, a rainfall deficient month, is different, with a higher value of k and a much lower value of λ. Interestingly, we do not see any difference between the values for pre-monsoon and monsoon months. Both at Thiruvananthapuram and Kochi, the values of k and λ during the pre-monsoon months are close to the values in the monsoon months. The only exception, if it can be considered so, is in the values of λ at Thiruvananthapuram during the pre-monsoon months, which appear to be slightly higher than in the monsoon months.

λ has the lowest value for July in Munnar, and the second lowest in October. The values of k at Munnar are all close together, unlike in any other case. Possibly by accident, λ has the same value for the three months June–August 2005. Overall, the values λ do not appear to have any consistent pattern at these sites.

The shape parameter (k) for all the stations for all the months is shown in figure 3.7. The value of k remains more or less same for each station during the southwest monsoon period. At Kochi, for July 2002, the shape parameter shows a higher value that probably indicates that July 2002 received lesser rainfall. Thiruvananthapuram shows a variation from year to year. Munnar does not have any variation with in the southwest monsoon period. All these characteristics suggest that southwest monsoon period has same characteristics with special reference to rainfall and rain rate distribution.

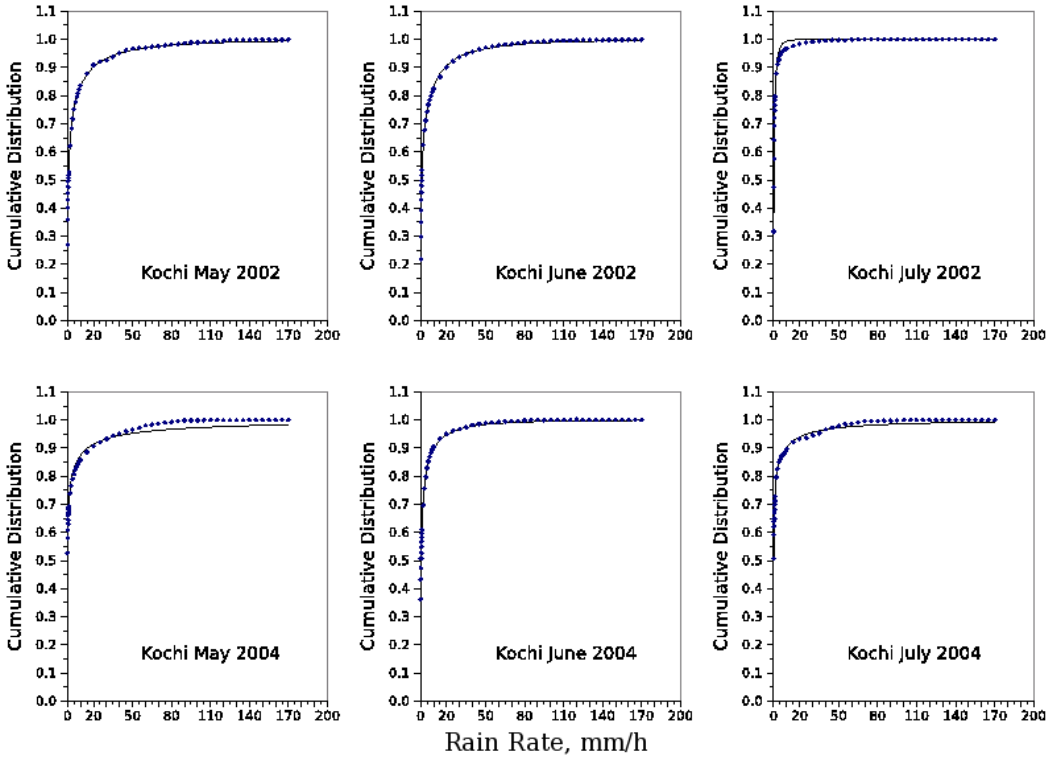

Figure 3.5. Cumulative frequency distribution of rain rate at Kochi. The points represent measured values and the line represents the fitted Weibull distribution.

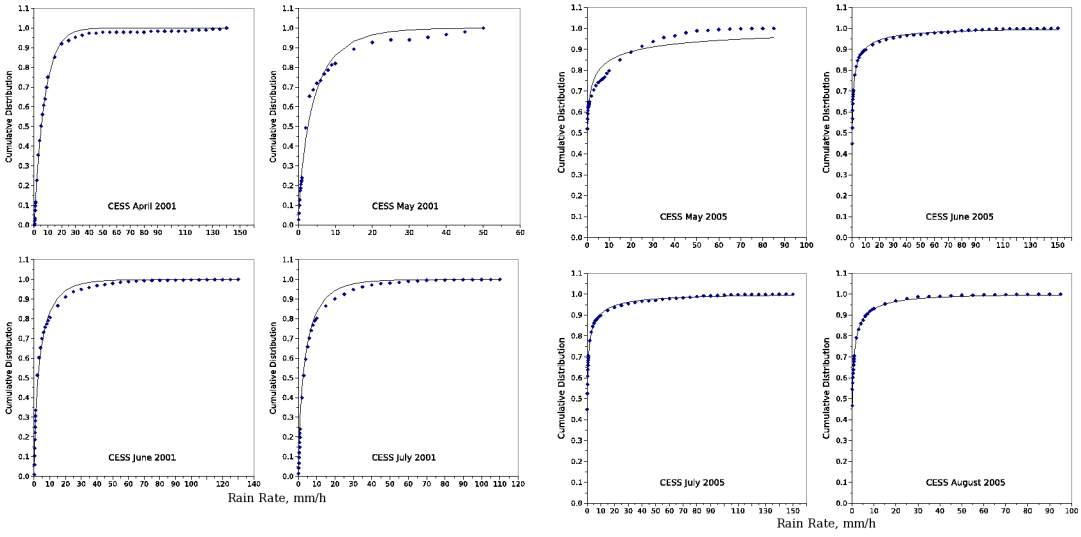

Figure 3.6. Cumulative frequency distribution of rain rate at Thiruvananthapuram in 2001 (left 2 panels) and 2005 (right 2 panels). The points represent measured values and the line represents the fitted Weibull distribution.

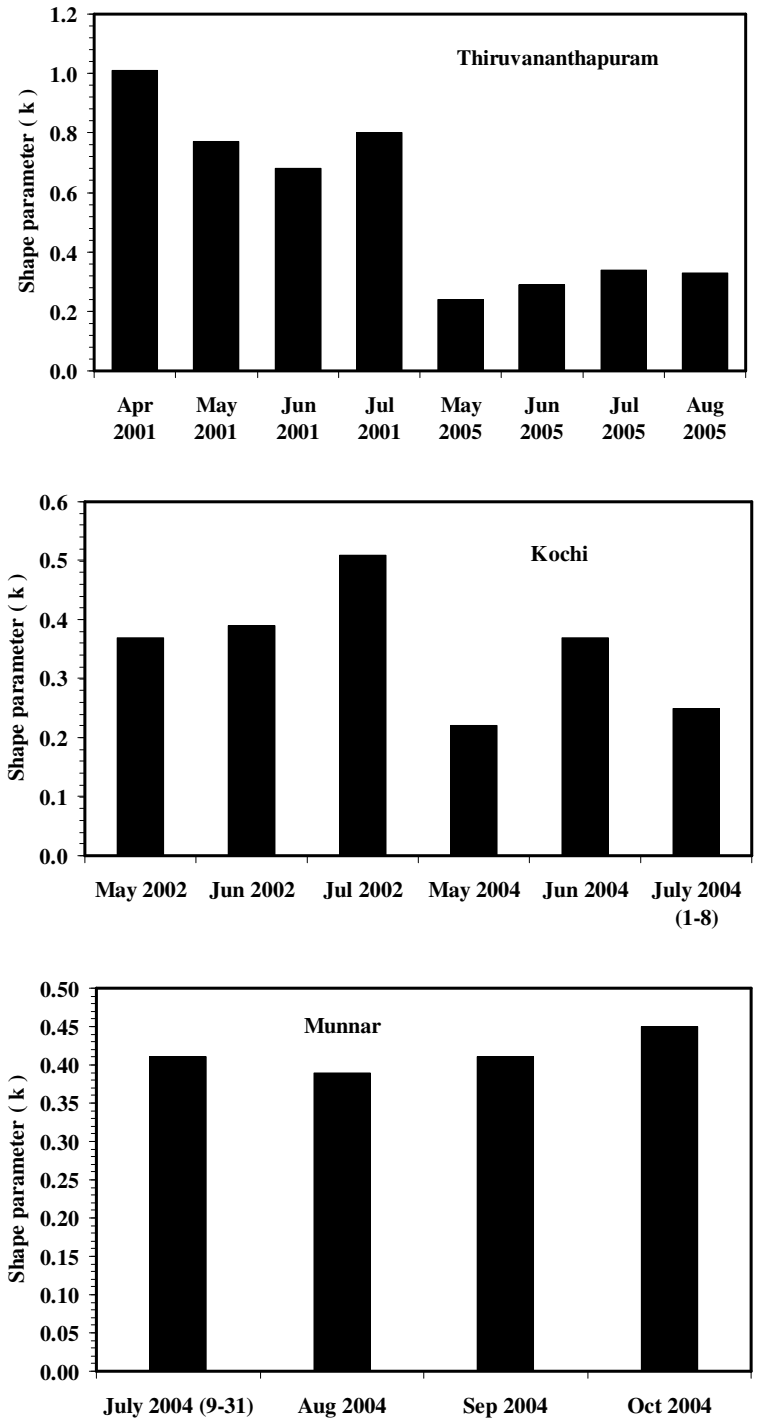

Figure 3.7. The Histogram showing the variation of shape parameter (k) for each station.

No.	Station	Month	k	λ
1	Thiruvananthapuram	April 2001	1.01 ± 0.03	7.52 ± 0.14
2		May 2001	0.77 ± 0.04	4.12 ± 0.19
3		June 2001	0.68 ± 0.02	4.22 ± 0.14
4		July 2001	0.80 ± 0.02	5.08 ± 0.13
5		May 2005	0.24 ± 0.015	0.73 ± 0.10
6		June 2005	0.29 ± 0.002	0.51 ± 0.01
7		July 2005	0.34 ± 0.003	0.51 ± 0.01
8		August 2005	0.33 ± 0.004	0.51 ± 0.01
9	Kochi	May 2002	0.37 ± 0.003	2.03 ± 0.02
10		June 2002	0.39 ± 0.006	2.27 ± 0.05
11		July 2002	0.51 ± 0.03	0.42 ± 0.02
12		May 2004	0.22 ± 0.004	0.44 ± 0.02
13		June 2004	0.37 ± 0.004	1.08 ± 0.02
14		July 2004 (1-8)	0.25 ± 0.004	0.37 ± 0.01
15	Munnar	July 2004 (9-31)	0.41 ± 0.004	0.18 ± 0.002
16		August 2004	0.39 ± 0.007	0.56 ± 0.01
17		September 2004	0.41 ± 0.003	0.54 ± 0.005
18		October 2004	0.45 ± 0.003	0.29 ± 0.001

Table III.II. Values of shape parameter, k and scale parameter, λ obtained when fitting the cumulative frequency distribution of rain rate with the Weibull function.

3.3.4. Contribution to total rainfall

We shall now look at the contribution of each rain rate range to total rainfall. We divided the observed rain rates into ranges of 5 mm/h interval and computed the amount of rainfall obtained in each range. This was plotted as a percentage of the total rainfall, and also as the cumulative percentage. The scale of the y axis has been kept the same in all graphs to facilitate comparison (except in some cases, as pointed out later). The results are given below.

The graphs for Thiruvananthapuram are shown in figure 3.8. What strikes one immediately on seeing these graphs is their large difference from the distribution graphs of rain rate with time for Thiruvananthapuram (figure 3.1). Unlike the latter, these graphs show that the higher rain rates do contribute significantly to the total rainfall, especially in the pre-monsoon months. During the pre-monsoon months in 2001, in fact, the lowest and highest rain rates have contributed more than the middle ranges in the pre-monsoon months. However, the total rainfall received in these months

is low, which could be one of the reasons why the occasional short duration heavy rain becomes important. But in May 2005, interestingly, the middle rain rates contribute more than the lowest and highest. During the southwest monsoon period, the contribution is highest from the lowest rain rate range in all cases, and the contribution decreases with increasing rain rate. The only exception is June 2005, when the distribution is almost flat.

The distribution at Kochi during the months of May, June and July in 2002 and 2004 are shown in figure 3.9. Here also we see that all rain rates contribute almost similarly during the pre-monsoon period, but the contribution decreases with increasing rain rate during the monsoon months – the only exception being July 2004. Another point to note is that the scale of the y axis is different for July 2002, in which month the contribution from the lowest rain rate range is very high. We had earlier found that rainfall during this month was less than 5 mm/hr for about 95% of the time, leading us to suspect that the reason for rainfall deficiency in the month was the lower presence of cumuliform clouds. The present finding tends to confirm this suspicion.

Munnar (figure 3.10) presents a different picture. The low rain rates are prominent here, with the range 0–5 mm/h contributing more than 30% in all months, and going up to 65% in October and more than 55% in July. In August, even the range 5–10 mm/h has contributed more than 25%, which is not seen at either of the other two stations in any month. It may be pointed out that the y scale is different in each of these graphs.

The cumulative contributions from the different rain rate ranges to the total rainfall at the three stations are given in figures 3.11, 3.12 and 3.13. Unlike the cumulative distributions shown earlier, most of these curves do not appear to follow any well-defined pattern. The graph for May 2001 for Thiruvananthapuram, for example, is almost a straight line, and so are those for May and June 2005 to an extent. The graphs for May and July 2004 for Kochi also show an almost linear increase except for small departures. In view of this, no attempt was made to fit any function to the data.

3.4. DISCUSSION

Ananthakrishnan et al. (1979), after analysing hourly rainfall data for the monsoon seasons of 1969 and 1970, found that "falls of intensity ≥10 mm/h account for 14% of the rainfall at Thiruvananthapuram in less than 2% of the rain hours". What we find in the present study is that rainfall of intensity ≥10 mm/h is present during 19.25% of the time in June 2001, 19.8% in July 2001, 10.23% in June 2005, 6.4% in July 2005 and 6.9% in August 2005. It accounted for 73.9%, 69.6%, 84.3%, 67.5% and 65.3% of the total rain in these months respectively. This is very different from what they found. They continue to state that "Such falls account for about a third of the rainfall at stations from Cochin to Goa and 40 to 50% at Vengurla and Bombay." In our study, we found that, in Kochi, rainfall of intensity ≥10 mm/h is present during 17.7%, 3.3%, 9.5% and 10.4% of the time in June 2002, July 2002, June 2004 and July 2004, respectively, and contributed 82.2%, 54.8%, 68.6% and 84%, respectively, of the total rainfall. These are not very different from the values for Thiruvananthapuram. This difference between these two studies needs to be explained. This is possibly a result of Ananthakrishnan et al. using the hourly rainfall value in place of rain rate, in the absence of rain rate measurements. A rainfall of 1 mm depth that lasted for one minute would be counted as a 1mm/h rain event, while, in fact, the intensity should be taken as 60mm/h. Thus, the intensity values used by Ananthakrishnan et al. could be highly underestimated. This problem would also have affected the other conclusions they have drawn, and is certainly the reason why their data do not show intensities greater than about 30 mm/h. Rainfall can be from stratiform or cumuliform clouds. The former is the dominant cloud form during the southwest monsoon season. They are generally expected to produce only light rainfall, while cumuliform clouds, especially cumulonimbus, can produce heavy rainfall. If we assume that a certain rain rate is the maximum that stratiform clouds can produce, then we can roughly determine from the graphs given earlier the relative prevalence of these two cloud types in a given month.

We need to keep in mind the fact that cumuliform clouds could produce light rainfall, though stratiform clouds cannot produce heavy showers.

Rain from stratiform clouds is often classified as slight, moderate or heavy if the rain rate is <0.5 mm/h, between 0.5 and 4 mm/h and > 4 mm/h. Rainfall from cumuliform clouds is said to be slight if it is <2 mm/h, moderate if it is between 2 and 10 mm/h, heavy if it is between 10 and 50 mm/h and violent if it is >50 mm/h. These are values corresponding to the Beaufort letters used for recording weather. We assume the maximum rain rate produced by stratiform clouds as 20 mm/h. This is not based on any study of stratiform cloud properties or rainfall, but is an arbitrary value. The maximum rain rate observed in any month in these measurements is at least 44 mm/h (at Munnar in July). What we have chosen is less than half this rain rate. However, we need to remember that all rainfall of rain rate less than this is not necessarily produced by stratiform clouds, and there would be some contribution from cumuliform clouds also. On the basis of this assumption, we find that rainfall is from stratiform clouds at least 88% of the time. At Thiruvananthapuram, rainfall is below 20 mm/h from 88.62 to 98.61 per cent of the time during the months the measurements were made. This rainfall contributes from 28% to 56% of the total rainfall for the month. No consistent difference between pre-monsoon and southwest monsoon months is seen. The values for the different stations for the different months are summarised in table III.III.

The table shows the predominance of low intense rainfall in Munnar. Rainfall is below 20 mm/h more than 99% of the time in three of the four months, contributing at least 88% of the total rainfall. In September, though the rainfall was below 20 mm/h more than 98% of the time, it contributed only about 60% of the total rainfall for that month. This, and the fact that the maximum rain rate observed in that month (132.6 mm/h) is much higher than in the other months indicate the greater presence of cumuliform clouds in this month. The reason for this is not clear.

No.	Station	Month	Normalised Frequency	Percentage of total rainfall
1	Thiruvananthapuram	April 2001	92.1	56.1
2		May 2001	92.7	55.7
3		June 2001	91.1	48.3
4		July 2001	90.1	49.8
5		May 2005	88.6	33.8
6		June 2005	93.6	27.7
7		July 2005	96.6	48.6
8		August 2005	96.8	55.3
9	Kochi	May 2002	90.9	31.8
10		June 2002	90.0	33.8
11		July 2002	98.5	61.5
12		May 2004	90.7	25.9
13		June 2004	95.1	48.5
14		July 2004 (1-8)	93.3	27.6
15	Munnar	July 2004 (9-31)	99.7	88.0
16		August 2004	99.4	89.5
17		September 2004	98.1	59.9
18		October 2004	99.7	88.2

Table III.III. The relative duration for which rainfall is below 20 mm/hr and the contribution from this to the total rainfall.

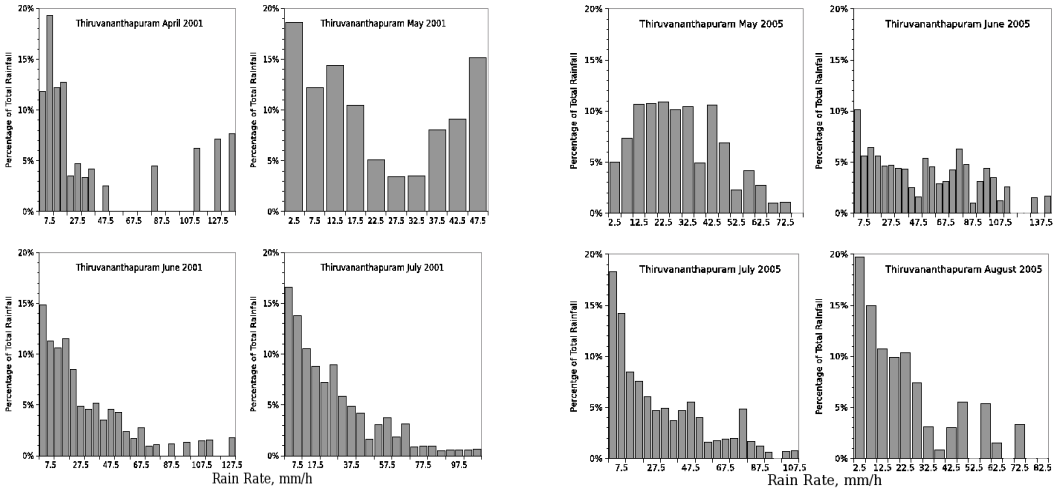

Figure 3.8. Histogram of the contribution of each rain rate range to total rainfall at Thiruvananthapuram in 2001 (left 2 panels) and 2005 (right 2 panels).

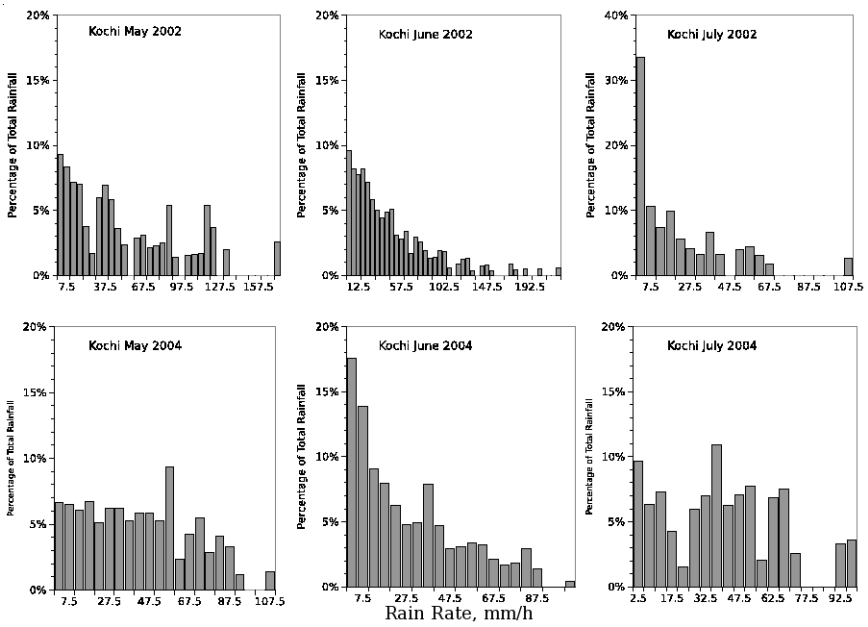

Figure 3.9. Histogram of the contribution of each rain rate range to total rainfall at Kochi in 2002 (top) and 2004.

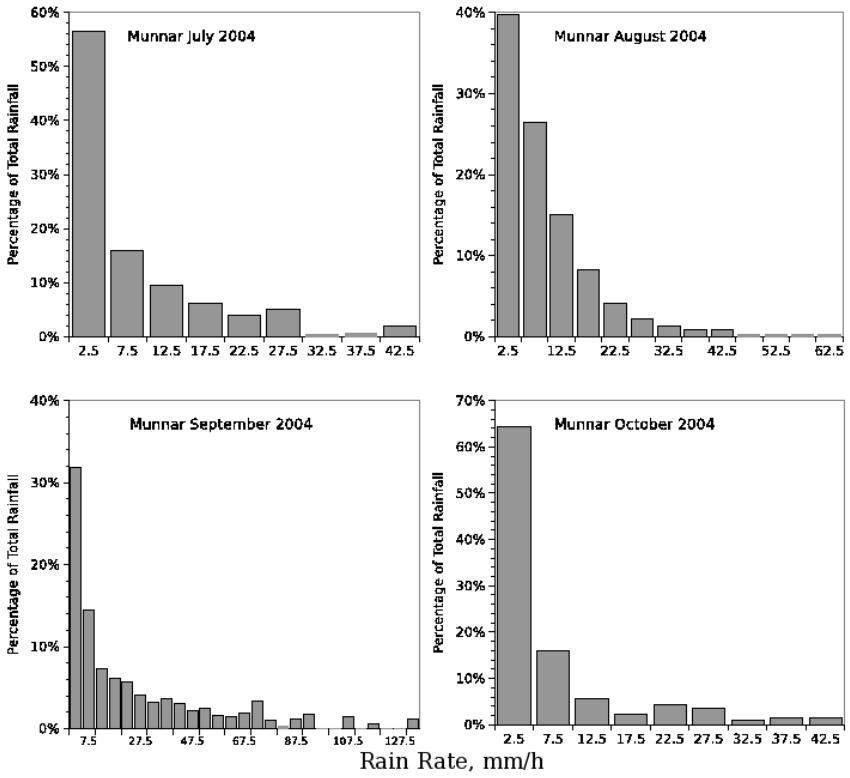

Figure 3.10. Histogram of the contribution of each rain rate range to total rainfall at Munnar in 2004.

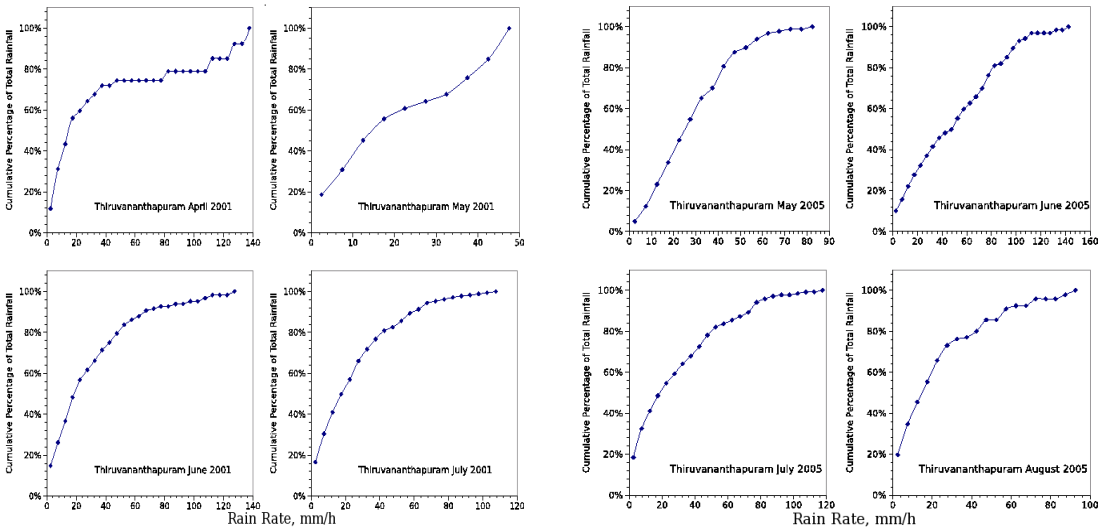

Figure 3.11. Cumulative contribution from each rain rate range to total rainfall at Thiruvananthapuram in 2001 (left 2 panels) and 2005 (right 2 panels).

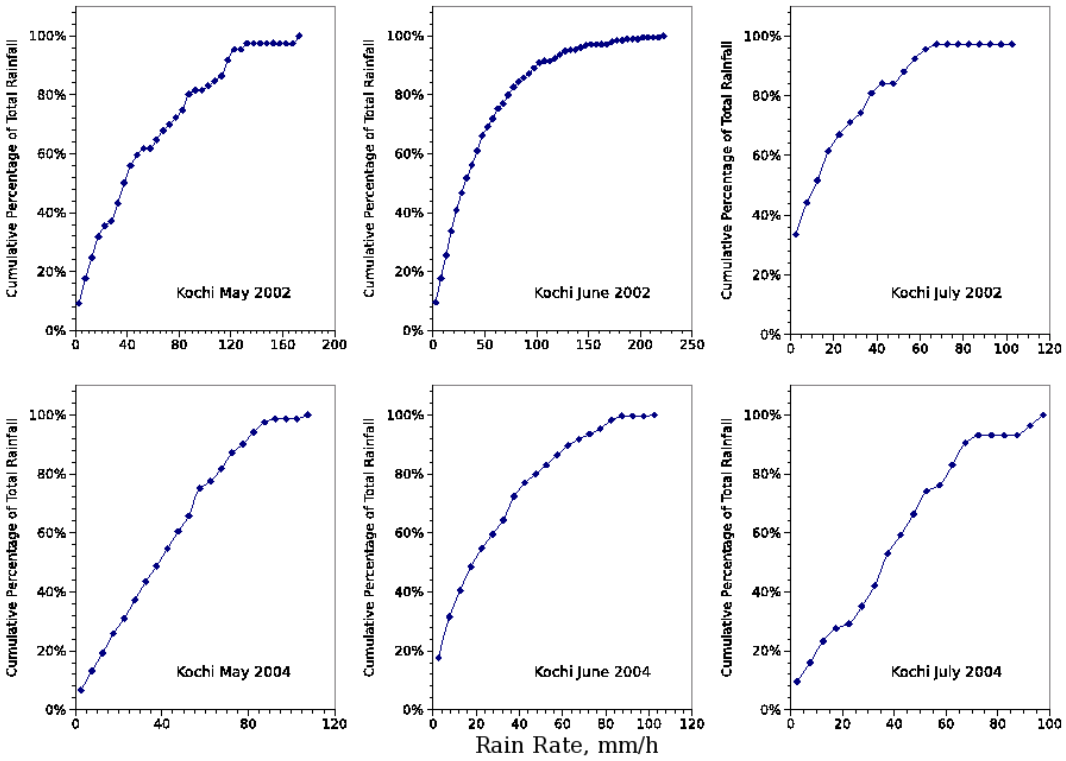

Figure 3.12. Cumulative contribution from each rain rate range to total rainfall at Kochi in 2002 and 2004.

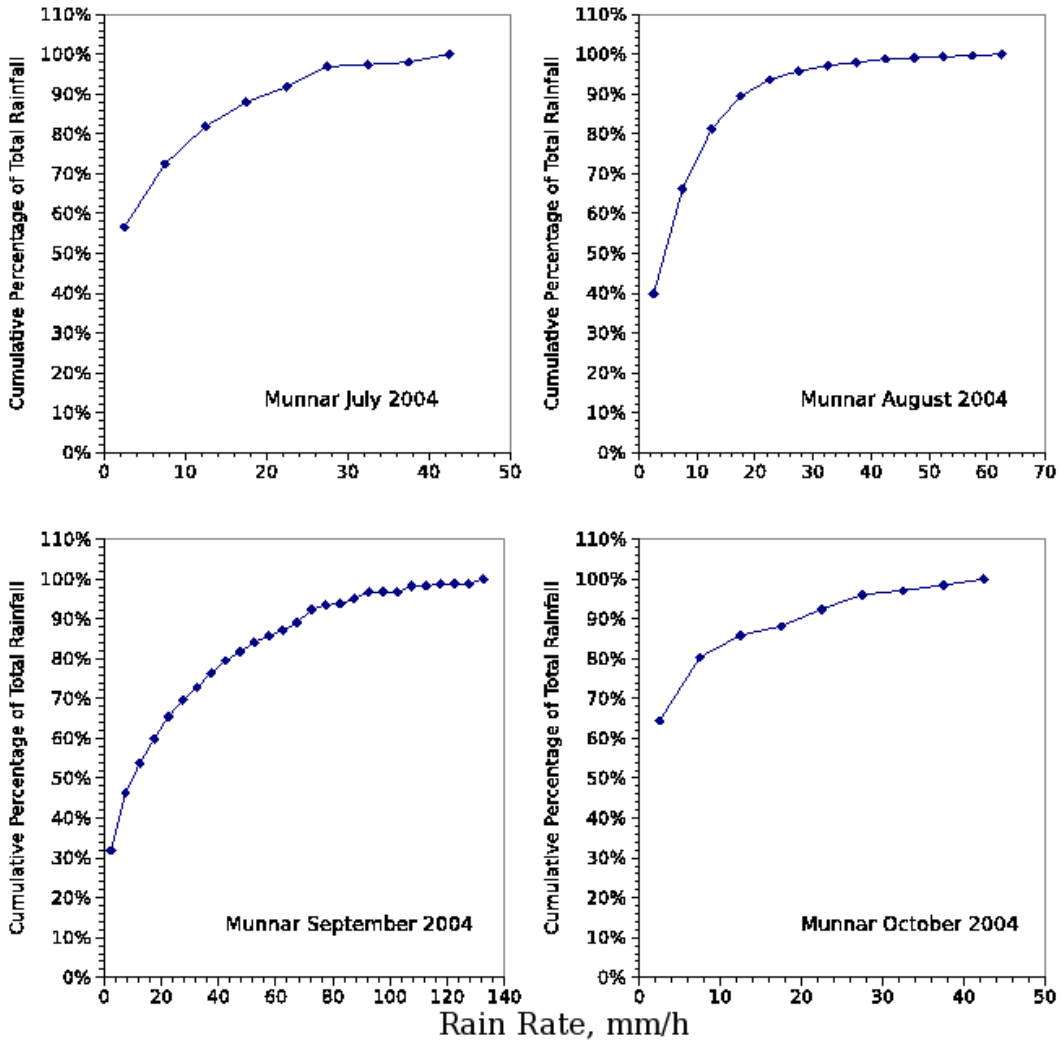

Figure 3.13. Cumulative contribution from each rain rate range to total rainfall at Munnar in 2004.

Another interesting point is the dominance of low intense rainfall in July 2002 at Kochi. Rainfall below 20 mm/h is present almost 99% of the time in July 2002, compared to around 90% of the time in the other months (except in June 2004, when it is 95%). Moreover, this has contributed about 62% of the total monthly rainfall in July 2002 while the highest in all the other months is only less than 49%. These figures strengthen our suspicion that the deficiency in rainfall was due to reduced presence of cumuliform clouds.

There does not appear to be any consistent difference between pre-monsoon and southwest monsoon months. But there are some interesting points that can be noted. The table shows that low intense rainfall was present for more time and contributed more to the total rainfall in April and May, 2001, compared to June and July, at Thiruvananthapuram. In 2005, the percentages are less in May, compared to the monsoon months. However, it is interesting that in June 2005, though low intensity rainfall was present almost 94% of the time, it contributed only less than 28% of the total rainfall (which is less than that for May 2005). The highest rain rate observed at Thiruvananthapuram is in this month. This possibly indicates the presence of a small number of very active cumuliform clouds that gave short duration very heavy rainfall.

In order to understand the distribution of rainfall with time, we plotted the normalised frequency against the percentage of total rainfall for all months for each station. The graphs are shown in figures 6.14, 6.15 and 6.16. We see that, at Thiruvananthapuram in June 2001, about 70% of the rainfall occurred in about 15% of the time and 90% in less than 50% of the time. In June 2005, however, about 90% of the rainfall was obtained in less than 20% of the time! In Kochi, around 90% of the rainfall was obtained in around 40% of the time in the year 2002, while in 2004, 80–90% of the rainfall was received in about 20% of the time. It may be noted that the distribution is more or less similar in both June and July 2002, although we had seen some differences between these two months in our earlier analysis. In Munnar, the behaviour is very similar in all the months, but is very different from that at the other stations. This information is very important for water conservation and management. The state of Kerala being a narrow strip of land with the Western Ghats on one side, rain water flows rapidly to the Arabian Sea. The short duration heavy rainfall tends to aggravate the loss of water and the related loss of top soil.

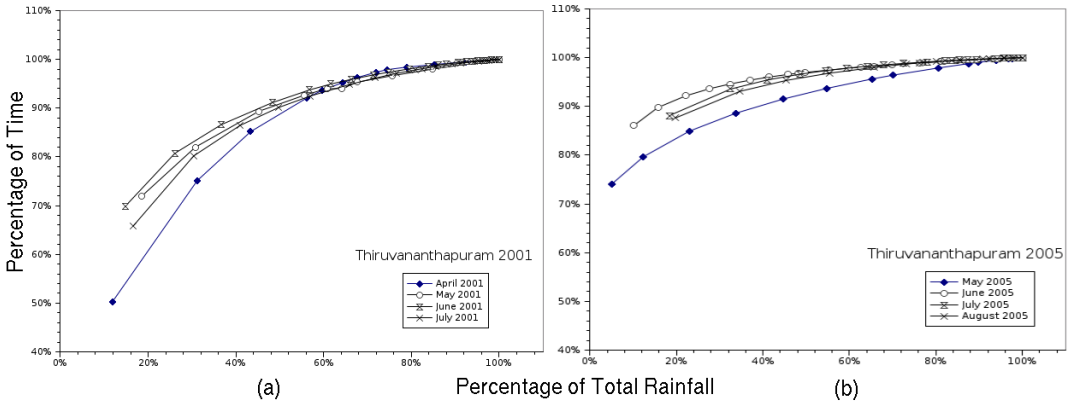

Figure 3.14. Variation of total rainfall with time at Thiruvananthapuram in (a) 2001 and (b) 2005.

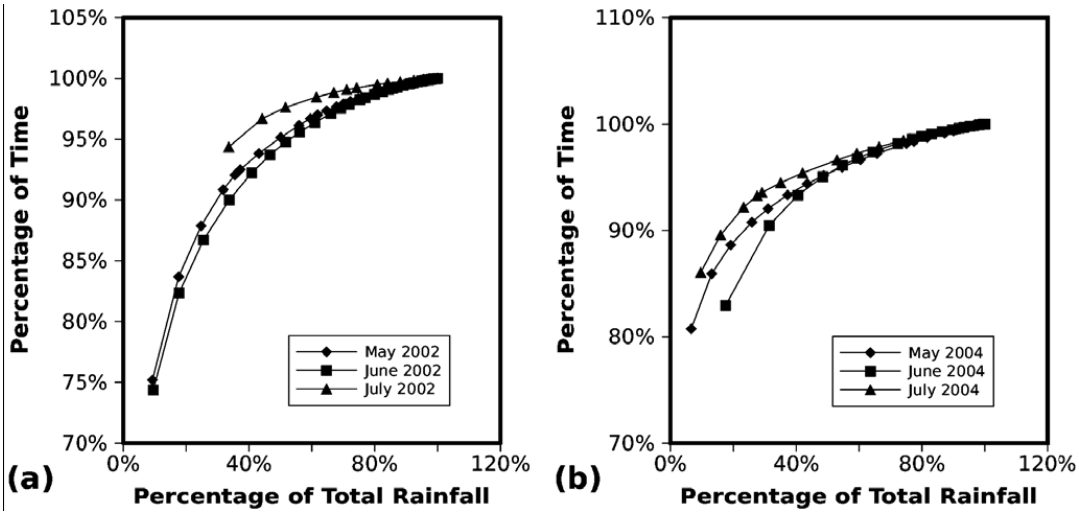

Figure 3.15. Variation of total rainfall with time at Kochi in (a) 2002 and (b) 2004.

3.5. CONCLUSION

This chapter presents the variation of rain rate at high time resolution conducted in Kerala. Though the measurements have been conducted only at three stations for durations of a few months at each station, the data give some insight into the behaviour of rainfall in this region. The important results are given below.

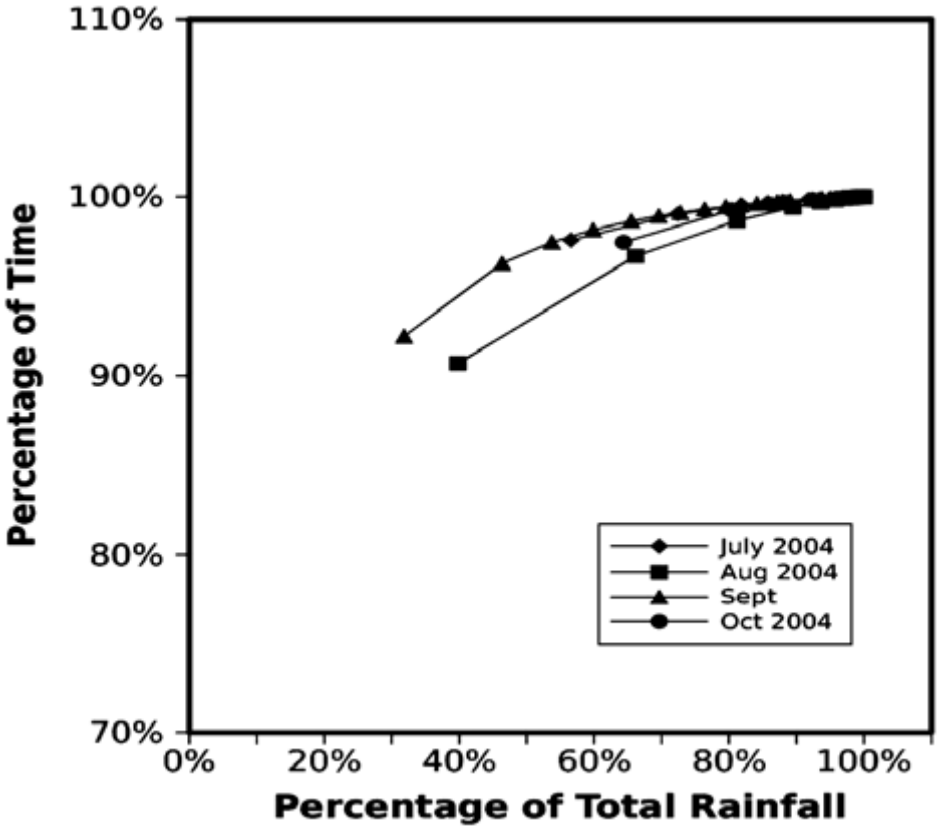

Figure 3.16. Variation of total rainfall with time at Munnar.

- Around 90 % of the time, the rain rate is below 5 mm/h, except at Thiruvananthapuram where it is around 65%. This indicates that stratiform clouds are more prevalent in these stations compared to cumuliform.
- The most interesting aspect was the apparently lower presence of cumuliform clouds during July 2002 at Kochi, which possibly contributed to the deficiency in rainfall.
- The rain rate temporal cumulative distribution could be fitted with a Weibull distribution function of the form

$$y = 1 - \exp\left(1 - \left(\frac{x}{\lambda}\right)^{k}\right)$$

The k is the shape parameter and λ is the scale parameter. It is found that the shape parameter is more or less the same at all stations during the southwest monsoon period.

- Rainfall is present only for less than 10% of the time (or about 4300 minutes) even during a rainy month like June or July. This indicates that rainfall could be actually present for lesser duration.

CHAPTER IV

RAIN DROP SIZE DISTRIBUTION (DSD): CHARACTERISTICS & DEVELOPING AN EMPIRICAL MODEL TO DERIVE DSD WHEN RAIN RATE ALONE IS AVAILABLE

CHAPTER IV

RAIN DROP SIZE DISTRIBUTION (DSD): CHARACTERISTICS & DEVELOPING AN EMPIRICAL MODEL TO DERIVE DSD WHEN RAIN RATE ALONE IS AVAILABLE

4.1. INTRODUCTION

Study of rain drop size distribution (DSD) is very useful in different areas like microwave communication, satellite meteorology, soil erosion and cloud physics. There is big interest in these areas for several reasons, including climatic change and increasing soil erosion due to expanding human activities. Accurate measurements of drop size distributions are important for many meteorological applications, including estimation of rainfall, cloud radiative transfer studies, and cloud model initialization and verification. For example, McGaughey et al. (1996), Viltard et al. (1998) and McKague et al. (1998) all demonstrated the large sensitivity of passive microwave algorithms to the prescribed drop size distribution of the precipitation originated from both convective and stratiform clouds. By tracking the rain DSD along their falling path is a direct way of even measuring rain evaporation (Li and Srivastava, 2001)

To overcome the time height ambiguity in radar measured reflectivity and surface rain rate, knowledge of hydrometeor size distribution within the precipitation layer is essential. The rain DSD is a critical factor in estimating rain rate using advanced dual-polarized weather radars (Vulpiani et al., 2006). A new neural-network algorithm to estimate the DSD from S-band dual-polarised radar measurement is presented in their paper. The corresponding rain rates are then computed assuming a commonly used raindrop diameter-speed relationship. Satellite measured rain parameters would be reliable and dependable if and only if the retrieval from the satellite primary data using the algorithm is accurate. Unfortunately, errors due to the seasonal dependence, back ground dependence etc. is very clear from the retrievals

carried out so far. Retrieval of the precipitation parameters from the active satellite measurements is found to be less accurate. The errors associated with the retrieval of rain rate from radar reflectivity factor can be eliminated, by knowing the target, which is the rain drop size distribution, from which the scattering of the electro magnetic radiation takes place. The same reflectivity may be obtained from different targets having different drop size distributions. Hence, there is a need to know the rain DSD in detail. The spatial, altitudinal and temporal variability of the Z-R relation is evident from the past measurements. Since the radar reflectivity factor is the 6^{th} moment of rain DSD, the radar back scattered power is not only merely dependant on the rain rate, but also it depends purely on the number and size distribution of the rain drops. So the radar reflectivity factor should necessarily be derived from the rain DSD, for the derivation of an empirical relation for the altitudinal and spatial variation of Z-R equation and here lies the importance of the need of more rain DSD data and analyses. Since there is no one to one relation between this Z and R, a wide range of Z-R relations are mentioned in the literature (Battan, 1973). A common technique for radar estimation of rainfall is to develop relationships between the backscattered energy return to the radar (i.e., reflectivity, *Z*) and rainfall rate (*R*). Both *Z* and *R* are dependent on the drop size distribution. The *Z–R* technique has the advantage of producing rainfall estimates over large areas (50 000 km^2) in relatively short time (several minutes). Unfortunately, the existence of various range-dependent errors can produce significant biases in the scanning radar estimate of rainfall (e.g., Wilson and Brandes 1979; Zawadzki 1984; Austin 1987). Moreover, many previous observational studies have shown that natural variations of the drop size distribution in time and space can lead to different *Z–R* parameterizations, ultimately producing different estimates of rain rates (e.g., Battan 1973; Ulbrich 1983; Austin 1987; Huggel et al. 1996). Different Z-R relations should be used for each rain rate range, for better rain DSD derivation (Mali et al., 2003).

In the context of microwave communication, the performance of the microwave links at frequencies above 10 GHz is constrained by the excess attenuation

due to precipitation, especially, rainfall. The lower atmosphere is absorptive, dispersive and inhomogeneous and therefore plays an important role in radio communication in the frequency range UHF to mm waves. The important parameters affecting the propagating wave are the shape of each rain drop and rain DSD. Rain attenuation increases with rain drop size and attains a maximum value at a particular drop size. Beyond this value of drop size, rain attenuation either remains constant or decreases (Verma and Jha, 1996b). Since the wavelengths of mm waves are of the same order as the rain drop sizes, the rate of attenuation is highly dependant on rain DSD (Verma and Jha, 1996a). In tropical climates, rain attenuation is severe due to higher rain rates (Jassel et al., 1994). "Sufficient data on propagation attenuation, rain rate and DSD are not available for tropical region and, in particular, for India where rainy season is characterised by the heavy monsoon rains. Due to the lack of rain DSD data in the tropics, the usage of available DSD data that are collected from the low rain rate regime like temperate regions, causes the attenuation prediction models are found to be very inadequate for tropics" they continued. These authors have developed a rain attenuation model based on the DSD data and compared with CCIR (International Radio consultative Committee) and other models. The usage of regional DSD data with its lognormal fit is very clear from their studies (and also Verma and Jha, 1996b) and the specific attenuation calculated using DSD with lognormal representation was more realistic compared to DSD with MP and gamma representations. So, these DSD measurements, their lognormal modelling and deep quantitative understanding have much relevance in the special scenario of attenuation of electromagnetic radiation with rain, especially with tropical heavy rainfall. Rain attenuation can be obtained directly through experiments or predicted from a knowledge of rain rate and DSD (Medhurst, 1965; Maciel and Assis, 1990; Ajai and Olsen, 1985). That is a model for the variation of DSD with rain rate is very essential. The difference in the experimental and theoretical attenuation results are due to the non-uniformity of DSD, which varies with the geographical locations (Medhurst, R.G., 1965). So, it will be helpful to understand more about the rain DSD for tropical climates, for improving the efficiency of

communication. Selection of frequency bands can be made on the basis of the DSD model derived for each location.

A number of recent studies have examined the applicability of separate *Z–R* relations for rain that originate from convective and stratiform clouds. Short et al. (1990) and Tokay and Short (1996) have shown, using Disdrometer data from Darwin, Australia, and the tropical western Pacific, that the DSD undergoes abrupt shifts between convective and stratiform precipitation and that rainfall rates derived are improved when two *Z–R* relations are used instead of one. However, Steiner and Houze (1997) showed that the use of two *Z–R* relations instead of one did not significantly improve monthly rain totals using radar data at Darwin, Australia. Also, Yuter and Houze (1997) have argued that convective and stratiform DSDs in the tropical western Pacific are not statistically distinct. Clearly, more research on the variability of the DSD in different precipitation regimes is required. The profiler retrievals for the MCS were partitioned into a three-tier classification scheme (i.e., convective, mixed convective–stratiform and stratiform) following a modified version of Williams et al. (1995) in order to isolate the microphysical characteristics in different precipitation types.

Kenji et al. (1999) has made measurements of rain DSD and kinetic energy of the rainfall at T-sukuba for 2 years and Ishigaki for 1 year, and compared the energy-rain rate equations. Their main finding on regional characteristics of Ishigaki was that, there were large sized raindrops below 30 mm/h rain rate and the distribution of raindrop size wide from 1 mm to 5 mm in diameter. But in Tsukuba the distribution of raindrop size concentrated between 1 mm to 2 mm. The impact of rain on soil that causes soil erosion at these different locations will be different because of the difference in DSD. So, the understanding about rain DSD will help us to take precautions in determining the agriculture field structure.

The gamma parameters have been derived on the ground with the Disdrometer and aloft with VHF and UHF radar measurements made at Gadanki in the southwest monsoon season by Narayana Rao et al. (2006). This is to study the μ-λ

(shape parameter-slope parameter) relation (parameter derived from the gamma fit to the rain DSD) with respect to this climatic regime and also as a function of height. This relation is different at Gadanki compared to other places like Florida and Oklahoma and also this relation is found to be varying with height. An experimental study of small scale variability of DSD has been carried out at Wallops Island, Virginia by Tokey and P.G. Bashor (2007). They also recognised the sampling issues of the Disdrometer and thus itself presented the findings for 1-, 3-, 6-, 10- and 15-minute averaged disdrometric measurements. Using the Disdrometer measurements at different climatic regions, constraints on the gamma distribution has been developed to retrieve DSD from the dual-frequency radars by Munchak and Tokey (2008). DSD data obtained from Disdrometer could be used for the simulation of algorithms to derive back the DSD (Tokey and Dickens, 2000).

The natural conclusion by Haddad et al. (2003) is that, in spite of the dual-frequency radar that GPM will carry, the careful a-priori modeling of the DSD, at scales commensurate with the GPM radars' resolution, will be crucial to the success of the GPM core retrieval algorithm. This enforces the fact that DSD should be modeled for its variation with rain rate very region specific.

According to Weischet (1969), the tropical area characteristically has a rainfall maximum between 1000 metres and 1500 metres. Still, there is possibility of many local or regional complications to occur (Barry, 1981). The rainfall characteristics over mountains are determined by several factors such as latitude, altitude and orography. A convective pattern of vertical precipitation distribution is widely found in the tropics. According to Rao (1958), the monsoon currents become convectively unstable when it is lifted by the mountains during travel along a short distance. The amounts of orographic precipitation depends on the air mass characteristics and synoptic-scale pressure pattern, local vertical motion due to the terrain, microphysical processes in the cloud and the evaporation of the falling rain drops (Sawyer, 1956).

Orographic effect of the western ghats on the monsoon rainfall has been studied for the southwest and northeast monsoon using normal rainfall data of 50 years (1901 to 1950). The precipitation is dependant on altitude over the western slope which is on the windward side with respect to the southwest monsoon, whereas it is independent of altitude over the eastern slope which is on the leeward side. The situation exactly reverses during the northeast monsoon rainfall. The study of Muralidharan et al. (1985) reveal that the amount of precipitation on the western slope of the western ghats above an altitude of about 600 metres increases with the altitude to a maximum at a height of about 1300 meters; and further up it decreases. Almost in a similar manner on the eastern slope of the Ghats above an altitude of about 370 metres the rainfall increases to a maximum about 1800 metres above mean sea level, and thereafter decreases continuously. Their rainfall profiles more or less agree with the results obtained from the global survey carried out by Lauer (1975) and also by Lauscher (1976) for other tropical mountains.

With the development of instruments that can give drop size data continuously and at relatively low costs, DSD measurements are becoming more common. However, there haven't been many measurements in India. Some of them are Jassal et al. (1994), Verma and Jha (1996a and 1996b), Reddy and Kozu (2003), Sasi Kumar et al. (2003), Mali et al. (2003), Krishna Reddy et al. (2005), Soma Sen Roy et al. (2005), Rao et al. (2006) and Harikumar et al. (2007; 2009). We present here the characterization of rain DSD and derivation of a rain DSD model for 4 different locations in southern India, viz. Thiruvananthapuram and Kochi, which are west coast stations; Munnar, a high altitude station in the Western Ghats and Sriharikota (SHAR), a station on the east coast, (Details of these stations are explained in the Chapter II) using a Joss-Waldvogel Disdrometer (JWD; Joss and Waldvogel, 1967). Some preliminary results from Thiruvananthapuram were presented in an earlier paper by Sasi Kumar et al. (2003) and the comparison of rain DSD between the stations in the eastern (SHAR) and western (Thiruvananthapuram and Kochi) coasts of India has also been presented by Harikumar et al. (2007).

Three different distribution functions are commonly used by different authors to describe rain drop size spectra, namely, the Marshall and Palmer (1948) type of exponential distribution, the gamma distribution (Ulbrich,1983) and the lognormal distribution (Feingold and Levin, 1986). It is generally agreed that the exponential distribution is valid only for data averaged over long periods of time (Joss and Gori, 1978), or over large volumes of space. However, the negative exponential is not appropriate for use in tropical regions and gamma model distribution too must be modified (Awang and Din, 2004). Thus, lognormal raindrop size distribution models are suitable and thus used it to estimate rain attenuation and compared to rain attenuation measurements from microwave links installed at Wireless Communication Centre (WCC), Universiti Teknologi Malaysia, UTM Skudai, Johor by these authors. Raindrop spectra often tend to have a monomodal distribution, which can be modelled by the gamma distribution function. This has the advantage that it tends to the exponential function as one of the parameters tends to zero. In the cases of the exponential and gamma distributions, however, the parameters have no physical significance.

The lognormal distribution was explored by Feingold and Levin (1986) and was found to be as good as, if not better than, the gamma distribution in terms of fitting with observations. While the former showed better fit with the observed raindrop size distribution, the computed rain rate was marginally better when the gamma function was used. However, the lognormal distribution has the advantage that the parameters have physical significance (Feingold and Levin, 1986). The variations in these parameters with rain rate or with time would, therefore, have implications on the physical processes that lead to the formation of rain drops and the processes that take place as the drops fall from the cloud to the ground.

Testud et al. (2001) developed a concept of normalization of DSD as normalizing raindrop spectra is an appropriate way to identify the shape of the distribution. The concept of normalization of DSD is based upon two reference

variables, the liquid water content LWC and the mean volume diameter *Dm*. This normalization procedure helps in clearly defining the stratiform and convective rain types and hence a better insight into the cloud microphysics. The major point of this approach is that this normalisation is totally free of any assumption about the shape of the DSD. This new normalization has been successfully applied to the airborne microphysical data of the Tropical Ocean and Global Atmosphere Coupled Ocean–Atmosphere Response Experiment (TOGA COARE) collected by the National Center for Atmospheric Research Electra aircraft. The classification of the TOGA COARE raindrop spectra into stratiform and convective have been done to impress on the usefulness of this approach.

In the present study, we have tried to understand the characteristics of DSD rather than use the DSD to distinguish the type of rainfall. Therefore, the approach of Testud et al. (2001) is not adapted here. However, the liquid water content (LWC) is varying linearly with rain rate at all the stations. So, the study of the variation of all the parameters with rain rate indirectly implies its variation with LWC too.

4.2. CHARACTERISTICS OF RAIN DROP SIZE DISTRIBUTION (DSD)

4.2.1. Data and Data Analysis

The data covers a period of roughly 34 months in which there was rainfall. This includes 22 months in the SW monsoon season, 8 months in the pre-monsoon season and 4 months in the NE monsoon season. Data for four months are from the high altitude station Munnar and for three months from the east coast station SHAR. The remaining data are from two stations on the west coast as explained in the Chapter I. One method for obtaining drop size distribution (DSD) functions requires previous normalization of both measured drop diameters and concentrations. This normalization, proposed by Sekhon and Srivastava (1971, 1978), and later by Willis (1984), was meant to comprise the entire dataset, thus achieving a universal distribution function independent of observation site or rain type. An alternative method is based on previous grouping of rain registers in different rain-rate classes to obtain mean size distributions. These distributions can then be fitted to theoretical

models whose parameters will depend on the rain rate, usually through a power law. (Cerro et al., 1999). We followed the second method to analyse and thus parameterize our DSD data.

4.2.2. Representing the Rain DSD – Best Fitting Distribution

The data obtained in each minute were corrected for dead time errors and the rain DSD was computed. The rain rate for each minute was then computed from the corrected data, and the entire data for each month were sorted in ascending order of rain rate. The data were then divided into different ranges of rain rate, as explained below. The values for each range were then averaged and the average DSD was computed for each range of rain rate. The mean rain rate for each range was also determined. The next step would be to find out the most suitable distribution that represents the rain DSD.

Three well known distribution functions have been used by different authors to represent the DSD.

Marshal Palmer (MP) distribution (Marshal and Palmer, 1948) of the form

$$N(D) = N_0 \exp(-\lambda D) \tag{4.1}$$

where N_0 is the Intercept parameter (signifies the number density in the first channel of the Joss Waldvogel Disdrometer) and λ is the Slope parameter,

a Gamma (Γ) distribution (Ulbrich, 1983) of the form

$$N(D) = N_0 D^{\mu} \exp(-\lambda D) \tag{4.2}$$

where N_0 is the Intercept parameter, λ is the Slope parameter and μ is the Shape parameter, and a lognormal distribution (LN) (Feingold and Levin, 1986) of the form

$$N(D) = \frac{N_T}{\sqrt{2\pi}\ln\sigma D} \exp\left[-\frac{\ln^2\left(D/D_g\right)}{2\ln^2\sigma}\right] \tag{4.3}$$

where N_T is the Total number of drops, D_g is the Geometric mean diameter and σ is the Standard geometric deviation of the drop size.

By substituting

$$\frac{N_T}{\sqrt{2\pi}\ln\sigma} = A \tag{4.4}$$

$$\ln D_g = B \text{ and} \tag{4.5}$$

$$\ln\sigma = C \tag{4.6}$$

and simplification, finally the equation (4.4) takes the form

$$N(D) = \frac{\exp(A)}{D}\exp\left\{-0.5\left[\frac{(\ln D - B)}{C}\right]^2\right\} \tag{4.7}$$

where D is the drop diameter, $N(D)$ is the number of drops per cubic meter per unit diameter interval, and A, B and C are fit parameters.

DSD corresponding to different rain rate ranges for the month of June 2005 at Thiruvananthapuram was selected as a sample and the data set was fitted with all the three distribution functions mentioned above. The correlation coefficient between the fitted data and the actual data was derived for each rain rate range. The variation of this correlation coefficient with rain rate is shown in Figure 4.1. A similar behaviour is seen in the data from the other three stations also.

From figure 4.1, it is clear that the correlation between the DSD derived using the Marshal Palmer distribution function fit and the DSD data decreases as the rain rate increases. Even though the correlation coefficients of both the Gamma and lognormal distributions with the data are very similar for most of the rain rates, Gamma distribution shows a somewhat lower correlation at higher rain rates compared to the lognormal distribution. According to Munchak and Tokey (2008), even though good relations between the gamma parameters are seen, the relations do not necessarily hold at all rain rates and for all precipitation events. Taking into consideration this result also, lognormal distribution was preferred to represent the DSD over this region.

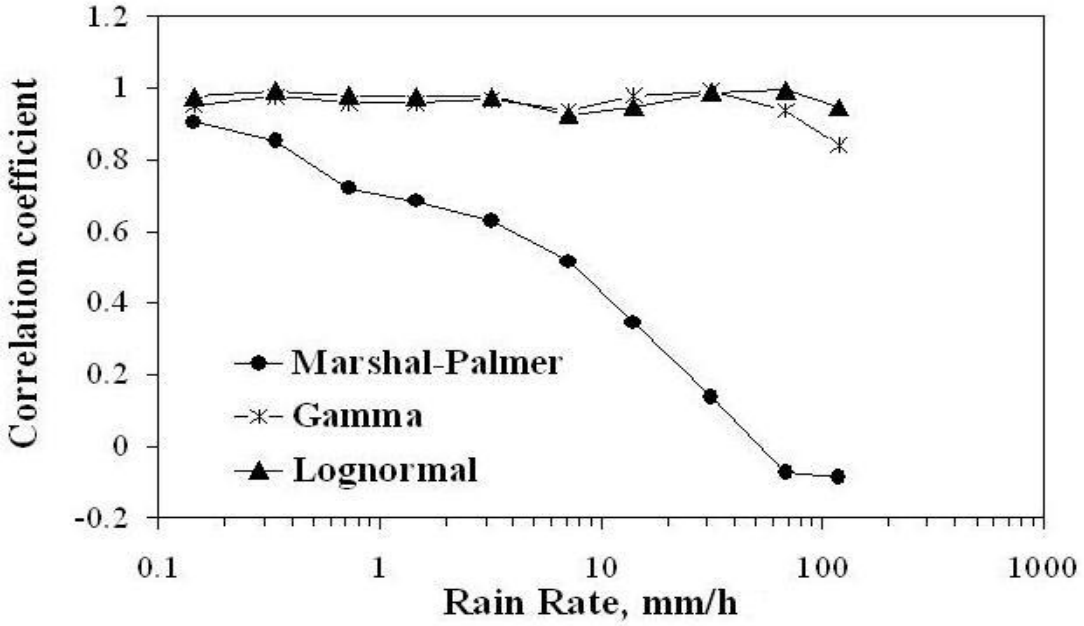

Figure 4.1. Variation of the correlation coefficient for the correlation analysis between the DSD derived from each functional fit and the DSD data to which the fit has applied with rain rate.

4.2.3. Drop Size Distribution Spectrum-General features

Figure 4.2 shows typical rain DSD spectrums with fitted lognormal curves for all the stations. The curves fit the data reasonably well in all the data ranges. The distribution is narrow when the rain rate is low and becomes significantly wider with increasing rain rate, indicating the increasing presence of larger drops. The initial increasing trend of number of drops with drop diameter is not very clearly seen at the low diameter end for low rain rates, though a tendency for that may be made out. We are not in a position to determine whether the number of drops actually increase with drop diameter in this region since we have data only from 0.313 mm onwards. However, this can be clearly seen in the case of DSDs corresponding to large rain rates. Therefore, it may be reasonable to assume that this trend extends to the low rain rates also. Though, there is a possibility of under estimation in the number of smaller drops in heavy rains due to instrument's electronic design for self-noise control as

explained earlier in the Chapter II. But there is no way as on today to eliminate this error completely. In the present case, the sensor is mounted such that acoustic noise and wind effects are reduced to a minimum.

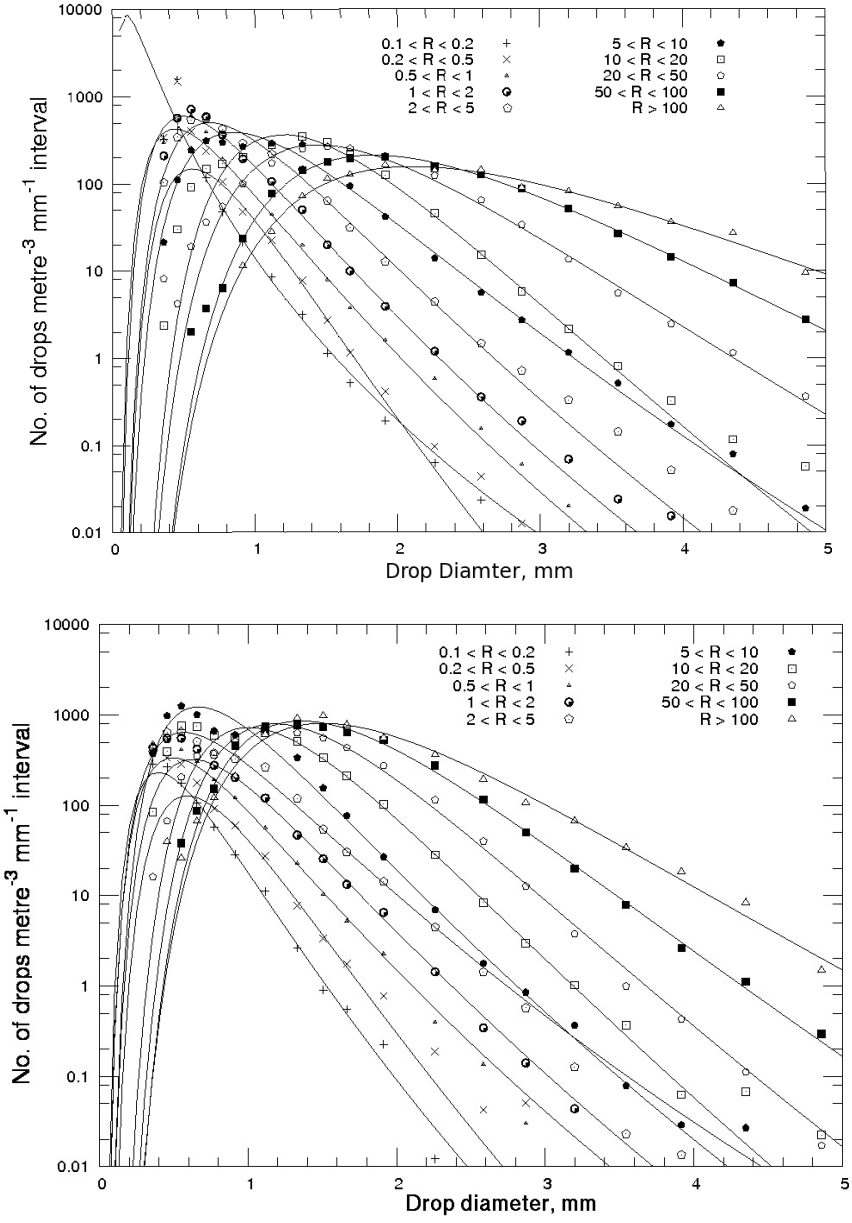

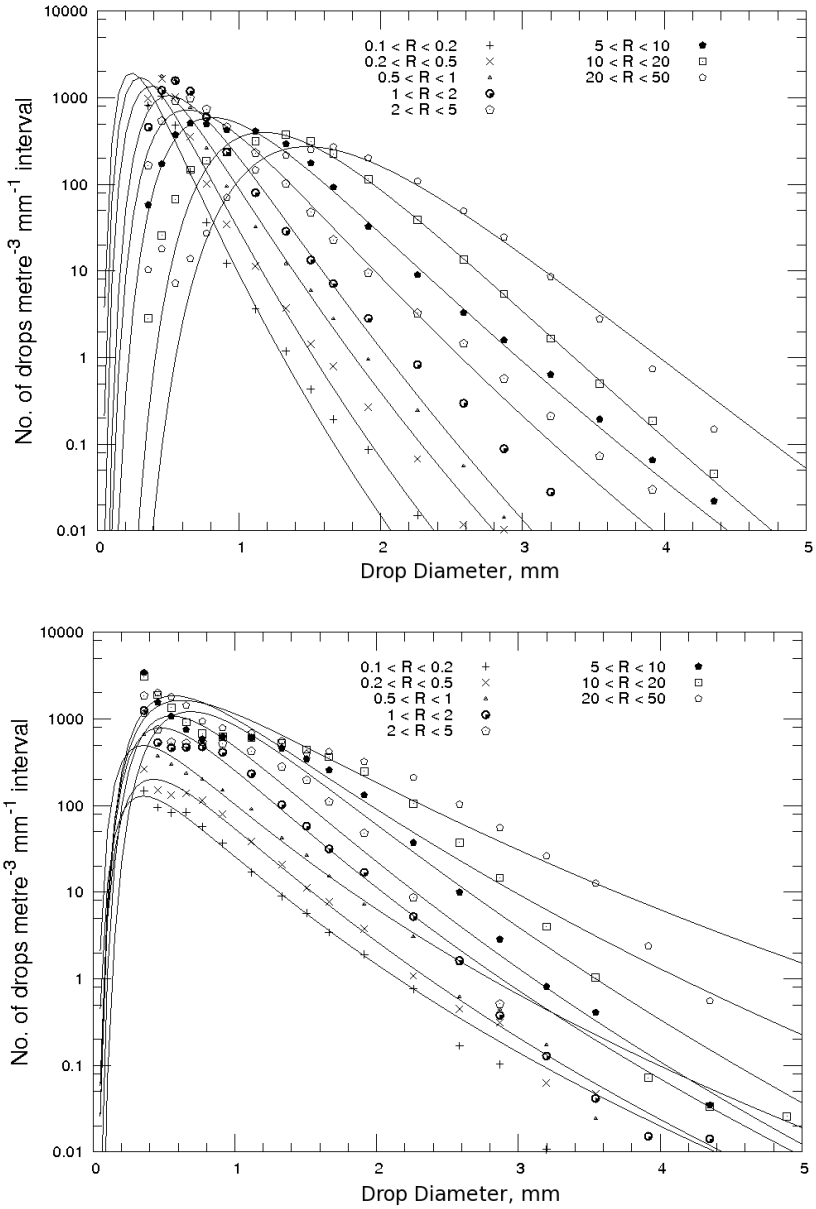

Figure 4.2. Rain DSD spectrum corresponding to the stations Kochi (July 2003; top panel) Thiruvananthapuram (July 2005; second panel), Munnar (July 2004; third panel) and SHAR (August 2003; bottom panel). The lognormal fit is shown as solid lines along with the DSD data. R in the legend represents the rain rate.

Behaviour of rain DSD at different locations is very clear from visual observations of these spectra (figure 4.2). At Thiruvananthapuram, an increase is seen in the drop diameter at which the distribution peaks with rain rate. The amplitude of this peak decreases as the rain rate increases. At kochi, the behaviour is very similar o that Thiruvananthapuram but the amplitude is found to be constant for all the rain rates. At Munnar, the characterstics are similar to Thiruvananthapuram, but the amplitude of the peak decreases very drastically as rain rate increases. But at SHAR, there is no shift in the peak and the amplitude increases as rain rate increases.

From the fitted lognormal distribution, the three physically meaningful parameters N_T, D_g and σ were evaluated to study the characteristics of DSD in our region.

4.2.4. Evaluation of N_T, D_g and σ

Feingold and Levin (1986) computed the fit parameters by using the observed total number concentration, N_T, and the number of drops in each size class to calculate the geometric mean diameter, D_g, and standard geometric deviation, σ, of the truncated distribution. They then used these values in the equation 4.3, to obtain the expression for number of rain drops per cubic metre per unit diameter interval ($N_{(D)}$), where D_g and σ are in millimetres. A different method has been followed here. Instead of computing the fit parameters, the DSD for each range was fitted with a lognormal distribution function. The functional fits were made using gnuplot, a graphing software that uses the Marquardt- Levenberg algorithm for non-linear curve fitting. . It is very easy to fit the data sets with lognormal distribution function using simple computer programs and to obtain fit parameters for huge long term data compared to the parameter estimate. Since the number of drops varies from 0 to thousands or tens of thousands, we took the natural logarithm of both sides of the equation before fitting so that all the points get equal weightage. Thus, the actual equation used for fitting was

$$\ln(N_{(D)}) = A - \ln(D) - (0.5(\ln(D) - B)/C)^2 \qquad (4.8)$$

where D is the drop diameter, $N_{(D)}$ is the number of drops per cubic metre per unit diameter interval and A, B, C are the fit parameters. Comparing this with Eqn. 3, we can, thus, derive the values of N_T, D_g and σ from A, B and C using the equations 4.4, 4.5 and 4.6 respectively.

Table IV.I shows the rain rate ranges into which the data were divided and the mean rain rate obtained in each range for a typical month in each station. The rain rate ranges were chosen such that the width of the range increases in a roughly exponential manner. The reason is that the data showed, in general, that the rainfall duration was high at the low rain rate end and decreased in a roughly exponential manner with increasing rain rate so that there was data for a longer duration for lower rain rate. A detailed analysis of the distribution of rain rate is given in our paper (Sasi Kumar et al. 2007). There we show that rainfall is below 5 mm/h, 70 to 90% of the time in most of the months, and sometimes even higher.

No.	Rain rate range	Tvpm July 2005		Kochi July 2003		Sriharikota Aug. 2003		Munnar July 2004	
		R	n	R	n	R	n	R	N
1	0.1 < R < 0.2	0.146	354	0.143	107	0.148	75	0.144	1039
2	0.2 < R < 0.5	0.336	635	0.329	146	0.338	101	0.329	1443
3	0.5 < R < 1	0.687	474	0.721	148	0.716	52	0.712	940
4	1 < R < 2	1.387	329	1.479	152	1.465	50	1.382	655
5	2 < R < 5	3.240	404	3.172	265	3.259	59	3.077	420
6	5 < R < 10	7.131	261	7.157	124	7.110	29	6.747	151
7	10 < R < 20	14.412	147	14.517	86	15.598	24	13.681	73
8	20 < R < 50	31.902	124	31.016	75	28.208	25	27.686	29
9	50 < R < 100	67.277	41	65.754	24	53.848	3	--	--
10	R > 100	109.27	3	113.26	3	--	--	--	--

Table IV.I. Mean rain rate obtained in each range for one month in each station. (R=rain rate. n=Number of minutes for which rain was measured).

The significance of taking the entire data for a month for the analysis, rather than taking each rainfall episode separately is discussed here. This was done for the following reasons: This region has mainly three seasons, as far as rainfall is concerned. These are the South-West (SW) monsoon (June–September), North-East (NE) monsoon (October–December) and Pre-monsoon (January–May). Rainfall during the SW monsoon is mostly from stratiform clouds, and during the other two seasons is from cumuliform clouds, mostly thunderstorms. Therefore, it is expected that the rainfall during a season is mostly from similar type of clouds. One important difference is there in the characteristics of rainfall between the stations in the west coast and those in the east coast, which is relevant to this study. Ie, during the SW monsoon period, rain fall over west coast is oceanic while rain fall at east coast is continental because the wind is mostly southwesterly or westerly. We took each month separately because it gave better time resolution compared to taking an entire season as a whole. This also helped to a certain extent to see whether there are changes within a season. It is found by Kozhu et al. (2006) that the DSDs are affected even by diurnal convective cycles and seasonal variations in precipitation characteristics. Further, we were trying to identify how DSD is influenced by rain rate, rather than to understand, for example, how DSD varied during the course of a rainfall event. The analysis procedure was selected to enable this.

In a previous paper (Sasi Kumar et al. 2003), it was stated that the distribution measured at Thiruvananthapuram in April (pre-monsoon) appears to be different from that in June (SW monsoon) for low rain rates. At that time, they had divided rainfall periods into five rain rate ranges and tried to fit the gamma function to the distribution. The low rain rate ranges in June showed a behaviour that was closer to the Marshall-Palmer type of distribution than to gamma. However, after analysing a much greater volume of data, and in greater detail than earlier, we find that the lognormal distribution is more appropriate and fits most of the data. The deviation from lognormal is limited to about a tenth of the data we have obtained so far.

4.2.5. Variation of N_T, D_g and σ with rain rate

N_T, D_g and σ for each rain rate range in each month was derived to study the variation of these parameters with rain rate to study the characteristics of DSD. These are discussed here.

Variation of σ with rain rate

Variation of σ is plotted against the mean rain rate. Typical graphs of σ for one month from each station are shown in Figure 4.3. It is seen that in general σ was almost constant for all rain rate ranges (Harikumar et al., 2007). A small variation can be seen, but it is very small compared to the values of σ.

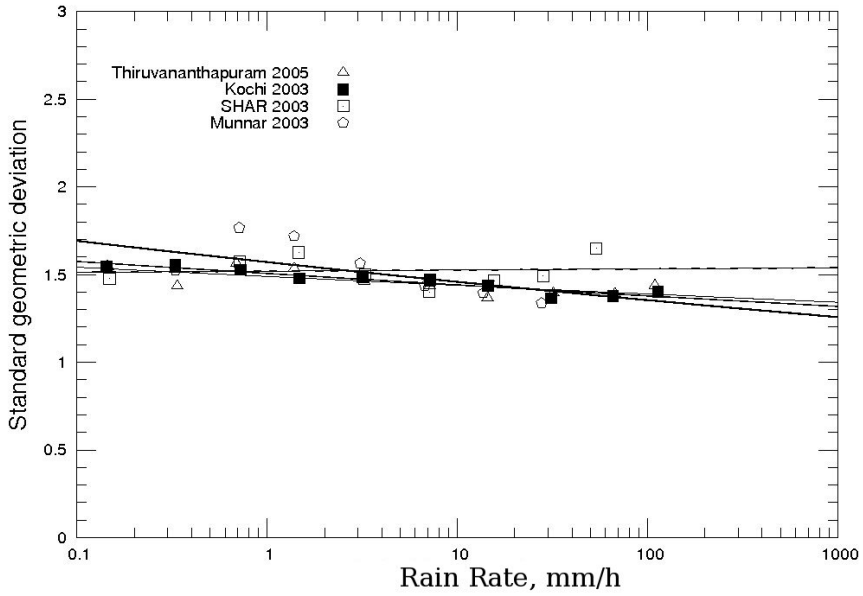

Figure 4.3. The variation of σ with rain rate in August at Sriharikota and in July in the other stations.

Variation of N_T and D_g with rain rate

The typical Variation of N_T, Dg (with fit of the form $Y=aX^b$) and $N_T Dg^3$ (a measure of LWC) (with fit of the form Y=mX+c) with rain rate at all the stations are shown in the figure 4.4.

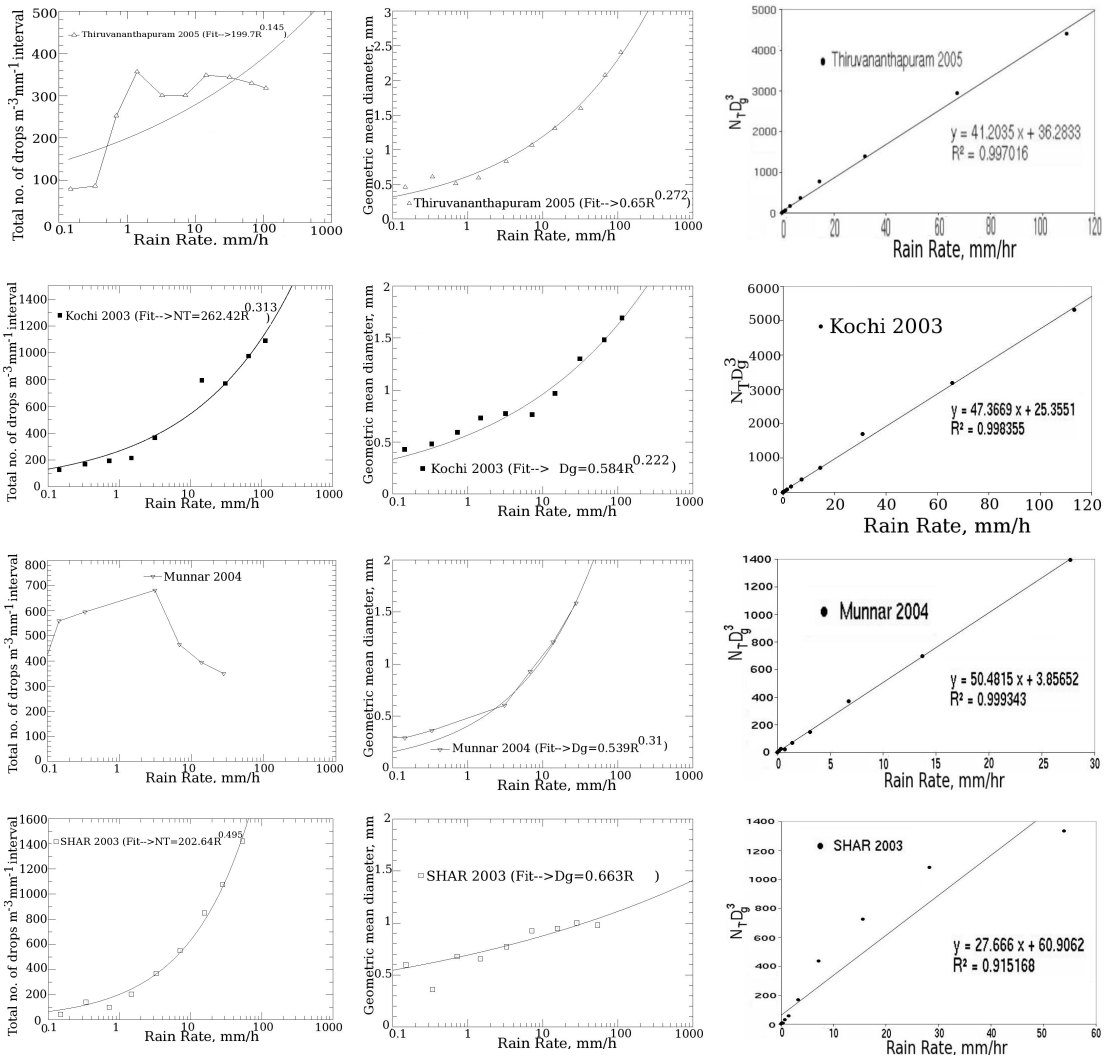

Figure 4.4. Variation of N_T(left panel), Dg (middle) (with fit of the form $Y=aX^b$) and N_TDg^3 (right) (with fit of the form $Y=mX+c$) with rain rate at stations Thiruvananthapuram (top panel), Kochi (2nd panel), Munnar (3rd panel) and SHAR (bottom panel). For all the stations except SHAR, the data shown here is for the month of July and for SHAR, it is for August.

The variation of these parameters with rain rate at all the stations have been included together in the figure 4.5. Comparison of the variation of theses parameters with rain rate between all the stations is explained in detail below. Since Kochi and SHAR behaved same they have been treated together and since Munnar and Thiruvananthapuram behave same they are being treated separately.

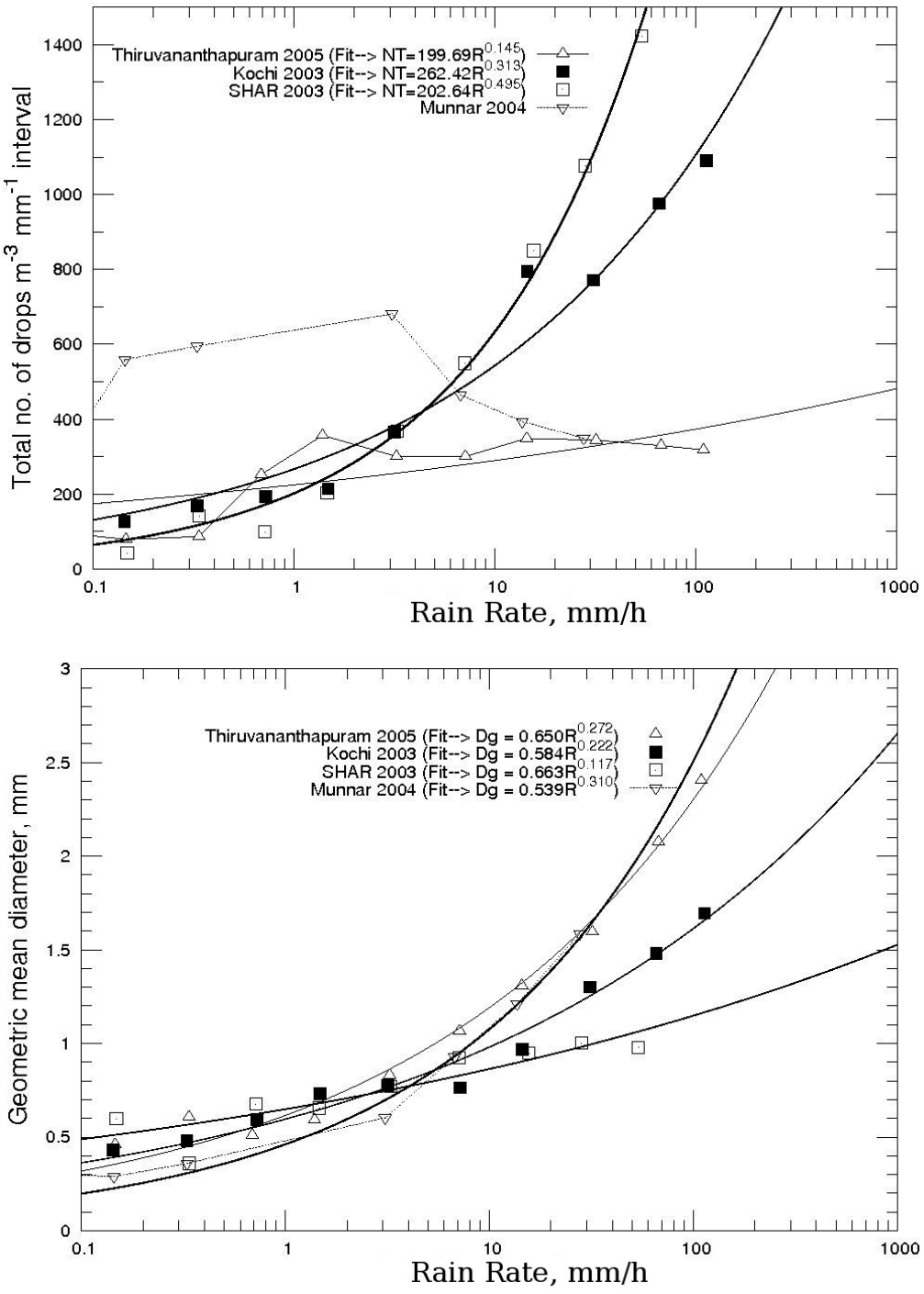

Figure 4.5. Comparisons of the Variation of N_T (top panel) and Dg (bottom panel) with rain rate at all the stations.

Kochi and SHAR

We see that N_T generally tends to increase exponentially with rain rate; but the rate of increase is different for these two stations (figure 4.5). The graph also shows fitted curves of the form $Y=aX^b$, where *a* and *b* are constants. It may be noted that the total number of drops is more or less the same at both the stations up to about 3mm/h. Above that the total number of drops increase faster with rain rate at SHAR compared to that at Kochi. This results in N_T being higher for large rain rates at SHAR. As a consequence, there should be more number of larger drops in Kochi during high rain rates. In other words, the mean drop size should be higher in Kochi during heavy rainfall, as we shall see below.

As in the case of N_T, we have fitted the Dg data with curves of the form $Y=aX^b$ and the fitted equations are also shown in the figure. The periods for which the data are taken are the same as in the case of N_T. The variation is very similar to that of N_T. We see that the values of Dg are more or less same up to around a rain rate of 3 mm/h. Above this rain rate, the rate of increase of Dg is high for Kochi and less for SHAR. Thus, a faster increase in the number of drops at SHAR is compensated by a slow rise in drop size.

An interesting observation at Kochi is that N_T was rather low in the three months of May, June and July 2004. Thus, for instance, for a rain rate of 3 mm/h, N_T was 366 in July 2003. But it came down to 138 in July 2004. D_g, on the other hand, increased from 0.774 in July 2003 to 1.101 mm in July 2004. Figure 4.6 shows the graphs for N_T and D_g for Kochi for July 2003 and July 2004 which makes the difference clear. i.e., during 2003 at Kochi, the geometric mean sizes of the drops are always smaller compared to that during 2004 for any particular rain rate. The presence of comparatively smaller drops in the convective clouds was explained by Tokay and Short (1996) is as given below. The time required for the growth of precipitation particles in convective clouds is much less than that in the stratiform clouds. Therefore, the precipitation particles originate and grow not far from the cloud base. With the existence of strong updrafts, it is possible that the precipitation particles in convective

clouds are carried upward and continue to grow until they become heavy enough to overcome the updraft and begin to fall relative to the ground. In convective clouds, growth by accretion of liquid water is the dominant mechanism followed by collisions, coalescence and breakup of raindrops.

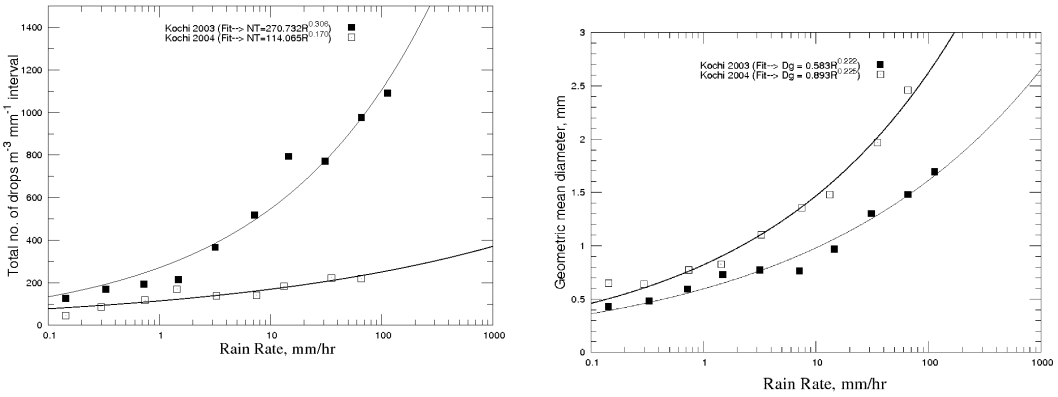

Figure 4.6. Comparison of variation of N_T (left panel) and D_g (right panel) with rain rate in July 2003 and July 2004 at Kochi. The fitted equations are also shown.

This indicates the possibility of rainfall being predominantly from convective clouds in 2003. To confirm the prevalence of convection in 2003 compared to 2004, we checked the Outgoing Longwave Radiation (OLR) data. The OLR data is downloaded for a maximum possible spatial resolution of 2.5º lat X 2.5º lon grid corresponding to Kochi (7.5ºN to 10ºN, 75ºE to 77.5ºE) from the NOAA website (Liebmann and Smith, 1996). The high convection in the year 2003 compared to 2004 is clear from the low OLR value (OLR~ 199.827 W/m^2) during July 2003 compared to July 2004 (OLR~ 209.542 W/m^2) at Kochi.

Munnar and Thiruvananthapuram

During the four months in which we measured DSD in Munnar, we find that N_T varies very differently. We see that N_T initially increases with rain rate up to about 3 mm/h, indicating that the increase in rain rate is primarily due to increase in the number of drops, as in other stations. This is supported by the fact that the increase in

D_g is small over this range. Beyond 3 mm/h, we see that N_T decreases rapidly and D_g increases rapidly. At Thiruvananthapuram, the variation up to about 3 mm/h more or less follows an incraesing pattern, but then N_T remains more or less constant or starts decreasing, though slightly. This kind of behaviour is found in most of the months at Thiruvananthapuram, though the rain rate at which the change in profile occurs is different for different months. D_g increases correspondingly to compensate for N_T remaining steady or decreasing. Table IV. II shows this clearly. It also shows how N_T and D_g for the same rain rate is different for different stations.

R	N_T				D_g				σ			
	Tvm July 2005	Kochi July 2003	Shk Aug. 2003	Mnr July 2004	Tvm July 2005	Kochi July 2003	Shk Aug. 2003	Mnr July 2004	Tvm July 2005	Kochi July 2003	Shk Aug. 2003	Mnr July 2004
0.33	86.5	168.9	140.9	594.8	0.61	0.48	0.59	0.36	1.43	1.55	1.60	1.52
3.20	300.7	366.4	367.6	681.6	0.83	0.77	0.77	0.60	1.46	1.49	1.50	1.56
30	343.9	770.8	1077	349.2	1.60	1.30	1.00	1.59	1.39	1.36	1.49	1.34
110	317.8	1090.7	--	--	2.40	1.69	--	--	1.44	1.40	--	--

Table IV. II. N_T, D_g and σ for same rain rate at different stations (Tvm = Thiruvananthapuram, Mnr = Munnar, Shk = Sriharikota).

To understand the differences in the magnitudes of these parameters at each station, the values of N_T and Dg are plotted together for a rain rate of 30 mm/h for all the stations are shown in figure 4.7. It is apparent from the figure that as total number of drops increases mean diameter decreases. The N_T (Dg) is lowest (most) for Thiruvananthapuram, is less (more) for Munnar, is more (less) for Kochi and most (lowest) for SHAR.

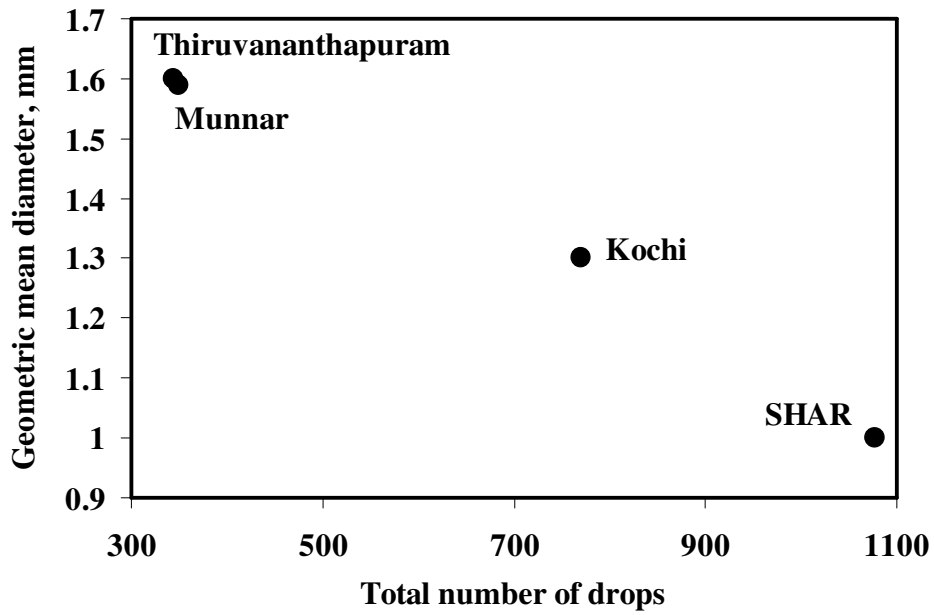

Figure 4.7. Station-wise variation of N_T-Dg pairs corresponding to a rain rate of 30 mm/h.

The comparison of the variation of these two parameters between a station at west coast (Kochi) and at a high altitude station (Munnar) lying in the same latitude during southwest monsoon period gave an insight to the orogrphic effect on rain DSD apart from the known orographical rainfall enhancement (Muralidharan et al., 1985). Recently, study of the satellite detection (TRMM satellite data) of rainfall (June-August 2002-2003, averaged) over the Indian peninsula by Harikumar et al. (2009a) shows the rainfall enhancement at windward side of the Western Ghats during southwest monsoon season. It is very clear from figure 4.5 that a heavy rainfall at Munnar consists of less number of bigger drops, while Kochi rain consists of more number of smaller drops at a particular rain rate. That means, the orography is seen to affect the drop size and thus orographic rain seems to have larger drops when rain rate is high. This situation is very crucial because larger drops could cause more soil erosion that may lead to the triggering of land slide. Therefore study of orographic effect on rainfall, especially on rain DSD would be useful and throw light on landslide triggering mechanisms.

Variation of $N_T D_g^3$ with rain rate

As mentioned earlier, we find that both N_T and D_g vary in a similar fashion with rain rate. We also find that when one of these parameters increases slowly with rain rate, the other parameter seems to compensate and increase more rapidly, and vice versa. This is natural since a certain quantity of water has to be provided by the drops to create particular rain rate. We plotted the function $N_T D_g^3$ against rain rate R and found that there existed a linear relationship between R and $N_T D_g^3$. In figure 4.4, the graphs for a month at each station are also shown. It is interesting to note that the regression coefficient is around 0.999 most of the time, even for Munnar where the variation of N_T and D_g with R is irregular, as mentioned above. The regression coefficient is, however, lower (0.91) for SHAR. Here, the points are away from the line and follow a kind of arc. This is possibly because DSD curves fitted badly with the lognormal distribution function, as mentioned earlier. The regression lines were not forced to go through the origin and hence the equations give a finite y-intercept. The values are, however, small and can be ignored.

4.2.6. Discussion

Lognormal distribution is found to be a very good representation for rain DSD for the entire rain rates. The parameters N_T and D_g vary with rain rate in such a manner that an increase or decrease in one parameter is compensated by an opposite change in the other. At Kochi and SHAR, N_T and D_g increases exponentially with rain rate. In Munnar, and in Thiruvananthapuram to some extent, we find that these parameters vary in a manner that is very different from that at the other two stations. N_T increases first up to a rain rate of around 3 mm/h and then decreases beyond as rain rate increases. At Thiruvananthapuram, for some months a constant value is also seen for N_T instead of decreasing beyond 3 mm/h. Dg increases very gradually up to around 3 mm/h and then increases very sharply beyond around 3 mm/h. For a particular rain rate The N_T (Dg) is lowest (most) for Thiruvananthapuram, is less (more) for Munnar, is more (less) for Kochi and most (lowest) for SHAR.

The difference in the behavior of these parameters at Munnar and SHAR in the southwest monsoon season, when the wind is westerly or south-westerly suggests that the effect of CCN may not be the possible reason for the DSD spatial variability. The more or less similar behaviour shown by Munnar and Thiruvananthapuram and that shown by Kochi and SHAR as explained above also suggests that, effect of orography on rainfall is a possible reason for the spatial variability of the rain DSD within the tropical areas. However, more detailed studies would be needed to confirm this.

$N_T D_g^3$ varies linearly with rain rate, with an exception at SHAR. This also points out the need to have more data at east coast stations.

4.3. EMPIRICAL MODEL FOR THE VARIATION OF RAIN DROP SIZE DISTRIBUTION WITH RAIN RATE

4.3.1. Derivation of the empirical model

An empirical model for DSD in this region was derived using the data. All the available data, except that for a few months, was used for this purpose. The data for the few months that was not used was kept aside for validating the derived model. The data thus kept aside was for the months of May, June and October 2005 at Thiruvananthapuram, May and July 2004 (up to 8th) at Kochi, July 2004 (from 9th onwards) at Munnar and August 2003 at Sriharikota. The method of deriving the empirical model is given below.

DSD data for each of the three monsoon periods was sorted according to rain rate, viz. southwest monsoon (June, July, August & September), northeast monsoon (October, November & December) and pre-monsoon (January to May). Then this data was grouped into the different rain rate ranges specified earlier. The mean DSD and the mean rain rate for each range for each season was then determined. This mean DSD corresponding to each rain rate range was fitted with the lognormal distribution function (Equation 4.7). The functional fits were made using gnuplot, a graphing software that uses the Marquardt-Levenberg algorithm for non-linear curve fitting as

mentioned earlier. A typical set of rain drop size distribution spectra along with lognormal fits for each station is shown in Figure 4.2.

The values of the lognormal fit parameters A, B and C for the fit corresponding to each rain rate range were obtained from the curve-fitting process. The variation of these parameters with rain rate was then studied. The variation of these three parameters with rain rate has the same form in all the monsoon seasons at all the stations. This variation of the fit parameter A could be fitted with an expression of the form

$$A = A_0 + A_1R + A_2\ln R \qquad (4.9)$$

where A_0, A_1 and A_2 are the fit parameters and R is the rain rate.

The fit parameter B also could be represented by a similar relation.

$$B = B_0 + B_1R + B_2\ln R \qquad (4.10)$$

where B_0, B_1 and B_2 are fit parameters and R is the rain rate. The parameter C was found to be almost a constant for all stations and all seasons.

Variation of these three parameters with rain rate during the southwest monsoon season at Thiruvananthapuram is shown in Figure 4.8.

Incorporating the expressions for A and B into the original lognormal distribution (Equation 4.7), we get a rain DSD equation in which number of rain drops is a function of both drop diameter and rain rate. Thus the empirical model can be written in the form

$$N_{(D,R)} = \frac{\exp(A_0 + A_1R + A_2\ln R)}{D}\exp\left\{-0.5\left[\frac{\left(\ln D - (B_0 + B_1R + B_2\ln R)\right)}{C}\right]^2\right\} \qquad (4.11)$$

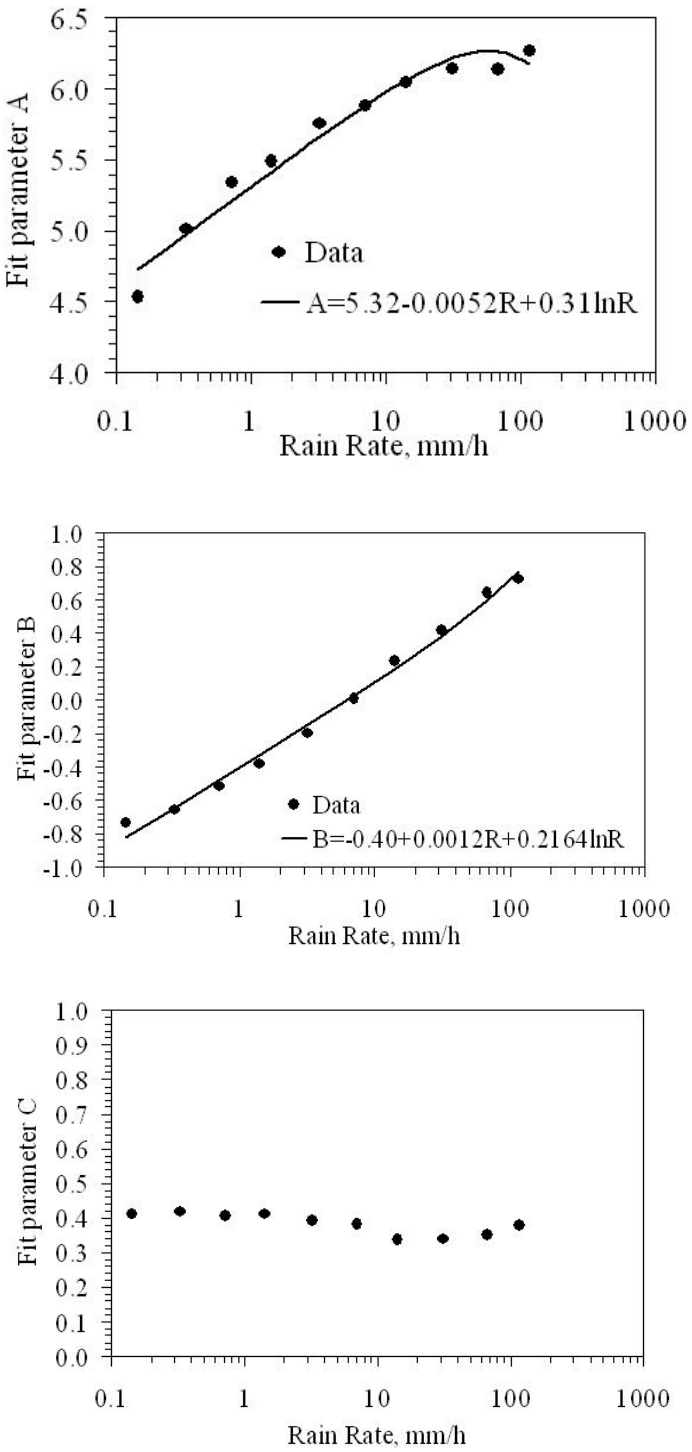

Figure 4.8. Variation of the fit parameters A, B and C with rain rate during southwest monsoon season at Thiruvananthapuram.

The same analysis was done for all the four stations. The values of all the seven fit parameters in the above expression corresponding to each season for all the stations are shown in Table IV.III. By incorporating these values in the basic empirical model, the DSD corresponding to each season at each station can be derived.

Station	Season	Parameters						
		A_0	A_1	A_2	B_0	B_1	B_2	C
Thiruvananthapuram	PRE	4.930	-0.013	0.489	-0.286	-0.005	0.152	0.370
	SW	5.318	-0.005	0.308	-0.404	0.001	0.216	0.383
	NE	4.968	-0.008	0.409	-0.320	0.002	0.192	0.386
Kochi	PRE	4.850	-0.014	0.327	-0.362	-0.002	0.310	0.388
	SW	5.080	0.003	0.297	-0.416	0.001	0.178	0.416
SHAR	ASO*	5.268	-0.005	0.558	-0.713	0.005	0.080	0.532
Munnar	SW	5.960	-0.008	0.115	-0.547	0.002	0.280	0.368

*Table IV. III. Parameters of the empirical model corresponding to each season at all the stations. * August, September and October.*

The values of most of the parameters are rather close to each other, except a few. With more data, it should be possible to reduce the scatter and improve the empirical model for DSD.

4.3.2. Validating the empirical model

In order to validate the empirical model derived, the model derived DSD values were compared with actual measurements. These actual measurements have not been used in deriving the model. Figures 4.9 to 4.15 show such comparisons for the stations Thiruvananthapuram, Kochi, Munnar and SHAR respectively for a few rain rates. The figures show a qualitative comparison. To evaluate the statistical significance of this comparison for all the rain rates, correlation between the model derived values and the actual measurements have been obtained.

Thiruvananthapuram

Pre monsoon

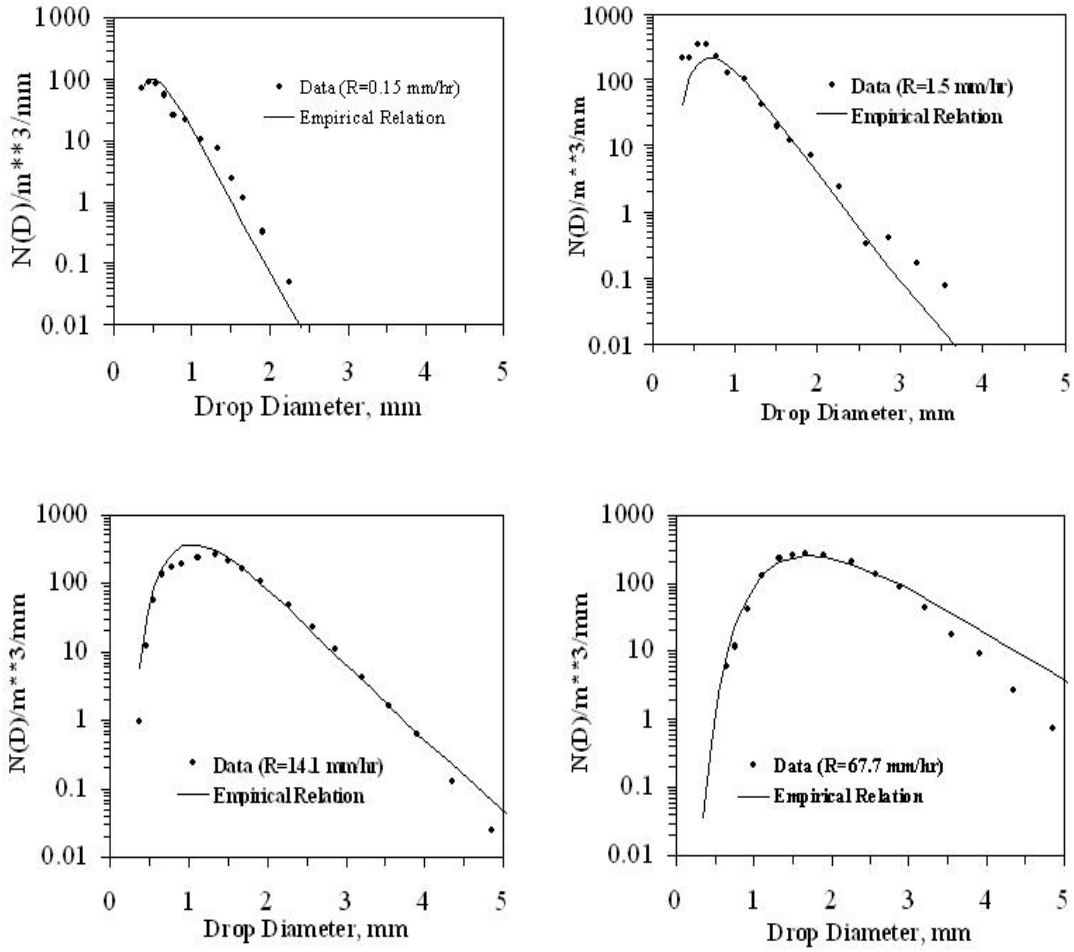

Figure 4.9. Comparison of the model with the observed DSD for the month of May 2005 at Thiruvananthapuram.

Southwest monsoon

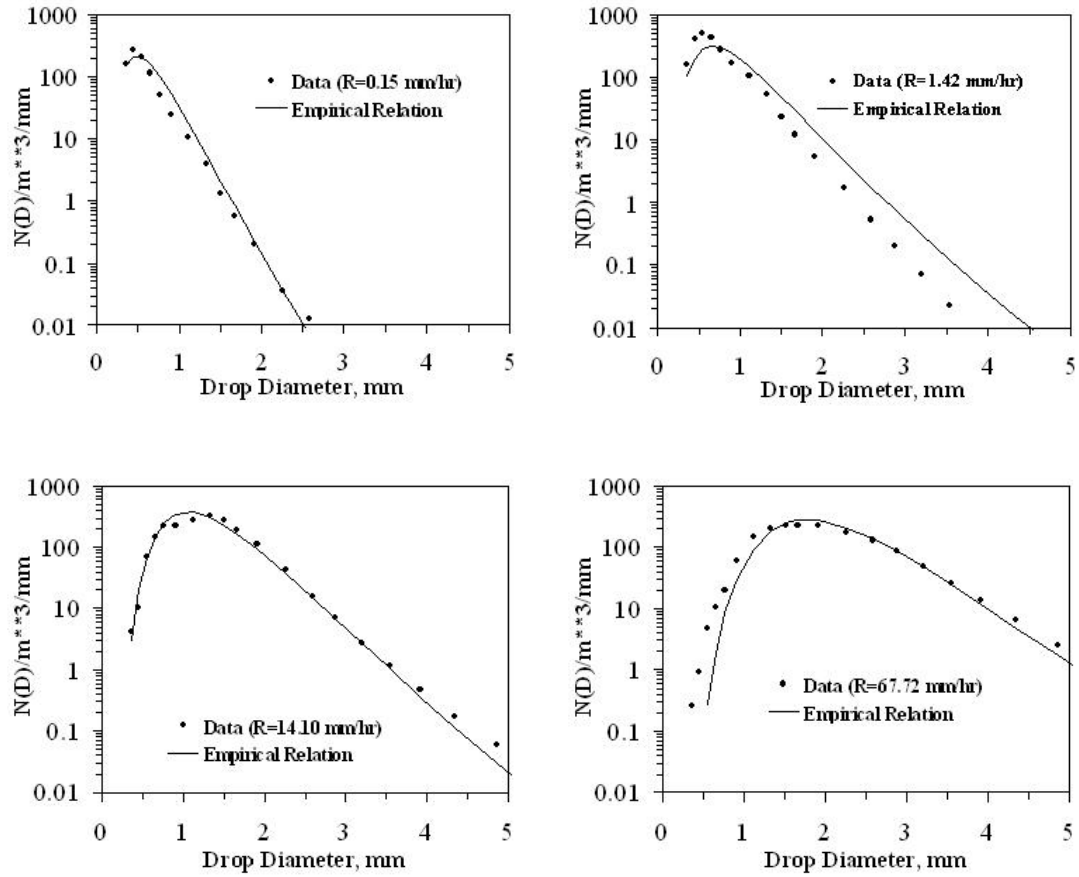

Figure 4.10. Comparison of the model with the observed DSD for the month of June 2005 at Thiruvananthapuram.

Northeast monsoon

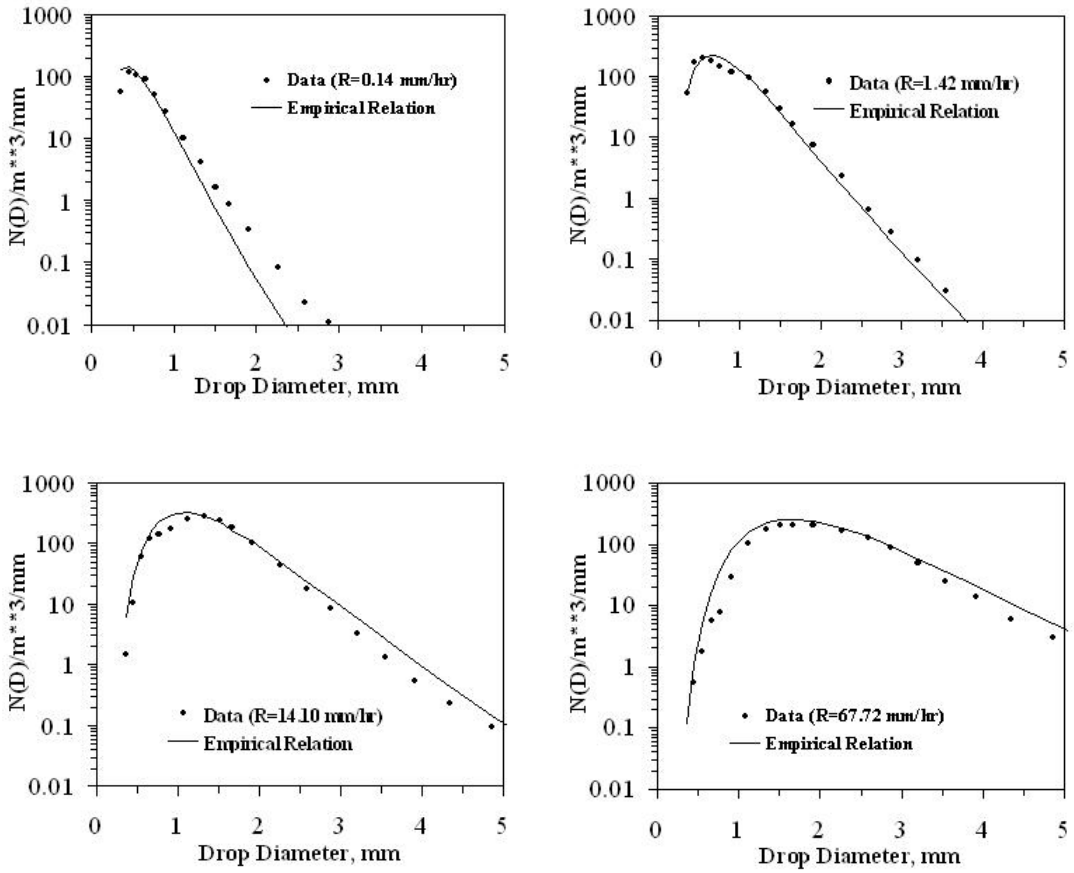

Figure 4.11. Comparison of the model with the observed DSD for the month of October 2005 at Thiruvananthapuram.

Kochi

Pre monsoon

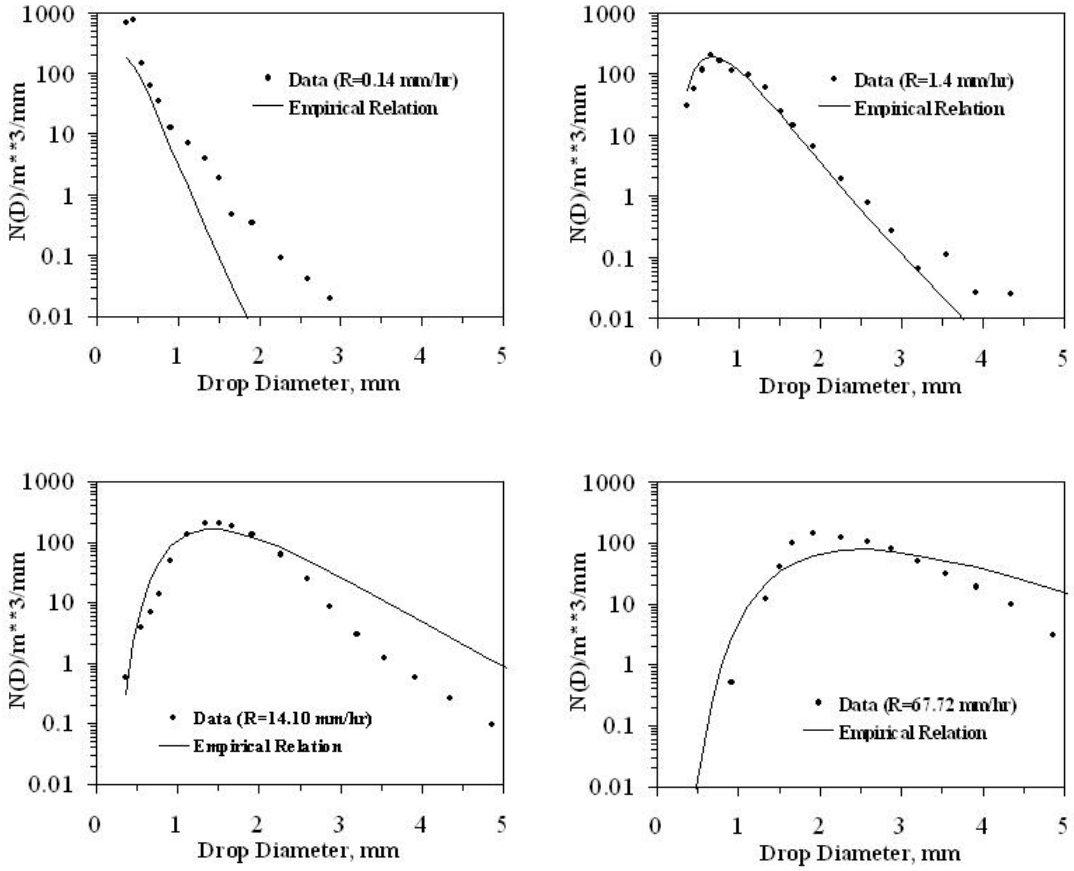

Figure 4.12. Comparison of the model with the observed DSD for the month of May 2004 at Kochi.

Southwest monsoon

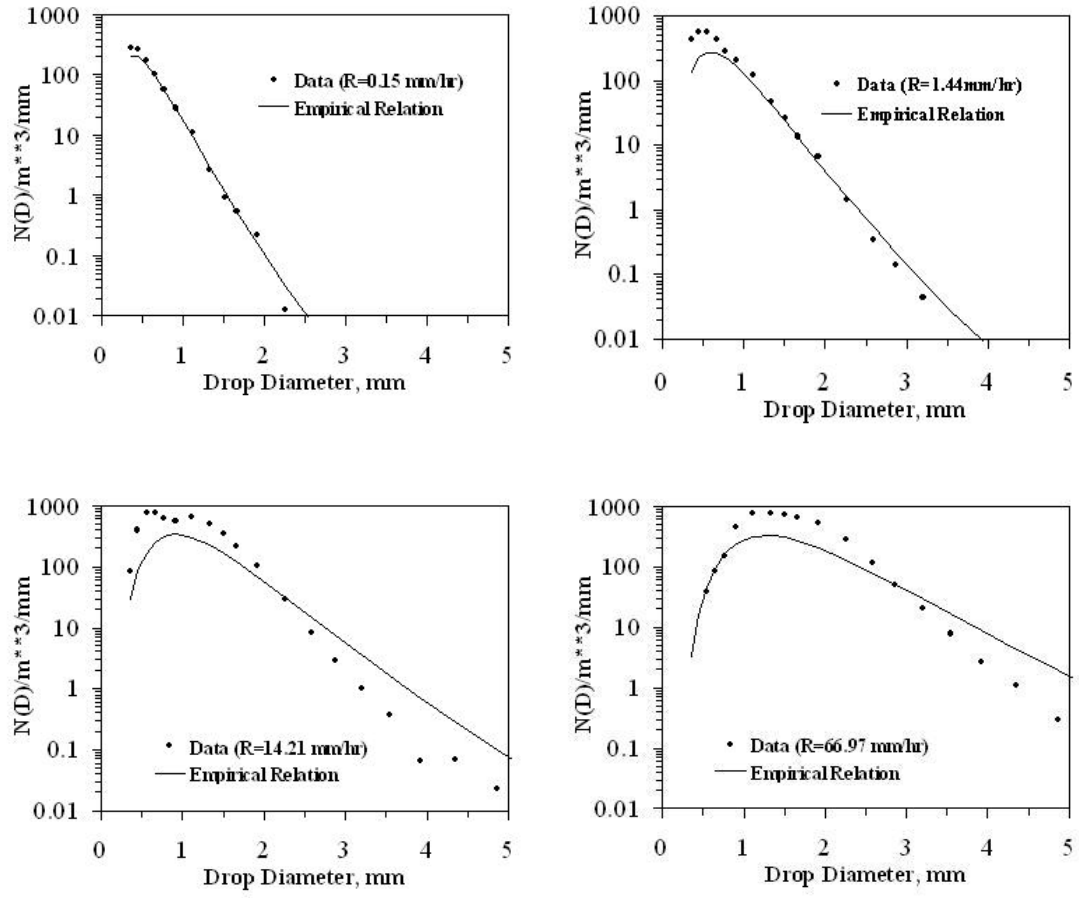

Figure 4.13. Comparison of the model with the observed DSD for the month of July 2004 at Kochi.

Munnar (Southwest Monsoon)

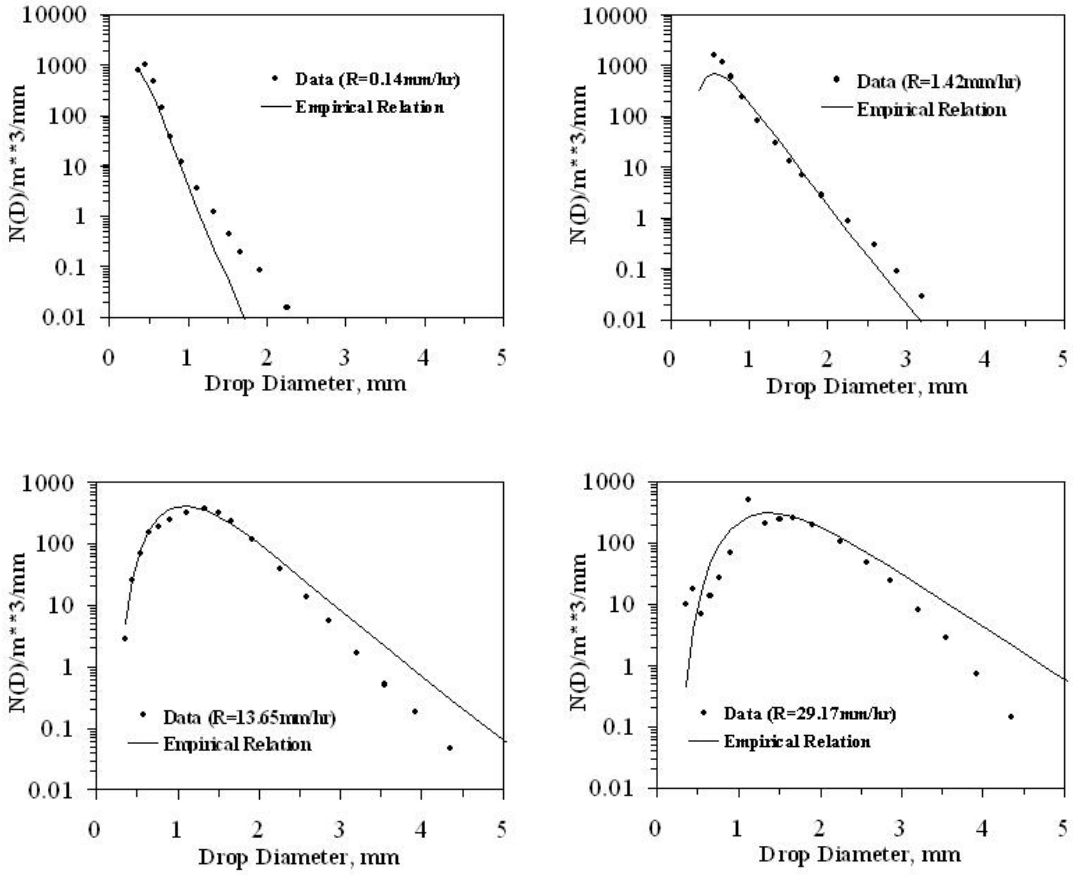

Figure 4.14. Comparison of the model with the observed DSD for the month of July 2004 at Munnar.

SHAR (August, September and October)

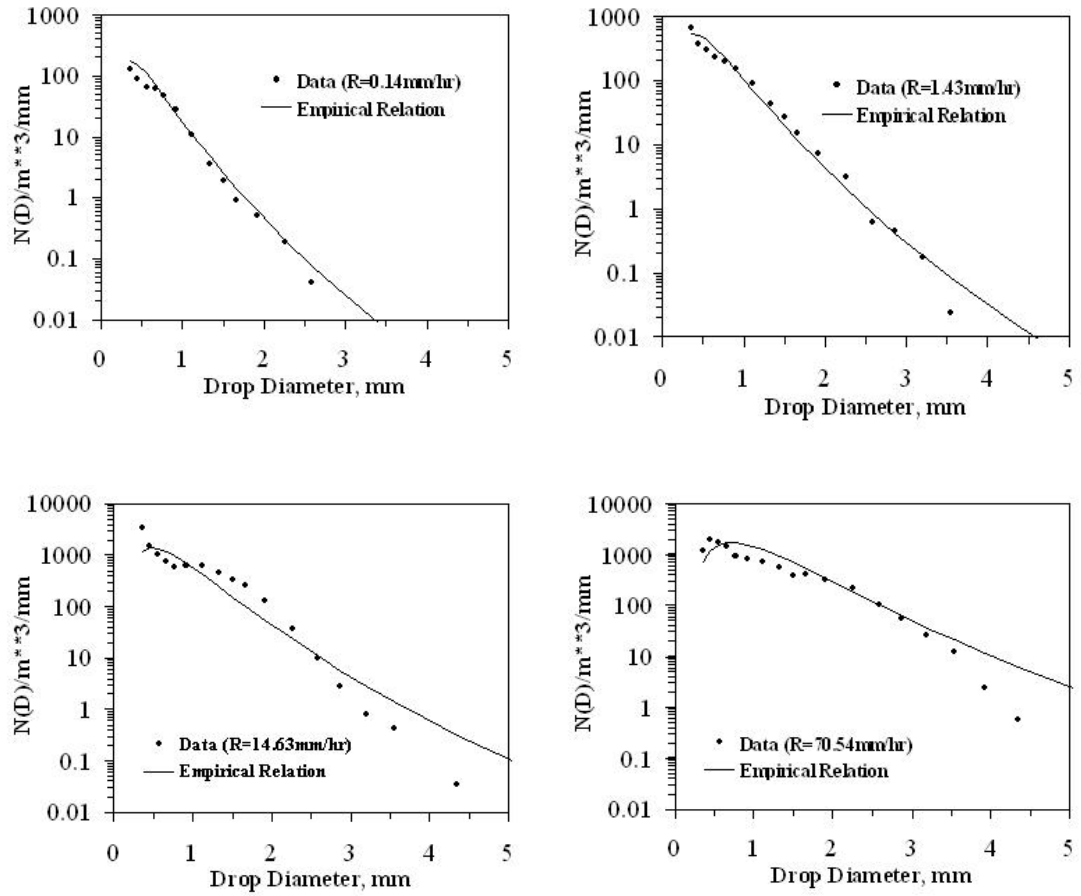

Figure 4.15. Comparison of the model with the observed DSD for the month of August 2003 at SHAR.

Figure 4.16 shows the correlation of the DSD derived from the empirical model with actual DSD data for all the rain rates for all the four stations. For all the stations, except SHAR and Kochi SW, the correlation coefficient is grater than 0.9. For SHAR, beyond 1 mm/h, correlation coefficient decreases as rain rate increases and reaches a minimum value of around 0.75. At Kochi during southwest monsoon season, correlation coefficient of 0.85 is shown for a rain rate of around 7 mm/h. The lowest correlation coefficient being 0.75 indicates that the empirical model represents the

DSD measurements well. This model can be improved further with more data available from these stations.

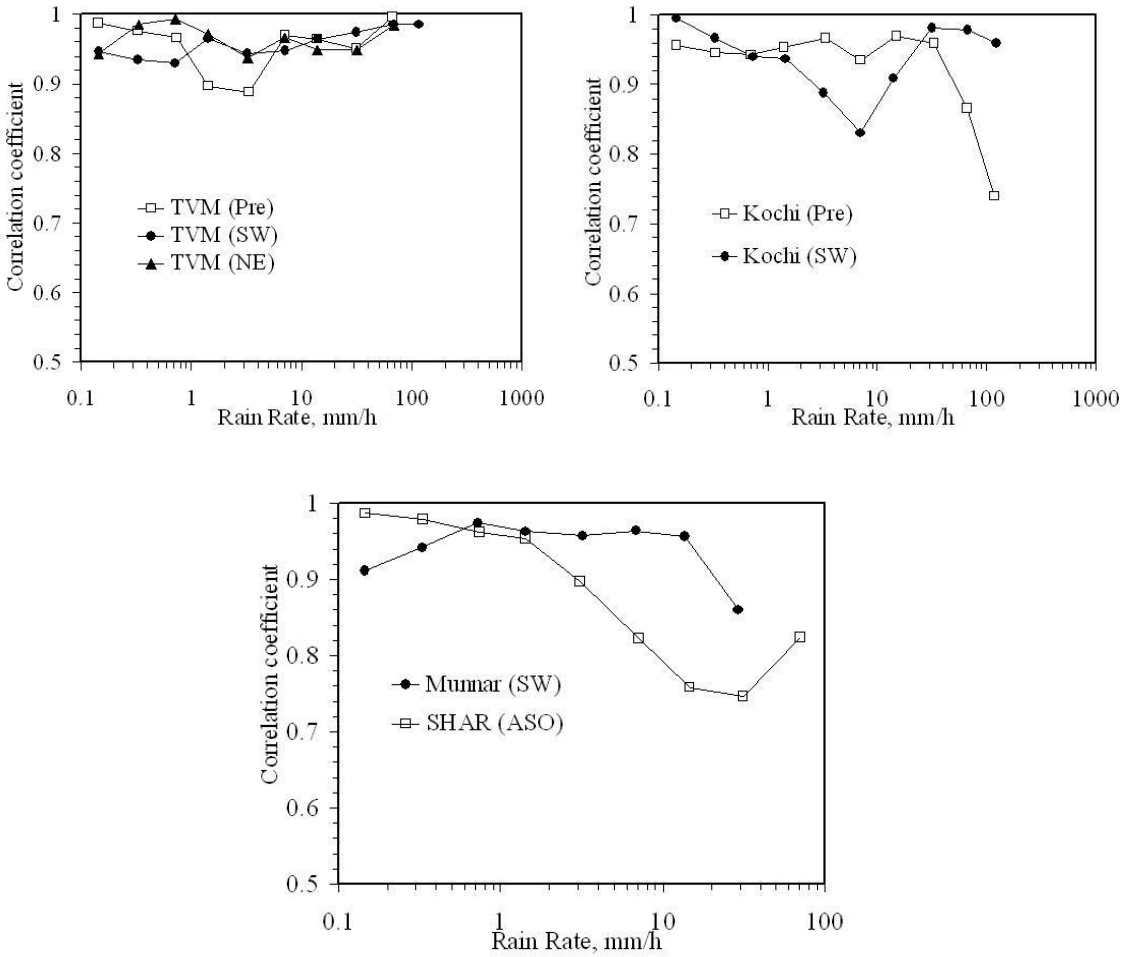

Figure 4.16. Correlation between the DSD derived from the empirical model and the actual DSD data for all the rain rates.

4.4. SUMMARY AND CONCLUSION

Rain DSD was observed using a JW type Disdrometer at four places, three of them coastal and one at an altitude of about 1500 m. The DSD data were divided into periods of different ranges of rain rate and fitted with the lognormal distribution function. The function fitted the data well, except in a few rare cases. The total number of drops, N_T, the geometric mean diameter, D_g, and the standard geometric deviation, σ

was derived from the fitted function. σ was found to be more or less constant for all rain rates. The other two parameters showed an exponential increase with rain rate, R. At two sites, namely, Munnar and Thiruvananthapuram, N_T was found to behave differently from the other two. At Munnar, N_T increased initially and decreased beyond around R= 3 mm/h. At Thiruvananthapuram, N_T increased with rain rate up to some value of R that was different for different months. But above this value of R, N_T remained more or less constant or decreased slightly. An interesting observation at Kochi is that N_T was rather low in the three months of May, June and July 2004 compared to that at 2003. Thus, for instance, for a rain rate of 3 mm/h, N_T was 366 in July 2003. But it came down to 138 in July 2004. D_g, on the other hand, increased from 0.774 in July 2003 to 1.101 mm in July 2004. This indicates the possibility of rainfall being predominantly from convective clouds in 2003 at Kochi. The high convection in the year 2003 compared to 2004 is evidenced from the low NOAA-OLR value (OLR~ 199.827 W/m^2) during July 2003 compared to July 2004 (OLR~ 209.542 W/m^2) at Kochi.

It was found that, in spite of the different kinds of behaviour observed in N_T, the function $N_T D_g^3$ increased linearly with rain rate. For SHAR, however, the variation was not strictly linear. The very different behaviour of N_T at Munnar could be attributed to the orographic effect. The situation in Thiruvananthapuram and Munnar is similar with respect to DSD. Since Thiruvananthapuram is closer to the Western Ghat mountains compared to Kochi, it is probable to expect an influence of the mountains on the rain DSD at this site. Grossman and Durran (1984) indicate that the influence of the Western Ghats could extend from 50 to 200 km to the windward side. Thiruvananthapuram is less than 50 km westward of the mountain. Thus we could expect the influence of mountain to be felt at Thiruvananthapuram also.

Since the rain DSD in this region could be best represented with the lognormal distribution function for all the rain rates, a lognormal empirical model has been derived for all the seasons for all the stations from where the data is available. The values of the lognormal distribution parameters are very close to each other in all

the cases. The correlation between the DSD values derived using the empirical model and the actually measured DSD has been found to be generally good. The correlation coefficient between the DSD derived using the empirical model and the DSD data used for validation is greater than 0.9 for all the seasons for the stations with a few exceptions. For SHAR, as rain rate increases beyond 1 mm/h, the correlation coefficient decreases and reaches a value of around 0.75. For southwest monsoon season at Kochi, the correlation coefficient shows a low value of 0.85 for a rain rate of around 7 mm/h. This derived empirical model can give an average DSD for particular values of rain rate. With more data sets when available could be used to update the model to represent the DSD even better.

Fitting the lognormal distribution function to measured DSD thus seems to give some insight into differences and similarities in the behaviour of rain rate and clouds at different places. It is expected that this could lead to a better understanding of clouds in this region, especially monsoon clouds.

CHAPTER V

ALTITUDINAL AND TEMPORAL VARIATION OF RAIN DROP SIZE DISTRIBUTION DURING A RAIN SPELL

CHAPTER V

ALTITUDINAL AND TEMPORAL VARIATION OF RAIN DROP SIZE DISTRIBUTION DURING A RAIN SPELL

5.1. INTRODUCTION

Deep awareness of rain drop size distribution (DSD), its vertical profiles and altitudinal and temporal evolution are very useful for the fields like microwave communication, radar meteorology and cloud micro-physics. But such measurements have been very few in the tropics. The altitudinal and temporal evolution of rain DSD is of much interest. According to Low and List, significant collisional growth, i.e., coalescence, occurred only when drops < 0.6 mm in diameter are struck by larger ones (Low and List, 1982). The coalescence efficiencies of raindrop pairs has been established by Low and List and using it, the collision breakup equations were expanded into general overall equations for all drop pairs as expected in natural rain. Special procedures have been developed by Philips and Brown (1986) to deal effectively with several computational problems that arise in calculating both the fragment distribution function and the Bleck expansion coefficients that appear in the discrete coalescence/breakup equation of Low and List. Theoretical and observational studies on the evolution of rain DSD by coalescence, breakup and evaporation have been done by Hu and Srivastava (1993 and 1995). They considered two models of evolution of the rain DSD. Model 1 was spatially homogeneous and model 2 was one dimensional (vertical), conditions being uniform in horizontal. In both models, the size distribution evolved with time by the process of coalescence, collisional breakup and evaporation. In model 2, they also considered vertical air motion. The model 1 may be considered to be a crude approximation to showery precipitation while model 2 approximates continuous stratiform rain. According to these authors, either the Low and List parameterization is greatly over estimating drop breakup and/or the number of drops formed by breakup or evaporation played a dominant role in shaping the DSD.

There are two currently accepted mechanisms for raindrop formation:

Wegener (1911) first suggested that rain originates from the melting of ice particles, an idea which was later elaborated by Bergeron (1935) and Findeisen (1938). According to a second theory, which is applicable to cloud regions not containing ice, raindrops could form directly by collision and coalescence of cloud droplets (Twomey, 1964). Reynolds (1876) proposed the collision process as a possible growth mechanism but a quantitative presentation of the concept was not formulated until Langmuir (1948) suggested a chain-reaction scheme of rain production from warm clouds. The fragmentation of large drops via aerodynamic breakup was thought to provide the feeder droplets for further collisional growth. Aerodynamic breakup involved the assumption that drops become unstable once they reach diameters of 0.6 cm. This limiting size proved to be incorrect according to experimental and theoretical (Prupacher and Pitter, 1971) studies which moved this limit to drop sizes of 1.0 cm in terms of equivalent spherical diameters. Hence, aerodynamic breakup is now considered unimportant. It is breakup after drop collisions which seem to govern the drop evolution in the larger size ranges (Magarvey and Geldart, 1962; McTaggart-Cowan and List, 1975b; Ryan, 1976; List and Gillespie, 1976), regardless of the origin.

The importance of collection process in warm rain is well established (Riehl, 1954). Although cloud droplets can grow to radii of approximately 10 μm by diffusion and condensation of water vapor, the time required for growth to raindrop sizes by the same process is prohibitive. Growth to drops of precipitation size is accomplished by two other processes. In clouds with tops above the freezing level, solid precipitation particles grow at the expense of super-cooled droplets, fall, accrete cloud droplets and finally melt at temperatures above 0°C to form rain. In warm clouds, however, raindrops grow by gravitational collection: larger drops, which fall faster, collide and coalesce with smaller drops in their path. Even under conditions in which the ice phase is responsible for the initiation of precipitation, collection is the dominant growth mechanism in the non-freezing regions of the cloud (Houghton, 1968) and is thus important in shaping the rain DSD.

In studies of the growth of cloud droplet populations into precipitation

particles, it is found that the collision of droplets does not necessarily result in 100% coalescence and that ice crystals do not always rebound. Information on the percentage coalescence of the colliding drops, usually defined as the coalescence efficiency, and on the percentage bounce of ice crystals, the separation probability, is so scarce and so poor that both coalescence and bounce are often assumed to occur 100% of the time. It has been known for a long time that drops with the order of one millimeter bounce almost 100% of the time if uncharged and not in an electrical field (Rayleigh, 1879). The addition of charges and electric fields increases the probability of coalescence following collision to the point where small charges and small fields cause almost 100% coalescence. In the presence of electric fields, or when the drops are charged, observations of Gunn (1965a, 1965b) and Sartor (1967) show that by controlling their relative velocity they can be made to coalesce with subsequent disruption and the production of rain drops. Further it has been showed by Sartor (1967) that even a small percentage of cloud and precipitation drops bouncing or disrupting in an electric field can be significant in the problems of cloud electrification.

The spatial variation in the rain DSD has been brought out by conducting study at a few stations in the southern peninsular India by Harikumar et al. (2007). An empirical model for the variation of rain DSD with rain rate at these locations in peninsular India has also been developed by Harikumar et al. (2009). The first experimental measurements of rain DSD at Thiruvananthapuram using the MRR were also presented by Harikumar et al. (2006). In that work, the averaged DSD over one hour of a continuous rain episode were presented and compared with the average over a five-minute interval of the same rainfall event. It was found that coalescence apparently happened at all the altitudes. Since, averaging of the data over a long period of time modifies the distribution, here we have taken 10 seconds instantaneous data to study the evolution of rain DSD with altitude. The MRR gives the DSD at different heights every 10 seconds.

5.2. DATA AND DATA ANALYSIS

The analysis uses the data during 16 continuous rainfall episodes during southwest monsoon (JJAS) season. Since all the episodes behaved similarly, here a single continuous rainfall episode from IST 16:10:01 o'clock to 16:12:31 o'clock on 12th August 2006 is considered. The rain DSD data at different heights has been measured using a Micro Rain Radar deployed at the premises of the Centre for Earth Science Studies, Thiruvananthapuram. Thiruvananthapuram is a tropical station situated nearly at the tip of peninsular India.

The analysis is carried out as follows. The reliability of the MRR data has been assessed by comparing the data obtained from MRR with that obtained from a collocated Joss-Waldvogel impact type Disdrometer. The variation of the rain rate and fall velocity with altitude and with time has been studied. Using this, the apt duration for which data need to be analysed for understanding the evolution has been determined. The rain DSD spectra at different time intervals of 10 seconds for the selected whole period has been compared and interpreted.

5.2.1. Comparison of the MRR and Disdrometer DSD for this event

Along with the MRR, Simultaneous measurement of DSD at the surface has also been done using a collocated Joss Waldvogel impact type Disdrometer. The data from the Disdrometer and MRR (data at a height of 35 m) has been compared and the data is in good agreement for this selected event (figure 5.1). The possible errors in the MRR and Disdrometer measurements are also discussed. The average rain rate was 2.028 mm/h for this duration. The rain DSD in this region follows a Log-normal distribution function of the form as shown in the equation 4.7 in the fourth chapter of this thesis (Harikumar et al., 2007).

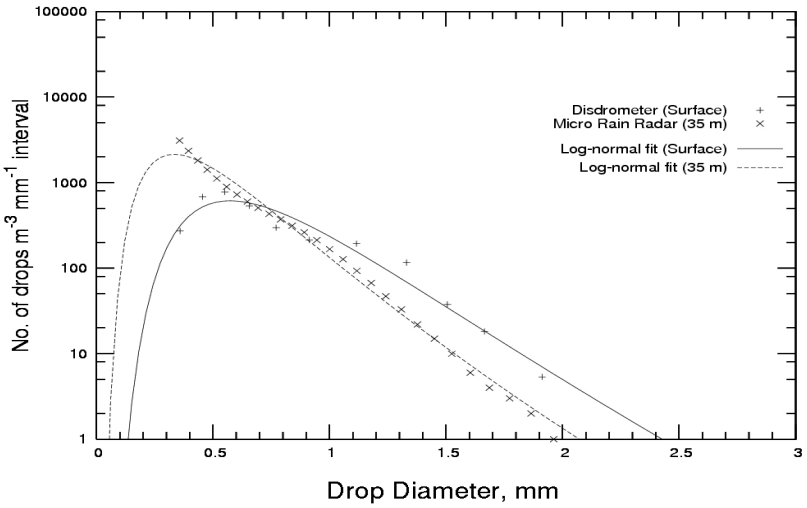

Figure 5.1. Comparison of rain DSD data obtained for the event from the Disdrometer and the MRR. The solid lines represent the log-normal fit to the data.

In the Figure 5.1., the solid lines represent the fitted log-normal function to the DSD data. The fit parameters obtained for the fitted function is shown in the Table V.I. The minimum height at which the MRR measurement is possible is at 35 m. So we compared the surface Disdrometer data with those at an altitude of 35 m. This itself may cause a difference in the DSD data. It is observed that the DSD at different heights does not follow the log-normal distribution (Harikumar et al., 2006). As height increases the departure of the rain DSD spectrum from the log-normal behavior is very clear. From figure 5.1, it is clear that the MRR number density data starts to decrease from a particular value, while Disdrometer data increases rapidly, reaches a maximum and then decreases gradually as diameter increases as expected for a log-normal distribution function. The difference shown in the fit parameter ***b*** clearly reflects this fact.

Fit parameter	Surface (Disdrometer data)	35 m (MRR data)
a	5.942	6.679
b	-0.695	-0.882
c	0.403	0.467

Table V.I. The fit parameters of the lognormal distribution function fitted to the DSD data from the Disdrometer and the Micro Rain Radar.

The possible errors in the measurement of rain DSD using the Disdrometer have been discussed in detail in the Chapter II (Harikumar et al., 2009). And the possible errors in the measurements of rain DSD and integral rain parameters using the MRR are explained below. For the relation of terminal fall velocity versus drop size stagnant air has been assumed.

The relation between terminal velocity and drop diameter is obtained in appropriate analytical form by Atlas et al. (1973)

$$\nu(D) = 9.65 - 10.3 \times \exp(-0.6D) \qquad (5.1)$$

where 0.109 mm ≤ D (mm) ≤ 6 mm

In real atmosphere the drops are carried with the wind (the inertial length scale of rain drops is on the order of 10 m). Thus the velocity in the equation 5.1 is relative to the ambient air velocity. But in this study, the event has been selected in such a way that the rain rate is always below 5 mm/h both with altitude and time. So, the error due to this assumption does not come into picture. Turbulence, i.e. the random fluctuations of vertical wind within the scattering volume or within the averaging time interval causes a systematic bias because the effects of up and downwind do not compensate each other completely due to the non-linear velocity-diameter relation. Usually turbulence leads to an underestimation of LWC and RR and does not affect the DSD measurement much. Other chance for error is due to the non-spherical shape of the rain drops. But, since the MRR has been calibrated for natural rain, this error is expected to be small. Because of the change of phase of water at heights like 0 degree isotherm, the back-scattered power will increase and thus cause an over estimation of drops. But here our analysis is limited to a height of 700 m and hence this is avoided. A chance of attenuation of the electro-magnetic radiation during higher rain rates and also at higher altitudes is possible. Since, in the present study we have used rain episodes having rain rates less that 5 mm/hr and also DSD measurements have also been made for lower heights, the possibility of error due to this fact is small.

5.2.2. Calculation of the time taken by rain to reach the ground

The objective is to understand the behavior of the altitudinal variation of DSD with time during any single precipitation event. For this, the time period of

the event is so chosen that during this interval, the fall velocity of the most dominant drop size remains the same. For the interval chosen here for the most dominant drop size, namely 1.179 to 1.242 mm, the fall velocity was 4.648 m/s. This fall velocity ensures that most dominant drops do not undergo change during this period.

The analysis uses the data from a single precipitation event from 16:10:01 o'clock to 16:12:31 o'clock on 12th August 2006 at Thiruvananthapuram. This period was chosen because the most dominant drops from the top of the region takes about two and a half minutes to reach the surface, as explained below in the next paragraph. The vertical height resolution of the Micro rain radar has been set in such a way that it gives the raw data on DSD and integral rain parameters from 35 m to 1050 m height with 35 m resolution at every 10 seconds. The cloud base height observed using a ceilometer deployed near the MRR is 700 m during this episode. So the analysis is limited to a height of 700 m.

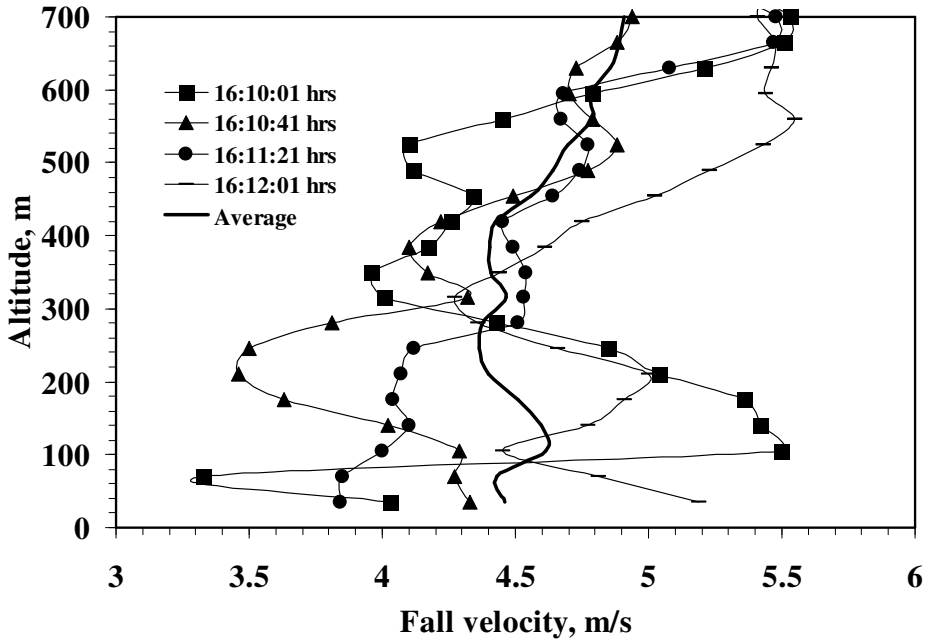

Figure 5.2. The variation of fall velocity with height for different time intervals.

MRR also gives the fall velocity that represents the terminal velocity of the drops that contribute most of the liquid water to the rain rate. The variation of

fall velocity with height for different time intervals is shown in Figure 5.2. The average variation is also represented with a thick line. We found that the fall velocity was more or less constant at different altitudes and at different times. Therefore, we took an average value (4.648 m/s with a standard deviation of 0.184 m/s, i.e., 4.648±0.184) and used this to determine the time taken by the drops to reach the ground from the top of the region used for the study, namely, 700 m. This is about 155 sec. Hence, this study used the data over a period of about 2½ minutes from 16:10:01 o'clock IST.

5.2.3. Altitudinal and temporal variation of rain rate and fall velocity

Variation of rain rate with altitude and with time is shown in the Figures 5.3 and 54. Throughout the entire time and throughout the altitude, the rain rate is below 5 mm/h. It was found out by Sasi Kumar et al. (2007) that around 70% of the time, the rain rate observed is less than 5 mm/h at Thiruvananthapuram. In this regard, the rainfall event having rain rate less than 5 mm/h that is considered in this analysis is very relevant. At the beginning of the rain episode, the value of rain rate increases from a height of 700 m to reach a maximum at 500m as height decreases and below this altitude the rain rate decreases. But for the next two time intervals, the rain rate is more or less constant at all the heights. For the last time interval it increases from 700 m to reach a maximum at 300m and then decreases below this altitude. This is similar to the one observed at the beginning of the episode. The average fall velocity has a value between 4 and 5 m/s in all the time intervals and in all different altitudes.

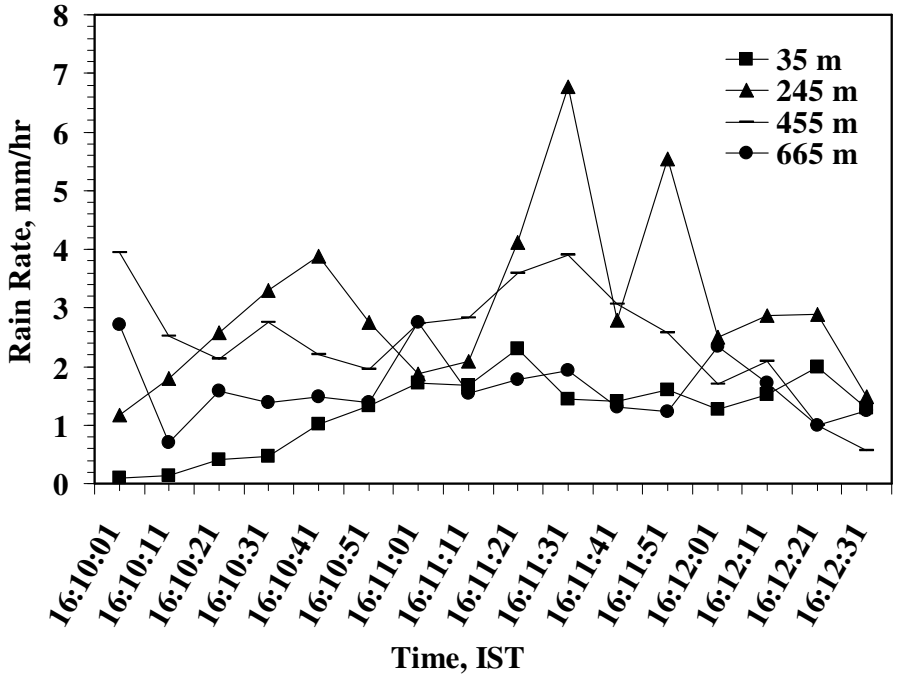

Figure 5.3. Variation of rain rate with time at different altitudes.

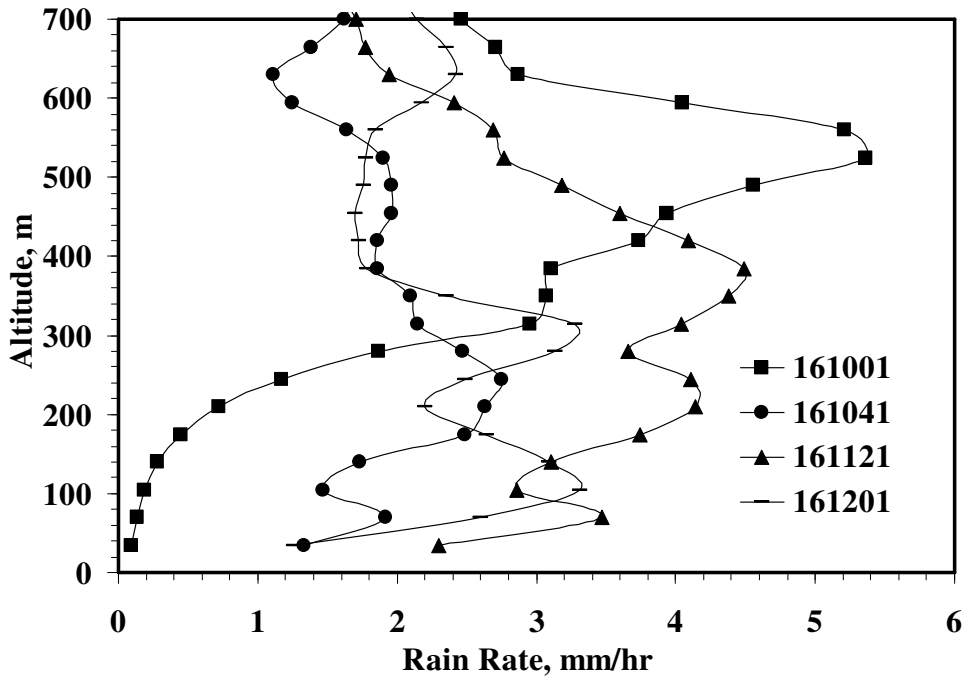

Figure 5.4. Variation of rain rate with altitude at different time intervals.

5.3. RESULTS AND DISCUSSION

To understand the variation of number of drops in each diameter range with time, the data is presented as contour diagrams at every 20 seconds interval in Figure 6. The x-axis shows the drop diameter while the y-axis gives the altitude. The logarithm of the number of drops is used in the z-axis. The variation of the log of the number of drops (log(N)) with altitude in a few size classes at 16:10:01 o'clock is shown in Figure 5.5 (a). We see that log(N) in the smallest drop size class varies between about 2.5 and about 5 over the altitude region from ground to 700 m. The maximum of about 5 is seen at about 500 m altitude. The number of drops at any given altitude is lower for larger drops. The log(N) in the largest size class varies from about 0.5 to about 1.5. All other drop size classes lie in-between. The figures 5.5 (b) to 5.5 (h) give the variation of the number of drops per cubic metre per mm interval with altitude for different drop diameter classes at 16:10:21 o'clock to 16:12:01 o'clock with 20 seconds interval respectively.

At 16:10:21 o'clock (figure 5.5 (b)), the maximum number of drops is seen at a height of around 350 m. The high log(N) valued part of the spectrum as such has been lowered from a height of 500 m to 350 m as an indication of mass movement of the particular water content as a patch of rain. In the next spectrum (figure 5.5 (c)), it is again found to be lowered from this 350 m to a height with its maximum at a height of around 200 m.

Fig. 5.5 (h) shows the rain DSD spectrum at 16:12:21 o'clock. We see that the number of drops in the smallest size class has reduced at almost all altitudes, while the number of drops in the larger size classes has increased at almost all the altitudes. For instance, log(N) in the smallest size class varies between 2.5 and 5. The number of drops in the largest size class has a minimum around 0.5 and maximum around 1.5. The values are similar to what they were at 16:10:01 hr, but from the graph it is apparent that the values are closer to the minimum value at most places in the earlier time period (16:10:01 o'clock) but closer to the maximum value at the later time period. Similar changes can be seen in the other drop size classes also. The number concentration corresponding to the average diameter of

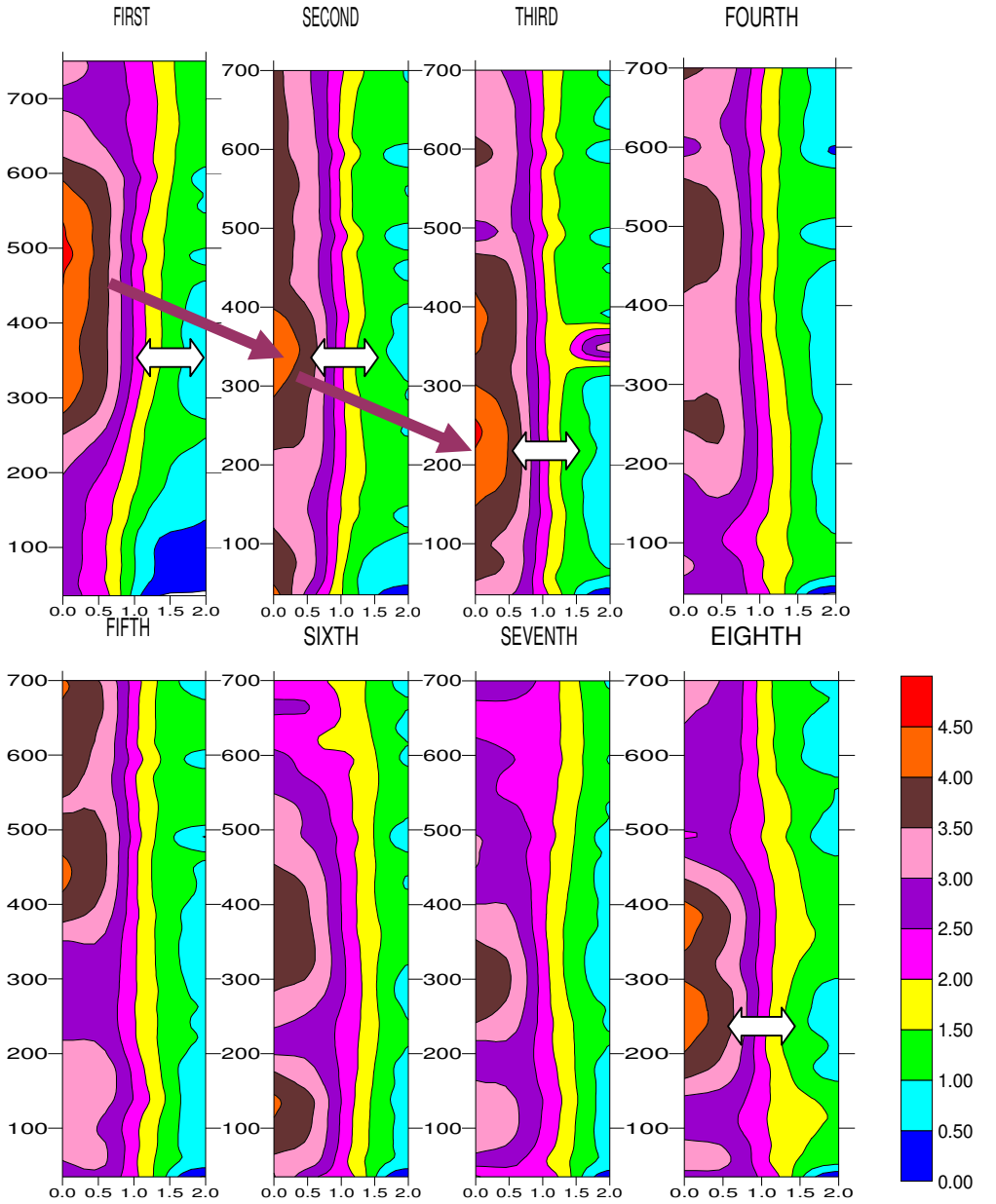

Figure 5.5. Variation of the number of drops per cubic metre per mm interval with altitude for different drop diameter classes on 12th August at (a) 16:10:01 o'clock (first), (b) 16:10:21 o'clock (second), (c) 16:10:41 o'clock (third), (d)16:11:01 o'clock (fourth), (e) 16:11:21 o'clock (fifth), (f) 16:11:41 o'clock (sixth), (g) 16:12:01 o'clock (seventh) and (h) 16:12:21 o'clock (eighth). Brown arrows show the "mass movement" while white arrows show the decrease (increase) in smaller (larger) drops.

1.2 mm of the diameter class namely 1.179 to 1.242 mm, that contributes maximum to the rain rate is not having that much noticeable variation troughout the entire duration and also through out the altitude. This is the reason why a less spread is seen in the fall velocity of the drops throughout the altitude and throughout the entire period, while we have taken fall velocities earlier to find out the time taken by rain to reach the ground.

In short, the following features are clearly seen in the eight contour diagrams in figure 6. Firstly, the number of drops in the middle size or medium diameters remains more or less same throughout the event. The larger diameter drops that are quite less in the beginning of the event show an increase with time as the event progresses. The smaller drops on the other hand show a tendency to decrease with time. Decreases in the number of smaller drops are seen with corresponding increases in larger drops indicating coalescence. Also seen are decreases in the smaller drops without corresponding increases in larger drops showing possible cases of evaporation. According to Low and List (1982), if the drops of size less than 0.6 mm are struck by larger drops, they will coalesce. This is very clearly evidenced from our present study; that is, small drops (whose diameter < 0.6 mm) have been reduced as rain comes down with passage of time. At the same time, the number concentration contour in the rain DSD spectrum has shifted towards the large sized drops end, meaning that size of the drops (> 6 mm diameter) has been increased because of the above mentioned coalescence. In short, what this indicates is that the smaller drops have been swept out by larger drops. Movement of 'rain clouds' are also seen indicating that rain fall without much changes with time can also be seen.

Theses results are the observational proof in the natural rain of the theoretical concepts of coalescence of Low and List (1982). We need to keep in mind that drops with terminal velocity equal to or greater than 4.648 m/s (corresponding to about 1.378 mm diameter) that were at the top of the region at 16:10:01 o'clock would have reached the ground at 16:12:21 o'clock. So the changes in the numbers of the larger drops would be also due to the variation with time in the drops that enter the region at the top. However, drops smaller than 1.378

mm has smaller terminal velocity and, hence, some of the drops of these sizes that were seen in the first graph are still visible in the second graph. For instance, the velocity of the smallest size class is only 1.48 m/s and they would have traveled only about 230 m during this period. Since the rain rate during this period was low (below 5 mm/h most of the time), this could be one reason for the relative absence of break up.

This case study brings out some of these interesting aspects of variation of rainfall with time and altitude. Further extension of similar analysis for startiform and cumuliform rain events will add to our understanding of the process of rain and its movement with time and altitude.

5.4. CONCLUSION

In this study of altitudinal and temporal evolution of rain DSD, we selected rainfall episodes, whose rain rate is always less than 5 mm/h. All these rainfall events showed similar behavior with special reference to evolution of rain DSD. Therefore only one event is explained in detail here. It is found by Sasi Kumar et al. (2007) that around 70% of the time, the rain rate observed is below 5 mm/h at Thiruvananthapuram. So the rainfall event having rain rate less than 5 mm/h in this analysis is very apt and relevant.

Time taken by rain to reach the ground from a height of 700 m has been evaluated first from the fall velocity during this period. Fall velocity gives the velocity of those rain drops that contribute maximum liquid water content to the rain rate. The time period of the event is so chosen that during this interval, the fall velocity of the most dominant drop size remains the same. For the interval chosen here for the most dominant drop size, namely 1.179 to 1.242 mm, the fall velocity was 4.648 m/s. This fall velocity ensures that most dominant drops do not undergo change during this period.

To understand the variation of number of drops in each diameter range with time, the data is presented as contour diagrams at every 20 seconds interval. The x-axis shows the drop diameter while the y-axis gives the altitude. The logarithm of the number of drops is used in the z-axis. The following features are

clearly seen in the eight contour diagrams. Firstly, the number of drops in the middle size or medium diameters remains more or less same throughout the event. The larger diameter drops that are quite less in the beginning of the event show an increase with time as the event progresses. The smaller drops on the other hand show a tendency to decrease with time. Decreases in the number of smaller drops are seen with corresponding increases in larger drops indicating coalescence. The larger drops coming from above collide with smaller drops and coalesce, thus sweeping out the smaller drops as they fall. Also seen are decreases in the smaller drops without corresponding increases in larger drops showing possible cases of evaporation. Movement of 'rain clouds' are also seen indicating that rain fall without much changes with time. This case study brings out some of these interesting aspects of variation of rainfall with time and altitude. Further extension of similar analysis for startiform and cumuliform rain events will add to our understanding the process of rain and its movement with time and altitude. Here, since the rain rate during this period was low (below 5 mm/h most of the time), this could be one reason for the relative absence of break up.

CHAPTER VI

VERTICAL PROFILES OF:
RAIN DROP SIZE DISTRIBUTION
&
RADAR REFLECTIVITY FACTOR-RAIN RATE (Z-R) RELATION

CHAPETR VI

VERTICAL PROFILES OF:
RAIN DROP SIZE DISTRIBUTION
&
RADAR REFLECTIVITY FACTOR-RAIN RATE (Z-R) RELATION

6.1. INTRODUCTION

Knowledge of the vertical profiles of Z-R relation and rain drop size distribution (DSD) are very useful for the fields like microwave communication, radar/satellite meteorology and cloud micro-physics. But such measurements that will help in measuring precisely the atmospheric parameters using remote sensing techniques need to be carried out more especially in the tropics. Since the global circulations are driven mainly by tropical weather, understanding its variability using observational techniques, especially satellite-based, is very crucial. Satellites like TRMM (Tropical Rainfall Measuring Mission), upcoming Indo-French satellite Megha-Tropiques, GPM (Global Precipitation Measurement) constellation etc. exclusively measures the tropical atmospheric parameters. So, for the retrieval of atmospheric parameters from the satellite-borne measurements and for calibration of the satellite sensors, vertical profiles of DSD and Z-R relations in the tropical sites are very essential. In this chapter, study of the variation of DSD with altitude has been discussed. The vertical variation of the Z-R relation is also derived and studied during radar bright band (BB)/stratiform and non-bright band (NBB)/convective conditions/rains of the southwest monsoon and premonsoon seasons.

In the Indian region, monsoon is a major phenomenon affecting agriculture, drinking water, potential of hydro electric energy and the overall economy. The lives of a large number of people in India and neighboring countries are affected. Hence we need to study and understand the vertical distribution of DSD parameters, which gives information concerning the generating processes of the monsoon precipitating systems (Reddy et al., 2005).

Understanding of the characteristics of melting layer is very useful to weather forecasters in predicting and monitoring the snow level, defined as the lowest level in a melting layer where snow or ice completely changes to rain. This information can also be useful to road maintenance workers, hydrologists, emergency managers, aviators and the ski industry (White et al., 2002). More importantly, the information of the freezing height and the melting layer are critically important in taking decision whether to do seeding experiment or not and in establishing an optimal seeding strategy that may lead to most profitable output (Cha et al., 2007). They have explained in detail the method to estimate from the Micro Rain Radar (MRR) data the freezing height and the melting layer depth, the altitude interval throughout which ice-phase precipitation melts as it descends.

Numerical modeling studies have demonstrated large sensitivity in terms of surface rainfall production, evaporation, and downdraft intensity to the parameterized hydrometeor size distribution below the melting level, especially in tropical mesoscale convective systems (MCS; Ferrier et al. 1995). Drop-size distributions in clouds are difficult to observe directly. These measurements are typically recorded using probes mounted on aircraft. The observations are limited to the regions where the planes fly, thus producing sporadic measurements in time and space (e.g., Rogers et al. 1993). Moreover, the sample volume is typically small so that it may not always be possible to obtain representative drop-size distributions (e.g., Richter and Hagen 1997). Three different algorithms of DSD retrieval by vertically pointing radar have been simulated utilising JWD measurements from Amazon basin of Brazil by Tokey and Dickens (2000). Thus they used the DSD data obtained from Disdrometer for the simulation of algorithms to derive back the DSD.

Li and Srivastava (2001) derived an analytical solution for the evaporation of a single raindrop. The results show that, for the detection of rain evaporation, reflectivity is more sensitive than differential reflectivity, whereas for the estimation of rainfall rate R, an empirical Z_{DR}–Z–R formula is more robust and accurate than a Z–R formula. Lee at al. (2006) concluded that, when using the ground Disdrometer to establish proper Z-R relationship, the spatial and temporal

extends should be considered very carefully. It is well established that rain evaporation plays an important role in inducing and maintaining downdrafts under cloud bases, in both convective-scale and mesoscale precipitation. It is also an important sink of atmospheric latent heat. However, quantitative measurement of rain evaporation remains extremely difficult (Li and Srivastava, 2001). A direct way of measuring rain evaporation is to track the drop size distribution (DSD) along their falling paths. Gori and Joss (1980), and Levin et al. (1991) used this approach in their investigations. They measured DSDs simultaneously along steep mountain slopes at different heights.

Weather radar yields improved hydrometeor detection and area coverage, but has remaining deficits when it comes to ground truth or quantitative precipitation estimation (QPE) due to the very variable relation between radar reflectivity (Z) and rain rate (R; Diederich et al., 2004). In this article, they present the MRR (Micro Rain Radar), which gives an alternative QPE method. This low cost Doppler radar measures vertical profiles of radar reflectivity as well as spectra of fall velocity of hydrometeors, and estimates the drop size distribution (DSD) of rain using a relation between terminal fall velocity and drop diameter for liquid precipitation. Tian et al. (2006) presents an initial investigation using airborne Doppler radar operating at 10 and 94 GHz to measure the light stratiform rain ($\leq$5 mm/h). It has been shown that the combination of 10 and 94 GHz is more sensitive to resolve the rain DSD in light rain than that of 14 and 35 GHz (Frequencies that will be used in the dual-frequency radar of Global Precipitation Measurement mission). The sensitivities of the retrieval to Gamma shape parameter are discussed.

Characteristics of precipitating clouds, such as microwave irradiance, cloud-top infrared irradiance, and radar reflectivity, can be measured remotely over large regions by sensors on satellites, aircraft, ships, and on the ground. The information from these indirect measurements of precipitation must be converted to the rain rate by using an appropriate algorithm. Although the basic physics behind these algorithms may be understood, algorithm parameters typically must be calibrated to the particular rain regime under study in order to produce accurate results. Often the approach to calibration is one of bootstrapping—using a small-

scale direct measurement to calibrate a larger-scale indirect measurement, which in turn is used to calibrate a still larger scale measurement successively until the scale needed is reached. Thus, it is vital that the initial relation upon whom this sequence of calibrations is based be as accurate as possible (Yuter and Houze, 1995)

Application of the information on vertical profiles of rain DSD and integral rain parameters is to correct algorithms for weather radar data. But the problem exists as weather radar measurements take place at a certain altitude whereas their calibration is usually done by ground based data-either the radar data is adjusted to surface based sensors or transferred to rain rate by Z-R-relationships established at ground-level. The vertically pointing radar provides measurements at different altitudes and thus closes the gap between ground based measurements and the weather radar as has been reported before (Wagner et al., 2004). Within the framework of APOLAS (Areal Precipitation measurements Over Land And Sea), a project under the German Climate Research Programme DEKLIM in the Baltic area (http://miraculix.dkrz.de/gerhard/apolas.html), they addressed this problem of understanding the vertical structure of precipitation. Diederich et al. (2004) studied the variability in the drop size distribution inside an area of 200 by 600 meters with a temporal resolution of 30 seconds using 3 Micro Rain Radars/Disdrometers and a 2d-video Disdrometer.

Whenever the weather radar has been used for areal precipitation measurement, the quantitative estimation and investigation of rain rate from radar reflectivity has been hampered by (1) The highly variable and ambiguous relation between rain rate and radar reflectivity, which depends strongly on the drop size distribution (DSD), (2) The occurrence of ice in the illuminated volume, (3) The evolution of rainfall from the height of the radar beam to the ground and (4) The dissimilar volumetric and temporal scales involved when measuring different rain characteristics. These effects have been investigated in numerous publications, but the progress in applied areal rainfall measurement with radar has been modest. Often additional information is needed to correctly identify, predict and correct the named effects. Fabry et al. (1992) suggested the use of a network of low cost vertically pointing radars to enhance weather Radar scans by measuring the vertical

reflectivity profile and detecting the melting layer, which yields potential to counter the errors caused by issue 2 and 3. For issue 1, the measurement of the drop size distribution (DSD) allowed the investigation of methods to associate rainfall structure with DSD characteristics at ground level (Uijlenhoet et al, 2003). This represents a significant progress compared to separately measuring reflectivity with radar and rain rate with gauges, as this is too strongly affected by issue 4 (Diederich et al., 2004).

Z-R relation shows clear distinction between southwest and northeast monsoon seasons (Reddy et al., 2003). During southwest monsoon precipitation generally has bigger drops than during northeast monsoon. Wilson et al. (2001) conducted a study using the Disdrometer data and found that there was no significant differences between DSDs in southwest and northeast monsoons. In the model study in this thesis, we find that the lognormal parameters are similar during different monsoon seasons at a particular station.

Measurements of rain were obtained with a vertically pointing micro radar (MRR) with 1 min time resolution and 50 (100) m height resolution at the German Baltic coast on the Zingst peninsula (54.43°N, 12.67°E) by Peters et al. (2002). Simultaneous estimates of rain rate and reflectivity factor with data of a C-band (frequency=6 GHz) weather radar suggest that the MRR may be used to support quantitative rain rate estimates with weather radars.

Conventional weather radar retrieval of areal quantitative precipitation suffers from mainly two problems (Peters et al., 2002). They are: (1) The relation between the radar reflectivity and rain rate depends on the structure of the drop size distribution. Parameterized distributions can deviate considerably from actual distributions. Richter and Hagen (1997) demonstrated that this problem can be mitigated by advanced radar techniques including, for example, polarimetry (2) The height of the measuring volume increases with increasing distance from the radar due to the earth curvature. In moderate zones the majority of weather radar data are obtained above the freezing level. Stratiform shallow rainclouds may be totally below the sampling height of the radar. In general the extrapolation from the radar measuring volume to the surface includes significant uncertainties. The influence of

vertical wind and turbulence was neglected in these MRR measurements, which represents probably the most important source of error of this method (e.g. Joss and Dyer, 1972, Richter, 1994).

Zhang et al. (2002) studied the sampling effect on radar measurements of inhomogeneous media and the resultant rain estimation. The dependence of statistical moments on the variation of DSD parameters is calculated and applied to radar-based rain estimation. Quantitative estimation of fallen precipitation at ground level using weather radar is hampered by numerous well documented problems: the variable relation between radar reflectivity and rain rate, a vertical evolution of rain intensity from ground to beam-height, attenuation, changes in water-phase, attenuation, and eventually insufficient temporal sampling (Diederich et al., 2004). Bendix at al. (2004) used MRR to study the rain in a tropical montane cloud forest of southern Ecuador and its chemical composition.

A bright band is the enhanced radar echo area that is associated with the melting of hydrometeors in stratiform precipitation (Cha et al., 2009). The top of the bright band can be considered as the melting level (or freezing height), commonly accepted as the altitude of the 0° C isotherm (Glickman, 2000).

Data from a long term measurement of MRR at a mountain site (Daegwallyeong, DG, one year period in 2005) and a coastal site (Haenam, HN, three years 2004–2006) in South Korea were analyzed by Cha et al. (2009) to compare the MRR measured bright band characteristics of stratiform precipitation at the two sites. On average, the bright band was somewhat thicker and the sharpness (average gradient of reflectivity above and below the reflectivity peak) was slightly weaker at DG, compared to those values at HN.

The characteristics of the bright band may reveal important cloud microphysical processes. Fabry and Zawadzki (1995) reported that the mixture of ice, air, and water leads to a greater increase in the radar reflectivity than that expected from the change from ice to water. They suggest several other factors that contribute to this bright band phenomenon. One such factor is the distribution of water within the particle, so called the density effect. That is, the distribution of melted water within the snow particle will appreciably affect the reflectivity value.

Zawadzki et al. (2005) focused more on the density effect and proposed a bright band model, showing that the difference between the peak reflectivity and the snow reflectivity increases with a decreasing density of snow particles.

Melting precipitation in stratiform rain produces a distinct signal in radar data, ie., the "bright band" (BB; Gettys et al., 2000). The case of the convective rain is different. The strong convective currents in active showers and thunderstorms tend to destroy the horizontal stratification essential for creating and sustaining the BB. As a result, the BB is broken (Farby and Zawadkzki, 1995; Neiman et al., 2005). The stratiform condition gives rise to radar bright band (BB) and during convective regime of rain there will not be any radar bright band (NBB). High-frequency radars do not measure an enhanced 'bright band' at the melting layer, rather a sudden increase of reflectivity as the ice particles become coated in water. This sudden step can be used to locate accurately the height of the WBZ (Wet-Bulb zero degree isotherm). This studies of Mittermaier and Illingworth (2003) suggests that, at least in the UK, operational model predictions of the freezing-level height are within the specified 200 m error, but that the use of volumetric scans, even under idealized conditions, cannot achieve this accuracy.

Recently, however, Loffler-Mang and Kunz (1999) and Harikumar et al. (2006; 2008b) demonstrated that a MRR, a vertically pointing Doppler radar, could be a very useful instrument to measure the vertical profiles of precipitation and the bright bands, with the advantage of a higher time resolution, a significantly lower cost than X-band radars, and the easiness of operation. The electronic noise correction rendered the radar particle size retrievals below 0.7 mm drop diameters invalid; exponential extrapolation of the spectrum below drop diameters of 0.7 mm decreased the rain intensity up to 20% (Loffler-Mang and Kunz, 1999).

For the first time in Korea, monthly mean melting layer height data measured using a MRR by Cha et al. (2009). Measurements are made at the Cloud Physic Observation System (CPOS) site at Daegwallyeong Weather Station (37º41 N, 128º46 E, 842 m ASL), located in Gangwon Province. An easy method is introduced to estimate the melting layer height from the MRR rain rate data in association with the bright band regions (Cha et al., 2009). In the Tropics, freezing

levels are highest (~5000 m) and both intramonth and interannual variability is lowest. Freezing levels are lower and variability is higher in the subtropics and midlatitudes (Harris et al., 2000). Sudden changes in the temporal behaviour of the DSD spectra are accompanied by rapid modifications in corresponding integral relationships of Z-R are seen (Clemens et al., 2006). So, the DSD evolution of the rain DSD has been studied in detail by these authors. The initial spectra below the melting layer seem to play an important role in the change of these modifications of the integral parameter's relation. In addition, the height of the melting layer or even the fall-distances allows for modifications of drop size distributions in terms of coalescence and drop-break up. Most of these described processes result in a vertical variability of the estimated reflectivity in contemporaneous constant rain intensity. This leads to height-dependent Z-R relationships in spite of temporal homogeneity which is of importance especially for quantitative radar rainfall estimation (Clemens et al., 2006)

Usually the Z-R-relationship ($Z=AR^b$) is established by using drop size spectra from Disdrometers at ground level and transferring it to radar data aloft. But the changes of spectra with height indicate that also Z-R relationships will be affected. Therefore, these relationships have been calculated from the mean spectra described before by regression with the independent variable R (rainfall) and the dependent variable Z (reflectivity). Variable *b* is equal to the regression coefficient (Wagner et al., 2004).

Within stratiform precipitation, the same rain rate could be produced by a drop spectrum dominated by numerous small drops (lower reflectivity) or by a few large drops (higher reflectivity) (Yuter and Houze, 1995). The usual specific Z-R relations are usually established on the basis of climatologies of rain gauge data versus simultaneous radar reflectivities (e.g. Michelson and. Koistinen, 2000). Lee and Zawadzki (2006) demonstrated that distrometer-based radar calibration providing the actual Z-R relation via the drop size distribution has the potential to eliminate important calibration uncertainties.

Reflectivity–rainfall (*Z–R*) relations of the form $Z = AR^b$ were developed for each precipitation category as a function of height using linear regressions to the

radar retrievals of *R* and *Z* in log space by Cifelli et al. (2000). The results of this study show that, despite large overlap in the distribution of the drop-size parameters, significant differences occur in the mean *Z–R* parameterization for each category as a function of height. Similar to findings from previous studies, the rainfall decreased *for a given reflectivity* as the precipitation type changed from convective to stratiform. The coefficient *A generally* increased downward with height in each category; the exponent *b* showed a small decrease (stratiform), almost no change (convective), or a slight increase (mixed convective–stratiform). In the stratiform region, the coefficient *A* increases by ~37% with decreasing height. Exponent *B* also decreases slightly in the stratiform category. There are large differences in the convective and stratiform rain rates (15%–85%) for a given reflectivity and emphasizes the fact that the *Z–R* relation varies, not only by precipitation category, but also as a function of height. The combined signature of *A* increasing and *B* decreasing in the stratiform category is consistent with the expected change in *Z–R* due to one or more of the following: coalescence, evaporation, or size sorting (Gunn and Marshall 1955; Atlas and Chmela 1957; Wilson and Brandes 1979; Ulbrich and Atlas 1998). The coefficient *A* in the $Z=AR^b$ relation increases with median volume diameter while the exponent *b* approaches unity (Ulbrich and Atlas, 2007). Apart from using the lognormal distribution to represents the rain DSD, radar reflectivity factor also has been derived by these authors (Feingold and Levin, 1986). It is found out that the use of MP Z-R relation ($Z=200R^{1.6}$) gives bias errors of about 1.5 dB or less in their measurements (Kozhu et al., 2006). Z-R relation will have significant variation in the area where the origin of rainfall and surrounding environment depend heavily on the season.

Using MST, LAWP and Disdrometer, Z-R relation has been studied for different tyepes of rain, stratiform, transition and convective type and also for different seasons by Rao et al., (2001). The exponent b (coefficient A) has been found to be smaller (larger) in the case of stratiform (convective) precipitation than in convective (stratiform) precipitation, in contrast to the earlier studies. The observed discrepancies are partially due to different methods of precipitation

classification and partially due to different data set at different locations. As per the shape of the Z-R relation, if we use a single Z-R relation for all the regions and also to different precipitation systems, there will be underestimation in the convective rain and overestimation in the stratiform rain (Rao et al., 2001).

According to Wagner et al. (2004), from 200 m to 2000 m height, the b has been reduced from 1.3 to 0.9. a is also decreasing with height (same as present result). Factor *A* is ranging between 60 and 210 for light, moderate and total rainfall, but for heavy rain it exceeds 500 at lower altitudes corresponding to Z-R relationships for severe convection (Wagner, 2004). Some kind of linearity between Z and R seems to exist (Jameson and Kostinski, 2002). Within stratiform precipitation, the same rain rate could be produced by a drop spectrum dominated by numerous small drops (lower reflectivity) or by a few large drops (higher reflectivity) (Yuter and Houze, 1995). A probability-matched Z–R relation for all the raindrop image data from the Electra collected between altitudes of 2.7 and 3.3 km in TOGA COARE is similar to the Z–R relation obtained at the sea surface in the Global Atmospheric Research Program Atlantic Tropical Experiment. I.e., A single Z-R relation using all the data has been derived rather than classifying as stratiform and convective type.

Cerro et al. (1999) shows the results of the modeling of drop size distributions (DSD) observed during a 2 year study in Barcelona. They collected the rain DSD and velocities and then grouped them into classes according to the rain rate. Good results of Z-R relations are obtained when the DSD is modelled with an exponential distribution. According to Jamson and Kostinski (2002), The non-linear power relations between them are purely depends on the number of samples. That is, as per these authors, the shape of the power relations depend on the number of drops considered in the analysis.

O. Fiser (2004) describes the accuracy of the Z-R relationships through the RMSE and correlation and to improve the accuracy using distinguished rain (DSD) types using the Czech DSD data that has been collected for one year. The accuracy is perfect when DSDs are distinguished in two classes according to Waldvogel criterion (Waldvogel A., 1974).

The Z-R relation derived by Baltas and Mimikou (2002) for a specific event was $Z=407R^{1.26}$, whereas for all events it was $Z=431R^{1.25}$. The rain rate could be derived from the radar reflectivity factor using the power Z-R law (Brandes, 1974). Lee and Kyung (2006) got Z-R relation as $Z=333R^{1.08}$. They concluded that, when using the ground Disdrometer to establish proper Z-R relationship, the spatial and temporal extents should be considered carefully. Early classification for Z-R relation by rain type by Fujiwara (1965), gives values of A and b as for thunderstorm (A =450; b =1.46), rain showers (A =300; b =1.37) and continuous rain (A =205; b =1.48).

Uijlenhoet et al. (2003) presents a case study of the variability of raindrop size distributions for a squall line passing over a small watershed in northern Mississippi. The intrastorm variability of raindrop size distributions as a source of uncertainty in single-parameter and dual-parameter radar rainfall estimates is studied using time series analyses of Disdrometer observations. Two rain-rate (R) estimators are considered: the traditional single-parameter estimator using only the radar reflectivity factor (Z) and a dual-polarization estimator using a combination of radar reflectivity at horizontal polarization (Z_H) and differential reflectivity (Z_{DR}). A scaling-law analysis reveals that the shapes of the scaled spectra are bent downward for small raindrop sizes in the leading convective line, slightly bent upward in the transition zone, and strongly bent upward in the trailing stratiform rain. The exponents of the resulting Z–R relationships are roughly the same for the leading convective line and the trailing stratiform rain (~1.4) and slightly larger for the transition region (~1.5), with prefactors increasing in this order: transition (~200), convective (~300), stratiform (~450). In terms of rainfall estimation bias, the best-fit mean $R(Z_H, Z_{DR})$ relationship outperforms the best-fit mean $R(Z)$ relationship, both for each storm phase separately and for the event as a whole.

A fundamental step in the hydrometeorological application of single-parameter weather radar is the conversion of radar-measured reflectivities aloft to estimates of the spatial and temporal distribution of rainfall at the ground. Although many different sources of error and uncertainty affect this conversion (e.g., Wilson and Brandes 1979; Zawadzki 1984; Joss and Waldvogel 1990; Steiner et al. 1999;

Sa´nchez-Diezma et al. 2001), a key issue is the limited spatial and temporal representativeness of radar reflectivity–rain rate (*Z–R*) relationships. Fixed *Z–R* relationships will inevitably lead to errors in radar rainfall estimates, because raindrop size distributions exhibit an appreciable amount of spatial and temporal variability e.g., Dingle and Hardy 1962; Waldvogel 1974; Carbone and Nelson 1978; Smith 1993; Smith and De Veaux 1994). Although the storm-to-storm (i.e., *inter*storm) variability of *Z–R* relationships is relatively well established (e.g., Fujiwara 1965; Battan 1973; Smith and Krajewski 1993; Steiner and Smith 2000), the variability within storms (i.e., *intra*storm variability) has received less attention until recently (e.g., Waldvogel 1974; Carbone and Nelson 1978). Yet, there exist appreciable spatial variations in microphysical environments within a storm at any given time and corresponding temporal variations through the course of a storm at any given place within that storm (e.g., Steiner et al. 1995; Houze 1997; Petersen et al. 1999). Since the coefficients of *Z–R* relationships are closely related to the microphysical structure of rainfall (e.g., Marshall and Palmer 1948; Battan 1973; Waldvogel 1974; Jameson and Kostinski 2001a), the intrastorm variability of *Z–R* relationships is inevitably a source of uncertainty in radar rainfall estimates.

Drop size distributions (DSD) associated with tropical rainfall at Cuddalore in the south-eastern part of India has been measured by a Joss-Waldvogel Disdrometer (RD–80 model) during September to November 2002 by Roy et al. (2005). Rainfall events were separated into convective and stratiform. During the rain event, at low rainrates, the convective phase of the rainfall event was marked by DSD spectra that have greater population of small droplets as compared to stratiform DSDs at the same rainrates. In our case, the stratiform (BB)-Z is large for a particular rain rate compared to convective (NBB). This also shows that stratiform rain consists of more large drops. At higher rain rates, the convective regime is characterised by narrow spectra centred at higher diameters.

An empirical stratiform-convective classification method based on N_0 (Intercept parameter of the gamma distribution fit to the DSD) and R is presented by Tokey and Short (1995). Regarding the Z-R relation, the exponent is lower and the intercept is higher in the tropical stratiform classification than in the tropical

convective classification. Precipitation is generally considered to be of two clearly distinguishable types - stratiform and convective. Stratiform precipitation falls from nimbostratus clouds, while convective precipitation falls from cumulus and cumulonimbus clouds (Houze, 1993). Atlas et al. (1984) stated that "when rain is composed of many small drops of low fall speed, the liquid water content is bound to be higher and the reflectivity lower than with an equal rain rate of larger fast falling drops. The Z-R relation obtained by Tokey and Short (1995) are $Z=315R^{1.20}$ when all data is used, $Z=139R^{1.43}$ for convective and $Z=367R^{1.30}$ for stratiform. The value of ***A*** for stratiform rain is larger than for convective.

In the first section of this chapter, the variation of rain DSD with altitude is studied. Since all the rain events have similar rain DSD spectrum through out the altitude, a sample continuous rainfall event has been taken and explained here. While in the second section, the data pertaining to one complete year has been explored, by classifying the rain events in to stratiform and non-stratiform to study the altitudinal variation of Z-R relation.

6.2. VERTICAL PROFILES OF DSD

6.2.1. Data and data analysis

The analysis uses the MRR data during a continuous rainfall event from 02:00 hrs to 03:00 hrs on 12th October 2005 at Thiruvananthapuram. The first measurement height set for MRR was 200 m and the resolution was 200 m. The rain rate was 3.34 mm/h for this duration. The DSD values from the Disdrometer, were fitted with the lognormal function given as equation 4.7. The averaged DSD for different heights obtained from the MRR do not follow this function, but shows an exponential decrease with drop diameter.

6.2.2. Results and discussion

Figure 6.1 shows the drop size distribution at the surface and at 200 m and 400 m altitudes (y-axis in log scale). The DSD at the surface (from the Disdrometer) clearly follows the lognormal function, as reported earlier (Harikumar et al., 2007). But this is not true for the DSD at 200 m and 400 m. The lower threshold of the diameter for MRR measurement is 0.245 mm while that for the

Disdrometer, it is 0.3mm. So the MRR has measurements at 3 drop sizes smaller than those of Disdrometer. This needs to be kept in mind while comparing the MRR and Disdrometer data.

Figure 6.2 shows the DSD at different altitudes from 400 m to 4400 m, in steps of 400 m. The DSD at all heights behave in a more or less similar manner, with a steep exponential fall at the lower diameter end (i.e. up to around 0.6 mm) and a more gradual decrease beyond. DSD shows different behaviour above and below 3200 m. Above 3200 m, all the DSD curves more or less coincide, with very little difference between them. This is because the data above this height may be polluted due to the effect of the melting layer in the back scattered radar spectrum. However, below this height, the distributions start behaving differently and below 1200 m, the difference between them is significant. Therefore, our discussion focuses on this region. We see that drops of diameter of about 0.6 mm have the same concentration at all heights. According to Low and List (1982), if the drops of size less than 0.6 mm are struck by larger drops, it will coalesce. This is very clearly evident from the present spell study explained in the Chapter V. That is, small drops (whose diameter < 0.6 mm) have been reduced as rain comes down with passage of time. Here, in this analysis, the number of small drops decreases (<0.6 mm), and that of large drops (>0.6 mm) increases, as the height decreases. i.e., as rain comes down, the DSD is modified in such a way that the drops whose size is less than 0.6 mm decreases along with an increase in drops whose size is larger that 0.6 mm. This may mean that coalescence of small drops is more probable than disruption during collisions. Evaporation may also attribute to this situation. The average rain rate of this event was only 3.34 mm/h and also all the rain rate event of 1 minute duration obtained from MRR has a value less that 5 mm/h and this could be one reason for relative absence of break up. However, we have to keep in mind that the MRR gives an average picture for the duration of measurement.

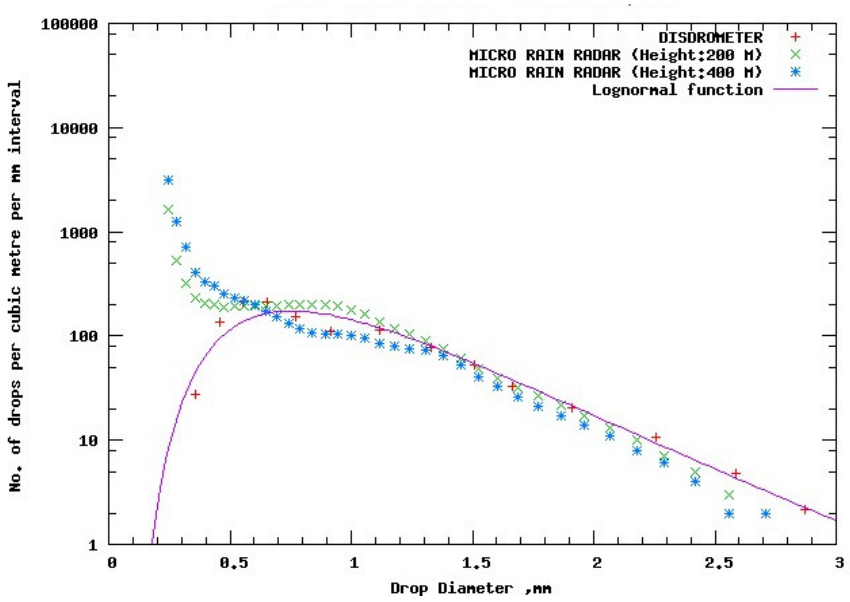

Figure 6.1. Comparison between DSD obtained from Disdrometer and from MRR.

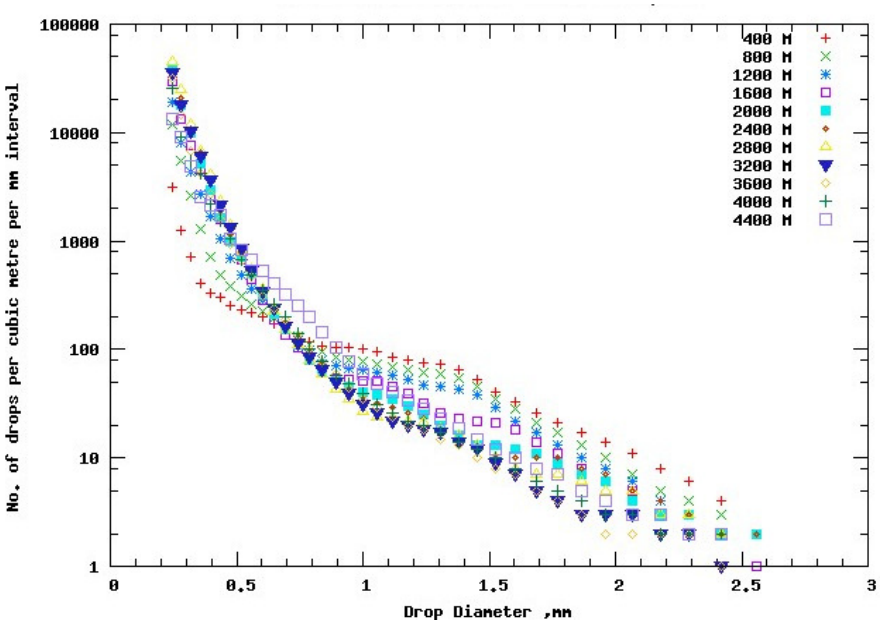

Figure 6.2. A typical Rain Drop Size Distribution Spectrum from the MRR (In the legend Altitude in meters is given).

The variation of number density with height is shown in figure 6.3. For lowest diameter range, it initially increases and then remains more or less constant. Figure 6.3 shows that the value remains almost constant at all altitudes for the

diameter range 0.559 mm to 0.603 mm. This diameter range exactly matches with 0.6 mm diameter given by Low and List (1982), as limit. Drops smaller than this will only be coalesce with bigger drops while they collide. But in the case of higher diameter ranges it decreases and then remains more or less constant.

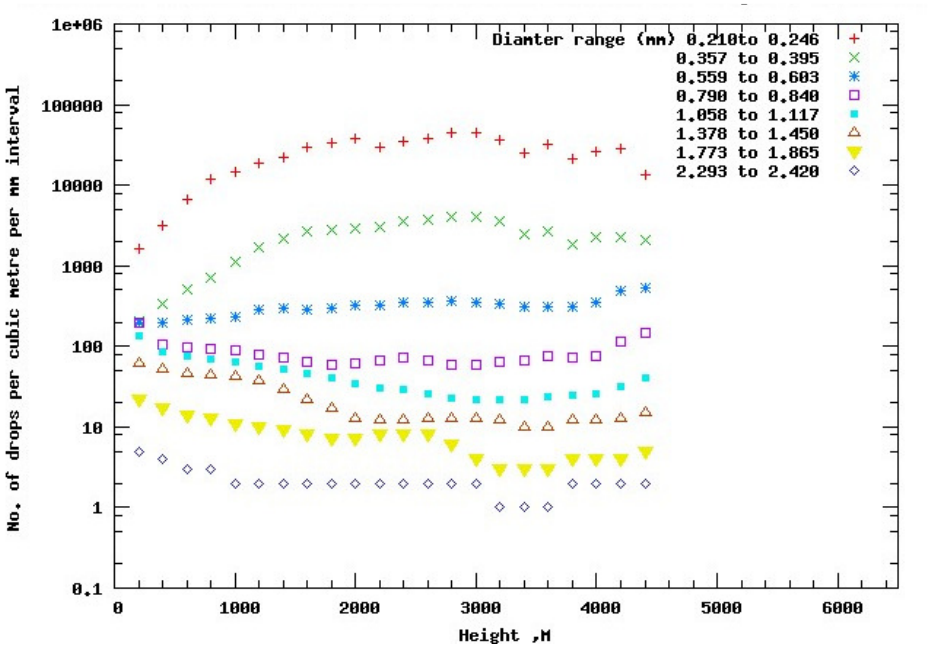

Figure 6. 3. Variation of number density with height for each diameter range (02:00 to 03:00 hrs, 12-10-05).

6.2.3. Summary of the results

DSD at the surface is lognormal in nature. DSD at 35 meters and even at a height of 200 metre with a short term averaged (five-minute averaged) DSD also show a lognormal behavior. But above this altitude, DSD changes from lognormal to exponential in character irrespective of the averaging time. The physical causes for such a change from lognormal to exponential distribution of DSD itself needs to be studied.

MRR data on many occasions, above about 3200 m, may not be useful due to the pollution in the back-scattered data obtained from the MRR due to the effect of melting layer.

It is seen that, up to 1200 m altitude, the DSD shows a marked change below and above 0.6 mm drop size. This behaviour indicates the prevalence of

coalescence.

6.3. VERTICAL PROFILES OF Z-R RELATION

6.3.1. Data and methodology

The back scattered power data from the MRR outdoor unit is automatically be logged on to a computer that is a part of the data acquisition system. The rain drop size distribution and integral rain parameters are be derived and stored in the assigned locations on the computer. Measurement principles of the Micro Rain Radar are explained in detail in the second chapter.

The height resolution set for the MRR measurement was 200 m and minimum measurement height was 200 m from January 2007 onwards, so that the data up to 6000 m height can be obtained and the radar bright band signature will be visible. The rain events (1 minute output of DSD and integral rain parameters from the MRR) from March to September 2007 at Thiruvananthapuram were separated into Bright Band (BB) and Non- Bright Band (NBB) cases (Harikumar et al., 2009b). Figure 6.4 is a schematic diagram that shows how we would be able to discern bright band or non-bright band condition from the rain rate vertical profile. Figure 6.5 shows the radar rain rate vertical profile spectrum obtained from the Micro Rain Radar. The above mentioned classification of the rain events into BB and NBB are done by interpreting this spectrum for the entire period. The bright band often leads to an overestimation of precipitation intensity (Rain rate; Rico-Ramirez et al., 2005) and several algorithms have been proposed to correct the effect of the bright band (e.g., Song and Marwitz, 1989; Kitchen et al., 1994; Hardaker et al., 1995; Gray et al., 2002; Neiman et al., 2002). This increase in the value of rain parameters is not due to the real increase in parameters but due to the phase change of the water that cause more reflection of the electromagnetic radiation.

The radar Bright Band signature, which is an indication of freezing height, is validated with the Wyoming radiosonde data (from the web site, http://weather.uwyo.edu/upperair/sounding.html) that tells us where the 0 degree isotherm is lying. This was at an average height of around 4500 m over the tropical station Thiruvananthapuram during this duration.

A well-marked radar "bright band" in stratiform clouds can be used as a criterion for discriminating between startiform and convective type rain (Williams et al., 1995). Radar echo tops during the non-brightband (NBB) periods are generally shallower and orographic forcing was stronger than for brightband (BB) periods (Martner et al., 2005). Based on the S-PROF reflectivity and vertical velocity data, White et al. (2003) concluded that the NBB rain contains more small drops and fewer large drops than the BB periods. Evidence from the studies of Neiman et al. (2005) and White et al. (2003), indicates that BB rain usually results from deep, cold-top clouds that produce ice crystals, which grow by deposition, aggregation and riming to become large snow flakes which then form large raindrops when they melt. In the NBB cases, however, large snowflakes are absent, and water drops grow by condensation aided by upslope flow and by coalescence of drops in a relatively shallow layer near the terrain. The "hybrid" category used by White et al. (2003) is same as Martner et al. (2005) classification into BB, beacause both exhibit a definite radar bright band. He categorised exactly like what has been done here, into BB (stratiform) and NBB (convective).

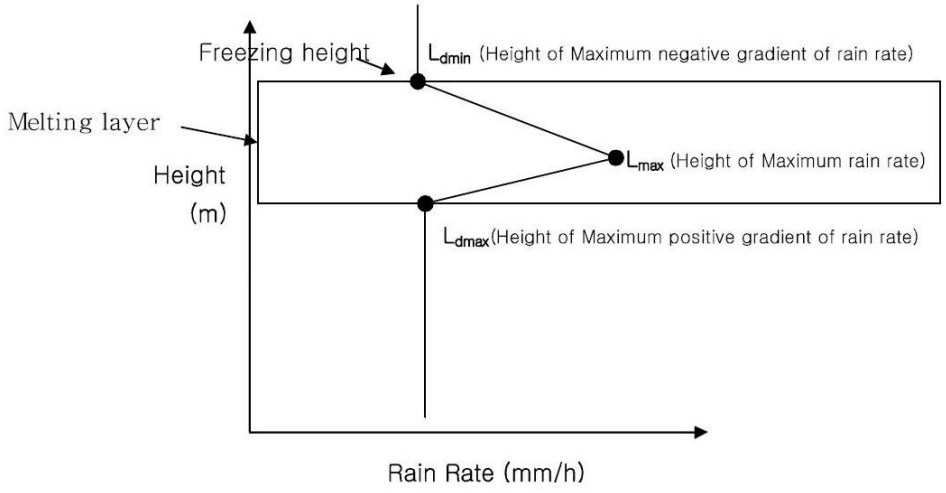

Figure 6.4. Schematic diagram that shows how to discern the presence or absence of radar bright band.

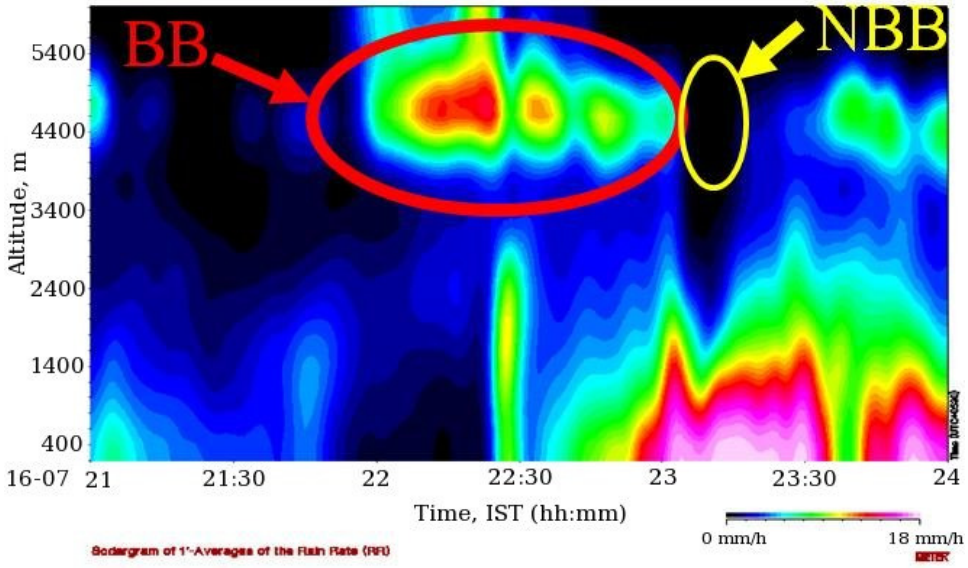

Figure 6.5. Rain rate vertical profile spectrum obtained from the MRR. Bright Band (BB) and Non Bright Band (NBB) regions of the rain event are shown.

As explained above, the radar bright band is an indication of stratiform rain. Stratiform rain has a maximum rain rate of about 10 mm/h, while convective rain will have a maximum rain rate even greater that 100 mm/hr. From the figure 6.5, it is clear that, when ever bright band is there, the rain rate at lower heights has low values, as a real evidence for stratiform condition. But when radar bright band is absent (23:00'o clock to around 23:35'o clock), which is a condition of convective rain and the rain rate at lower heights are found to be maximum in the present spectrum. That is at around 23:00'o clock, the rain has been transformed from stratiform origin (BB) to convective origin (NBB). This convective condition lasts up to around 23:35' o clock. After it, there is stratiform condition and by around 23:40' o clock, the convective condition has been revived again. The classification with respect to NBB or BB has been done in this manner, i.e., by looking into the radar rain rate spectrum.

6.3.2. Results and discussion

The presence of bright band is clearly discernible from the vertical profile of rain rate obtained from the MRR. The variation of radar reflectivity factor (Z) with rain rate for all the heights is fitted with a function of the form $Z = AR^b$

corresponding to the BB and NBB cases separately for Pre-monsoon and Southwest monsoon seasons. Clearly, two distinct fits with different slopes are obtained for BB and NBB cases during both the seasons (figure 6.6). The MRR data above 200 m alone is used in the analysis to eliminate the possible effect of radar ground clutter. The fit has good correlation coefficient of nearly 1 for all the Z-R relations during BB and NBB cases in both the seasons at all the heights. But in the NBB cases, it is noted that there is saturation in the radar reflectivity values beyond some rain rates at all the heights.

The Z-R relations for premonsoon-BB case is

$$Z = 496R^{1.26} \quad , \qquad (6.1)$$

for premonsoon-NBB case is

$$Z = 265R^{1.27} \quad , \qquad (6.2)$$

for southwest monsoon-BB case is

$$Z = 334R^{1.36} \qquad (6.3)$$

and for southwest monsoon-NBB case is

$$Z = 141\ R^{1.25} \qquad (6.4)$$

The parameters (intercept $\boldsymbol{A}$ and exponent $\boldsymbol{b}$) of the Z-R relation obtained from the present study have been compared with those obtained from the past studies. Figure 6.7 shows such a detailed comparison.

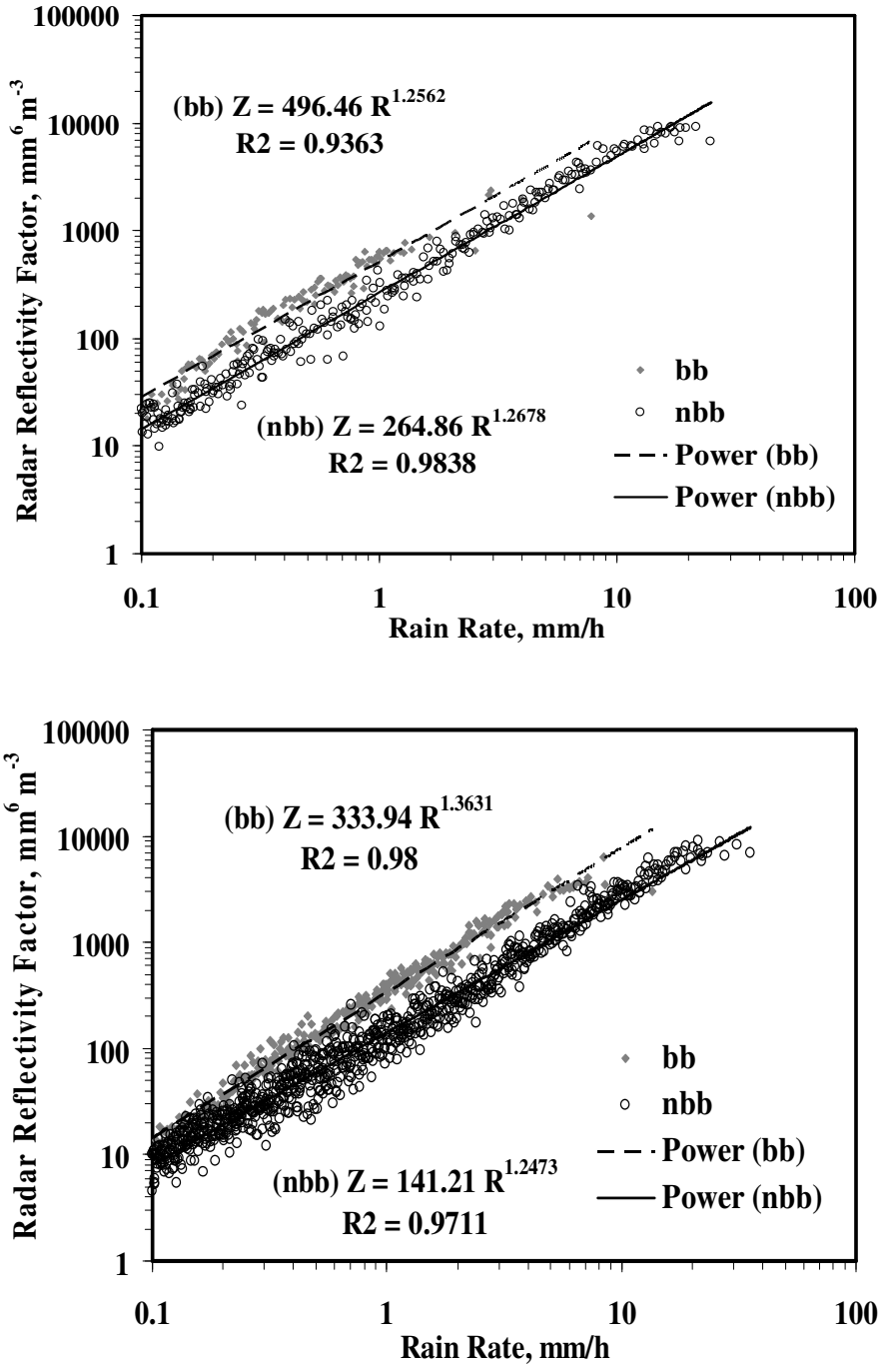

Figure 6.6. Variation Radar Reflectivity Factor with Rain Rate corresponding to the height 400 m for BB and NBB cases during Pre (top panel) and Southwest monsoon season at Thiruvananthapuram.

The values of these fit parameters for BB and NBB corresponding to each altitude has been studied for the altitudinal variation of these fit parameters for different seasons (Figure 6.8). In both the seasons and for BB and NBB, both ***A*** and ***b*** are decreasing with altitude except for southwest BB case. By incorporating the expressions of ***A*** and ***b*** shown in the figures for each case in the basic Z-R relation ($Z = A\ R^{b}$), an empirical relation for the variation of Z-R relation with altitude could be derived. In the southwest BB case, ***A*** and ***b*** are almost constant with little variation with altitude. The reason for such a difference in behavior of BB during the SW monsoon needs to be looked into in detail.

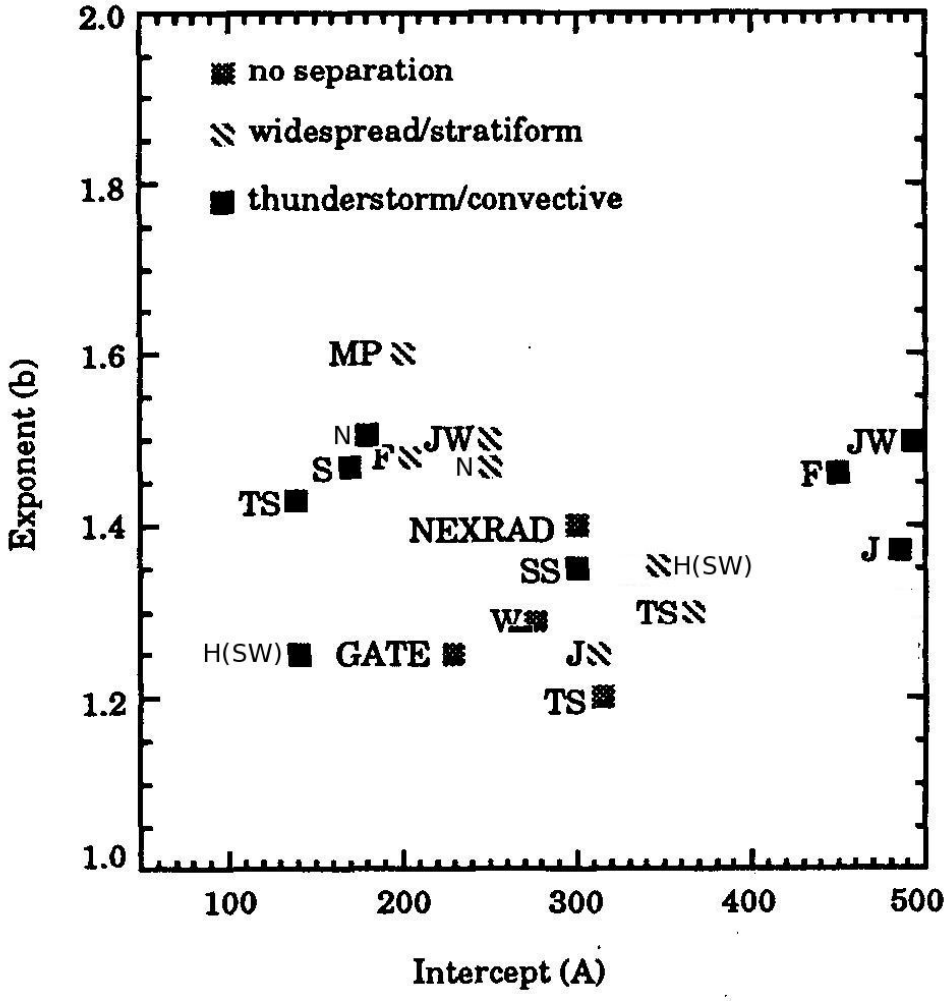

Figure 6.7. Summary of the $Z=AR^{b}$ relations [Figure reproduced from Tokey and Short (1996)] along with new results. The following abbreviations are used: JW: Joss

Waldvogel (1969), J: Jones (1956), F: Fujiwara (1965), S: Short et al. (1994), MP: Marshal and Palmer (1948), SS; Shekhon and Srivastava (1971), W: Willis (1984), GATE: Global Atmospheric Research Programme (GARP) Atlantic Tropical Experiment (Hudlow 1979), NEXRAD:Next Generation Weather Radar, TS: Tokey and Short (1996) and Present study [H (SW-southwestmonsoon]. N: Narayana Rao et al. (2001) also added shown in this figure.

Height of maximum positive gradient of rain rate (Ld_{max}; figure 6.4) was 3400 m during most of the time. So, the analyses were limited to a height of 3200 m to avoid possible pollution in the data due to the effect of radar bright band signature in the back-scattered radar spectrum.

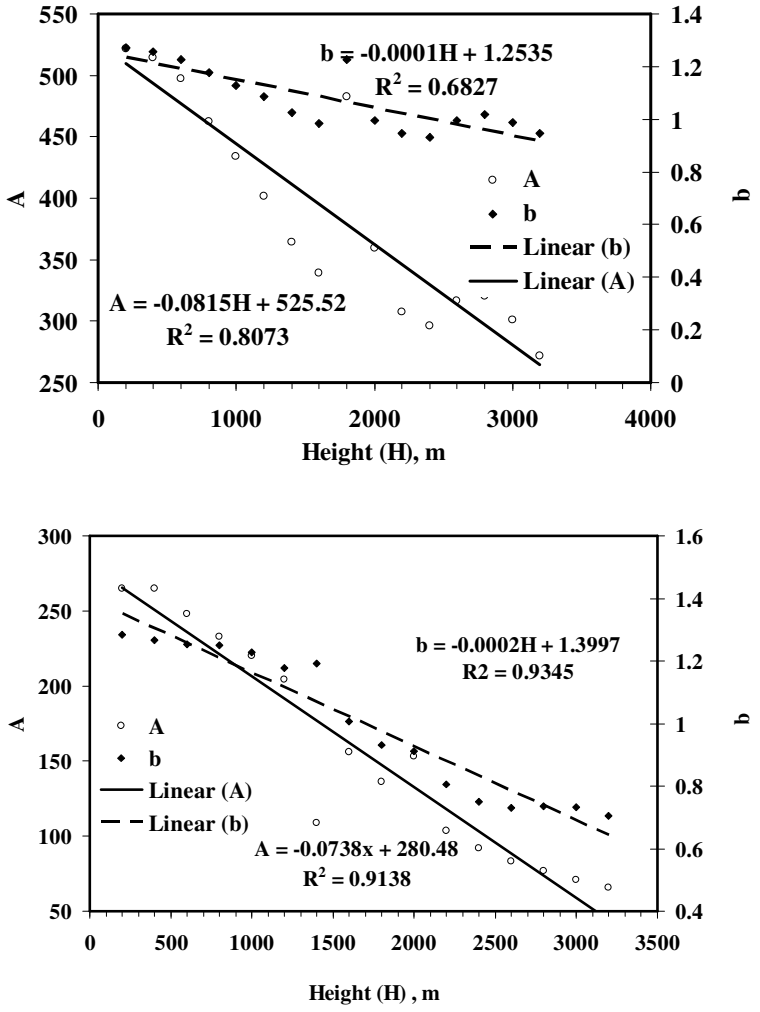

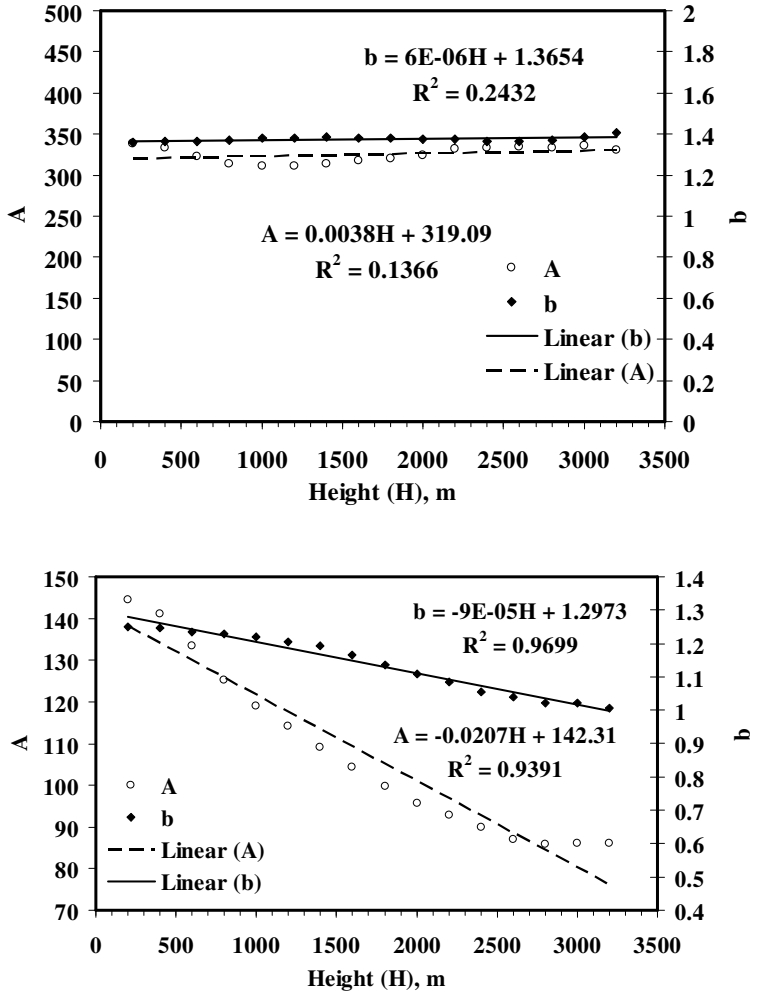

*Figure 6.8. The variation of fit parameters **A** and **b** with altitude for (1) Pre-monsoon-BB (top panel) (2) Pre-monsoon-NBB (second panel) (3) southwest-monsoon-BB (third panel) and (4) southwest-monsoon-NBB (bottom panel).*

The Z-R relation gives a new clear-cut method for classification of tropical precipitation as stratiform or convective origin using a Micro Rain Radar from the BB and NBB detections.

6.4. CONCLUSION

The vertical profiles of rain DSD and Z-R relation have been brought out in this chapter. The MRR data from 200 m to 6000 m height with a resolution of 200 m has been used for this purpose.

The Disdrometer data and MRR data agreed well. DSD at the surface is lognormal in nature. DSD at 35 meters and even at a height of 200 metre with a short term averaged (five-minute averaged) DSD also show a lognormal behavior. But above this altitude, DSD changes from lognormal to exponential in character irrespective of the averaging time. The physical causes for such a change from lognormal to exponential distribution of DSD itself needs to be studied.

MRR data on many occasions, above about 3200 m may not be useful due to the pollution in the back-scattered data obtained from the MRR due to the effect of melting layer.

It is seen that, up to 1200 m altitude, the DSD shows a marked difference below and above 0.6 mm drop size. This behaviour indicates the prevalence of coalescence. According to Low and List (1982), if the drops of size less than 0.6 mm are struck by larger drops, it will coalesce. This is very clearly evidenced from the present spell study explained in the Chapter V. That is, small drops (whose diameter < 0.6 mm) have been reduced as rain comes down with passage of time. Here, in this analysis, the number of small drops decreases (<0.6 mm), and that of large drops (>0.6 mm) increases, as the height decreases. Number of drops remains almost constant at all altitudes for the diameter range 0.559 mm to 0.603 mm.

As rain comes down, the DSD is modified in such a way that the drops smaller than 0.6 mm decrease in number and larger drops increase. This may mean that coalescence of small drops is more probable than disruption during collisions. It may also mean that evaporation is taking place. The average rain rate of this event was only 3.34 mm/hr. All the rain rate events of 1 minute duration obtained from MRR has a value less that 5 mm/h and this could be one reason for relative absence of break up.

The variation of the parameters of the Z-R relation also is studied for BB and NBB conditions of both pre-monsoon and southwest monsoon seasons. The rain events (1 minute output of integral rain parameters from the MRR) from March to September 2007 were separated into Bright Band (BB) and Non- Bright Band (NBB) cases. The radar Bright Band signature, which is an indication of freezing height, is validated with the Wyoming radiosonde data. A well-marked radar

"bright band" in stratiform clouds can be used as a criterion for discriminating between the startiform or convective type rain (Williams et al., 1995).

The presence of bright band is clearly discernible from the vertical profile of rain rate obtained from the MRR. The variation of radar reflectivity factor (Z) with rain rate for all the heights is fitted with a function of the form $Z = \boldsymbol{A}\ R^{\boldsymbol{b}}$ corresponding to the BB and NBB cases separately for Pre-monsoon and Southwest monsoon seasons. Clearly, two distinct fits with different slopes are obtained for BB and NBB cases during both the seasons. The values of the parameters of the Z-R relation is obtained and these have been compared with that obtained from the past studies.

In both the seasons and for BB and NBB, both ***A*** and ***b*** are decreasing with altitude except for southwest BB case. By incorporating the expressions of ***A*** and ***b*** shown in the figures for each case in the basic Z-R relation ($Z = \boldsymbol{A}\ R^{\boldsymbol{b}}$), an empirical relation for the variation of Z-R relation with altitude could be derived. The Z-R relation and the bright band detected using MRR gives a new clear-cut method for classification of tropical precipitation as stratiform or convective origin.

CHAPTER VII

COMPARISON OF SATELLITE (TRMM) PRECIPITATION DATA WITH GROUND-BASED DATA

CHAPTER VII

COMPARISON OF SATELLITE (TRMM) PRECIPITATION DATA WITH GROUND-BASED DATA

7.1. INTRODUCTION

Most of the earth's rain falls over the oceans, especially in the tropics. There fore, emphasis should be given to rainfall measurements over oceans, to understand the global hydrologic cycle. But, since the in-situ measurements are very difficult over oceans, we need to depend on satellite measurements that are validated sensibly. Tropical Rainfall Measuring Mission (TRMM) is the first satellite mission of National Aeronautics and Space Administration's (NASA), United States of America, launched in November 1997, dedicated for observing and understanding tropical precipitation and its relation with global climate. TRMM Merged High Quality/Infrared Precipitation estimates obtained from the TRMM '3B42' algorithm provide high resolution satellite-based rainfall estimates. To understand these measurements and to use the derived data products, it would be needed to compare/validate with ground-based measurements and also be aware of the seasonal and coastal dependence of the satellite measurements. This chapter presents such a comparison carried out for different monsoon seasons for all the stations out of which two coastal stations are on the west coast of India which experiences intense precipitation during the Indian summer monsoon (Xie et al., 2006), one high altitude station on the Western Ghats and one station on the east coast. The methodology and analysis followed here will eventually help in validating the precipitation data from the Indo-French upcoming satellite mission Megha-Tropiqes.

TRMM provides a unique platform for measuring rainfall from space using a passive sensor TRMM Microwave Imager (TMI; Kummerow et al., 1998), an active Precipitation Radar (PR) operating at 13.6 GHz, and a visible and infrared scanner (VIRS) radiometer. Precipitation Radar is the first satellite-based radar (active sensor) to measure rain parameters. TMI is a multi-channel/dual polarized (except in 22 GHz) microwave radiometer (10, 18, 22, 37 and 85 GHz), which provides rain rates over the tropical oceans besides sea surface temperature (SST),

sea surface wind speed (SSW), total water vapor (TWV) and cloud liquid water content (CLW). Passive estimates from the TMI are a less direct rainfall estimate since the radiometer responds to integrated liquid water, not just to raindrops. But by comparison, the more direct measurement of hydrometeors by the TRMM PR would seem to have less uncertainty; however, the PR operates at a single frequency (13.8 GHz) so that microphysical assumptions regarding drop size distributions come into play in the process of correcting the measured reflectivity for attenuation and relating reflectivity structure to rainfall rate (Franklin et al., 2003). Since the PR is a single-frequency, single-polarization, and non-Doppler one, the retrieval of rain intensity from the echo intensity data requires careful interpretation based on sophisticated algorithms which incorporate with peripheral ground validation data (Koru et al., 1996). Since, 13.6-GHz radar will only be sensitive to reflectivities higher than about 17 dB, there is disagreement between PR and TMI (Berg et al., 2006). Any way, the upcoming Global Precipitation measurement (GPM) mission will improve upon TRMM by employing a dual-frequency precipitation radar. The 13.6-GHz radar will only be sensitive to reflectivities higher than about 17 dB, whereas at 35 GHz, the minimum sensitivity will be 12 dB, according to recent design specification (Iguchi et al., 2003).

TRMM algorithm 3B42 provides adjusted 3-hour cumulative estimates of rain using merged microwave and infrared (IR) precipitation information (Adler et al., 2000). The TRMM adjusted Geostationary Observational Environmental Satellite (GOES) precipitation index (GPI) (AGPI) is produced by using cases of (nearly) coincident TRMM combined instrument (TCI) using the combined TMI and PR algorithm (Haddad et al., 1997) and VIRS IR data to compute a time and space varying IR-rain rate relationship that matches the TCI IR rain rate. This relation is used to calibrate IR estimates from geosynchronous satellite IR data to form the 3B42 product. Global estimates are made by adjusting the geosynchronous satellite Precipitation Index (GPI) to the TRMM estimates. The monthly TRMM and merged estimate is produced by merging the AGPI with information from rain gauges. The gauge analysis used in this procedure is from the GPCP (Rudolf, 1993). The merger is computed following Human et al. (1997). The 3B42 algorithm

provides daily precipitation and root mean square (RMS) error estimates at 1º x 1º latitude/longitude grids in the TRMM domain 40º N to 40º S (Human et al., 2001) for 3B42-V5 and in 3-hourly at 0.25º x 0.25º latitude/longitude grids over 50º N to 50º S for 3B42-V6.

Even though we have been using data from TRMM satellite for more than 10 years, the effect of coastal dependence and seasonal dependence on data products at each location is still a dilemma. Validation of TRMM 3B42-V5 data has been done using IMD rain gauge data by Narayanan et al. (2005) over Indian land. They found out that 3B42-V5 does not pick up small (< 1mm) and very high (> 80 mm per day) daily average rainfall. Thus, the daily variance (day-to-day variations within the season) estimated by 3B42-V5 is poor compared to the gauge data. The reasons may be related to deficiencies in the IR estimates. However at pentad (five-day) time scale the correspondence between the two datasets improves and intraseasonal and interannual variations are reasonable. The correlation coefficient over all of India on the monthly scale is high (r^2=0.92) in comparison to 5-day (r^2=0.89) and daily (r^2=0.79) time scale. Chokngamwong and Chiu (2005) have validated 3B42 data using rain gauge data from more than one hundred gauges over Thailand. Their results show that 5-year (1998-2002) daily average rainfall for gauge, 3B42-V5 and 3B42-V6 are 4.73, 5.62 and 4.58 mm/day respectively. The bias and root mean square deviation (RMSD) for V5 are 0.88 mm and 9.71 mm whereas for V6 it is 0.15 mm and 9.60 mm respectively. Scatter plots of daily gauge data versus 3B42 data show that 3B42-V6 correlates better with gauge (r^2=0.44) than V5 (r^2=0.37). The distribution of daily 3B42-V6 rain rate is quite similar to gauge while 3B42-V5 has more rain in the range 5-20 mm/day. The 3B42-V6 TRMM algorithm shows improvement over 3B42-V5 in terms of the bias, RMS difference, and mean absolute difference. Long-term mean rainfall rates from the Tropical Rainfall Measuring Mission (TRMM) Microwave Imager (TMI) and Precipitation Radar (PR) are compared with in-situ measurements by rain gauges on the NOAA TAO/TRITON buoy array in the tropical Pacific by Kenneth et al (2003) [12]. The buoy rain gauges have an advantage over most of the available ground truth data in that the local meteorological effects do not influence them.

The TRMM 3B42-V5 and 3B42-V6 daily rainfall data has been compared both with GPCP as well as IMD Indian gauge data for the duration 1998 to 2003 by Rahman and Gupta (2007). They have compared the all India seasonal (JJAS) total rainfall derived from IMD data with GPCP and 3B42-V6. In all the years the former is having more difference from the later two. Among known sources of errors in the rain retrieval, Toru et al. (1996) studied the vertical variability of the DSD and examined the partial beam-filling effect in terms of their significance with numerical simulations based on the MU radar data. Here, they examined the effect of the height variations of DSD using the MU radar data as realistic examples of the given 'truth' in the simulation. An accurate mean of the ground truth for the TRMM precipitation radar has been developed with the MU radar. Adeyewa and Nakamura (2003) have shown that TRMM PR data overestimates rain in the tropical rain forest region of Africa when compared with Global Precipitation Climatology Centre (GPCC) rain gauge data (Rudolf, 1993). The 3B43 product, which is the TRMM merged analysis on monthly scale, has the closest agreement with rain gauge data. Nicholson et al. (2003a), using rain gauge data from 515 stations over North Africa shows 3-4% bias for GPCC or GPCP with reference to seasonal rainfall fields (1988-1994). Nicholson et al. (2003b) and excellent agreement of TRMM-adjusted GOES precipitation Index (AGPI) and TRMM merged rainfall analysis with high density (920 stations) gauge data over West Africa on monthly to seasonal time scale. The RMSD of both satellite-derived products is 0.6 mm/day at seasonal scale and 1 mm/day at monthly resolution. The bias of AGPI is only 0.2 mm/day whereas the TRMM-merged product shows no bias over West Africa. The 1°x1° latitude/longitude product also shows excellent agreement at the seasonal scale and good agreement at monthly scale. In the present study, the comparison of TRMM and disdrometer data from four stations has been done. The details are explained below.

7.2. THE STATIONS AND THEIR CORRESPONDING TRMM GRIDS

The stations, duration for which data being compared and the corresponding TRMM grid that is chosen for comparison for each station are given in the Table VII.I. Thiruvananthapuram is a coastal station and about 25% of the

TRMM grid falls over the ocean. Kochi is also a coastal station with the same type of grid. Munnar is a high altitude station and an entire grid falls over the land. SHAR is a coastal station on the eastern coast and about 40 % of the grid could be over the oceans. The stations along with the corresponding TRMM grids are shown in a physiographical map shown in figure 7.1. The percentage of background that ocean or land occupies each of the grids can also be seen in the figure.

7.3. DATA AND DATA ANALYSIS

Satellite data

Algorithm 3B-42 produces Tropical Rainfall Measuring Mission (TRMM) merged high quality (HQ)/infrared (IR) precipitation and root-mean-square (RMS) precipitation-error estimates. These gridded estimates are on a 3-hour temporal resolution and a 0.25-degree by 0.25-degree spatial resolution in a global belt extending from 50 degrees south to 50 degrees north latitude. The main difference between TRMM 3B42-V5 and 3B42-V6 is that the resolution of 3B42-V5 is on a 1º x 1º grid and covers the global tropics (40º S-40º N latitude), whereas the 3B42-V6 product is in 3-hourly on a 0.25º x 0.25ºgrid and covers 50ºS-50ºN latitude. The 3B-42 estimates are produced in four stages, (1) the microwave estimates precipitation are calibrated and combined, (2) infrared precipitation estimates are created using the calibrated microwave precipitation, (3) the microwave and IR estimates are combined, and (4) rescaling to monthly data is applied. Each precipitation field is best interpreted as the precipitation rate effective at the nominal observation time.

The data has been downloaded from the web portal of NASA through anonymous FTP. The binary data obtained is converted into ASCII format. The data has a temporal resolution of 3 hours and corresponding to an area averaged over 0.25 x 0.25 degrees latitude longitude grid. The program written in FORTRAN, derives the needed data corresponding to the grid where the each station lies. The 3-hourly accumulated rainfall has then been derived from the 3-hourly rain rate for the comparison with the disdrometer data. The daily rainfall data has been compared by Rahman and Senguptha (2007). But in the current analysis, we have compared 3-hourly accumulated rainfall that is the maximum

temporal resolution of the rainfall data available from TRMM 3B42-V6 also apart from daily and monthly accumulation data.

No.	Station	From	To	TRMM Grid box
1	Thiruvananthapuram	March 2006	November 2006	8.375º N to 8.625º N; 76.875º E to 77.125º E
2	Kochi	a) May 2002 b) July 2003 c) May 2004	July 2002 August2003 July 2004*	9.375ºN to 9.625ºN 76.125ºE to 76.375ºE
3	Munnar	July 2004*	October 2004	9.875ºN to 10.125ºN; 76.875ºE to 77.125ºE
4	Sriharikota (SHAR)	August 2003	October 2003	13.375ºN to 13.625 ºN; 80.125 ºE to 80.375ºE

Table VII.I. The stations, duration for which data being compared and the corresponding TRMM grid that is chosen for comparison for each station.

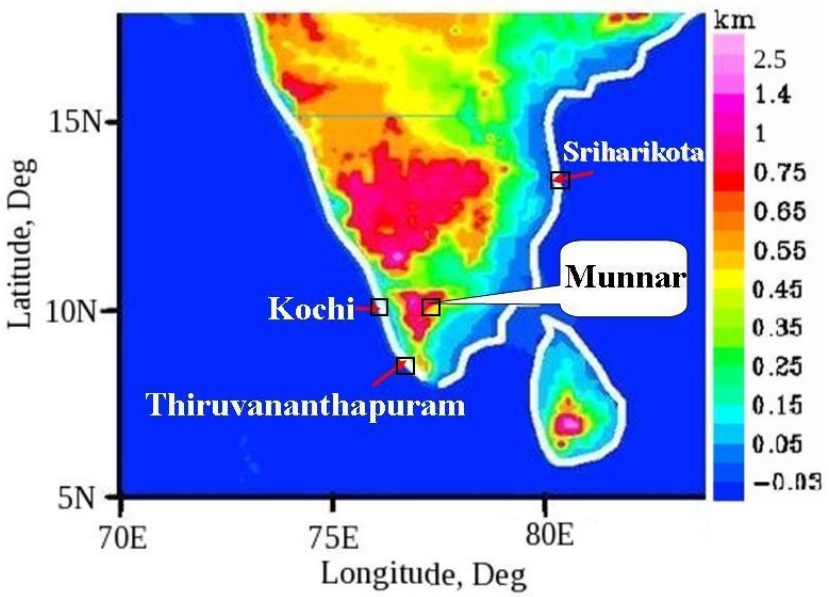

Figure 7.1. The Geographical locations of the 4 stations along with corresponding TRMM grid box shown in a physiographical map.

Ground-based data

At all the four stations disdromter was operated for differing periods. Therefore, the disdrometer data can be compared with the corresponding TRMM grid data. At Thiruvananthapuram, apart from the disdrometer Micro Rain Radar (MRR) and manual raingauge are also operational. Hence, at Thiruvananthapuram data from all these instruments have compared with the satellite data.

The disdrometer and MRR data obtained at one-minute interval were used to get the accumulated rainfall over 3 hour interval, over a day and for a month. Daily and monthly observations were obtained from the manual raingauge.

The analysis consisted of two parts. Firstly, the simultaneous detection of rain events by both ground-based and satellite measurements was found out. Then the correlation of the magnitude of the accumulated rain was done for only those events which were detected simultaneously.

The correlations for 3-hourly, daily and monthly precipitation data obtained from ground based and TRMM data have been evaluated.

7.4. RESULTS AND DISCUSSION

7.4.1. Simultaneous detection of rain

Before, correlating the measurements, the detection of daily rain events by these instruments simultaneously was evaluated as said earlier. The results for Thiruvananthapuram are shown as a pie diagram in figure 7.2. Both TRMM and ground-based instruments detected rain simultaneously for 35% time while 42% of time “no rain” was detected by both the instruments. Therefore for 77% time simultaneous detection of rain/no rain is seen. For the other 23% time only either one of the instruments has detected rain. This is not taken for the analysis. The 35% time when both detected is only used for analysis.

In the following sections, first the simultaneous detectability is shown by plotting the actual measurements from satellite and ground-based instruments. Then their magnitude was compared by doing a correlation analysis. By this way, the detectability and the efficiency of detection of rain events by all these instruments can be understood.

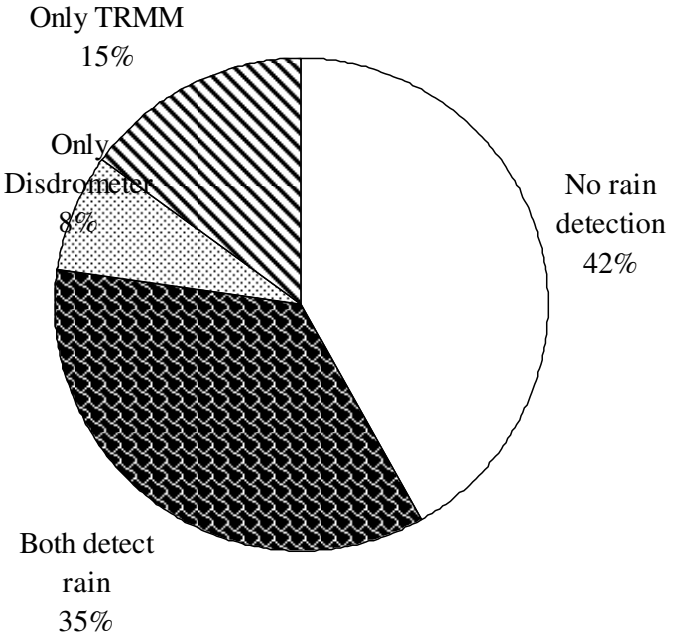

Figure 7.2. The detection of daily rain events at Thiruvananthapuram by TRMM and disdrometer.

7.4.2. Three-hourly rainfall

TRMM 3B42-V6, 3-hourly data has been compared with ground-based data. TRMM data is found to be matching with the ground-based measurements in the simultaneous sensing of rain. Munnar has a better correlation compared to other stations. Munnar is a high altitude station where the TRMM grid is wholly lying on the ground. That may cause the reduction in erroneous measurement for the microwave passive imager measurement when compared to other stations. Typical comparison for all the stations for each month is shown in the figure 7.3.

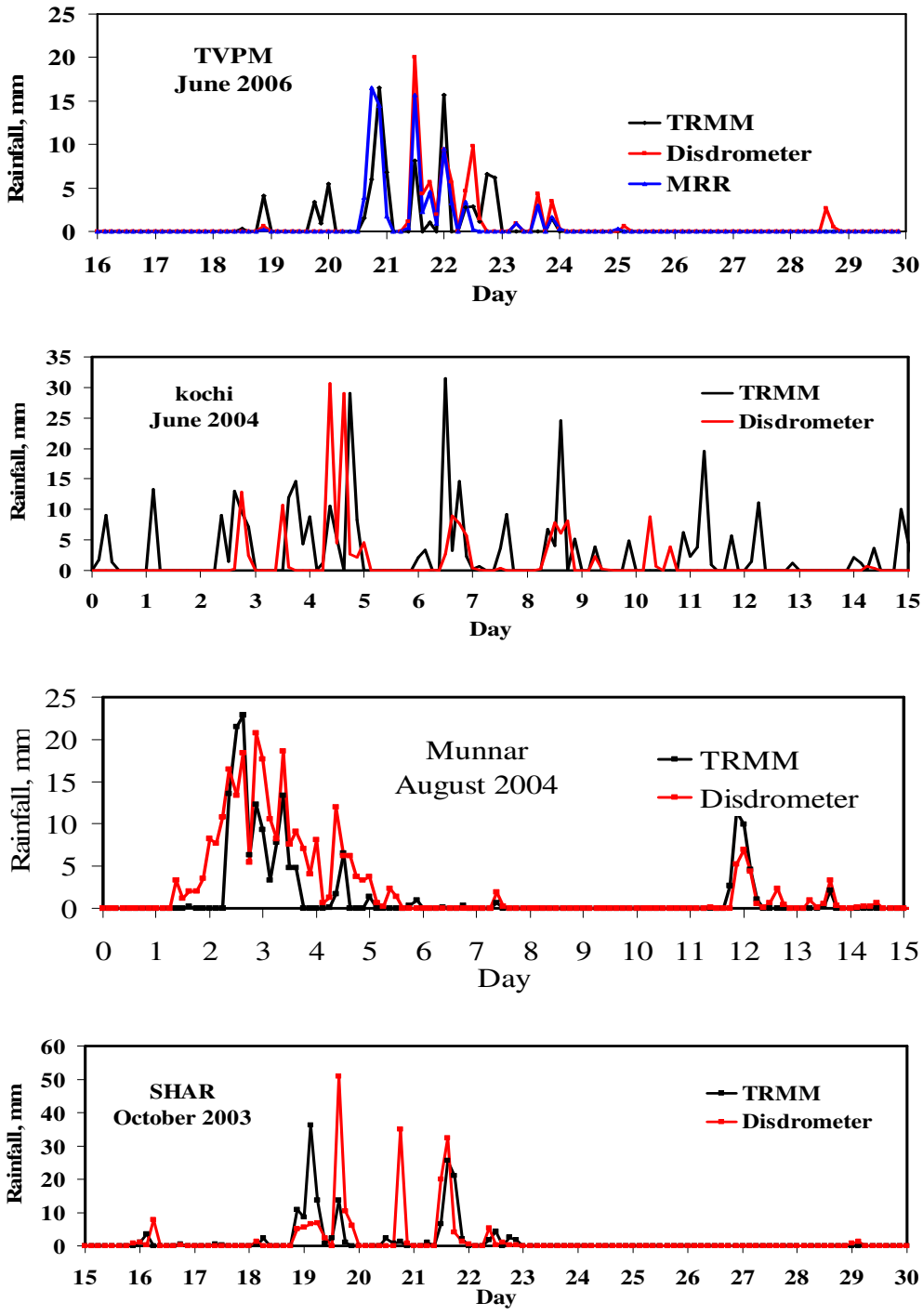

Figure 7.3. Comparison of TRMM 3-hourly rainfall data with Ground-based observations. [Disdrometer data is not available from 20th to 22nd and MRR data is also not available on 20th at Thiruvananthapuram (TVPM; panel 1)].

The next step of the analysis is to compare the magnitude of rainfall seen by ground-based and satellite measurements.

All the 3-hourly rainfall data points measured by disdrometer and TRMM at Thiruvananthapuram during the year 2006 have been plotted to find out the correlation (figure 7.4). The total number of data points is 132. The correlation coefficient obtained is only 0.4. Since the satellite gives an area averaged rainfall, the magnitude of the rainfall shown will be averaged for that particular grid. So, the magnitude appears to be underestimated. We are assuming that the rainfall over an area that is as small as a satellite grid got homogeneous clouds and thus homogeneous precipitation. But even for this much small area, it is seen that rainfall may not be homogeneous. Here the magnitude of the satellite rainfall measurement is seen to be on average about 50% of ground based measurement.

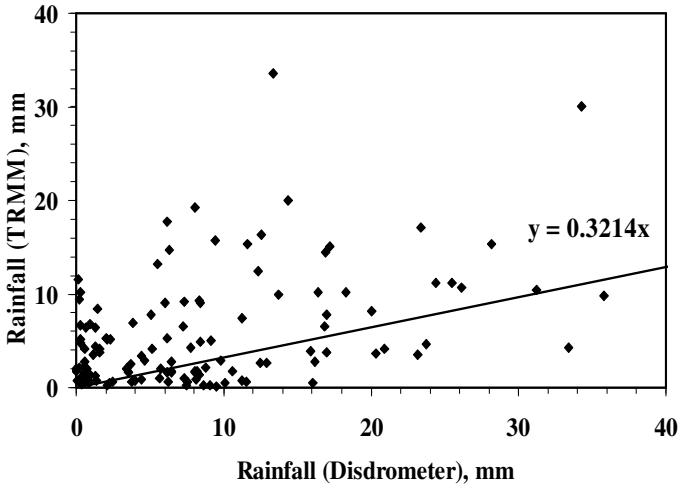

Figure 7.4. 3-hourly rainfall data measured by disdrometer and TRMM (number of data points=132).

To understand the seasonal dependence on the satellite measurements of rainfall, Thiruvananthapuram 2006 data has been grouped for that of pre-monsoon, southwest monsoon and that of north-east monsoon. Then each set of data obtained from the disdrometer and TRMM has been put together and plotted and fitted to study the correlation in each season (figure 7.5). The correlation was 0.48 for premonsoon, 0.44 for southwest monsoon and 0.3 for northeast monsoon season.

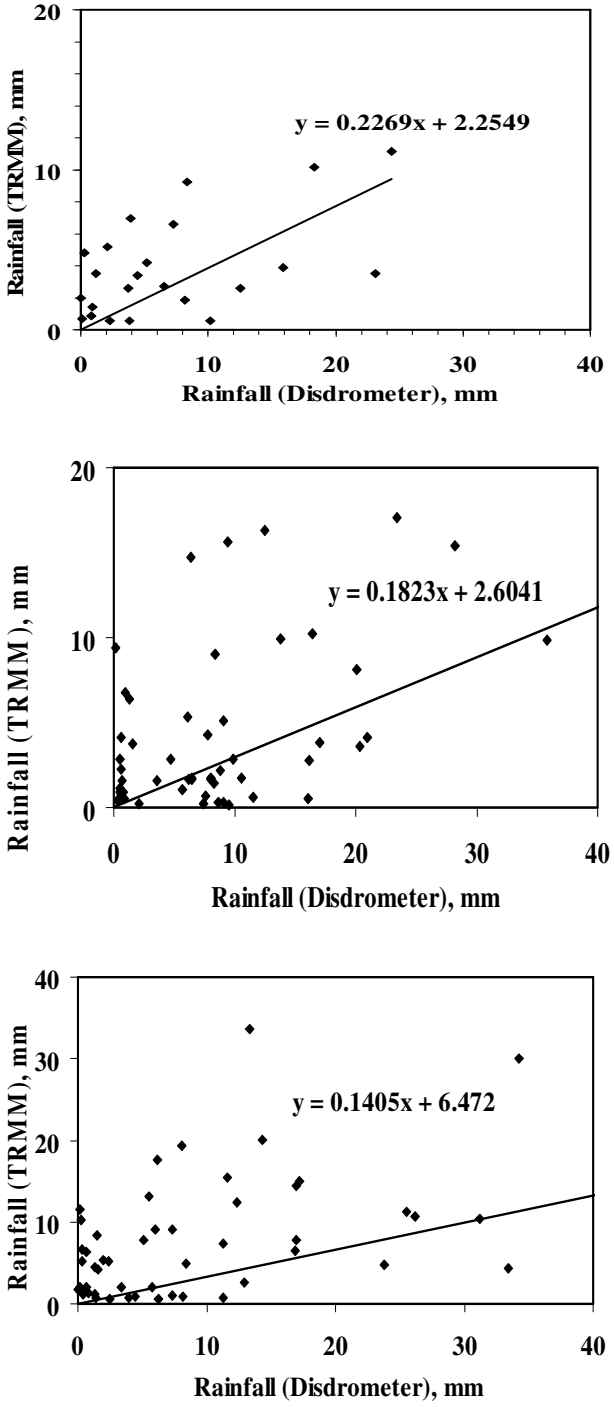

Figure 7.5. 3-hourly rainfall obtained from disdrometer and TRMM for (1) Pre-monsoon (top panel) (2) southwest monsoon (middle panel) and (3) northeast monsoon (bottom panel).

7.4.3. Daily rainfall accumulation

The daily accumulated rainfall data has been derived from the 3-hourly data. To understand the improvement in the correlation of the comparison when daily accumulations are taken, these daily TRMM data and ground-based data has been plotted in a bar-graph. Such comparisons for all the stations are shown in the figure 7.6. Since the manual rain gauge data was available at Thiruvananthapuram, data from it has also been incorporated in this analysis.

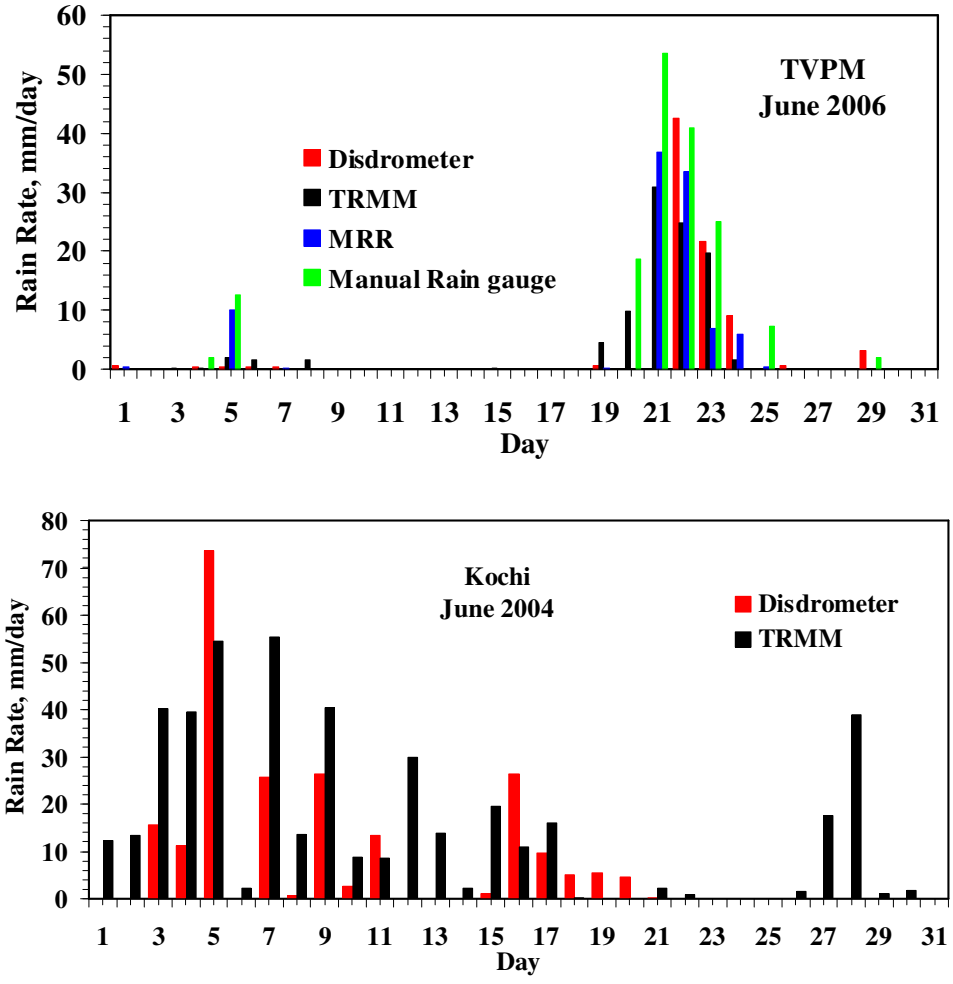

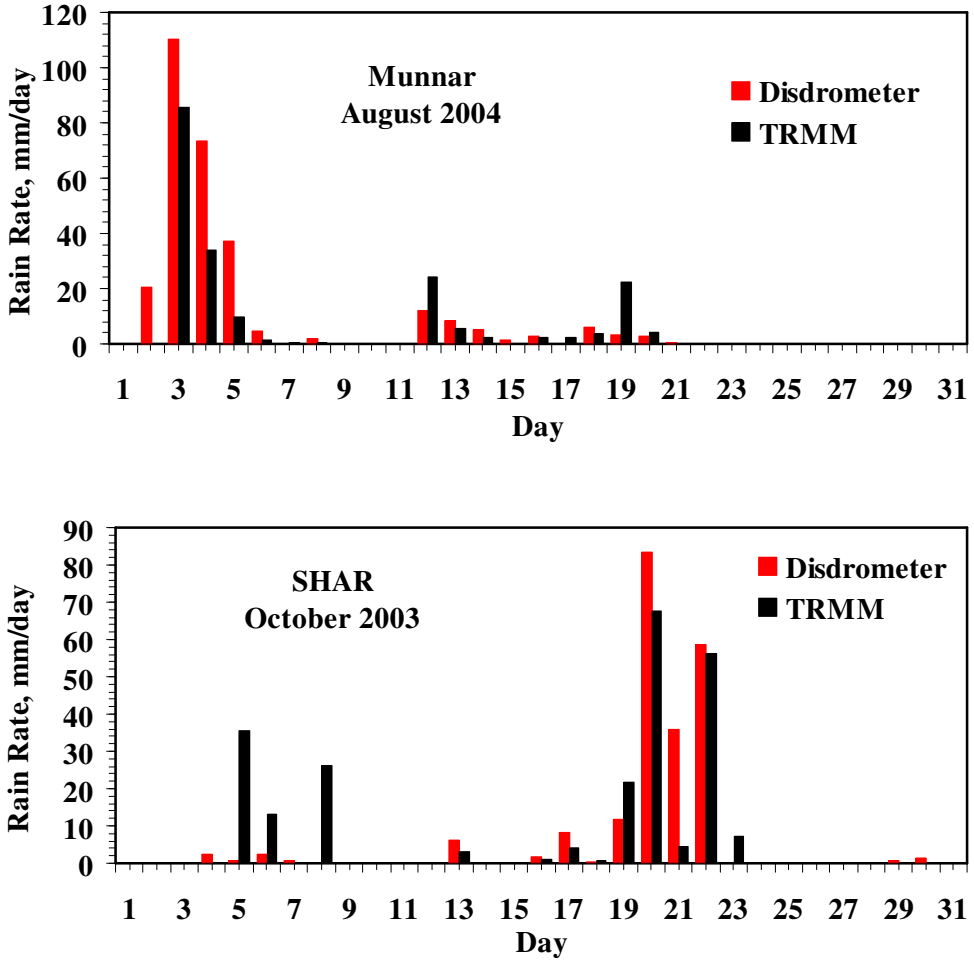

Figure 7.6. Comparison of TRMM rainfall/day data with Ground-based observations. [Disdrometer data is not available from 20th to 22nd and MRR data is also not available on 20th at Thiruvananthapuram (TVPM; panel 1)]

Exactly like the correlation study did for 3-hourly data, here also all the mm/day data points measured by disdrometer and TRMM has been plotted together to study the correlation between the measurements of the daily accumulations of rainfall (figure 7.7). Here the correlation coefficient has been improved from that at 3-hourly accumulation (0.4) to 0.6

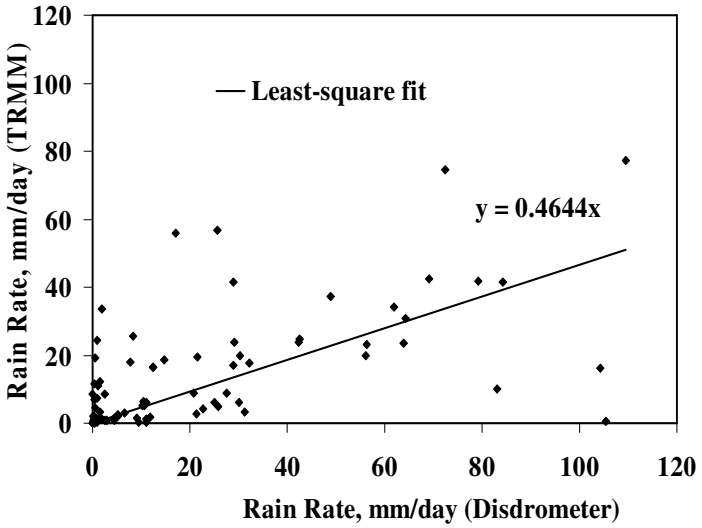

Figure 7.7. Daily rainfall obtained from TRMM and disdrometer. (number of data points = 78).

7.4.4. Monthly rainfall accumulation

Monthly accumulated rainfall data has been derived from the 3-hourly data from TRMM and from disdrometer. The daily manual raingauge data has been used to derive the monthly raingauge data. Root Mean Square Error (RMSE) in these comparisons has also been brought out and plotted along with the rainfall data. It is apparent from the figure that all the monthly accumulations obtained from the ground-based sensors compare well with the satellite detections.

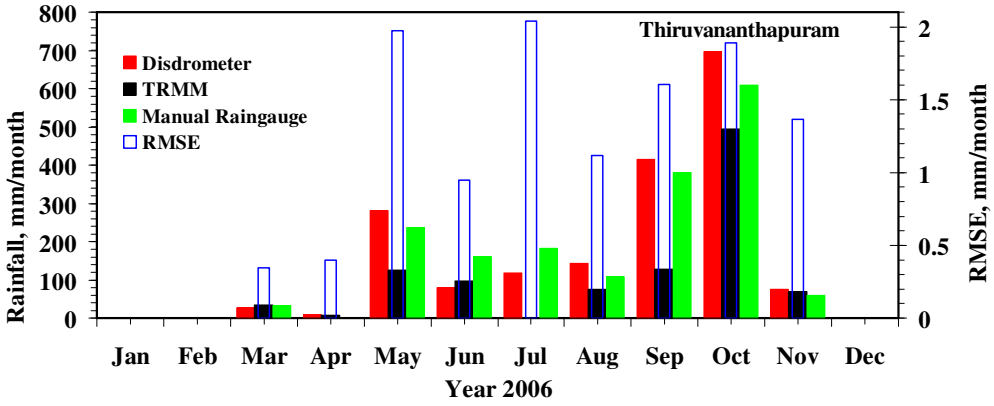

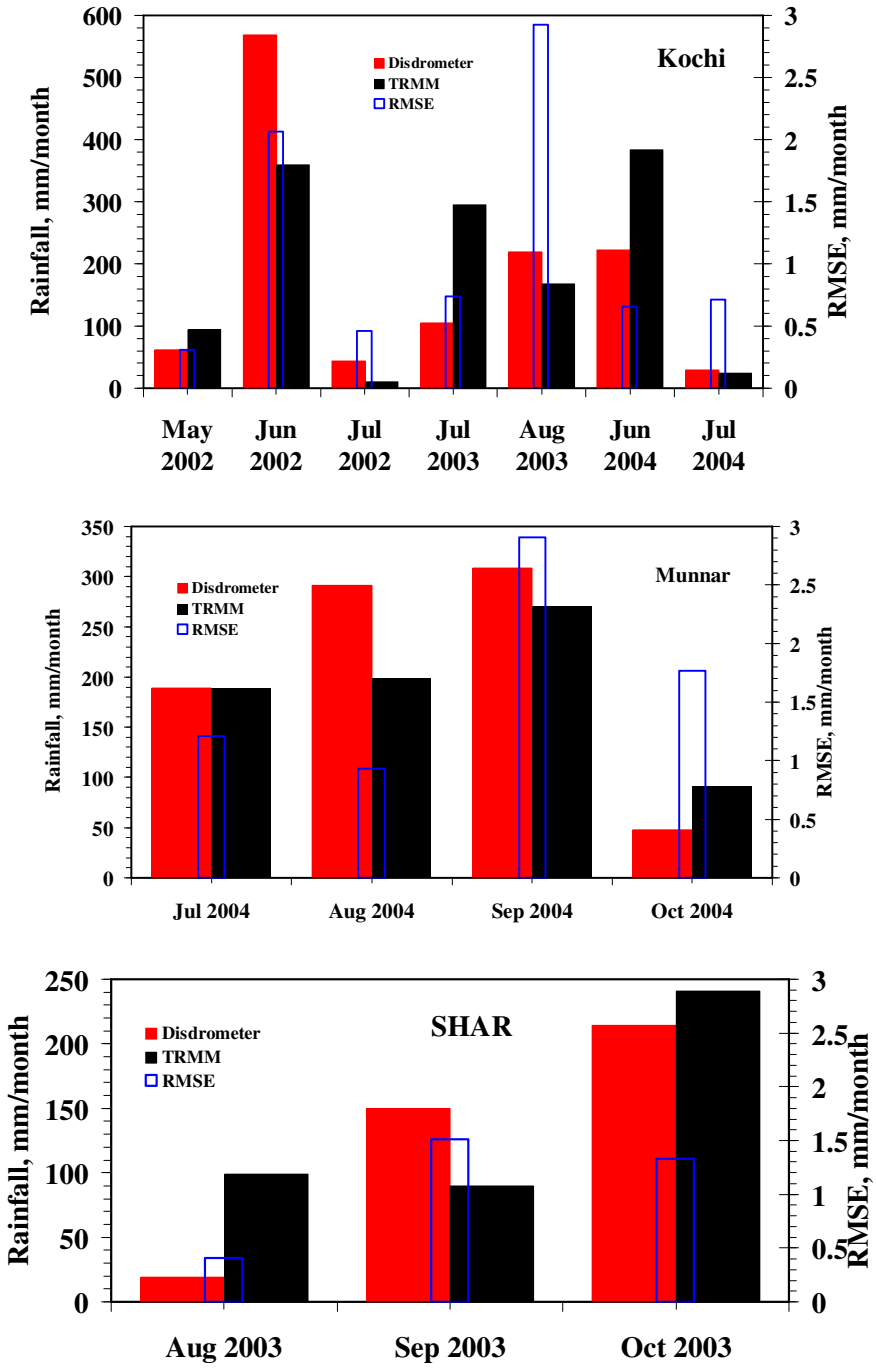

Figure 7.8. Comparison of the rainfall/month at (1) Thiruvananthapuram (top panel), (2) Kochi (2nd panel), (3) Munnar (3rd panel) and SHAR (bottom panel). RMSE is given for measurements between disdrometer and satellite.

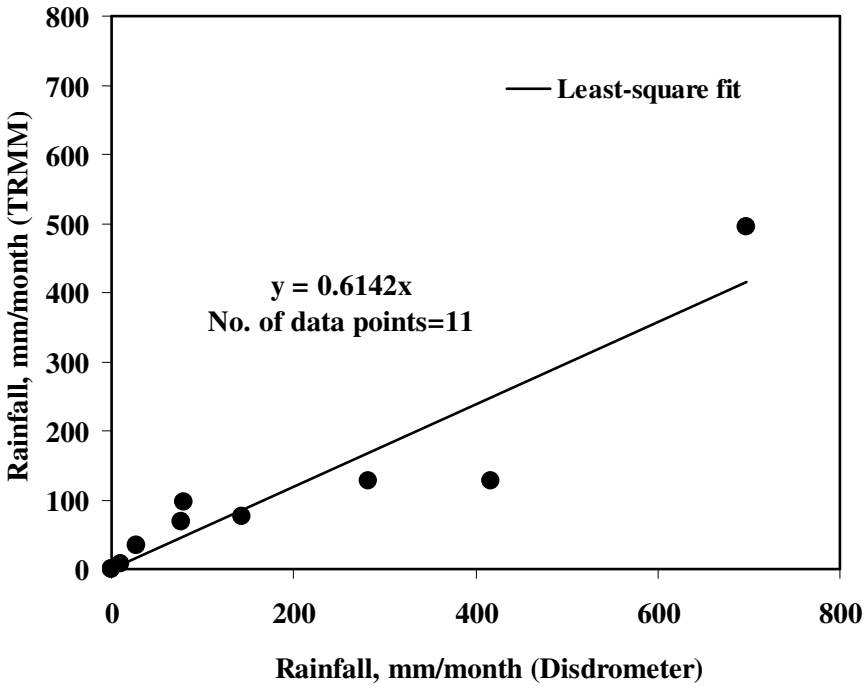

Figure 7.9. Correlation of the monthly accumulations of rainfall between the disdrometer and satellite measurements.

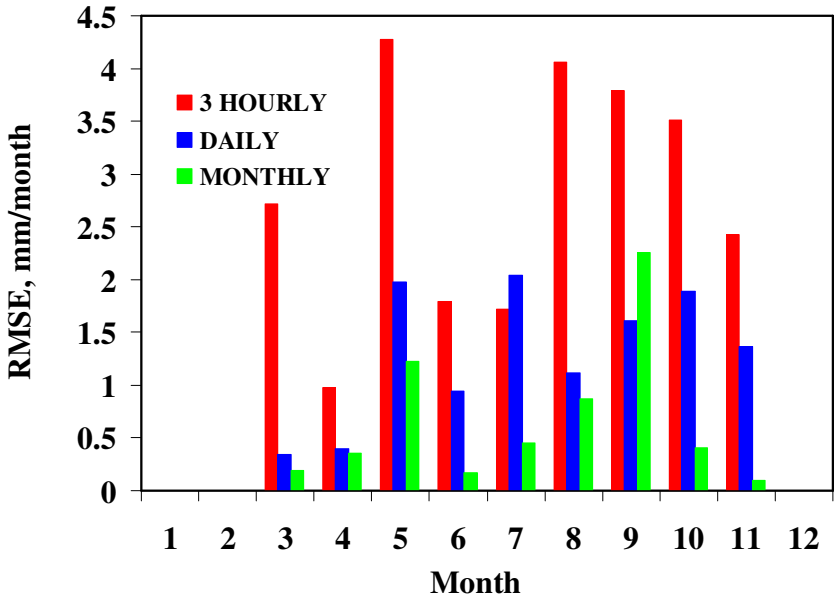

Figure 7.10. Comparison of the RMSE obtained for the comparison for different accumulations at Thiruvananthapuram for the year 2006.

Here also, all the monthly accumulations obtained from the disdrometer have been put together and plotted with that obtained from the TRMM. Here, the correlation has improved from a value of 0.6 for daily data to a value of 0.9.

7.4.5. Evaluation of the correlation for accumulations

The RMSE obtained when the comparison has been done using 3-hourly data, daily data and monthly data is shown in the figure 7.10. If RMSE is less, then correlation between the data from disdromter and TRMM is good. It is very clear from the figure that RMSE for 3-hourly is most, that of daily is more and that of monthly is less.

7.6. CONCLUSION

The major findings/conclusions from this study are given in brief below:

1. TRMM rainfall agrees well with the Manual rain gauge, Disdrometer and MRR rainfall, when monthly accumulation is taken (Correlation coefficient is > 0.9).
2. The same comparison for daily accumulated rainfall gives a correlation coefficient of around 0.6
3. For 3-hourly rainfall, the comparison gives a value of around 0.4
4. Magnitude of RMSE has no dependence on the magnitude of rainfall accumulation
5. RMSE varies from a low value for monthly accumulation to a high value for 3-hourly accumulation.
6. 79% of the total events could be detected together by the TRMM and disdrometer sensors.
7. Munnar shows a better correlation compared to other stations. This could be due the “coastal-grid effect”, as the other three stations are coastal stations. This could be due to the land and ocean back-ground emissivity within the same grid box in the scenario of satellite measurements.
8. To evaluate the ‘ground truth’ in a detailed way, it would be better to deploy more instruments within a single grid of 0.25º X 0.25º.
9. For rainfall events detected both by the satellite and ground based sensors, the TRMM rainfall appears to be under estimated in magnitude, on an

average, up to 50%. This could due to the fact that the satellite data is for an area averaged one over the 0.25º X 0.25º grid.

10. The number of events detected by single sensor only is being significant indicates that the rainfall may not be uniform even over a small grid size of 0.25X0.25 degrees. This also supports the need to have closely knit network of ground stations within the grid area.

CHAPTER VIII

SUMMARY OF THE RESULTS

CHAPTER VIII

SUMMARY OF THE RESULTS

The study of rain drop size distribution (DSD) and rain integrals is the focal theme of the thesis. Data from an impact type Disdrometer installed at four different locations for differing periods, from a Micro Rain Radar (MRR) and a conventional rain gauge have been used in the study. The results from this study have been described and discussed in the earlier chapters. Here a summary of the results are presented.

8.1. EVALUATION OF AN EMPIRICAL MODEL FOR THE VARIATION OF DSD WITH RAIN RATE

The one-minute DSD data has been sorted according to rain rate. Then the data is grouped into different rain rate windows. This DSD data for each rain rate group is averaged. It has been found that the DSD data for this region is represented by the lognormal distribution better than the Gamma and Marshal-Palmer distributions. Therefore for each of the rain rate group, the lognormal distribution is fitted and the constants are evaluated. Then the variation of these constants with rain rate was obtained. Using this, an empirical model to describe the variation of DSD with rain rate has been obtained. This empirical model has been tested using the actual measurements and found to be a good representation. The data used for testing was not included in the derivation of the model.

The lognormal distribution is given by

$$N(D) = \frac{\exp(A)}{D} \exp\left\{-0.5\left[\frac{(\ln D - B)}{C}\right]^2\right\} \tag{8.1}$$

The variation of parameter A with rain rate is

$$A = A_0 + A_1 R + A_2 \ln R \tag{8.2}$$

and that of B is given by

$$B = B_0 + B_1 R + B_2 \ln R \tag{8.3}$$

and C is found to be a constant.

Replacing these expressions in the above equation (8.1) we get the empirical model

$$N_{(D,R)} = \frac{\exp(A_0 + A_1 R + A_2 \ln R)}{D} \exp\left\{-0.5\left[\frac{(\ln D - (B_0 + B_1 R + B_2 \ln R))}{C}\right]^2\right\} \qquad (8.4)$$

where D is the drop diameter, $N(D)$ is the number of drops per cubic meter per unit diameter interval, and A_i, B_i and C are fit parameters.

The following table gives the constants for all the stations.

Station	Season	Parameters						
		A_0	A_1	A_2	B_0	B_1	B_2	C
TVM$^+$	PRE	0.930	0.013	0.489	0.286	0.005	0.152	0.370
	SW	0.318	0.005	0.308	0.404	0.001	0.216	0.383
	NE	0.968	0.008	0.409	0.321	0.002	0.192	0.386
Kochi	PRE	0.850	0.014	0.327	0.362	0.002	0.310	0.388
	SW	0.080	0.003	0.297	0.416	0.001	0.178	0.416
SHAR	ASO*	0.268	0.005	0.558	0.713	0.005	0.079	0.532
Munnar	SW	0.960	0.008	0.115	0.547	0.002	0.280	0.368

Table VIII.I. Parameters of the empirical model corresponding to each season at all the stations. (August, September and October, $^+$ Thiruvananthapuram).*

The rain rate measurements are available at a number of places, while DSD measurements are very less. Therefore this model could be used to derive DSD from rain rate alone. To make the model rigorously applicable and truly valid, measurements of DSD at more locations could be done and with this data, model can be updated.

8.2. RAIN RATE CHARACTERISTICS

The one-minute rain rate data from the Disrometer available from three stations, viz., Thiruvananthapuram, Kochi and Munnar has been used to study the characteristics of rain rate. The salient features of the results are given here.

- Around 90 % of the time, the rain rate is below 5 mm/h, except at Thiruvananthapuram where it is around 65%. This indicates that stratiform clouds are more prevalent in these stations compared to cumuliform.
- The most interesting aspect was the apparently lower presence of cumuliform clouds during July 2002 at Kochi, which possibly contributed to the deficiency in rainfall.

- The rain rate temporal cumulative distribution could be fitted with a Weibull distribution function of the form

$$y = 1 - \exp\left(1 - \left(\frac{x}{\lambda}\right)^{k}\right) \qquad (8.5)$$

The *k* is the shape parameter and **λ** is the scale parameter. It is found that the shape parameter is more or less the same at all stations during the southwest monsoon period.

- The value of shape parameter (k) of the weibull distribution fit to the temporal cumulative distribution remains more or less same for each station during the southwest monsoon period.
- Rainfall is present only for less than 10% of the time (or about 4300 minutes) even during a rainy month like June or July. This indicates that rainfall could be actually present for lesser duration.

8.3. DSD CHARACTERISTICS

Using the lognormal distribution, three physically significant parameters viz. Total number of drops (N_T), Geometric mean diameter (D_g) and Standard geometric deviation (σ) have been derived. Their variation with rain rates are presented here.

- The standard geometric deviation of drop size is constant for all rain rates at all the stations.
- Geometric mean diameter increases exponentially with rain rate at all the stations. This indicates heavier rainfall usually has more larger drops.
- Total number of drops increases exponentially with rain rate at Kochi and SHAR. However, at Thiruvananthapuram and Munnar, the total number of drops starts decreasing or remaining constant after a certain rain rate. This shows intense rainfall at these stations may not have the same increase in larger sized drops like in the other two stations.

8.4. VARIATION OF DSD DURING THE COURSE OF A RAINSPELL

The variation of the DSD during the course of a rain event lasting over 2½ minutes with an average rain rate of 2.028 mm/h has been studied. It is seen that:

- At the beginning of the rainfall event, the smaller drops are more in number compared to larger drops.
- During the course of the event, the number of smaller drops is seen to decrease while that of larger drops seen to increase showing the possibility of coalescence.
- Decrease in smaller drops without the corresponding increase in larger drops showing the possibility of evaporation.
- The movement of rain patches downward is also seen during the course of the event.

8.5. RADAR REFLECTIVITY AND RAIN RATE (Z-R)

The variation of radar reflectivity with rain rate has been derived using the MRR data. The stratiform and convective clouds could be distinguished from the presence of Bright band or otherwise, from the MRR data.

The results from the study are given below.

- The Z-R relations (of the form $Z=AR^b$) derived is given in the table VIII.II.

Rain type→	Stratiform		Convective	
Season	***A***	***b***	***A***	***b***
Pre-monsoon	496	1.26	265	1.27
Southwest monsoon	334	1.36	141	1.25

Table VIII.II. The parameters A and b of the Z-R relation for different rain type during different seasons.

- The values of A and B are seen to decrease with height except for southwest stratiform where they are found to be constant with height.

8.6. COMPARISON OF SATELLITE DATA WITH GROUND-BASED MEASUREMENTS

The rain rate data from the Disdrometer, MRR, Manual rain gauge and the TRMM are compared both for the simultaneous detection and for the amplitude of the magnitude.

- 77% of the total events could be detected together by the TRMM and Disdrometer sensors.
- TRMM rainfall agrees well with the Manual rain gauge, Disdrometer and MRR rainfall, when monthly accumulation is taken (Correlation coefficient is > 0.9). The same comparison for daily accumulated rainfall gives a correlation coefficient of around 0.6. For 3-hourly rainfall, the comparison gives a value of around 0.4.
- Magnitude of Root Mean Square Error (RMSE) has no dependence on the magnitude of rainfall accumulation.
- Munnar shows a better correlation compared to other stations. This could be attributed to the "coastal-grid effect", as the other three stations are coastal stations. This could be due to the land and ocean back-ground emissivity within the same grid box in the scenario of satellite measurements.
- The number of events detected by single sensor only is being significant indicates that the rainfall may not be uniform even over a small grid size of 0.25º X0.25º.
- Hence to evaluate the 'ground truth' in a detailed way, it would be better to deploy more instruments within a single grid of 0.25º X 0.25º.

In short, the major results pertain to the development and testing of an empirical model to represent the variation of DSD with rain rate in the tropics. The evaluation of the vertical profiles of Z-R relations for our region is another important result of this study. The correlation between satellite measured rainfall and ground-based measurements has brought out a broad agreement between them. However the need to have a closer look at the satellite retrieval is required. The

behaviour of the intensity of rain fall or rain rate at tropical stations and the possible effect of orography on DSD has been also brought out.

8.7. SCOPE OF FUTURE WORK

The empirical model developed in this study could be updated with more data and from other locations. Using the collocated MRR for classification of rain into stratiform and convective origin on the basis of radar bright band signature, DSD model could be derived separately for stratiform and for convective rain. The shape and scale parameters of the weibull-distribution fitted to the cumulative rain rate distributions could be explored during different monsoon seasons to understand the spatial variability in rainfall and even the prevalence of stratiform and convective clouds. More Disdrometers could be deployed within a single TRMM grid to get a better resolution and comparison with satellite data. This will ultimately help in evaluating the ground truth accurately. The DSD data could be collected from more west coast stations and high altitude stations in the western ghat and comparison could be done between those coastal and high altitude stations in the same latitude for getting more evidence for the orographic effect on rain DSD. The behaviour of DSD with altitude using the micro rain radar data would throw some light on the possible effects of the atmospheric medium on rain processes itself.

REFERENCES

Adeyewa, Z. D., Nakamura Â. Validation of TRMM Radar Rainfall Data over Major Climatic Regions in Africa. J. Appl. Meteorol. 42(2), 331-347, 2003.

Adler, R.F., Bolun, D.T., Curtis, S., Nelkin, E.J. Tropical rainfall Distributions determined using TRMM combined with other satellite and raingauge information, J. Appl. Meteorol. 39, 2007-2023, 2000.

Ajai, G.O., Olsen, R.L. Modelling of a tropical raindrop size distribution for microwave and millimeter wave applications. Radio Sci. (USA), 20, 193, 1985.

Ananthakrishnan, R., Aralikatti, S.S., Pathan, J.M. Some features of the southwest monsoon rainfall along the West Coast of India. Proc. Indian Acad. Sci. 88A, 177–199, 1979.

Atlas, D. Advances in radar meteorology. Advances in Geophysics, 10, Academic Press, 317–478, 1964.

Atlas, D., Chmela, A.C. Physical-synoptic variation of drop-size parameters. Proc. Sixth Weather Radar Conf., Cambridge, MA, Amer. Meteor. Soc. 21-29, 1957.

Atlas, D., Srivastava, R.C., Sekhon, R. Doppler radar characteristics of precipitation at vertical incidence. Rev. Geophys. Space Phys. 11, 1-35, 1973.

Atlas, D., Ulbrich, C.W., Meneghini, R. The multiparameter remote measurement of rainfall. Radio Sci. 19, 3-22, 1984.

Austin, P. M. Relation between measured radar reflectivity and surface rainfall. Mon. Wea. Rev. 115, 1053–1070, 1987.

Baltas, E.A., Mimikou, M.A. The use of Joss-type disdrometer for the derivation of Z-R relationships, Proc. ERAD, 291-294, 2002.

Barry, R.G. Mountain weather and climate, Methuen, London, pp. 180, 185-188, 1981

Battan, L. J. Radar Observation of the Atmosphere. The University of Chicago Press. 324 pp, 1973.

Bendix, J., Fabian, P., Rollenbeck, R. Gradients of fog and rain in a tropical montane cloud forest of southern Ecuador and its chemical composition. Proc. 3rd Int. Conf. on Fog, Fog Collection and Dew, Cape Town ZA, 11-15 Oct. 2004.

Bergeron, T. On the physics of clouds and precipitation. Proc. 5th Assembly U.G.G.I., Libson. 2, 156-178, 1935.

Brandes, E.A. Optimising rainfall estimates with the aid of radar. J. Appl. Meteor. 14, 1339-1345, 1974.

Bringi, V.N., Chandrasekar, V., Hubbert, J., Gorgucci, E., Randeu, W.L., Schoenhuber, M. Raindrop Size Distribution in different climatic regimes from Disdrometer and dual-polarised radar analysis. J. Atmos. Sci. 60, 354-365, 2003.

Carbone, R. E., Nelson, L.D. The evolution of raindrop spectra in warm-based convective storms as observed and numerically modeled. J. Atmos. Sci. 35, 2302–2314, 1978.

Cha, J., Chang, K., Yum, S.S., Cho, Y.J. Comparison of the Bright Band Characteristics Measured by Micro Rain Radar (MRR) at a Mountain and a Coastal Site in South Korea, Adv. Atmos. Sci. 26 (2), 211–221, 2009.

Cha, J.W., Yum, S.S., Chang, K., Oh, S.N. Estimation of the melting layer from a micro rain radar (MRR) data at the cloud physics observation system (CPOS) site at Daegwallyeong Weather Station, J. korean meteorological soc. 43 (1), p. 77-85, 2007.

Chapon, B., Delrieu, G., Gosset M., Berne, A. Study of the Z-R relationship sensitivity on the precipitation type using concomitant ground-based drop size distribution and vertically pointing radar measurements, Cosis.net, abstracts, ERAD3, 00057.

Chokngamwong, R., Chiu, L. TRMM and Thailand daily gauge rainfall comparison, http://ams.confex.com/ams/pdfpapers /103039.pdf., 2005.

Cifelli, R., Williams, C.R., Rajopadhyaya, D.K., Avery, S.K., Gage, K.S., May, P.T. Drop-Size Distribution Characteristics in Tropical Mesoscale Convective Systems. J. Appl. Meteorol. 39(6), 760-777, 2000.

Clemens, M., Peters, G., Seltmann, J., Winkler, P. Time-height evolution of measured raindrop size distributions. Proc. ERAD, 2006.

Diederich, M., Crewell, S., Simmer, C., Uijlenhoet, R. Investigation of rainfall microstructure and variability using vertically pointing radar and disdrometer. Proc. ERAD, 2004.

Diederich, M., Simmer, C., Battaglia, A. Spatial and temporal variability of drop size distribution from vertically pointing micro rain radar (MRR). 2nd Workshop of the International Precipitation Working Group.

Distromet LTD, Analyser-ADA 90, Instruction manual, 1997

Distromet LTD, Disdrometer RD-69, Instruction manual, 1997

Doviak, R.J., Zrnic, D.S. Doppler radar and Weather Observations. Academic Press, pp. 562, 1993.

Fabry, F., Zawadzki, I. Long-term radar observation of the melting layer of precipitation and their interpretation. J. Atmos. Sci. 52, 838–851, 1995.

Feingold, G., Levin, Z. The lognormal fit to raindrop spectra from frontal convective clouds in israel. J. Clim. Appl. Meteorol. 25, 1346-1363, 1986.

Ferrier, B. S., Tao, W. K., Simpson, J. A double-moment multiple-phase four-class bulk ice scheme. Part II: Simulations of convective storms in different

large-scale environments and comparisons with other bulk parameterizations. J. Atmos. Sci. 52, 1001–1033, 1995.

Findeisen, W. Die kolloidmeteorologischen Vorgaenge beider Niederschlagsbildung. Meteor. Z. 55, 121, 1938.

Fiser, O. Radar Reflectivity- Rain Rate relationships derived from Czech Disdrometer Data. Proc. ERAD, 2004.

Franklin, R., Robertson, Fitzjarrald, D.E, Kummerow, C.Q. Effects of uncertainty in TRMM precipitation radar path integrated attenuation on interannual variations of tropical oceanic rainfall, Geophys. Res. Let. 30(4), 1180, doi:10.1029/2002GL016416, 2003.

Fujiwara, M. Raindrop-size distribution from individual storms. J. Atmos. Sci., 22, 585–591, 1965.

Glickman, T.S. Glossary of Meteorology. 2d Ed., Amer. Meteor. Soc., 855pp., 2000.

Gordon, H.B., Whetton, P. H., Pittock, A.B., Fowler, A.M., Haylock, M.R. Simulated changes in daily rainfall intensity due to the enhanced greenhouse effect: implications for extreme rainfall events. Clim. Dyn. 8, 83–102, 1992.

Gori, E. G., Joss, J. Changes of shape of raindrop size distributions simultaneously observed along a mountain slope. J. Rech. Atmos. 14, 239–300, 1980.

Gray, W. R., Uddstrom, M. J., Larsen, H.R. Radar surface rainfall estimates using a typical shape function approach to correct for the variation in the vertical profile of reflectivity factor. Int. J. Remote Sens. 23, 2489–2504, 2002.

Grossman, R., Durran, D. Interaction of low level flow with the western ghat mountains and offshore convection in the summer monsoon. Mon. Wea. Rev. 112, 652–672, 1984.

Gunn, K. L. S., Marshall, J. S. The effect of wind shear on falling precipitation. J. Meteor. 12, 339–349, 1955.

Gunn, R. Collision characteristics of freely falling water drops. Science. 150, 695-701, 1965.

Gunn, R. Thunderstorm Electrification and Raindrop Collisions and Disjection in an Electric Field. Science. 150, 3698, 888-889, 1965.

Haddad, Z. S., Smith, E. A. C., Kummerow, D., Iguchi, T., Farrar, M. R., Durden, S. L., Alves, M., Olson, W. S. The TRMM day-1 radar/radiometer combined rain-profiling algorithm., J. Meteor. Soc. Japan, 75, 799_809. 1997.

Hardaker P. J., Holt, A. R. Collier, C. G. A melting layer model and its use in correcting for the bright band in single polarization radar echoes. Quart. J. Roy. Meteor. Soc., 121, 495–525, 1995.

Harikumar, R, Sasi Kumar, V., Sampath, S., Vinayak P.V.S.S.K. Comparison of Drop Size Distribution between stations in Eastern and Western coasts of India. J. of Indian Geophysical Union. 11(2), 111-116, 2007.

Harikumar, R. Sampath, S. Altitudinal and temporal Evolution of Rain Drop Size Distribution observed over a tropical station using a Micro Rain Radar. Proc. COSPAR meeting 2008, Montreal, Canada, 2008b.

Harikumar, R., Hamza Varikoden, Sampath, S., Mohan Kumar, G. and Gairola, R.M., Comparison of TRMM precipitation data with Micro Rain Radar and Disdrometer data during different Monsoon seasons, Proc. COSPAR meeting 2008, Montreal, Canada, 2008c.

Harikumar, R., Sampath, S., Mohan Kumar, G. Spatial Variability of Rain Drop Size Distribution-Study at High Altitude and Coastal Tropical Stations in Peninsular India. Proc. International Conference on Megha-Tropiques Science and Applications, Bangalaru, India, 2009a.

Harikumar, R., Sampath, S., Mohan Kumar, G., Sasi Kumar, V. Simultaneous Evidence for the origin of rain from Stratiform or Convective Clouds from the Micro Rain Radar Bright Band Signature and the Vertical profiles of

Z-R Empirical relation. Proc. International Conference on Megha-Tropiques Science and Applications, Bangalaru, India, 2009b.

Harikumar, R., Sampath, S., Sasi Kumar V. An Empirical Model for the variation of Rain Drop Size Distribution with Rain Rate at a few locations in Southern India. Adv. Space Res. 43, 837-844, doi: 10.1016/j.asr.2008.11.001, 2009

Harikumar, R., Sasi Kumar, V., Sampath, S., Vinayak, P. V. S. S. K. Rain Drop Size at different heights. Proc. 18th Kerala Science Congress. 244-45, 2006.

Harris, G.N. JR., Bowman, K.P., Shin, D.B. Comparison of Freezing-Level Altitudes from the NCEP Reanalysis with TRMM Precipitation Radar Brightband Data. J. clim. 13, 4137-4148, 2000.

Haylock, M.R., Nicholls, N. Trends in extreme rainfall indices for an updated high quality data set for Australia, 1910–1998. Internat. J. Climatol. 20, 1533–1541, 2000

Houghton, H.G. On Precipitation Mechanisms and their Artificial Modification. Journal of Applied Meteorology. 7(5), pp.851-859, doi: 10.1175/1520-0450(1968)007, 1968.

Houze, R. A., Jr. Stratiform precipitation in regions of convection: A meteorological paradox?. Bull. Amer. Meteor. Soc. 78, 2179–2196, 1997.

Houze, R.A. Cloud Dynamics. Academic Press. 573 pp, 1993.

Hu, Z., Srivastava, R.C. Evolution of Rain Drop Size Distribution by Coalescence, Breakup and Evaporation: Theory and Observations, Technical Report No. 56. Laboratory for Atmospheric Probing, Department of the Geophysical Sciences, University of Chicago, 1993.

Hu, Z., Srivastava, R.C. Evolution of rain drop size distribution by coalescence, breakup and evaporation: Theory and observations. J Atmos Sci. 52, 1761-1783, 1995.

Huggel, A., Schmid, W., Waldvogel, A. Raindrop size distributions and the radar bright band. J. Appl. Meteor. 35, 1688–1701, 1996.

James, E.J, Saseendran S.A., Chandrasekharan, M.E., Anitha, A.B. Rainfall frequency studies for Kerala region. J. Inst. Engineers (India) 68(C), 74–81, 1987.

Jameson, A. R., Kostinski, A. B. Reconsideration of the physical and empirical origins of Z–R relations in radar meteorology. Quart. J. Roy. Meteor. Soc. 127, 517–538, 2001a.

Jameson, A. R., Kostinski, A. B. Spurious power-law relations among rainfall and radar parameters. Q. J. R. Meteorol. Soc., 128, 2045–2058, 2002.

Jassal, B., Verma, A., Singh, L. Raindrop size distribution and attenuation for Indian climate. Indian J. Radio and Space Phys. 23(3), 193-196, 1994.

Joss, J. and Gori, E. Shapes of raindrop size distributions. J. Appl. Meteorol. 17, 1054-1061, 1978.

Joss, J., Dyer R. Large errors involved in deducing drop size distributions from Doppler radar data due to vertical air motion. 15th Radar Meteorology Conf. Amer. Meteor. Soc. pp. 179–180, 1972.

Joss, J., Gori, E. Shapes of raindrop size distributions. J. Appl. Meteorol. 17, p. 1054, 1978.

Joss, J., Waldvogel, A. Ein Spektrograph fur Neider-schlagestrophen mit automatisher Auswerting (A spectrigraph for rain drops with automatic analysis). Pur Appl. Geophys. 68, 240-246, 1967

Joss, J., Waldvogel, A. Precipitation measurements and hydrology. Radar in Meteorology. D. Atlas. Ed. Amer. Meteor. Soc. 577–606, 1990.

Kenji, B., Tamon, F., Yoshinari, O., Kazuo, S. Measurement of Raindrop Size Distribution and and Kinetic Enery using Disdrometer. Transactions of the Japanese Society of Irrigation, Drainage and Reclamation Engineering, 204, pp. 777-783, 1999.

Kitchen, M., Brown, R., Davies, A.G. Real time correction of weather radar data for the effects of bright band, range and orographic growth in the widespread precipitation. Quart. J. Roy. Meteor. Soc., 120, 1231–1254, 1994.

Kozu, T., Reddy K.K., Mori, S., Thurai, M., Ong, T., J., Rao, D. N., Shimomai, T. Seasonal and Diurnal Variations of Raindrop Size Distribution in Asian Monsoon Region. J. Meteorol. Soc. Jap., 84A, 195-209, 2006

Kunhikrishnan, P.K., Sivaraman, B.R., Kiran Kumar, N.V.P., Alappattu, D.P. Rain observations with micro rain radar (MRR) over Thumba. Optical Engineering, 6408, doi: 10.1117/12.694115, 2006.

Langmuir, I. The production of rain by a chain reaction in cumulus clouds at temperatures above freezing. J. Meteor. 5, 175-192, 1948.

Lauer, W. Klimatische, Grundzuge der Hohenstufung, tropischer Gebirge, in Tagungsberichtund Wissenschafiliche Abhandlungen, 40 Deutscher Geogrphentag. Innsbruck, F. Steiner, pp. 76-90, 1975.

Lauscher, F. Weltwiete Typen der Hohenabhangigkeit des Niederschlags, Wetter u Luben, 28, pp. 80-90, 1976.

Lee, C.K., Lee, G.W., Kim, K.E. The Impact of DSD Variability on the Radar Rainfall Estimation, Seventh radar workshop, Meteorological Research Institute, Nov 16-17, 2006.

Lee, G.W., Zawadzki, I. Radar calibration by gage, disdrometer, and polarimetry: Theoretical limit caused by the variability of drop size distribution and application to fast scanning operational radar data. J. Hydrol., In Press, Available online 17 February, 2006.

Levin, Z., Feingold, G., Tzivion, S The evolution of rain drop spectra: Comparisons between modeled and observed spectra along a mountain slope in Switzerland. J. Appl. Meteor., 30, 893–900. 1991

Li, X., Srivastava, R.C. An Analytical Solution for Raindrop Evaporation and Its Application to Radar Rainfall Measurements, J. Appl. Meteorol. 40, 1607-1616, 2001.

Liao, L., Ghini, R.M., Iguchi, T. Bright-Band Modeling of Air/Space-Borne Microwave Radars, IEEE International Geoscience and Remote Sensing Symposium and the 24th Canadian Symposium on Remote Sensing, June 24-28, Canada.

Liebmann, B., Smith, C. A. Description of a complete (interpolated) outgoing longwave radiation dataset. Bull. Amer. Meteor. Soc. 77, 1275–1277, 1996.

List, R., Gillespie, J.R. Evolution of raindrop spectra with collision -induced breakup, J. Atmos. Sci. 33, 2007-2013, 1976.

Loffler-Mang, Kunz, M. On the performance of a low-cost K-band Doppler radar for quantities rain measurements. J. Atmos. Ocean. Technol. 16, 379-387, 1999.

Low, T. B., List, R. Collision, Coalescence and Breakup of Raindrops. Part I: Experimentally Established Coalescence Efficiencies and Fragment Size Distributions in Breakup. J American Met. Society. 39, 1591-1605, 1982.

Low, T. B., List, R. Collision, Coalescence and Breakup of Raindrops. Part II: Parameterization of Fragment Size Distributions. J. American Met. Soc. 39, 1607-1618, 1982.

Maciel, L.R. and Assis, M.S. Tropical rainfall drop-size distribution. Int. J. Satell Commun (UK), 8, 181, 1990.

Magarvey, R.H., Geldart, J.W. Drop collisions under conditions of free fall. J. Atmos. Sci. 19, 107-113, 1962.

Mali, P., Sarkar, S., Das, J. Rain drop size distribution from radar reflectivity measurements. Indian J. Radio and Space Phys. 32, 296-300, 2003.

Marshall, J., Palmer, W. The distribution of raindrop with size. J. Meteorol. 5, 165-

166, 1948.

Martner, B.E., Yuter, S.E., White, A.B., Kingsmill, D.E., Ralph, F.M. Raindrop Size Distribution and Z-R Relations in Coastal Rainfall for Periods With and Without a Radar Brightband, AMS, 11th Conference on Mesoscale Processes, Albuquerque, NM, 2005.

Martner, B.E., Yuter, S.E., White, A.B., Kingsmill, D.E., Ralph, F.M. Raindrop Size Distribution and Z-R Relations in Coastal Rainfall for Periods With and Without a Radar Brightband, American Meteorol. Soc. 11th Conference on Mesoscale Processes, Albuquerque, NM, 2005.

McGaughey, G., Zipser, E. J., Spencer, R. W. Hood, R. E. High-resolution passive microwave observations of convective systems over the tropical Pacific Ocean. J. Appl. Meteor., 35, 1921–1947, 1996.

McKague, D., Evans, K. F., Avery, S.K. Assessment of the effects of drop size distribution variations retrieved from UHF radar on passive microwave remote sensing of precipitation. J. Appl. Meteor., 37, 155–165, 1998.

McTaggart-Cowan, J.D., List, R. Collision and breakup of water drops at terminal velocity. J. Atmos. Sci. 32, 1401-1411, 1975b.

Medhurst, R.G., Rainfall attenuation of centimeter waves: comparison of theory and measurement. 1965, IEEE Trans Antenna and Propag (USA), 13, pp. 550.

Meetschen, D., Battaglia, A., Simmer, C. A combined Micro-Rain-Radar (MRR) and weather radar system for improved real-time quantitative precipitation measurement (QPM), Malte Diederich, 32nd conference on radar meteorology, 13R. 4, Alvarado.

Metek GmbH, METEK, Graphic User manual, Version 2.9, 2005.

Metek GmbH, MRR-2, Physical Basis, Version 1.3, 2001.

Metek GmbH, MRR-2, User manual, 2005.

Michelson, D. B., Koistinen, J. Gauge-Radar Network Adjustment for the Baltic Sea Experiment, Phys. Chem. Earth (B), 25, pp. 915-920, 2000

Mittermaier, M.P., Illingworth, A.J. Comparison of model-derived and radar-observed freezing-level heights: Implications for vertical reflectivity profile-correction schemes, Qurt. J. R. Met. Soc., 129(587), 83-95, 2003.

Munchak, S. J., Tokey,A. Retrieval of Raindrop Size Distribution from simulated Dual-Frequency Radar Measurements, J. Appl. Meteorol. Clim. 47, pp. 223-239, January 2008.

Muralidharan. V., Kuriyan, P. P., Sampath, S. A brief study of the orographic effect of Western Ghats on monsoon rainfall. Geogr. Rev. India. 47, 32–37, 1985.

Neiman, P. J., Ralph, M., White, A. B., Kingsmill, D.A., Persson, P. O. G. The statistical relationship between upslope flow and rainfall in California's coastal mountains: Observations during CALJET. Mon. Wea. Rev., 130, 1468–1492, 2002.

Nicholson, S. E., Some, B., McCollum, J., Nelkin, E., Klotter, D., Berte, Y., Diallo, B. M., Gaye, I., Kpabeba, G., Ndiaye, O., Noukpozounkou, J. N., Tanu, M. M., Thiam, A., Toure, A. A., Traore, A. K. Validation of TRMM and Other Rainfall Estimates with a High-Density Gauge Dataset forWest Africa. Part I: Validation of GPCC Rainfall Product and Pre-TRMM Satellite and Blended Products. J. Appl. Meteorol. 42 (10), 1337_1354, 2003a.

Nicholson, S. E., Some, B., McCollum, J., Nelkin, E., Klotter, D., Berte, Y., Diallo, B. M., Gaye, I., Kpabeba, G., Ndiaye, O., Noukpozounkou, J. N., Tanu, M. M., Thiam, A., Toure, A. A., Traore, A. K. Validation of TRMM and Other Rainfall Estimates with a High-Density Gauge Dataset for West Africa. Part II: Validation of TRMM Rainfall Products. J. Appl. Meteorol. 42 (10), 1355_1368, 2003b.

Nystuen, J. A. Relative Performance of Automatic Rain Gauges under Different Rainfall Conditions. J. Atmos. Oceanic Technol. 16, 1025-1042, 1999.

Peter, G., Fischer, B., Clemens, M., Areal homogeneity of Z-R-relations, Proc. ERAD, 2006.

Peters, G., Fischer, B., Andersson, T. Rain observations with a vertically looking Micro Rain Radar (MRR). Boreal Environmental Res., 7, 353–362, 2002.

Petersen, W. A., Coauthors, Mesoscale and radar observations of the Fort Collins flash flood of 28 July 1997. Bull. Amer. Meteor. Soc. 80, 191–216, 1999.

Philip, S., Brown, J.R. Analysis of the Low and List Drop-Breakup formulation. J. American Met. Society. March 1986, 313-321, 1986.

Pruppacher, H.R., Pitter, R.L. A semi-empirical determination of the shape of cloud and raindrops. J. Atmos. Sci. 28, 86-94, 1971.

Rahman, H. and Sengupta. Preliminary comparison of daily rainfall from satellite and Indian gauge data. Tech. Rep. 2007AS1, 26pp, Indian Institute of Science, Bangalore, India. 2007.

Rao, K.N. Monsoons of the world, Basu, S. et al. (editors), Hindi Union Press, New Delhi, p. 44, 1958.

Rao, T. N., Kumar, N. K., Radhakrishna, B., Rao, D. N. On the variability of the shape-slope parameter relations of the gamma raindrop size distribution model. Geophy. Res. Lett. 33, L22 809. doi:10.1029/2006GL028440, 2006.

Rao, T. N., Narayana Rao, D., Mohan, K., Raghavan. S. Classification of tropical precipitating systems and associated Z-R relationships. J. Geo-phys. Res. 106, 17, 699-711, 2001.

Rayleigh, L. On the capillary phenomena of jets. Proc. R. Sot. London. 29, 71-79, 1879.

Reddy, K.K., Kozhu, T., Ohno, Y., Jain, A.R., Rao,D.N. Estimation of vertical profiles of raindrop size distribution from the VHF wind profiler radar Doppler spectra. 34, 319-327, 2005

Reddy, K.K., Kozu, T. Measurements of raindrop size distribution over Gadanki during south-west and north-east monsoon. Indian J. Radio and Space Phys. 32, 286-295, 2003.

Reddy, K.K., Kozu, T., Ohno, Y., Jain, A. R., Rao, D.N. Estimation of vertical profiles of raindrop size distribution from the VHF wind profiler radar Doppler spectra. Indian J. Radio and Space Phys. 34, October,319-327. 2005

Reynolds, O. On the manner in which raindrops and hailstones are formed. Proc. Lit. Fil. Soc. Manchester, 16, 23-33, 1876.

Richter, C. Niederschlagsmessungen mit dem vertikal ausgerichteten FM-CW-Dopplerradar-RASS-System, Validierung und Anwendung. Dissertation Universität Hamburg. Berichte aus dem Zentrum für Meeres- und Klimaforschung Nr. 12, 143 pp., 1994.

Richter, C., Hagen,M. Drop-size distributions of raindrops by polarization radar and simultaneous measurements with disdrometer, wind profiler and PMS probes. Quart. J. Roy. Meteor. Soc., 123, 2277–2296, 1997.

Rico-Ramirez, M. A., Cluckie, I. D., Han, D. Correction of the bright band using dual-polarization radar. Atmospheric Science Letters. 6, 40–46, 2005.

Riehl, H. Tropical Meteorology. New York. McGraw Hill. 392pp, pp 281-357, 1954.

Rogers, R. R., Baumgardner, D., Ether, S. A., Carter, D. A., Ecklund, W. L. Comparison of raindrop size distributions measured by radar wind profiler and by airplane. J. Appl. Meteor., 32, 694–699, 1993.

Roy, S.S., Datta, R.K., Bhatia, R.C., Sharma, A.K. Drop size distributions of tropical rain over south India. Geofizika. 22, 105-130, 2005.

Rudolf, B. (1993), Management and analysis of precipitation data on a routine basis, in precipitation and evaporation, Proc. Int. WMO/IAHS/ETH Symp. Precipitation and Evaporation. pp. 69_76, Slovak Hydrometeorology Institution, Bratislava, Slovakia.

Sa´nchez-Diezma, R., Torres, S., Creutin, D., Zawadzki, J.D., I., Delrieu,G. Factors affecting the precision of radar measurement of rain. An assessment from a hydrological perspective. Preprints, 30th Conf. on Radar Meteorology, Munich, Germany, Amer. Meteor. Soc. 573–575, 2001.

Sampath, S., Vinayak, P.V.S.S.K. Rainfall in Kerala. Report of the Centre for Earth Science Studies, Thiruvananthapuram, 1989.

Sartor, J. D. The role of particle interactions in the distribution of electricity in thunderstorms. J. Atm. Sci. 24, 6, 1967.

Sasi Kumar, V., Sampath, S., Vinayak, P.V.S.S.K. Drop size distribution of rainfall of different intensities. Indian J. Radio and Space Phys. 32, 217-220, 2003.

Sasi Kumar, V., Sampath, S., Vinayak, P.V.S.S.K., Harikumar, R. Rainfall intensity characteristics at coastal and high altitude stations in Kerala. J. Earth System Sci. 116(5), 451-463, 2007.

Sato, T., Radar principles, in MAP Hand book, Ed. S. Fukao, **30**, pp. 19-53, 1989.

Satoy, T., Teraokay, T., Kimuray, I. Validation and Ground Truth for TRMM Precipitation Radar Using the MU Radar, IEICE trans. commun., vol. e79–b, 6, 1996.

Sawyer, J.S. The physical and dynamical problems of orographic rain, Weather, 11, pp. 375-381, 1956.

Sheppard, Joe P. I., Comparison of rain drop size distribution measurements by a Joss-Waldvogel disdrometer, a PMS 2DG spectrometer, and a POSS Doppler radar. J. Atmos. Oceanic Technol. 11, 874-887, 1994.

Short, D.A., Kozu, T., Nakamura, K. Rainrate and raindrop size distribution observations in Darwin, Australia. Proc. URSI Commission F Open Symp. on Regional Factors in Predicting Radiowave Attenuation Due to Rain, Rio de Janeiro, Brazil, International Union of Radio Science Commission, 35–40, 1990.

Smith, J. A. Marked point process models of raindrop-size distributions. J. Appl. Meteor. 32, 284–296, 1993.

Smith, J. A., De Veaux, R. D. A stochastic model relating rainfall intensity to raindrop processes. Water Resour. Res., 30, 651–664, 1994.

Smith, J. A., Krajewski, W. F. A modeling study of rainfall rate–reflectivity relationships. Water Resour. Res. 29, 2505–514, 1993.

Song, N., Marwitz, J. A numerical study of the warm rain process in orographic cloud. J. Atmos. Sci., 46, 3479–3489, 1989.

Sreedharan, K.E., James E.J. A frequency study of rainfall for the Periyar basin of Kerala. Mausam. 39, 429–432, 1988.

Steiner, M. A new relationship between mean Doppler velocity and differential: reflectivity. J. Atmos. Oceanic Technol. 8, 430–443, 1991.

Steiner, M., Houze, R.A.Jr. Sensitivity of the estimated monthly convective rain fraction to the choice of Z–R relation. J. Appl. Meteor., 36, 452–462, 1997

Steiner, M., Smith, J. A. Reflectivity, rain rate, and kinetic energy flux relationships based on raindrop spectra. J. Appl. Meteor., 39, 1923–1940, 2000.

Strauch, R.G. Theory and application of the FM-CW Doppler radar. Ph. D. Electrical Engineering, University of Colorado, 97 pp, 1976.

Testud, J., Oury, S., Amayenc, P. The concept of `normalized` distribution to describe raindrop spectra: a tool for hydrometeor remote sensing. Phys. Chem. Earth-Part B, 25 (10-12), 897-902, doi: 10.1016/S1464-1909(00)00122-2, 2001.

Testud, J., Oury, S., Black, R.A., Amayenc, P. The Concept of `Normalized` Distribution to Describe Raindrop Spectra: A Tool for Cloud Physics and Cloud Remote Sensing. J. Appl. Meteor. 40(6), 1118-1140, doi: 10.1175/1520-0450(2001), 2001.

Tian, L., Heymsfield, G.M., Li, L., Srivastava, R.C. Properties of light stratiform rain derived from 10- and 94-GHz airborne Doppler radars measurements. J. Geophys. Res. 112, D11211, doi: 10.1029/2006JD008144, 2007.

Tokay, A., Bashor, P. G. An Experimental Study of Small-Scale Variability of Raindrop Size Distribution. Geophysical Research Abstracts, Vol. 9, 04685, SRef-ID: 1607-7962/gra/EGU2007-A-04685, 2007.

Tokay, A., Bashor, P.G., Wolff, K.R. Error Characteristics of Rainfall Measurements by collocated Joss-Waldvogel Disdrometers. J. Atmos. Oceanic Technol. 22(5), 513-527, 2005.

Tokay, A., Short, D. A. Evidence from tropical raindrop spectra of the origin of rain from stratiform versus convective clouds. J. Appl. Meteor. 35, 355–371, 1996.

Tokey, A., Dickens. On the retrieval of Drop Size Distribution by Vertically Pointing Radar. J. EOS Trans. AGU, 81(48), Fall Meet. Suppl., Abstract A22B-07, 2000.

Tropical Rainfall Measuring Mission (TRMM） Precipitation Radar, Algorithm, Instruction Manual, For Version 6, TRMM Precipitation Radar Team, JAXA and NASA, 2005

Twomey, S. Statistical effects in the evolution of a distribution of cloud droplets by coalescence. J. Atmos. Sci. 21, 553-556, 1964.

Uijlenhoet, R., Steiner, M., Smith, J.A. Variability of Raindrop Size Distributions in a Squall Line and Implications for Radar Rainfall Estimation. J. Hydro meteorol. 4, 43-61, 2003.

Ulbrich, C. W. Natural variations in the analytical form of the raindrop size distribution. J. Climate Appl. Meteor., 22, 1764–1775, 1983.

Ulbrich, C. W., Atlas, D. Rainfall microphysics and radar properties:Analysis methods for drop size spectra. J. Appl. Meteor., 37, 912–923, 1998.

Ulbrich, C.W., Atlas, D. Microphysics of Raindrop Size Spectra: Tropical Continental and Marine Storms. J. Appl. Meterol. Clim., 46, 1777-1791, 2007.

Verma A.K., Jha, K.K. Influence of rain drop size distribution on specific attenuation for mm waves. Ind. J. Radio Space Phys. 25, 179-186, 1996b.

Verma, A., Jha, K.K. Raindrop size distribution model for Indian climate. Indian J. Radio and Space Phys. 25(1), 15-21, 1996a.

Viltard, N., Obligis, E., Marecal, V., Klapisz, C. Retrieval of precipitation from microwave airborne sensors during TOGA COARE. J. Appl. Meteor. 37, 701–716, 1998.

Vulpiani, G., Marzano, F.S., Chandrasekar, V., Berne, A., Uijlenhoet, R. Polarimetric Weather Radar Retrieval of Raindrop Size Distribution by means of a Regularised Artificial Neural Network. IEEE Transactions on Geosciences and Remote Sensing 44 (11), P. 3262-3275, 2006.

Wagner, A., Clemens, M., Seltmann, J. Vertical profile of drop size spectra, Proc. ERAD (2004), 402–406, 2004.

Wagner, A., Seltmann, J., Diederich, M., Peters, G. Coupling a vertically looking K-band radar and a C-band weather radar to obtain a complete profile of reflectivity, EGS Nizza 2003, Geophys. Res. Abstr., 5, 11, 993, 2003.

Waldvogel, A. The No jump of raindrop spectra. J. Atmos. Sci. 31, 1067-1078, 1974.

Wegener, A. Thermodynamik der Atmosphare. J.A. Barth, Leipzig. pp. 81 and 289, 1911.

Weischet, W. Klimatologiche Regeln Zur Vertikal verteilung der Niederschlage in Trophengebirgen, Die Erde, 100, pp. 287-306, 1969.

Williams, C.R., coauthors, Comparison of Simultanious Rain Drop Size Distributions Estimated from Two Surface Disdrometers and a UHF Profiler. 27(12), 1763-1766, 2000.

Williams, C.R., Ecklund, W.L., Gage, K.S. Classification of precipitating clouds in the Tropics using 915-MHz wind profiler. J. Atmos. Oceanic Technol. 12, 996-1012, 1995.

Willis, P.T., Marks, F., Gottschalck, J. Rain Drop Size Distributions and Radar Rain Measurements in South Florida, Preprints, 2005.

Wilson C.L., Eastment, J.D., Tan J., Ladd, D.N., Ong, J.T., Timothy, K.I. Overview of TRMM related tropical precipitation measurements in Singapore using radar and disdrometer techniquee, Preprints, EGS XXVI General Assembly, NH006, Nice, France, March 2001.

Wilson, J. W., Brandes, E. A. Radar measurement of rainfall-A summary. Bull. Amer. Meteor. Soc. 60, 1048–1058, 1979.

Woodley, W.L., Precipitation results from a pyrotechnic cumulus seeding experiment, J. Appl. Meteor. 9, 242-257, 1970

Xie, S. P., Xu, H., Saji, N.H., Wang, Y. Role of Narrow Mountains in Large-Scale Organization of Asian Monsoon Convection. Jour. of Climate. 19, 3420-3429, 2006.

Yuter, S. E., Houze R. A.Jr. Three-dimensional kinematic and microphysical evolution of Florida cumulonimbus. Part II: Frequency distributions of vertical velocity, reflectivity, and differential reflectivity. Mon. Wea. Rev., 123, 1941–1963, 1995.

Yuter, S.E., Houze, R.A. Measurements of Raindrop Size Distributions over the Pacific Warm Pool and Implications for Z–R Relations. J. Appl. Meteorol. 36, 847-867, 1995.

Zawadzki, I. Factors affecting the precision of radar measurements of rain. Preprints, 22nd Conf. on Radar Meteorology, Zurich, Switzerland, Amer. Meteor. Soc. 251–256, 1984.

Zawadzki, I., Szyrmer, W., Bell, C., Fabry, F. Modeling of the melting layer. Part III: The density effect. J. Atmos. Sci. 62, 3705–3723, 2005.

Zhang, G., Vivekanandan, J., Brandes, E. Effects of Random Inhomogeneity on Radar Measurements and Rain Rate Estimation, IEEE Transactions on Geoscience and Remote Sensing. 40(1), 2002.